IN-PLANE, FLEXURAL, TWISTING AND THICKNESS-SHEAR COEFFICIENTS FOR STIFFNESS AND DAMPING OF A MONOLAYER FILAMENTARY COMPOSITE

Final Report (Part I)
NASA Research Grant NGR-37-003-055

by

C.W. Bert & S. Chang
School of Aerospace, Mechanical & Nuclear Engineering
The University of Oklahoma
Norman, Oklahoma 73069

Prepared for

National Aeronautics and Space Administration
Washington, D.C.

March 1972

1. Report No.	2. Government Accession No.	3. Recipient's Catalog No.
NASA CR-112141		

4. Title and Subtitle	5. Report Date
IN-PLANE, FLEXURAL, TWISTING AND THICKNESS-SHEAR COEFFICIENTS FOR STIFFNESS AND DAMPING OF A MONOLAYER FILAMENTARY COMPOSITE	6. Performing Organization Code
7. Author(s)	8. Performing Organization Report No.
C. W. Bert and S. Chang	10. Work Unit No. 501-22-03-03
9. Performing Organization Name and Address School of Aerospace, Mechanical, and Nuclear Engineering The University of Oklahoma Norman, Oklahoma 73069	11. Contract or Grant No. NGR-37-003-055
12. Sponsoring Agency Name and Address National Aeronautics and Space Administration Washington, D. C. 20546	13. Type of Report and Period Covered Contractor Report
	14. Sponsoring Agency Code

15. Supplementary Notes

16. Abstract

Results are presented for elastic and damping analyses resulting in determinations of all of the various stiffnesses and associated loss tangents for the complete characterization of the elastic and damping behavior of a monofilament composite layer. For the determination of the various stiffnesses, either an elementary mechanics-of-materials formulation or a more rigorous mixed-boundary-value elasticity formulation is used. For determining the loss tangents associated with the various stiffnesses, either the viscoelastic correspondence principle or an energy analysis based on the appropriate elastic stress distribution is used.

The numerical results obtained from this analysis compare favorably with some existing analytical and experimental results for various practical combinations of constituent materials, specifically boron-epoxy, boron-aluminum, and E glass-epoxy composites. Finally a complete set of property curves for a boron-epoxy monofilament composite for a frequency range of 50 to 2,000 Hz are presented to facilitate elastic and damping analyses of a structure consisting of multiple layers of such a composite. Design data for other composites, namely, boron-aluminum and E glass-epoxy, which are valid for a similar frequency range, are summarized in tabulated form. Complete computer program documentation and listing are given to facilitate calculations of monolayer property values for other composites.

17. Key Words (Suggested by Author(s))	18. Distribution Statement
Composite materials Vibration damping Stiffness Vibration Micromechanics	Unclassified - Unlimited

19. Security Classif. (of this report)	20. Security Classif. (of this page)	21. No. of Pages	22. Price*
Unclassified	Unclassified	338	

*For sale by the National Technical Information Service, Springfield, Virginia 22151

IN-PLANE, FLEXURAL, TWISTING AND THICKNESS-SHEAR COEFFICIENTS FOR STIFFNESS AND DAMPING OF A MONOLAYER FILAMENTARY COMPOSITE

CONTENTS

ABSTRACT

To make a static or dynamic structural engineering analysis of a structure laminated of fiber-reinforced composite material, one must know beforehand the macroscopic equivalent orthotropic plate properties of a single layer. In the case of a monofilament composite layer, which consists of only a single row of parallel, equally spaced reinforced filaments embedded in the matrix material, flexural and twisting stiffness analyses must be carried out in addition to the in-plane and thickness-shear stiffness analyses owing to the inhomogeneous property distribution along the thickness direction of the layer.

In this work are carried out elastic and damping analyses resulting in determinations of all of the various stiffnesses and associated loss tangents for the complete characterization of the elastic and damping behavior of a monofilament composite layer.

For the determination of the various stiffnesses, either an elementary mechanics-of-materials formulation or a more rigorous mixed-boundary-value elasticity formulation is used. The solution for the latter formulation is obtained by means of the boundary-point least-square error technique.

Kimball-Lovell type damping is assumed for each of the constituent materials. For determining the loss tangents associated with the various stiffnesses, either the viscoelastic correspondence principle or an energy analysis based on the appropriate elastic stress distribution is used.

The numerical results obtained from this analysis compare favorably with some existing analytical and experimental results for various practical combinations of constituent materials, specifically boron-epoxy, boron-aluminum, and E glass-epoxy composites. Finally a complete set of property curves for a boron-epoxy monofilament composite for a frequency range of 50 to 2,000 Hz are presented to facilitate elastic and damping analyses of a structure consisting of multiple layers of such a composite. Design data for other composites, namely, boron-aluminum and E glass-epoxy, which are valid for a similar frequency range, are summarized in tabulated form. Complete computer program documentation and listing are given to facilitate calculations of monolayer property values for other composites.

SYMBOLS

A	cross-sectional area of a typical rectangular monofilament element
$\tilde{A}$	a general m x n coefficient matrix
$\tilde{A}^T$	transpose of $\tilde{A}$
$\tilde{A}^*$	an n x n symmetric matrix defined in eq. (A-5)
A_f, A_m	cross-sectional areas of the respective fiber and matrix regions in a typical rectangular element
A_i	heredity constants, eq. (B-21)
$a(x_1), a(x_2)$	wave amplitudes at positions x_1 and x_2
a_i, a_{i+1}, a_{i+n}	free-vibration amplitudes corresponding to the i-th, (i+1)th, and (i+n)th cycles
a_k	coefficients of the fiber-region series solution to the Prandtl torsion problem
a_o	initial amplitude
a_n^i, a'^i_n	coefficients of the biharmonic series solution to eq. (20) valid in the respective fiber and matrix regions (i=f,m)
B	constant defined in eq. (118)
$\tilde{B}$	n-dimensional column vector of prescribed boundary values
$\tilde{B}^*$	an n-dimensional column vector defined in eq. (A-6)
b	material damping coefficient defined in eq. (B-10)
b_c	critical material damping coefficient
b_k, b_{-k}	coefficients of the matrix-region series solution to the Prandtl torsion problem
b_n^i, b'^i_n	coefficients of the biharmonic series valid in the respective fiber and matrix regions (i=f,m)
C_d	damping coefficient defined in eq. (B-22)
C'_d	damping coefficient defined in eq. (B-8)
C_{V_f}	empirical constant factor

C_1, C_2, C_3	fiber-matrix interface, inter-element, and external boundaries, respectively
c	viscous damping coefficient
$\bar{c}$	Kelvin-Voigt complex damping coefficient defined in eq. (B-4)
D_{11}	longitudinal flexural stiffness
D_{12}	Poisson flexural stiffness
D_{22}	transverse flexural stiffness
D_{66}	twisting stiffness
d	distance between the origin and the center of the n-th element fiber; see fig. 7
E	Young's modulus
E_f, E_m	Young's moduli of the fiber and matrix materials, respectively
$\bar{E}_i$	equivalent Young's moduli (i=x,y,z)
E_{11}, E_{22}, E_{33}	Young's moduli of a specially orthotropic material in x_i-directions (i=1,2,3)
$E_{11}^{(b)}$	equivalent Young's modulus for flexural loading
E^2	mean-square error
Ei(u)	exponential integral defined in eq. (B-18)
e	base of the natural logarithms, e ≈ 2.7183
$F(\eta)$	function defined in eq. (51)
$\bar{F}$	exciting force amplitude
F_d	damping force
$F_n(\rho), F_n'(\rho)$	functions of the normalized radial coordinate ρ defining the series representation of the matrix-region Airy stress function, eq. (55)
F_s	spring force
F_1, F_2, F_3, F_4	integrals defined in eqs. (136,137,182, and 183)
G	shear modulus

G_f, G_m	shear moduli of the respective fiber and matrix materials
G_{44}, G_{55}, G_{66}	composite shear moduli: transverse thickness-shear, longitudinal thickness-shear, in-plane
g	loss tangent
g_1	parameter of the Biot model
$g_{E_{11}}$, etc.	subscripted loss tangents where the subscripts (i.e. E_{11}) refer to the associated moduli or stiffnesses; for example, $g_{E_{11}}$ signifies the loss tangent associated with the major Young's modulus E_{11}
HPMF	half-power magnification factor
h	total thickness of a single layer
I	centroidal rectangular moment of inertia per unit length of a longitudinal cross section
I_x, I_y	principal rectangular moments of inertia of a typical repeating cross section
I_E	weighted moment of inertia defined in eq. (119)
i	unit imaginary number $\doteq \sqrt{-1}$
K	shear coefficient
$k, \bar{k}$	spring constant, complex spring constant
k'	stiffness associated with the total in-plane force
$\bar{k}''$	complex spring stiffness defined in eq. (B-12)
$\bar{k}$	Kelvin-Voigt complex stiffness defined in eq. (B-3)
$\bar{k}'$	Kimball-Lovell complex stiffness defined in eq. (B-11)
L	effective length of spring
ℓn	natural logarithm
log	logarithm with base 10
N	bending moment per unit width
MF, MF'	magnification factors defined in eqs. (B-38) and (B-16)
m	mass
n	normal coordinate; degree of heredity, eq. (B-21)

P	axial tensile force
P'	expression defined in the first of eqs. (C-30)
Q	total shear force (Section 2.7)
Q	quality factor (Appendix B)
Q_f, Q_m	shear forces in the respective fiber and matrix regions
Q_{ij}	elastic coefficients for the plane-stress state (i,j=1,2,6)
R_1, R_2, R_3, R_4	integrals defined in eqs. (C-24)
RMF	resonant magnification factor
r	radius of the fiber
S_1, S_2, S_3, S_4	integrals defined in eqs. (C-25)
S_{44}	transverse thickness-shear stiffness
S_{55}	longitudinal thickness-shear stiffness
t	time
t_1, t_2	two different specific values of time
U	mean displacement defined in eq. (86)
U	strain energy per cycle defined in eq. (148)
U_b	flexural strain energy in an elemental volume
U_d	damping energy per cycle
U_{dv}	specific dissipative energy defined in eq. (B-22)
U^f, U^m	strain energies per cycle respectively of the fiber and matrix materials
U_s	shear energy per unit length
U_v	strain energy per unit length
U_d^f, U_d^m	damping energy per cycle respectively of the fiber and matrix materials
u, v, w	rectangular components of a displacement vector
u	displacement
$\tilde{u}$	displacement amplitude of vibration

u^i, v^i, w^i	rectangular components of a displacement vector in the fiber (i=f) and matrix regions (i=m)
u_r, u_θ	plane polar components of a displacement vector
u_{st}, u'_{st}	static displacements; see Appendix B
$\bar{u}, \bar{v}, \bar{w}$	mean rectangular components of a displacement vector
$\hat{u}, \hat{w}$	residual displacements defined in eqs. (87)
V	volume
V_f, V_m	fiber and matrix volume fractions, respectively
v_s	spatial attenuation constant defined in eq. (B-33)
v_t	temporal decay constant defined in eq. (B-30)
W	mean z-component of displacement defined in eq. (86)
x, y, z	rectangular coordinates; see figs. 3-9
x_1, x_2, x_3	rectangular coordinates associated with the fiber (x_1), transverse (x_2), and thickness (x_3) directions
x_1, x_2	two different specific values of position (Appendix B only)
$\vec{xy}$	the arrow symbols signify that the expression is also valid with the roles of x and y interchanged
α	angle of twist per unit length
α, β, γ	constants defined in eqs. (31)
α_i	heredity constants in eq. (B-21)
$\alpha_{,x}$	transverse flexural curvature
$\alpha_{,z}$	longitudinal flexural curvature
γ	loss angle
$\gamma_{average}$	average thickness-shear strain
$\gamma_{effective}$	effective thickness-shear strain
$\gamma_{r\theta}$	plane polar component of the shear strain
γ_s	spatial attenuation rate defined in eq. (B-34)

γ_t	decay rate defined in eq. (B-31)
$\gamma_{yz}, \gamma_{zx}, \gamma_{xy}$	rectangular components of shear strain
δ	ratio of height to width of the typical composite cross section
δ	logarithmic decrement defined in eq. (B-28)
δ_s	logarithmic attenuation defined in eq. (B-32)
ϵ	Biot parameter in eq. (B-17)
$\epsilon_r, \epsilon_\theta$	plane polar components of the normal strain
$\epsilon_x, \epsilon_y, \epsilon_z$	rectangular components of the normal strain
$\bar{\epsilon}_i$	average normal strains (i=x,y,z)
$\epsilon_1, \epsilon_2, \epsilon_6$	generalized plane-stress-state strain components
ζ	damping ratio
ξ, η	normalized rectangular coordinates; see eq. (74)
ρ, θ	normalized polar coordinates; see fig. 4(b)
Γ, Δ	functions defined in eqs. (174)
λ	$\lambda \equiv 1-\nu_{12}\nu_{21}$
λ	ratio of constituent-material shear moduli, $\lambda \equiv G_f/G_m$
λ'	ratio of constituent-material Young's moduli, $\lambda' \equiv E_f/E_m$
λ_1	$\lambda_1 \equiv (\lambda-1)/(\lambda+1)$
μ	ratio of width to fiber diameter of a typical monofilament cross section
ν	Poisson's ratio
ν_f, ν_m	Poisson's ratios of the fiber and matrix materials
ν_{ij}	Poisson's ratios of an orthotropic material (i,j = 1,2,3)
$\bar{\nu}_{ij}$	equivalent mean Poisson's ratios
π	pi $\approx$ 3.1415962
$\sum$	summation symbol

σ_f, σ_m	axial stress components in the respective fiber and matrix regions
σ_i	plane-stress-state stress components in rectangular coordinates (i=1,2,6)
$\bar{\sigma}_i$	equivalent mean plane-stress components (i=1,2,6)
σ_o	tensile stress; cf., figs. 4 and 6
$\tilde{\sigma}$	stress amplitude
τ	dummy time variable in eq. (B-19)
τ_{xz}, τ_{yz}	longitudinal and transverse thickness-shear stresses, respectively
$\Phi(t)$	hereditary kernel defined in eq. (B-21)
Φ^f, Φ^m	Airy stress functions for the respective fiber and matrix regions
φ	phase angle
$\hat{\varphi}^i, \varphi^i$	Neumann torsion functions (i=f,m)
$\bar{\varphi}$	mean angle of rotation of the cross section
$\hat{\chi}^i, \chi^i$	Saint-Venant flexure function (i=f,m)
$\hat{\psi}^i, \psi^i$	Dirichlet torsion function (i=f,m)
ω	angular frequency, rad/sec
ω_n	resonant angular frequency
ω_1, ω_2	angular frequencies defining the half-power points of the frequency spectrum
∇^2	Laplace operator; $\nabla^2 \equiv (\partial^2/\partial x^2)+(\partial^2/\partial y^2)$
$\hat{\nabla}^2$	dimensionless Laplace operator; $\nabla^2 \equiv (\partial^2/\partial \xi^2) + (\partial^2/\partial \eta^2)$

Superscripts:

f,m	signifies the respective fiber and matrix materials
I,R	signifies the respective imaginary and real parts of the quantity represented by the main symbol
$\cdot$	denotes differentiation with respect to time

SECTION I

INTRODUCTION

1.1 Introductory Remarks

Engineering structural design requirements for aerospace vehicle structures demand a maximum of strength and stiffness at minimum weight. In order to fulfill these requirements, engineers have been searching for new and better materials. This led to the development of glass-fiber-reinforced plastics in the case of pressure vessels, and to the use of carbon or boron filamentary composites in the case of stiffness-critical structures such as fuselage panels. In addition to being highly efficient structurally (strength/weight and stiffness/weight), the modern composite structures present modern structural designers with a unique advantage over the conventional homogeneous materials in that they can be designed to give different properties in different directions as required by the particular application. This is commonly achieved by laminating several layers of the monofilament* composites with the filaments of each layer oriented in some prescribed direction. Before macroscopic properties of such laminates can be predicted, it is necessary to determine the macroscopic behavior of a single monofilament layer.

---

*In contrast with those filamentary composites with many small reinforcing filaments randomly distributed throughout the entire cross section, there is only a single row of regularly-spaced filaments embedded in the midplane of the layer for the monofilament composites (reference 1).

Owing to their oriented nonhomogeneous nature, one-layer filamentary composite materials behave as an orthotropic material on a macroscopic basis. Thus, to use these advantages fully, orthotropic properties of the composites must be characterized from the knowledge of constituent material properties and their respective geometrical configurations. In the case of a one-layer filamentary composite with many small parallel filaments more or less randomly distributed throughout the cross section, the complete characterization of the in-plane macroscopic composite properties requires four independent elastic coefficients. These coefficients are: two moduli or elasticity E_{11}, E_{22}; one modulus of rigidity G_{66}; and one independent Poisson's ratio ν_{12} (reference 2)*. The flexural and twisting stiffnesses are then related to the in-plane moduli by the formula (reference 3),

$$(D_{11}, D_{12}, D_{22}, D_{66}) = \int_{-h/2}^{h/2} (E_{11}/\lambda,\ \nu_{12}E_{22}/\lambda,\ E_{22}/\lambda,\ G_{66})\ z^2\ dz$$

where

$$\lambda = 1 - \nu_{12}\nu_{21}$$

However, for a monofilament composite such as boron-epoxy, consisting of only one row of filaments whose diameter is relatively large in comparison with the thickness dimension, there is a large amount

*In usual notations, "1" is the filament direction, "G_{ij}" (i,j=1,2,3) denoted the shear modulus in the ij-plane, and ν_{ij} (i,j=1,2,3) denotes the j-direction normal strain due to unit i-direction normal stress.

of relatively flexible matrix material located at an appreciable distance from the filament axis. (See figure 1). Thus, the conventional practice (references 3 and 4) of assuming homogeneous property distribution in the thickness direction will not be expected to be valid in predicting the macroscopic flexural and twisting stiffnesses of a monofilament composite. In view of this, flexural and torsional analyses must be carried out in addition to the in-plane analyses in order to describe the behavior of such a composite completely. Furthermore, owing to the presence of a relatively flexible matrix material, the thickness-shear* flexibility is expected to be significant (references 5 and 6) for the filamentary composites.

In the dynamic analysis of a structure consisting of multiple layers of filamentary composites, the damping characteristics are just as important as the stiffness characteristics. The damping properties of a composite may be characterized in a number of ways (reference 7; also, see Appendix B).

There have been a few experimental investigations on damping characteristics of sandwich materials and filamentary composites (references 8-19).

Pottinger (ref. 8) measured the temporal decay of axial vibrations of bars of glass fiber-epoxy and boron fiber-aluminum composites in the frequency range of 1 kHz to 100 kHz.

---

*Often referred to as transverse-shear, here the term thickness-shear is used, so that the term transverse can be reserved to refer to the direction normal to the longitudinal (filament) direction and contained in the plane of the layer.

Schultz and Tsai (refs. 9 and 10) used the free vibration decay and resonant response of cantilever beams made of unidirectional and angle-plied glass fiber-epoxy composites in the 10 to 10,000 Hz range.

James (ref. 11) and Bert et al. (ref. 12 and 13) used the temporal decay of free-free sandwich beams. The facings of the ref. 12-13 beams were of glass fiber-epoxy.

Clary (ref. 14) conducted resonant response experiments of free-edge plates made of unidirectional boron fiber-epoxy composite material to study the effect of fiber orientation.

Bert et al. (refs. 15-17) carried out resonant response measurements on a free-edge, circular, truncated conical shell with an aluminum honeycomb core and glass fiber-epoxy facings.

Richter (ref. 18) used the rotating beam deflection technique to determine the damping characteristics of glass fiber-epoxy at low frequency (0.01 to 1.07 Hz.).

Kerr and Lazan (ref. 19) made hysteresis measurements on a sandwich beam with both core and facings of glass fiber-epoxy.

Analytically, Hashin (references 20 and 21) determined complex moduli of viscoelastic composites (particulate and filamentary) by developing a correspondence principle which relates the effective elastic moduli and creep compliances of the viscoelastic composites. However, his analyses are not applicable to those cases where the effective elastic moduli are not explicitly obtained. Since the steady-state response of the filamentary composite structure is of our main concern in this investigation, the wavelengths of the modal profiles are in general much greater than the filament diameter or the thickness dimensions; thus,

the Kimball-Lovell type material damping (reference 22) is assumed to hold. The analysis similar to reference 13 is carried out by using the numerically obtained stress distributions for the effective elastic coefficients, and the results are presented in terms of complex moduli for each assumed loading mode: in-plane, flexural, twisting, and so forth.

In the following subsection 1.2, the current literature on micromechanics analyses of filamentary composites are briefly surveyed. In Section II, detailed elasticity and mechanics-of-materials analyses are made to obtain various macroscopic elastic properties pertinent for the characterization of one-layer composites. In Section III, the elastic-analysis results are used to calculate the damping properties of the composites; and in Section IV, the damping properties in terms of complex moduli are summarized, and some typical numerical results are compared with existing analytical and experimental results.

1.2. A Brief Survey of Micromechanics Analysis of Filamentary Composite Materials

Since the development of practical methods for manufacturing parallel-filament-reinforced layers of composite materials in the 1950's (references 23, 24), the field of micromechanics analysis mushroomed rapidly starting with the pioneering analyses of Outwater (reference 25) in the United States and of Beer (reference 26) in Germany. By micromechanics analysis is meant an analysis which leads to the prediction of the macroscopic properties--elastic moduli-- of the composites based only on reinforcement configurations, and the properties and volume fractions of the

constituent materials.

Chamis and Sendeckyj, in their recent survey of the field (ref. 4), listed 109 references concerned with the prediction of thermoelastic properties of the fibrous composites. Since a unidirectional filamentary composite will behave macroscopically as an orthotropic materials, a complete description of the elastic properties of the composite requires nine independent elastic coefficients: three Young's moduli (E_{11},E_{22},E_{33}), three shear moduli (G_{44},G_{55},G_{66}), and three Poisson's ratios (ν_{12},ν_{23},ν_{31}), where the subscript (or subscripts) refers to the orthotropic axes of the composite along which the properties are measured (see figure 1.) The analytical methods which have been used in previous micromechanics analyses may be categorized as:

(1) Netting analysis method

(2) Mechanics-of-materials method

(3) Self-consistent model method

(4) Variational method

(5) Exact classical elasticity method

(6) Statistical method

(7) Discrete element (finite element) method

(8) Semiempirical method

(9) Microstructural method

In netting analysis, fibers are assumed to provide all of the longitudinal stiffness and the matrix material is assumed to provide the transverse and shear stiffnesses and the Poisson's effect. This is

equivalent to assuming the disjointed fiber-matrix model, and thus predicts relatively low values for E_{22} and G_{12} (references 25 and 27).

The mechanics-of-materials methods were pioneered by Ekvall (reference 28). In his analysis, the macro-composite properties are expressed in terms of the averaged stress-strain states, which, in turn, are expressed in terms of the constituent properties using displacement continuity and force equilibrium conditions at the matrix-fiber interface. In general, the predicted transverse and shear stiffnesses are lower than the experimental values. Thus, the method was later improved upon by using the concept of restrained matrix model in which the strain in the matrix parallel to the fiber is assumed to be zero (ref. 1). This method was later extended to account for the effect of voids in the composite by Greszczuk (reference 29), and the effects of misalignment by Nosarev (reference 30).

The self-consistent model method is based on the assumption that the strain field of a single fiber embedded in an infinite (reference 31) or a finite (reference 32) matrix is indistinguishable from that of the composite. The results of such analyses are generally accurate for the case of low-fiber-volume fractions only.

The variational method is based on the energy theorems of classical elasticity (reference 33) in which lower and upper bounds of the layer properties are obtained from the theorems of complementary and potential energy, respectively (references 34 and 35). The upper and lower bounds are very far apart for composites with high fiber-matrix-stiffness ratio such as boron-epoxy composites. Thus, correction factors such as contiguity and misalignment factor, etc. need to be brought in to obtain closer

agreement between the theoretical predictions and the experimental results (references 34 and 36).

The exact classical elasticity method has many variations depending on the methods of solution (references 37-39). With the exception of the relatively simple case of a circular fiber embedded in a circular matrix material, the solution cannot be obtained in a closed form and thus various numerical methods must be used. These are practical now with the aid of modern high-speed digital computers. In all cases, the problem is formulated with an assumption that the fibers form a regular array (rectangular or hexagonal); a solution is sought for the resulting mixed boundary-value problem, subjected to the usual assumption of perfect bonds between the fiber-matrix interface and a set of imposed boundary conditions (uniform tension, shear, etc.). The elastic field thus obtained is then averaged over the cross section and the boundary to yield the desired equivalent macroscopic elastic properties of the composite.

In the statistical methods, the composite is modelled by the random distribution of the fibers in the matrix materials. Very little success has been achieved by this method (ref. 20) owing to the statistical averaging process that leads to insurmountable computational difficulties.

The discrete element method was pioneered by Foye (references 40 and 41) for the prediction of E_{22}, G_{12}, ν_{12}, and ν_{23}. His results for circular filaments in square arrays are in good agreement with those of Ekvall (ref. 28) and Greszczuk (ref. 29). The method may also be applied to cases with nonlinear matrix behavior as well as random array arrangements (ref. 41); however, so far its use has been relatively limited.

The semiempirical method which is most commonly used to date is due to Tsai (ref. 34). He assumed that the properties of a filamentary composite with non-contacting fibers may be predicted by a linear interpolation between the lower and upper bounds obtained from the variational method. This linear interpolation was improved upon by Tsai and Halpin with a more refined nonlinear interpolation (ref. 3). There are other semiempirical models (ref. 4) based on the equivalent section concept, parallel and series connected elements, and the incorporation of certain empirical factors.

The microstructural method was proposed by Bolotin (reference 42). Postulating that the fiber behaves as a small rod and that the distances between the fibers are small in comparison with the characteristic distance of the body and using a variational principle, he derived the displacement equilibrium equation similar to those for a Cosserat medium, that is, a medium possessing an unsymmetric stress tensor containing couple stresses. Later, this microstructural model was applied by Herrmann et al. to investigate the transverse wave propoagation in filamentary composites (reference 43).

Most of the micromechanics analyses described above are based on the hypotheses* that: (1) The fibers are regularly spaced and aligned. (2) The fiber and matrix materials are homogeneous and linearly elastic. (3) There is a complete bond at the fiber-matrix interface. (4) The composite is free of voids. (5) The composite is initially at a stress

---

*As a rule, these hypotheses are adhered to in the above discussed analyses. However, there are exceptions in which one or more hypothesis is relaxed, for example, perfect interface bond is not assumed for the netting analyses.

free state. (6) The composite behaves as a homogeneous general orthotropic material macroscopically.

There have been a few experimental investigations on the damping characteristics of composites (refs. 8-19). In general, it was agreed upon that for small oscillations, the filamentary composites exhibit anisotropic, linear viscoelastic behavior. Damping properties of some non-metallic materials are summarized and tabulated in reference 44.

Analytically, Hashin developed a correspondence principle which relates the effective macroscopic elastic moduli to the effective viscoelastic moduli (reference 45). This correspondence principle was then applied to particulate and fibrous composites for the determination of macroscopic complex moduli of such composites (refs. 20 and 21). Unfortunately, this correspondence principle cannot be applied to cases where the effective elastic moduli are not explicitly obtained in a closed form. Bert et al., in their investigation of the damping in a shear-flexible sandwich beam (ref. 13), observed that the damping characteristics of composites may be related to the ratio of the dissipated energy per cycle to the total potential energy stored per cycle. The analysis is based on the assumption that the wave length of the normal modes is large in comparison with the thickness dimension of the beam.

SECTION II

ELASTIC ANALYSES

This section is concerned with the detailed elastic analyses leading toward predictions of macroscopically equivalent orthotropic properties of a monofilament composite layer. The composite layer is modelled by a typical repeating cross section consisting of a rectangular matrix with a centrally oriented circular-cross-section fiber. Various in-plane, flexural, twisting, and thickness-shear properties are obtained from the solutions of a series of mixed boundary value problems with approximately prescribed boundary conditions.

2.1 Introduction and Hypotheses

Macroscopically, a single layer of filamentary composite material behaves as a specially orthotropic material with respect to three mutually orthogonal planes: the plane normal to the fibers, the plane of the layer, and the plane normal to the first two planes. The intersection of these three planes forms three mutually orthogonal axes: the longitudinal (or fiber) direction, the transverse direction (normal to the fibers and contained in the plane of the layer), and the thickness direction (normal to the plane of the layer). Therefore, a complete characterization of the elastic properties in three dimensions requires nine independent elastic coefficients (ref. 2). However, in many structural engineering applications of filamentary composite materials or the laminates of such, they are used in the form of thin panels or plates

due to the weight considerations in such applications. In view of this, the thickness dimension of the composites is usually much smaller than the other dimensions and the radius of curvature of the structure. The three stress components σ_3, σ_4, and σ_5 therefore may be regarded negligibly small in comparison with the remaining three stress components, namely, σ_1, σ_2, and σ_6*. This is referred to as the generalized plane stress state. The constitutive equation for the generalized plane stress state is given by

$$\begin{Bmatrix} \sigma_1 \\ \sigma_2 \\ \sigma_6 \end{Bmatrix} = \begin{bmatrix} Q_{11} & Q_{12} & 0 \\ Q_{21} & Q_{22} & 0 \\ 0 & 0 & 2Q_{66} \end{bmatrix} \begin{Bmatrix} \epsilon_1 \\ \epsilon_2 \\ \frac{1}{2}\epsilon_6 \end{Bmatrix} \tag{1}$$

where the elastic coefficients Q_{ij} are symmetric, i.e.,

$$Q_{ij} = Q_{ji} \quad (i = 1,2)$$

Hence, there are only four independent elastic coefficients. Equation (1) may also be written in terms of the engineering moduli E_{11}, E_{22}, G_{12}, and Poisson's ratios ν_{12} and ν_{21} as

---

*In terms of double-subscript stress notation (ref. 3. p. 16),

$$\sigma_1 \equiv \sigma_{11},\ \sigma_2 \equiv \sigma_{22},\ \sigma_3 \equiv \sigma_{33},\ \sigma_4 \equiv \sigma_{23},\ \sigma_5 \equiv \sigma_{31},\ \sigma_6 \equiv \sigma_{12}$$

where the x_3-direction is normal to the plane of the layer.

$$\begin{Bmatrix} \sigma_1 \\ \sigma_2 \\ \sigma_3 \end{Bmatrix} = \begin{bmatrix} E_{11}/\lambda & \nu_{12}E_{22}/\lambda & 0 \\ \nu_{21}E_{11}/\lambda & E_{22}/\lambda & 0 \\ 0 & 0 & 2G_{12} \end{bmatrix} \begin{Bmatrix} \epsilon_1 \\ \epsilon_2 \\ \frac{1}{2}\epsilon_6 \end{Bmatrix} \tag{2}$$

where

$$\lambda \equiv 1 - \nu_{12}\nu_{21}$$

Again, there are only four independent coefficients since the symmetry in the coefficient matrix, which is a consequence of the existence of the elastic potential (ref. 2), demands that

$$\nu_{12}/E_{11} = \nu_{21}/E_{22}$$

It follows readily from equations (1) and (2) that,

$$\left.\begin{aligned} Q_{ii} &= E_{ii}/\lambda \quad (i=1,2) \\ Q_{12} &= \nu_{12}Q_{22} \\ Q_{66} &= G_{66} \end{aligned}\right\} \tag{3}$$

Hence, for a single layer of filamentary composite with many small filaments more or less randomly distributed throughout the entire cross section, in-plane macroscopic behavior is characterized by specifying the four elastic coefficients Q_{11}, Q_{22}, Q_{12}, and Q_{66} or equivalently, by the in-plane engineering moduli E_{11}, E_{22}, G_{66}, and one of the Poisson's ratios ν_{12} or ν_{21}.

Owing to the presence of the relatively flexible matrix material, the thickness-shear flexibility is expected to be significant (refs. 5 and 6) for the filamentary composites. Therefore, for complete macroscopic property characterization, one will need to specify flexural, twisting, thickness shear stiffnesses, and flexural Poisson's ratios, in addition to the in-plane properties. The above-mentioned type of composite has a more or less homogeneous distribution of properties through the thickness. Thus, only two additional stiffnesses, namely the thickness-shear moduli G_{55} and G_{44}, need to be calculated, since the flexural and twisting stiffnesses may be obtained by the previously stated formula,

$$(D_{11},D_{12},D_{22},D_{66}) = \int_{-h/2}^{h/2} (E_{11}/\lambda,\nu_{12}E_{22}/\lambda,E_{22}/\lambda,G_{66})\ z^2\,dz \qquad (4)$$

where D_{11},D_{12},D_{22}, and D_{66} denote the longitudinal, Poisson, transverse, and twisting stiffnesses, respectively, and h ≡ the thickness of the layer. However, for a monofilament composite, equation (4) is not expected to hold because of a more predominant inhomogeneity in the property distribution through the thickness. In view of this, for the complete characterization of macroscopic elastic behavior, flexural, as well as torsional, analyses must be carried out.

Given constitutive properties of the constituent materials and the fiber-matrix geometrical configurations, determinations of these macroscopic equivalent orthotropic properties may be carried out in a number of ways as summarized in reference 4. In the subsequent analyses, approaches based on mechanics-of-material and classical elasticity theories are used

to obtain solutions which are manipulated to yield the required equivalent orthotropic properties. The elastic solutions obtained in this way are used in Section III to analyze the damping characteristics of the filamentary composite materials where Kimball-Lovell type material damping (see Appendix B) is assumed to prevail.

The longitudinal in-plane and flexural stiffnesses and the transverse thickness-shear stiffness are handled easily for mechanics-of-materials analyses. For the remainder of the elastic properties, classical elasticity analyses are used to formulate a series of appropriate mixed boundary value problems. Then these problems are solved numerically by means of the boundary-point-least-square method, as described in Appendix A, to yield the desired equivalent macroscopic properties.

The monofilament composite material is exemplified by a repeated rectangular cross section consisting of a circular-cross-section fiber centrally located, and surrounded by matrix material as depicted in figure 2.

The basic hypotheses used consistently in the subsequent analyses are summarized as follows:

H1. Fibers and matrix respectively are homogeneous, linearly elastic, and isotropic.

H2. Both fibers and matrix are free of voids.

H3. The fiber-matrix interface bonds are perfect without transitional region between them.

H4. Initially, the composite is in a stress-free state and all thermal effects are neglected.

H5. Inertial and damping* effects are neglected.

2.2 Longitudinal In-Plane Stiffnesses

In this subsection, two in-plane engineering moduli of elasticity, namely, major Young's modulus E_{11} and in-plane longitudinal shear modulus G_{66}, will be discussed. The major Young's modulus E_{11} is estimated from the law of mechanical mixtures; whereas, the in-plane longitudinal shear modulus G_{66} is obtained from the result of classical theory of elasticity analysis by Adams and Doner (reference 46).

Major Young's Modulus E_{11}. - A typical repeating element of a monofilament composite element is subjected to a uniform longitudinal strain ϵ_1 as shown in figure 2. The longitudinal stresses induced in the fiber and matrix, respectively, are:

$$\sigma_f = E_f \epsilon_1, \quad \sigma_m = E_m \epsilon_1 \tag{5}$$

where E_f and E_m are the longitudinal Young's moduli of elasticity of the filament and matrix, respectively.

The total equivalent longitudinal force P in the composite is

$$P = \sigma_f A_f + \sigma_m A_m \tag{6}$$

where A_f and A_m are the cross-sectional areas of the filament and matrix, respectively.

The equivalent major Young's modulus E_{11} of the composite is readily

*Damping is treated separately in Section III.

obtained from equations (5 and 6) as

$$E_{11} = P/(A\epsilon_1) = (E_f A_f + E_m A_m)/A \tag{7}$$

where

$$A = A_f + A_m \tag{8}$$

The volume fractions of fiber and matrix are defined as

$$V_f = A_f/A \ , \ V_m = A_m/A \tag{9}$$

In terms of the volume fractions V_f and V_m, the major Young's modulus E_{11} is written as

$$E_{11} = E_f V_f + E_m V_m \tag{10}$$

or

$$E_{11} = E_m + (E_f - E_m) V_f \tag{11}$$

since

$$V_m = 1 - V_f \tag{12}$$

Since $E_f > E_m$ in general, equation (11) shows that E_{11} varies linearly with respect to V_f from the matrix modulus (at $V_f \approx 0$) to the fiber modulus (at $V_f = 1$). For a monofilament composite with a square typical element,

the fiber volume fraction ranges between 0 and 0.785. Therefore, the values of E_{11}/E_m can vary between 1 and 94.4 for $E_f/E_m = 120$ (boron-epoxy).

Equation (11) is usually known as the simple law of mechanical mixtures or "law of mixtures" for brevity. This relationship is also valid for the cases where the filament material is transversely isotropic with the plane of isotropy coinciding with the cross section of the filament. The Young's modulus E_f in eq. (11) is then interpreted as the longitudinal Young's modulus of the fiber.

Since the interaction between the constituent materials, owing to the difference in their Poisson's ratios, is neglected completely in this simplied analysis, the major in-plane Young's modulus E_{11} calculated from eq. (11) is the lower bound as demonstrated by Hill (reference 47). However, the effects of the difference in the Poisson's ratios of the constituent materials have been shown theoretically to be minute (references 39, 47 and 48) and confirmed experimentally. Therefore, for all practical purposes eq. (11) may be deemed satisfactory for the prediction of E_{11}.

In-plane Longitudinal Shear Modulus G_{66}. - Consider one quarter of a typical repeating element of a monofilament composite as depicted in figure 3. The displacement field corresponding to the applied longitudinal shear loading is then assumed to be of the form

$$u = v = 0, \quad w = w(x,y) \tag{13}$$

with the corresponding stress components:

$$\tau^i_{xz} = G_i \partial w^i/\partial x , \quad \tau^i_{yz} = G_i \partial w^i/\partial y \quad (i=f,m) \tag{14}$$

Substitution of equation (14) into the equations of equilibrium yields the governing partial differential equations that must be satisfied in the fiber and matrix regions

$$G_i \left[(\partial^2 w^i / \partial x^2) + (\partial^2 w^i / \partial y^2) \right] = 0 \quad (i=f,m) \tag{15}$$

The boundary conditions depicted in figure 3 are

$$\left.\begin{aligned} & G_m \, \partial w^m / \partial y = 0 \quad \text{along } y = 0 \quad \text{and } y = \mu\delta r \\ & w^m = 0 \quad \text{along } x = 0 \\ & w^m = \tilde{w} \quad \text{along } x = \mu r \end{aligned}\right\} \tag{16}$$

In solving the problem posed by equations (15) and (16), the interfacial continuity conditions on the displacement and the shearing stress need to be considered. This leads to:

$$w^f = w^m \quad \text{on } C_1 \tag{17}$$

and,

$$G_f \, \partial w^f / \partial n = G_m \, \partial w^m / \partial n \text{ on } C_1 \tag{18}$$

where n signifies the outward normal to the boundary C_1. The boundary-value problem defined by eqs. (15-18) are then solved by the finite difference method (ref. 46), and the effective macroscopic shear modulus

of the composite is determined from

$$G_{66} = \tau_{xz}/(\bar{w}/\mu r) \tag{19}$$

Comparisons of the shear modulus predicted by eq. (19) to those obtained from other analyses (refs. 35 and 38) showed that equation (19) is in closer agreement with the experimental values (ref. 46).

2.3 Transverse In-plane Stiffnesses

Consider a typical repeating element subjected to a uniform tensile stress of magnitude σ_o in the y direction as depicted in figure 4(a). Because of symmetry about both coordinate axes, only one quarter of the repeating-element cross section needs to be considered, as shown in figure 4(b).

Assuming that a state of plane strain exists in the xy (or $\xi\eta$) plane and further that each constituent material is isotropic in this same plane (that is, the fibers can be transversely isotropic), one can formulate the problem in terms of the Airy stress function Φ (reference 49). This requires satisfaction of the following governing partial differential equation in the absence of body forces which vary nonlinearly with the spatial coordinates:

$$\nabla^4 \Phi^i = 0, \qquad \text{in } A_i \ (i=f,m) \tag{20}$$

where ∇^4 is the biharmonic operator, f denotes fiber, and m denotes matrix.

The general solutions of equation (20) in polar coordinates (ρ,θ)

are of the form (ref. 49):

$$\phi^f(\rho,\theta) = b_o^f \rho^2 + b_1^f \rho^3 \cos\theta + \sum_{n=2,3,\ldots}^{\infty} (a_n^f \rho^n + b_n^f \rho^{n+2}) \cos n\theta \quad (21)$$

$$\phi^m(\rho,\theta) = a_o^m \log\rho + b_o^m \rho^2 + b_1^m \rho^3 \cos\theta + a_1'^m \rho^{-1} \cos\theta + \sum_{n=2,3,\ldots}^{\infty} (a_n^m \rho^n + b_n^m \rho^{n+2} + a_n'^m \rho^{-n} + b_n'^m \rho^{-n+2}) \cos n\theta \quad (22)$$

Owing to the symmetry about the x-axis, only those series terms which are even functions with respect to θ are retained in equations (21 and 22). In the usual notations, stress, strain, and displacement components are related to the Airy stress function ϕ by*:

$$\left.\begin{aligned} \sigma_r &= \rho^{-1}(\partial\phi/\partial\rho) + \rho^{-2}(\partial^2\phi/\partial\theta^2) \\ \sigma_\theta &= \partial^2\phi/\partial\rho^2 \\ \tau_{r\theta} &= -\partial/\partial\rho\,(\rho^{-1}\,\partial\phi/\partial\theta) \end{aligned}\right\} \quad (23)$$

$$\left.\begin{aligned} \epsilon_r &= (1+\nu)\,E^{-1}[(1-\nu)\,\sigma_r - \nu\,\sigma_r] \\ \epsilon_\theta &= (1+\nu)\,E^{-1}[(1-\nu)\,\sigma_\theta - \nu\,\sigma_r] \end{aligned}\right\} \quad (24)$$

*The superscripts f and m which signify fiber and matrix regions, respectively are omitted from equations (23-27) for brevity.

$$\left.\begin{aligned}
\varepsilon_z &= E^{-1}[\sigma_z - \nu\,(\sigma_r + \sigma_\theta)] = 0 \\
\gamma_{r\theta} &= 2\,(1+\nu)\,E^{-1}\,\tau_{r\theta} \\
u_r/R &= (1+\nu)\,E^{-1}\int[(1-\nu)\,\sigma_r - \nu\,\sigma_\theta]\,d\rho \\
u_\theta/R &= (1+\nu)\,E^{-1}\int\rho[(1-\nu)\,\sigma_\theta - \nu\,\sigma_r]\,d\theta - \int u_r\,d\theta
\end{aligned}\right\} \quad (25)$$

where ν is the Poisson's ratio.

The rectangular components of stress and displacement components are then related to polar components of stresses and displacements by:

$$\left.\begin{aligned}
\sigma_x &= \sigma_r \cos^2\theta + \sigma_\theta \sin^2\theta - \tau_{r\theta} \sin 2\theta \\
\sigma_y &= \sigma_r \sin^2\theta + \sigma_\theta \cos^2\theta + \tau_{r\theta} \sin 2\theta \\
\tau_{xy} &= (1/2)(\sigma_r - \sigma_\theta) \sin 2\theta + \tau_{r\theta} \cos 2\theta
\end{aligned}\right\} \quad (26)$$

$$\left.\begin{aligned}
u &= u_r \cos\theta - u_\theta \sin\theta \\
v &= u_r \sin\theta + u_\theta \cos\theta
\end{aligned}\right\} \quad (27)$$

The unknown coefficients of the series solutions, namely, a_n^i, b_n^i, $a_n'^i$, $b_n'^i$ $(i = f,m)$, are then determined from the symmetry conditions and the boundary conditions depicted in figure 4(b), and those on C_1, the fiber-matrix interface.

From the symmetry of geometry and loading, it is apparent that the

coefficients of the odd terms in the series must vanish.

$$\left.\begin{aligned} & b_1^f = b_1^m = a_1'^m = 0 \\ & a_n^f = b_n^f = a_n^m = b_n^m = a_n'^m = b_n'^m = 0 \quad (n=\text{odd}) \end{aligned}\right\} \quad (28)$$

Also, in view of the interfacial continuity conditions, the following relationships must be satisfied.

$$u_r^f = u_r^m \,,\; u_\theta^f = u_\theta^m \,,\; \sigma_r^f = \sigma_r^m \,,\; \tau_{r\theta}^f = \tau_{r\theta}^m \qquad (29)$$

Thus, coefficients b_o^f, a_n^f, b_n^f, a_n^f, $a_n'^m$ may be expressed in terms of b_n^m and $b_n'^m$.

$$\left.\begin{aligned} & b_o^f = 2\,[\lambda(1-\nu_m)]\,[\lambda + (1-2\nu_f)]^{-1}\, b_o^m \\ & a_n^f = [-(n+1)\,\alpha\, b_n^m + \beta\, b_n'^m]/n \\ & b_n^f = \alpha\, b_n^m \\ & a_n^m = [-(n+1) b_n^m + \gamma\, b_n'^m\,]/n \\ & a_n'^m = [(1-\alpha) b_n^m - (n-1)\, b_n'^m\,]/n \end{aligned}\right\} \quad (30)$$

where

$$\left.\begin{aligned} & \lambda \equiv G_f/G_m \\ & \alpha \equiv \lambda(3-4\nu_m+1)/(3-4\nu_f+\lambda) \\ & \beta \equiv 4\lambda(1-\nu_m)/(\lambda-1) \end{aligned}\right\} \quad (31)$$

$$\gamma = [\lambda(3-4\nu_m) + 1]/(\lambda-1)$$

Finally, the remaining coefficients a_o^m, b_o^m, b_n^m, and $b_n'^m$ are so chosen that the boundary conditions on the external boundary are satisfied at a discrete set of points. (See Appendix A; also, references 50-52).

The macroscopic equivalent transverse in-plane properties may now be determined from the average of the displacements on the boundary. The plane-strain stress-strain relations of an equivalent homogeneous rectangular element that undergoes the same average deformation as the monofilament composite element are of the form (ref. 2),

$$\left.\begin{aligned} \bar{\epsilon}_x &= \bar{\sigma}_x/\bar{E}_x - \bar{\nu}_{yx}\bar{\sigma}_y/\bar{E}_y - \bar{\nu}_{zx}\,\bar{\sigma}_z/\bar{E}_z \quad \overrightarrow{xy} \\ \bar{\sigma}_z &= \bar{E}_z\,(\bar{\nu}_{xz}\bar{\sigma}_x/\bar{E}_x + \bar{\nu}_{yz}\bar{\sigma}_y/\bar{E}_y) \end{aligned}\right\} \quad (32)$$

where $\overrightarrow{xy}$ indicates that the same equation holds with the roles of x and y interchanged, and a superscript bar indicates the average stress, strain, and property values of the equivalent homogeneous orthotropic material. Also, because of symmetry of the stiffness coefficient matrix,

$$\bar{\nu}_{ij}\bar{E}_j = \bar{\nu}_{ji}\bar{E}_i \qquad (i,j = x,y,z, \quad i \neq j) \qquad (33)$$

For the case considered,

$$\bar{\sigma}_y = \sigma_o\,, \quad \bar{\sigma}_x = \bar{\epsilon}_z = 0 \qquad (34)$$

Substitution of equations (34) into the second and the third of equations

(32) yields two simultaneous equations for the determination of $\bar{E}_y$ and $\bar{\nu}_{yz}$.

$$\left.\begin{aligned} \bar{\epsilon}_y &= \sigma_o/\bar{E}_y - \bar{\nu}_{zy}\bar{\sigma}_z/\bar{E}_z \\ \bar{\sigma}_z &= \bar{\nu}_{yz}\,\sigma_o/\bar{E}_y \end{aligned}\right\} \quad (35)$$

From equation (35), the minor Young's modulus E_{22} and the major Poisson's ratio ν_{12} are determined as

$$\left.\begin{aligned} E_{22} &= \bar{E}_y = \bar{E}_z\,\sigma_o^2 \,/\, (\bar{E}_z\bar{\epsilon}_y\sigma_o+\bar{\sigma}_z^2) \\ \nu_{12} &= \bar{\nu}_{zy} = \bar{\sigma}_z/\sigma_o \end{aligned}\right\} \quad (36)$$

where,

$$\left.\begin{aligned} \bar{E}_z &= E_{11} = E_m + (E_f - E_m)\,V_f \\ \bar{\sigma}_z &= \int_{\frac{1}{4}(A_f+A_m)} \sigma_z\, d\xi\, d\eta \,/\, (\mu^2\delta)^2 \\ \bar{\epsilon}_y &= \partial\bar{v}/\partial y = \int_o^{\mu} [v]_{\eta=u\delta}\, d\xi \,/\, (\mu^2\delta r) \end{aligned}\right\} \quad (37)$$

Although the major Poisson's ratio ν_{12} may be obtained from the second of equations (36), many experimental and analytical results (references 28,41,48, and 53) show that the rule of mixtures may be used to predict ν_{12} with sufficient accuracy. In view of this, the following

simplified formula for ν_{12} instead of the latter of eqs. (36) will be used in Section 3.3 for the determination of the loss tangent associated with ν_{12}.

$$\nu_{12} = \nu_f V_f + \nu_m V_m \tag{38}$$

On the other hand, elementary model prediction (Reuss estimate) of the minor Young's modulus E_{22} results in the following expression

$$E_{22} = [(V_f/E_f) + (V_m/E_m)]^{-1} \tag{39}$$

which gives much lower values than those obtained experimentally. In fact, Hill (reference 54) and Paul (reference 55) showed that equation (39) gives the lower bound on the elastic modulus for a macroscopically isotropic composite. There are some mechanics-of-materials analyses (ref. 1) which predict greater values for E_{22} at low fiber volume fractions and smaller values for E_{22} at high fiber volume fractions. In contrast, the classical theory of elasticity approach (ref. 56) predicts a value of E_{22} which is consistently higher than the experimental values.

2.4 Longitudinal and Poisson Flexural Stiffnesses

As stated previously, for a monofilament composite layer, the longitudinal and Poisson flexural stiffness D_{11} and D_{12} cannot be calculated from the in-plane properties E_{11}, E_{22}, ν_{12} and ν_{21} due to the fact that the assumption of macroscopic homogeneity of the material in the thickness direction is no longer valid. Therefore, in this subsection

a relatively simple mechanics-of-materials analysis is used to obtain the effective flexural stiffnesses.

Longitudinal flexural stiffness D_{11}. - An element of a monofilament composite layer subjected to a pure bending moment is shown in figure 5. Owing to symmetry of the loading and geometry, only one quarter of the cross section needs to be considered for the analysis. As a first approximation, assume that the Bernoulli-Euler hypothesis holds throughout the cross section; then the strain distribution is given as

$$\epsilon = \alpha,_z y \tag{40}$$

where $\alpha,_z$ = longitudinal bending curvature, and z = distance from mid-plane.

Then, the longitudinal stress in the fiber and matrix are given by:

$$\sigma_f = E_f \alpha,_z y \ , \quad \sigma_m = E_m \alpha,_z y \tag{41}$$

The flexural strain energy in an elemental volume one unit long and having cross-sectional area $(a_f + a_m)$ is:

$$U_b = (1/2)\int_{a_f} (\sigma_f^2/E_f)\, da_f + (1/2)\int_{a_m} (\sigma_m^2/E_m)\, da_m$$

or

$$2U_b/\alpha,_z^2 = (E_f - E_m)\int_o^r y^2 \, (r^2 - y^2)^{\frac{1}{2}} dy + E_m \int_o^{\mu\delta r} \mu r y^2 \, dy$$

which integrates to give

$$U_b/\alpha_z^2 = (E_f-E_m)(\pi r^4/32) + E_m(\mu r)^4\delta^3/6 \qquad (42)$$

For an equivalent homogeneous orthotropic one-quarter section:

$$U_b/\alpha_z^2 = E_{11}^{(b)}(\mu r)^4\delta^3/6 \qquad (43)$$

where $E_{11}^{(b)}$ is the equivalent longitudinal Young's modulus for flexural loading.

Equating the right-hand sides of equations (42 and 43), and solving for $E_{11}^{(b)}/E_m$, one obtains

$$E_{11}^{(b)}/E_m = 1 + (\lambda'-1)(3\pi/16\mu^4\delta^3) \qquad (44)$$

where

$$\lambda' \equiv E_f/E_m \qquad (45)$$

Finally, the layer flexural stiffness is given by the equation

$$D_{11} = E_{11}^{(b)}/(1-\nu_{12}\nu_{21})\int_{-\mu\delta r}^{\mu\delta r} y^2 dy$$

or

$$D_{11} = E_{11}^{(b)}/(1-\nu_{12}\nu_{21})[2(\mu\delta r)^3/3] \qquad (46)$$

Recalling that the in-plane Young's modulus E_{11} is estimated from the law of mechanical mixtures (see Section 2.2):

$$E_{11}/E_m = 1 + (\lambda'-1)\ V_f = 1+(\lambda'-1)\pi/(4\mu^2\delta) \qquad (47)$$

the ratio $E_{11}^{(b)}/E_{11}$ is expressed as

$$E_{11}^{(b)}/E_{11} = [1+ (\lambda'-1)(3\pi/16\mu^4\delta^3)]/[1+(\lambda'-1)\pi/4\mu^2\delta] \qquad (48)$$

In general, λ', μ, and δ are greater than 1; thus, the ratio in equation (49) gives a value less than 1. This shows that for a monofilament composite, the longitudinal flexural stiffness D_{11} as estimated, eq. (4), by using the in-plane Young's modulus will be unconservative.

Poisson flexural stiffness. - Due to the nonuniform distribution through the thickness, the transverse Young's modulus E_{22} and the Poisson's ratios ν_{12} and ν_{21} are dependent locally on the thickness coordinate of the composite. To carry out the integration indicated in eq. (4), E_{22}, ν_{12}, and ν_{21} must be expressed explicitly in terms of the thickness coordinate. In the following analysis, a typical monofilament composite element is considered to be made from the thin dy strip depicted in figure 5(b). Thus, on assuming eqs. (38 and 39)* to hold for the estimates of E_{22} and ν_{12} of the elemental strip, one obtains the following expressions:

For $0 \le y \le r$, (or $0 \le \eta \le 1$)

$$E_{22}(\eta) = E_m\, \mu\lambda'/[\mu\lambda - (\lambda'-1)(1-\eta^2)^{\frac{1}{2}}]$$

* The Reuss estimate, eq. (39), gives excellent results for computing the effective transverse Young's modulus for a thin strip, fig. 5(b), consisting of discrete rectangular aggregates of constituent materials.

$$\left.\begin{aligned} \nu_{12}(\eta) &= [\mu\nu_m+(\nu_f-\nu_m)(1-\eta^2)^{\frac{1}{2}}]/\mu \\ E_{11}(\eta) &= E_m[\mu+(\lambda'-1)(1-\eta^2)^{\frac{1}{2}}]/\mu \end{aligned}\right\} \quad (49)$$

where λ' is the moduli ratio as defined in eq. (46) and η is the normalized thickness coordinate ($\eta \equiv y/r$).

In view of eqs. (49), the Poisson flexural stiffness for the monofilament composite element is calculated by the following equation:

$$D_{12}/D_{12}^m = \left\{ \int_0^1 F(\eta)\, d\eta + \nu_m[(\mu\delta)^3-1]/[3(1-\nu_m^2)] \right\} [3(1-\nu_m^2)/\nu_m]/(\mu\delta)^3 \quad (50)$$

where D_{12}^m is the Poisson flexural stiffness of a homogeneous element of the same size and consisting entirely of matrix material, and the function $F(\eta)$ is defined as follows:

$$\left.\begin{aligned} D_{12}^m &= (2/3)E_m(\mu\delta r)^3\nu_m/(1-\nu_m^2) \\ F(\eta) &= \eta^2[\nu_{12}(\eta)E_{22}(\eta)/E_m]/[1-\nu_{12}^2(\eta)E_{22}(\eta)/E_{11}(\eta)] \end{aligned}\right\} \quad (51)$$

2.5 Transverse Flexural Stiffness

The transverse flexural stiffness is obtained in a way similar to that discussed for transverse tension (Section 2.3). Here, two edges of a typical element are subjected to linearly varying stress distributions that are equivalent to pure bending moments. (See figures 6(a) and (b).)

In view of the antisymmetry condition, the Airy stress functions in polar coordinates are of the form

$$\Phi^f(\rho,\theta) = b_1^f\rho^3 \cos\theta + \sum_{n=3,5,\ldots}^{\infty} (a_n^f\rho^n + b_n^f\rho^{n+2}) \cos n\theta \quad (52)$$

$$\Phi^m(\rho,\theta) = b_1^m\rho^3 \cos\theta + a_1'^m \rho^{-1} \cos\theta$$

(Cont'd. on next page)

$$+ \sum_{n=1,3,\ldots}^{\infty} (a_n^m + b_n^m \rho^{n+2} + a_n'^m \rho^{-n} + b_n'^m \rho^{-n+2}) \cos n\theta \qquad (53)$$

Equations (52 and 53) satisfy the biharmonic equations, equations (20) (Section 2.3). In view of equations (29) (Section 2.3), that specify continuity of displacements and stresses at the fiber-matrix interface, those coefficients defining the series solutions may be readily interrelated as:

$$\left.\begin{aligned} a_n^f &= [-(n+1)\alpha\, b_n^m + \beta\, b_n'^m]/n \\ b_n^f &= \alpha\, b_n^m \\ a_n^m &= [-(n+1)\, b_n^m + \gamma\, b_n'^m]/n \\ a_n'^m &= [(1-\alpha) b_n^m - (n-1) b_n'^m]/n \end{aligned}\right\} \qquad (54)$$

where α, β, and γ are as defined previously in equations (31).

In view of equations (54), the matrix-region Airy stress function may be written as

$$\Phi^m(\rho,\theta) = b_1^m \rho^3 \cos\theta + a_1'^m \rho^{-1} \cos\theta + \sum_{n=1,3,\ldots}^{\infty} [F_n(\rho)\, b_n^m + F_n'(\rho) b_n'^m] \cos n\theta \qquad (55)$$

where

$$F_n(\rho) \equiv [-(n+1)\ \rho^n + n\rho^{n+2} + (1-\alpha)\ \rho^{-n+2}]/n$$

$$F_n'(\rho) \equiv [\gamma\rho^{-n} - (n-1)\rho^{-n} + n\rho^{-n+2}]/n$$

The coefficients b_1^m, $a_1'^m$, b_n^m, and $b_n'^m$ $(n=3,5,\ldots)$ are then determined from the boundary conditions depicted in figure 6(b):

$$\left.\begin{aligned} &\sigma_x = \tau_{xy} = 0 && \text{on } \xi = \mu \\ &\sigma_x = v = 0 && \text{on } \xi = 0 \\ &\tau_{xy} = v = 0 && \text{on } \eta = 0 \\ &\sigma_x = \sigma_o\xi/\mu,\ \tau_{xy}=0 && \text{on } \eta = \mu\delta \end{aligned}\right\} \quad (56)$$

Since the second and third of equations (56) are identically satisfied by equation (55), these coefficients are determined from the first and fourth of eqs. (56) in the sense of least square error at a discrete set of points on the outer boundary $\xi = \mu$ and $\eta = \mu\delta$ (see Appendix A).

The macroscopic equivalent flexural stiffness D_{22} of a typical element may now be calculated from the applied bending moment M, and average weighted curvature $\partial\bar{\phi}/\partial y$ on the $\eta = \mu\delta$ edge.

$$D_{22} = M/[\partial\bar{\phi}/\partial y]_{y=\mu\delta r} \quad (57)$$

where

$$M = 2\ (\mu r)^2\sigma_o/3$$

$$\bar{\varphi} = (2r^2/I) \int_0^{\mu} \xi\, [v]_{\eta=u\delta}\, d\xi$$

$$I = 2\mu^3 r^3/3 \qquad \Bigg\} \quad (58)$$

Finally, substitution of equation (58) into equation (57) yields the desired result:

$$D_{22} = (2\, \sigma_o \mu^5 r^4/9) \left\{ \int_0^{\mu} \xi\, [\partial v/\partial \eta]_{\eta=u\delta}\, d\xi \right\}^{-1} \qquad (59)$$

2.6 Twisting Stiffness

To determine the macroscopic equivalent twisting stiffness D_{66} of a one-layer monofilament composite, a rectangular cross section consisting of N repeating typical elements is considered. (See figure 7.) Because of the symmetry condition, only the quarter of the cross section, which lies in the first quadrant of the xy plane, needs to be considered.

In the usual notation, u,v, and w are the displacements; and α is the angle of twist per unit ξ-length. Then, for a small angle of twist α, we have (reference 57):

$$u = -\alpha yz, \quad v = \alpha xz, \quad w = \alpha \hat{\varphi}^{i}(x,y) \text{ in } R_i \quad (i=f,m)$$

where $\hat{\varphi}^{i}(x,y)$ are the z-component displacement functions to be determined from the equilibrium and boundary conditions. The strain and stress components are readily found to be:

$$\epsilon_x = \epsilon_y = \epsilon_z = \epsilon_{xy} = 0$$

$$\epsilon_{xz}^{i} = \tfrac{1}{2}\,\alpha\,[\partial\hat{\varphi}^{i}/\partial x) - y],\quad \epsilon_{yz}^{i} = \tfrac{1}{2}\,\alpha\,[(\partial\hat{\varphi}^{i}/\partial y) + x],\quad (i=f,m)$$

and

$$\left.\begin{aligned} &\sigma_x = \sigma_y = \sigma_z = \tau_{xy} = 0 \\ &\tau_{xz} = \alpha\, G_i[(\partial\hat{\varphi}^{i}/\partial x) - y]\ ,\ \tau_{yz} = \alpha\, G_i[(\partial\hat{\varphi}^{i}/\partial y) + x],\ (i=f,m) \end{aligned}\right\} \quad (60)$$

On application of the equations of equilibrium, one finds that the first and the second of these equations are identically satisfied and the third equation gives

$$\hat{\nabla}^2\,\hat{\Psi}^{i} = 0 \qquad \text{in } A_i\ (i = f,m) \quad (61)$$

where

$$\hat{\nabla}^2 = (\partial^2/\partial x^2) + (\partial^2/\partial y^2) \quad (62)$$

The stress equilibrium condition across the fiber-matrix interface C_1 requires the satifaction of

$$\lambda\,(d\hat{\varphi}^{f}/dn) = (d\hat{\varphi}^{m}/dn) + (\lambda-1)[y\,(dx/dn) - x(dy/dn)] \text{ on } C_1 \quad (63)$$

where n is the outward normal to the boundary C_1.

Displacement continuity requires that:

$$\hat{\varphi}^f = \hat{\varphi}^m \qquad \text{on } C_1 \tag{64}$$

or, equivalently,

$$d\hat{\varphi}^f/ds = d\hat{\varphi}^m/ds \qquad \text{on } C_1 \tag{65}$$

where s is the arc length along the boundary C_1. Similarly, on the vertical inter-element boundary C_2 (see figure 7),

$$[\partial\hat{\varphi}^m/\partial\xi]_j = [\partial\hat{\varphi}^m/\partial\xi]_{j+1} \text{ , and } [\partial\hat{\varphi}^m/\partial\eta]_j = [\partial\hat{\varphi}^m/\partial\eta]_{j+1} \text{ on } C_2 \tag{66}$$

where j and j+1 refer to the jth and (j+1)-th repeating elements. Finally, the stress-free condition on the outer boundary C_3 (see figure 7) leads to

$$d\hat{\varphi}^m/dn = [y\,(dx/dn) - x\,(dy/dn)] \quad \text{on } C_3 \tag{67}$$

The aforementioned torsion problem, equations (61-67), may also be formulated alternatively in terms of the complex conjugate $\hat{\Psi}^i$ that satisfies the Riemann-Cauchy equations

$$\partial\hat{\varphi}^i/\partial x = \partial\hat{\Psi}^i/\partial y \text{ , } \quad \partial\hat{\varphi}^i/\partial y = -\partial\hat{\Psi}^i/\partial x \tag{68}$$

It is readily shown, in view of equation (68), that the alternative formulation leads to:

$$\hat{\nabla}^2 \hat{\psi}^i = 0 \quad , \quad \text{in } R_i \ (i=f,m) \tag{69}$$

$$\lambda \hat{\psi}^f = \hat{\psi}^m + \tfrac{1}{2}(\lambda-1)(x^2+y^2) + \text{constant} \quad \text{on } C_1 \tag{70}$$

$$d\hat{\psi}^f/dn = d\hat{\psi}^m/dn \quad \text{on } C_1 \tag{71}$$

$$[\partial\hat{\psi}^m/\partial\eta,\ \partial\hat{\psi}^m/\partial\xi]_j = [\partial\hat{\psi}^m/\partial\eta,\ \partial\hat{\psi}^m/\partial\xi]_{j+1} \quad \text{on } C_2 \tag{72}$$

$$\hat{\psi}^m = (1/2)(x^2+y^2) + \text{constant} \quad \text{on } C_3 \tag{73}$$

For later convenience in numerical analysis, these equations are normalized by introducing the following notations:

$$\xi = x/r, \quad \eta = y/r, \quad \varphi = \hat{\varphi}/r^2, \quad \psi = \hat{\psi}/r^2, \quad \nabla^2 = (\partial^2/\partial\xi^2)+(\partial^2/\partial\eta^2) \tag{74}$$

Then, the governing differential equations and the boundary conditions become:

$$\nabla^2\psi^i=0 \ , \ \nabla^2\varphi^i=0 \quad \text{in } A_i \ (i = f,m) \tag{75}$$

$$\left.\begin{aligned} &\lambda\psi^f=\psi^m + \tfrac{1}{2}(\lambda-1)(\xi^2+\eta^2) \\ &\lambda\,(d\varphi^f/dn) = (d\varphi^m/dn) + (\lambda-1)\,[\eta\,(d\xi/dn) - \xi\,(d\eta/dn)] \\ &d\psi^f/dn=d\psi^m/dn \ , \ d\varphi^f/ds = d\varphi^m/ds \end{aligned}\right\} \text{on } C_1 \tag{76}$$

$$(\partial/\partial\xi \ , \ \partial/\partial\eta)[\psi^m,\varphi^m]_j = (\partial/\partial\xi, \ \partial/\partial\eta)\,[\psi^m,\varphi^m]_{j+1} \quad \text{on } C_2 \tag{77}$$

$$\left.\begin{aligned} \psi^m &= \tfrac{1}{2}\,(\xi^2 + \eta^2) \\ d\varphi^m/dn &= [\eta\,(d\xi/dn) - \xi\,(d\eta/dn)] \end{aligned}\right\} \text{ on } C_3 \qquad (78)$$

and the stress components are:

$$\left.\begin{aligned} \tau_{xz}{}^i &= \alpha\, G_i\, r\,[(\partial\varphi^i/\partial\xi) - \eta] = \alpha\, G_i\, r\,[(\partial\psi^i/\partial\eta) - \eta] \\ \tau_{yz}{}^i &= \alpha\, G_i\, r\,[(\partial\varphi^i/\partial\eta) + \xi] = -\alpha\, G_i\, r\,[(\partial\psi^i/\partial\xi) - \xi] \end{aligned}\right\} (i=f,m) \qquad (79)$$

The solution to the problem is obtained by assuming series solutions for each of the fiber and matrix regions in all N elements that satisfy the governing partial differential equation exactly in their respective regions. For example, in terms of polar coordinates with the origin at the center of the N-th fiber, the solution for the fiber and matrix regions takes the form:

$$\left.\begin{aligned} \psi^f_{(n)} &= a_o^{(n)} + \sum_{k=1,2,\ldots}^{\infty} a_k^{(n)}\, \rho_{(n)}^k \cos k\,\theta_{(n)} \\ \psi^m_{(n)} &= b_o^{(n)} + \sum_{k=1,2,\ldots}^{\infty} [b_k^{(n)} \rho_{(n)}^k + b_{-k}^{(n)} \rho_{(n)}^{-k}] \cos k\,\theta_{(n)} \end{aligned}\right\} \qquad (80)$$

It is interesting to note the fiber-region solution coefficients a_k may be readily expressed in terms of matrix-region solution coefficients b_k by the use of boundary conditions on C_1, equation (76).

$$
\left.
\begin{aligned}
a_o &= [b_o + (\lambda-1)(1+d^2)/2]/\lambda \\
a_1 &= 2\,b_1/(\lambda+1) + \lambda_1 d \\
a_k &= 2\,b_k/(\lambda+1) \quad (k=2,3,\ldots) \\
b_{-1} &= \lambda_1(b_1-d) \\
b_{-k} &= \lambda_1 b_k \quad (k=2,3,\ldots)
\end{aligned}
\right\} \quad (81)^*
$$

where

$$
\lambda_1 = (\lambda-1)/(\lambda+1) \quad , \quad d = 2(n-1)\,\mu \tag{82}
$$

In view of equations (81), only the coefficients b_k need to be determined from the boundary conditions on C_2 and C_3, namely, equations (77 and 78), since a_k and b_{-k} may be readily calculated from b_k by the use of (81). On writing b_{-k} in terms of b_k, one has

$$
\psi^m = b_o - (\lambda_1 d)\rho^{-1}\cos\theta + \sum_{k=1,2,\ldots}^{\infty} b_k(\rho^k+\lambda_1\rho^{-k})\cos k\theta \tag{83}
$$

The problem is now reduced to the determination of the coefficients b_k by the satisfaction of equations (77 and 78) at a discrete set of points on C_2 and C_3 in the sense of least square error (see Appendix A).

After determining b_k, one can calculate readily the stress components from equation (79). Finally the torsional stiffness D_{66} is obtained from

*Superscripts $^{(n)}$ are omitted here for brevity.

the following equation in a closed form. (See Appendix C for details.)

$$D_{66} = \iint_{A_f+A_m} (-y\,\tau_{xz} + x\,\tau_{yz})\,dx\,dy/\alpha$$

$$= 2\,r^4\,G_m \left\{ \lambda \iint_{A_f} [\Psi_f - \tfrac{1}{2}(\xi^2+\eta^2)]\,d\xi\,d\eta + \iint_{A_m} [\Psi_m - \tfrac{1}{2}(\xi^2+\eta^2)]\,d\xi\,d\eta \right\} \tag{84}$$

2.7 Longitudinal Thickness-Shear Stiffness

Owing to the presence of relatively flexible matrix material, the effect of thickness-shear deformation needs to be considered in the structural application of monofilament composite materials. As the thickness-shear stresses are not distributed uniformly across the cross section, the effective thickness-shear strain needs to be known for the calculation of effective thickness-shear stiffnesses. It is a commonly accepted practice to relate the effective shear strain to the average shear strain by means of a correction factor K which is usually referred to as the shear coefficient (reference 58).

$$K \equiv \gamma_{average}/\gamma_{effective} \tag{85}$$

Since the thickness-shear strain distribution is dependent on the shape of the cross section on which the thickness-shear stress acts, it is also referred to as shear shape factor.

In 1921, Timoshenko derived a theory of flexural beam vibration in which the effects of rotatory inertia as well as that of thickness shear

were taken into account (reference 59). The shear coefficient K was defined as the ratio between the average shear strain and that at the midplane. This yielded a value of 2/3 for a homogeneous, rectangular-section beam. However, this value of the shear coefficient gave poor agreement with experimental results. In view of this, numerous attempts were made to obtain a better value for K which would be in closer agreement with experimental results. Based on the high-frequency mode of beam vibration, Mindlin and Deresiewicz (reference 60) obtained a value of 0.822 for a rectangular cross section; whereas, based on the static mode, Roark (reference 61) gave a value of K of 5/6. Recently, Cowper (reference 62) used a different static approach to derive a formula for K which is in good agreement with those obtained by other investigators. This latter approach is deemed to be satisfactory for long-wavelength, low-frequency deformations such as those encountered in the vibration of monofilament composites.

Therefore, in this subsection, Cowper's analysis (ref. 62) is extended to the nonhomogeneous case consisting of a typical repeating element of a monofilament composite to obtain the effective thickness-shear strain. The thickness-shear stiffness, which is defined as the resultant shear force divided by the effective shear strain, can then be obtained as a direct consequence of the analysis.

First, the thickness-shear distribution is obtained from the analysis of a tip-loaded monofilament cantilever beam shown in figure 8(a).

Denoting the displacement components as u,v, and w, one defines the mean displacements of the cross section and mean angle of rotation of the cross section φ by the following equations:

$$\left.\begin{aligned} U &= (1/A) \iint_A u \, dx \, dy \\ W &= (1/A) \iint_A w \, dx \, dy \\ \bar{\varphi} &= (1/I_y) \iint_A xw \, dx \, dy \end{aligned}\right\} \quad (86)$$

where A denotes the entire cross-sectional area, and I_y is the moment of inertia of the cross-sectional area with respect to the y axis. Then the actual displacements of a point on the cross section are written as

$$u = U + \hat{u} \quad , \quad w = W + x\,\bar{\varphi} + \hat{w} \quad (87)$$

where $\hat{u}$ and $\hat{w}$ are the residual displacements which are equal to the deviations of the actual displacements from the weighted mean displacements. In view of the definitions, equations (86),

$$\iint_A \hat{u} \, dx \, dy = \iint_A \hat{w} \, dx \, dy = \iint_A x\hat{w} \, dx \, dy = 0 \quad (88)$$

The stress-strain relation

$$\tau_{xz}/G = u_{,z} + w_{,x} \quad (89)$$

where a comma represents partial differentiation with respect to the spatial variable that follows it, may now be written as

$$W_{,z} + \bar{\varphi} = (\tau_{xz}/G) - \hat{w}_{,x} - \hat{u}_{,z} \quad (90)$$

where the shear modulus G is to be interpreted as that of the fiber or matrix material depending on whether the material point is located in the fiber or the matrix region of the cross section. Finally, the integration of equation (90) yields the desired kinematic relations among the mean values of the midplane slope $W_{,z}$; flexural slope φ; and the effective shear strain γ_{eff}:

$$W_{,z} + \bar{\varphi} = (1/A) \iint_A [(\tau_{xz}/G) - \hat{w}_{,x}] \, dx \, dy = \gamma_{eff} \tag{91}$$

For a tip loading, the shear force Q is uniform along the entire length of the beam, hence, the first part of the integral in equation (91) is evaluated as

$$\iint_A (\tau_{xz}/G) \, dx \, dy = (Q_f/G_f) + (Q_m/G_m) \tag{92}$$

where Q_f and Q_m represent the respective shear forces that act on the fiber and matrix regions and are related to the total shear force Q by

$$Q = Q_f + Q_m \tag{93}$$

In view of eq. (87), the remaining term in the integral of eq. (91) is

$$\iint_A \hat{w}_{,x} \, dx \, dy = \iint_A (w_{,x} - \bar{\varphi}) \, dx \, dy \tag{94}$$

where $\bar{\varphi}$ is defined in the third of eqs. (86). Combining eqs. (91-94), one obtains the effective thickness-shear strain expression,

$$\gamma_{eff} = w,_z + \bar{\varphi} = (1/A)\ [(Q_f/G_f)+(Q_m/G_m)\ -\iint_A (w,_x - \bar{\varphi})\,dx\,dy] \qquad (95)$$

where $\bar{\varphi}$ and hence w, the displacement field, needs to be known in terms of the parameters defining the geometrical configuration and the constituent properties before the integration can be carried out. Assuming that the deformation of the cross section can be approximated by that of a tip-loaded cantilever, and allowing the constituent materials to be transversely isotropic with the plane of isotropy normal to the fiber axis, one can readily formulate the problem using the Saint-Venant semi-inverse method (refs. 57 and 63).

First, displacement components are assumed to be:

$$\left.\begin{aligned} u^i &= B\left[\tfrac{1}{2}\,\nu_i\,(\ell-z)\,(x^2-y^2) + \tfrac{1}{2}\,\ell\,z^2 - (1/6)\,z^3\right] \\ v^i &= B\,\nu_i\,(\ell-z)\,xy \qquad\qquad (i=f,m) \\ w^i &= -B\left\{x\,(\ell z - \tfrac{1}{2}\,z^2) + \hat{\chi}^i + \left[(E_i/G_i)-2\nu_i\right](\tfrac{1}{2}xy^2)\right\} \end{aligned}\right\} \qquad (96)$$

where B is a constant to be determined from the boundary conditions; E_i is the Young's modulus in the fiber direction; G_i is the shear modulus in the vertical plane parallel to the fiber axis; ν_i is to be interpreted as the Poisson's ratios $\nu_{31}=\nu_{32}$; and $\hat{\chi}^i = \hat{\chi}^i\,(x,y)$ $(i=f,m)$ are functions to be so chosen as to satisfy equilibrium conditions in their respective regions.

The stress components are readily calculated from equation (96) to be:

$$
\left.
\begin{aligned}
&\sigma_x^i = \sigma_y^i = \tau_{xy}^i = 0 \\
&\tau_{xz}^i = -BG_i \{ \hat{\chi}_{,x}^i + (1/2)\nu_i x^2 [(E_i/G_i) - 3\nu_i](\tfrac{1}{2}y^2) \} \\
&\qquad\qquad\qquad\qquad\qquad\qquad\qquad\qquad (i=f,m) \\
&\tau_{yz}^i = -BG_i \{ \hat{\chi}_{,y}^i + [(E_i/G_i) - \nu_i] xy \} \\
&\sigma_z^i = -BE_i (\ell - z) x
\end{aligned}
\right\} \qquad (97)
$$

If the constituent materials are isotropic, E_i, G_i, and ν_i respectively of the constituent materials are related by

$$E_i = 2(1+\nu_i) G_i \qquad (i=f,m) \qquad (98)$$

Substitution of the stress components in equations (97) into the equilibrium equation yields the following governing partial differential equations (Laplace's equations in two dimensions):

$$\hat{\nabla}^2 (\hat{\chi}^i) = 0 \qquad (i=f,m) \qquad (99)$$

which must be satisfied in the respective regions A_f and A_m.

Consideration of displacement continuity at the fiber-matrix interface C_1 requires that:

$$u^f = u^m, \; v^f = v^m, \; w^f = w^m \quad \text{on } C_1 \qquad (100)$$

Apparently, the first and the second of equations (100) cannot be satisfied unless the two Poisson's ratios are equal. However, the interaction

between the constituent materials due to the differences in the Poisson's ratios has only weak effects as evidenced by many theoretical analyses (refs. 39, 47, and 48). Hence, it will be assumed for the subsequent analysis that

$$\nu_f = \nu_m = \bar{\nu} \tag{101}$$

With this assumption, equation (101), the first two of equations (100) are identically satisfied and the third leads to

$$\hat{\chi}^f = \hat{\chi}^m \qquad \text{on } C_1 \tag{102}$$

Continuity of surface traction at the interface C_1 requires that

$$\tau^f_{xz}\,(dx/dn) + \tau^f_{yz}\,(dy/dn) = \tau^m_{xz}\,(dx/dn) + \tau^m_{yz}(dy/dn) \tag{103}$$

where n denotes the outward normal coordinate to C_1, hence, (dx/dn) and(dy/dn) are the direction cosines of the unit normal vector to the interface C_1.

In terms of the stress components defined in equations (97), the condition of equilibrium at the interface, equation (103), is cast readily in the following form:

$$G_f\,(d\hat{\chi}^f/dn) - G_m(d\,\hat{\chi}^m/dn)$$

$$= -(G_f - G_m)\left\{\left[\tfrac{1}{2}\,\bar{\nu}\,x^2 + (1-\tfrac{1}{2}\,\bar{\nu})\,y^2\right](dx/dn) + (2+\bar{\nu})\,xy\,(dy/dn)\right\}$$

$$\text{on } C_1 \tag{104}$$

The condition that the lateral surface is free from surface traction

leads to

$$(d\hat{\chi}^m/dn) = -\left\{[\tfrac{1}{2}\bar{\nu}\,x^2 + (1-\tfrac{1}{2}\bar{\nu})y^2](dx/dn) + (2+\bar{\nu})xy(dy/dn)\right\}$$

$$\text{on } C_2 \qquad (105)$$

The solutions to the problems posed by the governing differential equations (99) and the boundary conditions, eqs. (102,104,105) are now obtained by assuming a pair of series solutions which are harmonic in the respective fiber and matrix regions. The coefficients of these series solutions are determined so as to satisfy the boundary conditions in the least-square-error sense (see Appendix A, also Section 2.6.)

Since the solution procedure is very similar to that of Section 2.6, it will be high-lighted by listing those equations which are pertinent to the solution.

With the introduction of the following transformation,

$$\left.\begin{aligned} &\xi = x/r,\ \eta = y/r,\ \chi^i = \hat{\chi}^i/r^3 \quad (i=f,m) \\ &\nabla^2 = (\partial^2/\partial\xi^2) + (\partial^2/\partial\eta^2) \end{aligned}\right\} \qquad (106)$$

eqs. (99), 102, 104, and 105) are rewritten in the following form, which is convenient for numerical analysis:

$$\nabla^2 \chi^i = 0 \qquad \text{in } A_i \ (i = f,m) \qquad (107)$$

$$\chi^f = \chi^m \qquad \text{on } C_1 \qquad (108)$$

$$\lambda(d\chi^f/dn) - (d\chi^m/dn) = -(\lambda-1)\left\{[\tfrac{1}{2}\bar{\nu}\xi^2 + (1-\tfrac{1}{2}\bar{\nu})\eta^2](d\xi/dn)\right.$$

$$\left. + (2+\bar{\nu})\,\xi\eta\,(d\eta/dn)\right\} \qquad \text{on } C_1 \qquad (109)$$

$$(d\chi^m/dn) = -\left\{\left[\tfrac{1}{2}\,\bar{\nu}\,\xi^2 + (1-\tfrac{1}{2}\bar{\nu})\,\eta^2\right](d\xi/dn) + (2+\bar{\nu})\,\xi\,\eta\,(d\eta/dn)\right\} \qquad \text{on } C_2 \tag{110}$$

The series solutions, which are harmonic in the respective regions, are assumed to be:

$$\chi^f = a_o + \sum_{k=1}^{\infty} a_k \rho^k \cos k\theta$$

$$\chi^m = b_o + \sum_{k=1}^{\infty} (b_k \rho^k + b_{-k}\rho^{-k}) \cos k\theta \tag{111}$$

In view of eqs. (108 and 109), which warrant displacement continuity and stress equilibrium conditions, the coefficients a_o, a_k, and b_{-k} $(k = 1,2,\ldots)$ may be expressed in terms of b_k as:

$$a_o = b_o$$

$$a_k = 2\,b_k/(\lambda+1) - \lambda\,(3+2\bar{\nu})/4$$

Because of the anti-symmetry of the displacement component w with respect to the ξ axis, it may be shown readily that those coefficients with even subscripts are zero. The condition that the lateral surface is free from surface traction, eq. (110), takes the form:

$$\left.\begin{aligned}
&\sum_{k=1,3,\ldots}^{\infty} k\, b_k \left[\rho^{k-1} \cos (k-1)\,\theta + \lambda_1 \rho^{-k-1} \cos (k+1)\,\theta\right] \\
&\quad = -\frac{\lambda_1}{4}\left[(3+2\bar{\nu})\rho^{-2} \cos 2\theta - 3\rho^{-4} \cos 4\theta\right] \\
&\qquad - (\lambda-1)\left[\tfrac{1}{2}\bar{\nu}\,\xi^2 + (1-\tfrac{1}{2}\bar{\nu})\eta^2\right] \\
&\qquad\qquad (0 \le \theta \le \tan^{-1}\delta,\ \xi = \mu,\ 0 \le \eta \le \mu\delta) \\
&\sum_{k=1,3,5}^{\infty} k\, b_k \left[-\rho^{k-1} \sin (k-1)\,\theta + \lambda_1 \rho^{-k-1} \sin (k+1)\,\theta\right] \\
&\quad = -\frac{\lambda_1}{4}\left[(3+2\bar{\nu})\,\rho^{-2} \sin 2\theta - 3\rho^{-4} \sin 4\theta\right] \\
&\qquad - (\lambda-1)\,(2+\bar{\nu})\,\xi\,\eta \\
&\qquad\qquad (\tan^{-1}\delta \le \theta \le \pi/2,\ 0 \le \xi \le \mu,\ \eta = \mu\delta)
\end{aligned}\right\} \qquad (113)$$

Next the coefficients b_k ($k = 1,3,\ldots$) are obtained according to the boundary-point least-square method as described in Appendix A.

With the coefficients b_k thus obtained, the constant B which appears in eqs. (96 and 97) is calculated from the condition that the resultant shear force is equal to the externally applied tip load Q:

$$\iint_A \tau_{xz}\, dx\, dy = Q \qquad (114)$$

Since the stress components in eqs. (97) satisfy equations of equilibrium in the absence of body forces, the following relation must hold:

$$\tau^i_{zz,z} = BE_i\, x = -\tau^i_{zx,x} - \tau^i_{zy,y} \quad (i=f,m) \tag{115}$$

or

$$\tau^i_{zx,x} + \tau^i_{zy,y} + BE_i\, x = 0 \quad (i = f,m) \tag{116}$$

In view of eq. (116), eq. (114) may be written as

$$\begin{aligned} Q &= \sum_{i=f,m} \iint_{A_i} \tau^i_{xz}\, dx\, dy \\ &= \sum_{i=f,m} \iint_{A_i} [(x\,\tau^i_{zx})_{,x} + (y\,\tau^i_{zy})_{,y}]\, dx\, dy \\ &\quad + B \sum_{i=f,m} E_i \iint_{A_i} x^2\, dx\, dy \\ &= B \sum_{i=f,m} E_i \iint_{A_i} x^2\, dx\, dy \\ &= B\, I_E \end{aligned} \tag{117}$$

where A_f and A_m are the cross-sectional areas of the respective fiber and matrix regions and I_E is the weighted moment of inertia of the cross section. From eq. (117), the constant B is readily obtained as

$$B = Q/I_E \tag{118}$$

where

$$I_E \equiv \sum_{i=f,m} E_i \iint_{A_i} x^2 \, dx \, dy \tag{119}$$

Finally, the longitudinal thickness-shear flexibility S_{55} is obtained from eq. (95) as

$$S_{55} = [Q/(2\mu\delta r)]/\gamma_{eff}$$

$$= A \, I_E \left[\tfrac{1}{2}\bar{\nu} \, (I_x - I_y) - (A/I_y) \iint_A x \, (\hat{\chi}^i + xy^2) \, dx \, dy\right]^{-1} \tag{120}$$

For an equivalent homogeneous beam with a rectangular cross section, the longitudinal thickness-shear stiffness is given by

$$S_{55} = KA \, G_{55}/(2\mu\delta r) \tag{121}$$

where the shear coefficient K is obtained as (ref. 60)

$$K = 10 \, (1+\bar{\nu}) / (12+11\bar{\nu}) \tag{122}$$

Thus, on equating eqs. (120) and (121), one obtains the equivalent shear modulus G_{55} as

$$G_{55} = I_E \, (12+11\bar{\nu}) [10(1+\bar{\nu})]^{-1} \left[\tfrac{1}{2}\bar{\nu}(I_x - I_y) - (A/I_y) \iint_A x \, (\hat{\chi}^i + xy^2) \, dx \, dy\right]^{-1} \tag{123}$$

2.8 Transverse Thickness-Shear Stiffness

A typical repeating one-quarter cross section shown in figure 9 is considered. As a first approximation assuming that the Bernoulli-

Euler hypothesis holds, we make an elementary Jourawski-type mechanics-of-materials analysis to obtain the shear stress and strain distributions in the cross section due to the application of shear force Q_x along the vertical boundary of the cross section. (See figure 9(a).) Then the strain energy is calculated and Castigliano's principle is applied to obtain the macroscopic shearing strain γ_x. The transverse thickness-shear stiffness S_{44} is then obtained in terms of definite integrals arising from the strain energy calculations.

Assuming that the cross section remains plane, one obtains the flexural strain distribution as

$$\epsilon_x = - \alpha,_x \, y \tag{124}$$

where ϵ_x denotes the flexural strain of an element located at a distance y from the midplane, and $\alpha,_x$ denotes the bending curvature of the midplane. The corresponding stress distribution is

$$\sigma_x^{\,i} = - \alpha,_x \, y \, E_i \qquad (i=f,m) \tag{125}$$

Summing the moment due to the stress distribution, one finds that the flexural moment acting on the cross section is

$$M_x = \begin{cases} (2/3)\, E_m (\mu\delta r)^3 [1+(\lambda'-1)(\mu\delta)^{-3}(1-\xi^2)^{3/2}]\alpha,_x & 0 \le \xi \le 1 \\ (2/3)\, E_m (\mu\delta r)^3 \, \alpha,_x & 1 < \xi \le \mu \end{cases} \tag{126}$$

where

$$\lambda' \equiv E_f/E_m \quad , \quad \xi \equiv x/r \tag{127}$$

From equation (126), the flexural stiffness of a strip Δx in width is found to be

$$D_{22} = \begin{cases} (2/3)\ E_m(\mu\delta r)^3\ [1+(\lambda'-1)(\mu\delta)^{-3}(1-\xi^2)^{3/2}] & 0\le\xi\le 1 \\ (2/3)\ E_m(\mu\delta r)^3 & 1\le\xi\le\mu \end{cases} \tag{128}$$

In view of equations (125-128), the flexural stress distribution is now given by the expression:

$$\sigma_x^{\ i} = -\ (M_x/D_{22})\ y\ E_i \qquad (i=f,m) \tag{129}$$

The thickness-shear distribution τ_{xy} is then obtained readily from the equilibrium of the forces acting on the strip. (See figure 9(b).)

$$-\int_y^{\mu\delta r} [\sigma_x^{\ i}]_x\ dy + \int_y^{\mu\delta r} [\alpha_x^{\ i}]_{x+\Delta x} dy = \tau_{xy}\ \Delta x \tag{130}$$

Solving for τ_{xy} in equation (130) and using equation (126), one obtains

$$\tau_{xy} = (\Delta\ M_x/\Delta x)\ D_{22}^{-1} \int_y^{\mu\delta r} E_i\ y\ dy \tag{131}$$

where

$$\Delta\ M_x \equiv [M_x]_{x+\Delta x} - [M_x]_x \tag{132}$$

Since the shear force $Q_x = \Delta\ M_x/\Delta x$ and the integral on the right-hand side of equation (131) can be evaluated, the thickness-shear

distribution is given by:

For $0 \le x \le r$

$$\tau_{xy} = G_f \gamma_{xy}$$

$$= \begin{cases} (Q_x/2D_x) E_m r^2 [(\lambda'-1)(1-\xi^2) - \lambda' \eta^2 + (\mu\delta)^2] & 0 \le y \le (r^2-y^2)^{\frac{1}{2}} \\ (Q_x/2D_x)\ E_m r^2\ [(\mu\delta)^2 - \eta^2)]; & (r^2-y^2)^{\frac{1}{2}} \le y \le \mu\delta e \end{cases} \quad (133)$$

and, for $r \le x \le \mu r$

$$\tau_{xy} = G_m \gamma_{xy} = (Q_x/2\,D_x)\ \ E_m\ r^2 [(\mu\delta)^2 - \eta^2]; \quad 0 \le y \le \mu\delta r \quad (134)$$

In view of equations (133 and 134), that part of the strain energy per unit z-length due to shearing stresses is readily calculated.

$$U_s = (1/2) \int\int_{A_f + A_m} \tau_{xy} \gamma_{xy}\, dx\, dy$$

$$= [3Q_x^2/(5G_m\mu\delta)](\mu-1) + (9Q_x^2/8\,G_f) F_1 + (9Q_x^2/8G_m) F_2 \quad (135)$$

where

$$F_1 = \int_o^1 \Big\{ [(\lambda'-1)(1-\eta^2) + (\mu\delta)^2]^2 (1-\eta^2)^{\frac{1}{2}}$$

$$- (2/3)[(\lambda'-1)(1-\eta^2) + (\mu\delta)^2] \lambda' (1-\eta^2)^{3/2}$$

$$+ (\lambda'^2/5)(1-\eta^2)^{5/2} \Big\} \cdot [(\mu\delta)^3 + (\lambda'-1)(1-\eta^2)^{3/2}]^{-2}\, d\eta \quad (136)$$

$$F_2 = \int_o^1 \Big\{ (8/15)(\mu\delta)^5 - (1-\eta^2)^{\frac{1}{2}} [(\mu\delta)^4 - (2/3)(\mu\delta)^2 (1-\eta^2) + (1/5)(1-\eta^2)^2] \Big\} \cdot$$

$$\cdot\left[(\mu\delta)^3 + (\lambda'-1)(1-\eta^2)^{3/2}\right]^{-2}\, d\eta \qquad (137)$$

Using Castigliano's theorem, one can compute the mean macroscopic shearing strain $\bar{\gamma}_{xy}$ from equation (135) as

$$\gamma_{xy} = (\partial U_s/\partial Q_x)(\mu r)^{-1}$$

$$= (3Q_x/2\mu r)\left\{[2/(5\, G_m \mu\delta)](\mu-1)+(3/4)G_f^{-1}F_1+(3/4)G_m^{-1}F_2\right\} \qquad (138)$$

The average transverse thickness-shear stiffness S_{44} is given by

$$S_{44} = Q_x/\bar{\gamma}_{xy} = KAG_{44}$$

$$= (2\mu r\, G_m/3)\left[(2/5)(\mu-1)/(\mu\delta) + (3/4)(F_1\lambda^{-1}+F_2)\right]^{-1} \qquad (139)$$

where

$$\lambda = G_f/G_m \qquad (140)$$

For a homogeneous rectangular corss section, Cowper's shear factor K is given by eq. (122). Thus, the equivalent transverse thickness-shear modulus G_{44} is given by

$$G_{44} = S_{44}/(2\mu\delta r\, K) \qquad (141)$$

SECTION III

DAMPING ANALYSES

This section is concerned with the analyses leading toward the characterization of dynamic properties of a single layer of monofilament composites. Many solids, whether they are metallic or otherwise, exhibit a damping effect ; this phenomenon is essentially due to the dissipation of energy associated with the deformation. It is convenient, especially in the case of steady-state vibrational analysis, to represent the dynamic properties of the solid by the use of complex dynamic moduli. For example, the major Young's modulus E_{11} may be considered to be of the form

$$E_{11} = E_{11}^{R} + i\, E_{11}^{I} \tag{142}$$

where $i \equiv \sqrt{-1}$, E_{11}^{R} is the storage modulus and E_{11}^{I} is the loss modulus, since the latter is associated with that component of the strain 90^{o} out of phase from the stress component which gives rise to the energy dissipation (reference 64). Alternatively, equation (142) may also be written as

$$E_{11} = E_{11}^{R}(1+ig_{E_{11}}) \tag{143}$$

where $g_{E_{11}}$ is referred to as the loss tangent which is related to the storage and loss moduli by the equation,

$$g_{E_{11}} = (E_{11}^{I}/E_{11}^{R}) = \tan \gamma \qquad (144)$$

Here the term, γ, is the phase angle by which the sinusoidally varying strain component lags behind the accompanying stress component on the phase plane, and is referred to as the loss angle. (See Figure 10.)

In the following subsections, detailed analyses based on the results of Section II are made to obtain the loss tangents associated with all the stiffnesses necessary for the characterizing of the damping properties of a single layer of monofilament composite.

3.1 Introduction

As previously discussed in Section 1.1, one of the main advantages that composite materials have over conventional homogeneous materials is their macroscopic anisotropic nature which gives the modern structural designer the ability to design stiffness and damping properties and strengths to fit the requirements of the application by means of lamination. In the dynamic analysis of a structure consisting of multiple layers of composites, as in the case of elastic characteristics, damping characteristics of a single layer must be known beforehand in order to predict the dynamic behavior of the laminated structure.

There have been numerous experimental investigations on damping characteristics of sandwich and filamentary composite materials (ref. 8-19). Analytically, Hashin (ref. 20-21) derived a correspondence principle for the determination of complex moduli of viscoelastic composites (particulate and filamentary). This correspondence principle is particularly suitable when the elastic moduli are of a form explicit in terms of the moduli of the constituent materials. However, Hashin's approach cannot be applied to cases where the moduli are given in terms of numerical elastic results.

Kimball and Lovell (ref. 22) observed that many engineering materials undergoing sinusoidal motion exhibited energy losses which were proportional to the square of the amplitude and independent of the frequency. Bert et al. (ref. 13), in their investigation of damping in sandwich beams, assumed Kimball-Lovell type damping for the facing and core materials and obtained good agreements between the theoretically-calculated and experimentally-obtained values of the logarithmic decrement for free vibration.

It is noted that the ratio of the total damping energy dissipated per cycle U_d to the total potential energy stored per cycle U can be related to the logarithmic decrement δ as follows (reference 65):

$$\delta = (1/2)\ \ln[1-(U_d/U)] \tag{145}$$

For most structural materials, where the logarithmic decrement is small, it may be approximated by

$$\delta = (1/2)(U_d/U) \tag{146}$$

In turn, the loss tangent g may be related to δ by (See Appendix B for details.)

$$g = (1/2\pi)(U_d/U) \tag{147}$$

The total potential and dissipative energy per cycle of a solid undergoing sinusoidal motion are given by *

$$U = \frac{1}{2}\iiint_V \sigma_{ij}\epsilon_{ij}\,dV \tag{148}$$

$$U_d = C_d\iiint_V \sigma_{ij}\sigma_{ij}\,dV \tag{149}$$

*Repeated subscripts denote summation where i,j = 1,2,3.

where σ_{ij} and ϵ_{ij} denote respective stress and strain amplitudes, C_d the damping coefficient, and V the total volume (fiber and matrix) occupied by the composite.

In performing the integration indicated in equations (148 and 149), the stress distributions are approximated by those obtained from the elastic analyses of Section II. Inherently, the stress distributions are dependent on the excitation frequency; however, for the frequency range of interest here (well below any micro-scale resonance), the stress distributions obtained from the elastic analyses of Section II are expected to be valid.

For the monofilament composite element under consideration here, with the exceptions of in-plane longitudinal shear modulus G_{66} and the Poisson's ratio ν_{12}, the following general procedure is adopted for the calculation of loss tangent of the composite element:

1. First, with the composite element subjected to an appropriate loading*, the strain energy is calculated for the respective fiber and matrix regions (U^f and U^m).

2. In view of equation (147), the damping energies for the respective fiber and matrix regions are obtained as follows:

$$U_d^i = 2\pi\, g_i\, U^i \qquad (i=f,m) \tag{150}$$

*By an appropriate loading, we mean the type of loading which is appropriate for the property under consideration, i.e., longitudinal tension for E_{11}, etc.

3. Then, the composite loss tangent associated with the property under consideration is computed as

$$g = (1/2\pi) \sum_i U_d^i / \sum_i U^i \quad (i=f,m) \tag{151}$$

The determinations of the real parts of the complex moduli; namely, the storage moduli; are carried out in an analogous manner to that of Section II by simply replacing the elastic property parameters with their respective counterparts in the complex moduli.

As for the determinations of the loss tangents for the in-plane longitudinal shear modulus G_{66} and the Poisson's ratio ν_{12}, Hashin's correspondence principle is used. The equivalence of the correspondence principle and the general procedure described above is substantiated analytically for the case of the longitudinal Young's modulus E_{11} and numerically for the case of the transverse Young's modulus E_{22}.

In the subsections that follow, detailed analyses are carried out for the loss tangents corresponding to all of the stiffnesses characterizing the composite properties.

3.2 Longitudinal In-plane Loss Tangents

Two loss tangents, namely $g_{E_{11}}$ and $g_{G_{66}}$, will be obtained in this subsection. As previously discussed in Section 2.2, the major Young's modulus E_{11} is obtained explicitly from the law of mixtures, whereas the longitudinal in-plane shear modulus G_{66} is based on the results of the elasticity analysis of Adams and Doner (ref. 46).

Loss tangent $g_{E_{11}}$ associated with the Major Young's modulus E_{11}. -

In terms of the notations used in Section 2.2, the total strain energy per cycle in the respective fiber and matrix regions are calculated as follows:

$$U^f = (1/2) \iint_{A_f} \sigma_f \epsilon_1 \, dx \, dy = (1/2) \, A_f \sigma_f \epsilon_1$$

$$U^m = (1/2) \iint_{A_m} \sigma_m \epsilon_1 \, dx \, dy = (1/2) \, A_m \sigma_m \epsilon_1 \qquad (152)$$

In view of equations (152 and 150), the total strain energy per cycle in the composite and the damping energy per cycle are readily calculated as follows:

$$U = U^f + U^m = \tfrac{1}{2} (A_f \sigma_f + A_m \sigma_m) \epsilon_1 \qquad (153)$$

$$U_d = U_d^{\,f} + U_d^m = \pi \, (g_f A_f \sigma_f + g_m A_m \sigma_n) \epsilon_1 \qquad (154)$$

where g_f and g_m are the loss tangents associated with the longitudinal Young's moduli of the fiber and matrix materials. The composite loss tangent $g_{E_{11}}$ associated with the major Young's modulus E_{11} is now readily calculated on substituting equations (153 and 154) into equation (151).

$$g_{E_{11}} = (g_f A_f \sigma_f + g_m A_m \sigma_m) / (\sigma_f A_f + \sigma_m A_m) \qquad (155)$$

In view of equations (5 and 9), equation (155) may be written in terms of volume fractions V_f and V_m and λ' as follows:

$$g_{E_{11}} = (\lambda' V_f g_f + V_m g_m)/(\lambda' V_f + V_m) \tag{156}$$

where

$$\lambda' = E_f^R/E_m^R \tag{157}$$

The composite storage modulus E_{11}^R is obtained from eq. (10) as

$$E_{11}^R = V_f E_f^R + V_m E_m^R \tag{158}$$

It is interesting to note that identical results for the storage modulus and the loss tangent can also be obtained on utilizing the elastic-viscoelastic correspondence principle of ref. 21. Replacing the elastic moduli in the right-hand side of eq. (10) with the corresponding complex moduli, and separating the real and the imaginary parts, one obtains

$$E_{11} = (V_f E_f^R + V_m E_m^R)[1 + i\,(g_f V_f E_f^R + g_m V_m E_m^R)/(V_f E_f^R + V_m E_m^R)] \tag{159}$$

from which equations (156 and 158) readily follow. This substantiates the equivalence of the correspondence principle and the formula (151).

Loss tangent $g_{G_{66}}$ associated with the in-plane longitudinal shear modulus G_{66}. - As mentioned previously, the storage modulus G_{66}^R is approximated by the elastic analysis of Adams and Doner (ref. 46). To calculate the loss tangent $g_{G_{66}}$ according to eq. (151) would require

lengthy numerical analyses for the determinations of the stress and strain distributions. To avoid this, it is surmised here that the results of ref. 47 may be empirically approximated by a much simpler formula due to Hashin and Rosen (ref. 35), which is given here in modified form as follows:

$$G_{66}/G_m = C_{V_f} \left[\lambda(1+V_f)+(1-V_f)\right]/\left[\lambda(1-V_f)+(1+V_f)\right] \tag{160}$$

where C_{V_f} is an empirical factor brought in here so that the shear modulus as calculated by equation (160) coincides with that given in ref. 46, λ is the fiber and matrix shear-moduli ratio defined in eq. (31), and V_f is the fiber volume fraction.

In view of the explicit expression of eq. (160), the loss tangent $g_{G_{66}}$ is readily obtained on replacing λ by its complex counterpart.

$$\lambda = \lambda^R (1 + i g_\lambda) \tag{161}$$

where

$$\left.\begin{aligned} \lambda^R &= (G_f^R/G_m^R)\ (1+g_{G_f}\ g_{G_m})/(1+g_{G_m}{}^2) \\ g_\lambda &= (g_{G_f} - g_{G_m})\ /\ (1+g_{G_f}\ g_{G_m}) \end{aligned}\right\} \tag{162}$$

Substitution of equations (161 and 162) into eq. (160) yields:

$$G_{66}^R/G_m^R = C_{V_f}\left\{(1-V_f^2)[\lambda^{R^2}(1-g_\lambda^2)+1] + 2\lambda^R(1+V_f^2) - 4\lambda^R g_\lambda g_{G_m} V_f\right\} \cdot$$

$$\cdot\left\{[\lambda^R(1-V_f)+(1+V_f)]^2 + [\lambda^R(1-V_f)g_\lambda]^2\right\}^{-1} \qquad (163)$$

$$g_{G_{66}} = \left\{g_{G_m}[(1-V_f^2)[\lambda^{R^2}(1-g_\lambda^2)+1] + 2\lambda^R(1+V_f^2)] + 4\lambda^R g_\lambda V_f\right\} \cdot$$

$$\cdot\left\{(1-V_f^2)[\lambda^{R^2}(1-g_\lambda^2)+1]+2\lambda^R(1+V_f^2)-4\lambda^R g_\lambda g_{G_m} V_f\right\}^{-1} \qquad (164)$$

3.3 Transverse In-plane Loss Tangents

Based on the result of elastic analysis and the observation made in section 2.3, two loss tangents $g_{E_{22}}$ and $g_{\nu_{12}}$ associated with the in-plane transverse Young's modulus E_{22} and the major Poisson's ratio ν_{12} will be obtained as follows.

Loss tangent $g_{E_{22}}$ associated with the transverse in-plane Young's modulus. - Owing to symmetry in the loading depicted in fig. 4, shear stresses τ_{xz} and τ_{yz} vanish. Hence, the total strain energies per cycle for the fiber and the matrix regions, respectively, are:

$$U^i = [1/(4G_i)]\iint_{A_i}[(1-\nu_i)(\sigma_x^2+\sigma_y^2) - 2\nu_i\sigma_x\sigma_y + 2\tau_{xy}^2]dx\,dy \qquad (i = f,m) \qquad (165)$$

where the stress components $\sigma_x, \sigma_y, \tau_{xy}$ are given by the equations (C-4, 5, and 6). In view of equations (150 and 165), the damping energies per cycle are:

$$U_d^i = (\pi g_i / 2G_i) \iint_{A_i} [(1-\nu_i)(\sigma_x^2+\sigma_y^2) - 2\nu_i \sigma_x \sigma_y + 2\tau_{xy}^2] dx\, dy \quad (i=f,m) \quad (166)$$

The loss tangent $g_{E_{22}}$ is then readily calculated from eq. (151).

The storage modulus E_{22}^R is calculated from the first of equations (36) by means of appropriate storage moduli of the constituent materials corresponding to the particular frequency of excitation.

Loss tangent $g_{\nu_{12}}$ associated with the in-plane major Poisson's ratio. - Since the in-plane major Poisson's ratio ν_{12} is related to the constituent Poisson's ratios ν_m and ν_f by a simple law-of-mechanical-mixture formula, eq. (38), the complex Poisson's ratio ν_{12} is readily obtained in a manner similar to that used for E_{11}, eq. (159), by the use of Hashin's correspondence principle as follows:

$$\nu_{12} = (V_f \nu_f^R + V_m \nu_m^R)([1+i(g_{\nu_f} V_f \nu_f^R + g_{\nu_m} V_m \nu_m^R)/(V_f \nu_f^R + V_m \nu_m^R)] \quad (167)$$

where

$$\left.\begin{aligned} \nu_{12}^R &= V_f \nu_f^R + V_m \nu_m^R \\ g_{\nu_{12}} &= (g_{\nu_f} V_f \nu_f^R + g_{\nu_m} V_m \nu_m^R)/(V_f \nu_f^R + V_m \nu_m^R) \end{aligned}\right\} \quad (168)$$

3.4 Longitudinal Flexural Loss Tangents

In this subsection are treated damping analyses for determining

the loss tangents $g_{D_{11}}$ and $g_{D_{12}}$ associated with the longitudinal and Poisson flexural stiffnesses. The former is obtained according to eq. (151), whereas the latter is obtained by the application of Hashin's correspondence principle.

Loss tangent $g_{D_{11}}$ associated with the longitudinal flexural stiffness. - In view of eq. (42) derived previously in Section 2.4, the strain energies per cycle in the fiber and matrix regions are readily obtained as follows:

$$U^f = \alpha_z^2 E_f^R \pi r^4/32$$
$$U^m = \alpha_z^2 E_m^R \left\{[\delta^3(\mu r)^4/6] - (\pi r^4/32)\right\} \tag{169}$$

Using eqs. (150 and 151), one can readily obtain the following expression for the longitudinal flexural stiffness:

$$g_{D_{11}} = \left\{[(\lambda' g_f - g_m)\pi/32] + (g_m \delta^3 \mu^4/6)\right\} \cdot \left\{[(\lambda'-1)(\pi/32) + (\delta^3\mu^4/6)\right\}^{-1} \tag{170}$$

The storage stiffness D_{11}^R is readily calculated from eq. (46) with the help of eq. (44) by replacing the static moduli and the Poisson's ratios with their respective real parts of the corresponding complex moduli and ratios.

Loss tangent $g_{D_{12}}$ associated with the Poisson flexural stiffness. - According to Hashin's correspondence principle, the complex Poisson flexural stiffness D_{12} may be calculated from equation (50) by replacing

the elastic moduli and Poisson's ratios appearing on the right-hand side of the equation with their respective complex moduli and Poisson's ratios as follows:

$$D_{12} = D_{12}^R (1+i\, g_{D_{12}})$$

$$= 2\, r^3\, E_m^R (1+i\, g_{E_m}) \left\{ \int_o^1 [F^R(\eta) + i\, F^I(\eta)]\, d\eta \right.$$

$$\left. + (1/3)[(\mu\delta)^3 - 1]\nu_m^R (1+i\, g_{\nu_m}) / [1-\nu_m^{R^2} (1+i\, g_{\nu_m})^2] \right\} \qquad (171)$$

where $F^R(\eta)$ and $F^I(\eta)$ are the real and imaginary parts of the function $F(\eta)$ defined in equation (51). Separating the real and imaginary parts on the right-hand side of equation (171), one readily obtains:

$$D_{12}^R = 2\, E_m^R\, r^3 \left\{ \int_o^1 [F^R(\eta) - g_{E_m} F^I(\eta)]\, d\eta + (1/3)[(\mu\delta)^3 - 1]\nu_m^R\, \Lambda^R \right\} \qquad (172)$$

$$D_{12}^I = 2\, E_m^R\, r^3 \left\{ \int_o^1 [g_{E_m} F^R(\eta) + F^I(\eta)]\, d\eta + (1/3)[(\mu\delta)^3 - 1]\nu_m^R\, \Lambda^I \right\} \qquad (173)$$

where

$$\left.\begin{aligned} \Lambda &= (1+i\, g_{E_m})(1+i\, g_{\nu_m}) / [1-\nu_m^{R^2} (1+i\, g_{\nu_m})^2] \\ \Lambda^R &= \text{Real}\,(\Lambda) \\ &= \left\{ (1-g_{E_m} g_{\nu_m}) - (1+g_{E_m} g_{\nu_m})\, \nu_m^{R^2} (1+g_{\nu_m}^2) \right\} / \Lambda_\Delta \\ \Lambda^I &= \text{Imaginary}\,(\Lambda) \\ &= \left\{ (g_{E_m} + g_{\nu_m}) + (g_{\nu_m} - g_{E_m})\, \nu_m^{R^2} (1+g_{\nu_m}^2) \right\} / \Lambda_\Delta \end{aligned}\right\} \qquad (174)$$

$$\Lambda_{\Delta} = [1-\nu_m^{R^2}(1-g_{\nu_m}^2)]^2 + [2\,\nu_m^{R^2}\,g_{\nu_m}]^2$$

The loss tangent $g_{D_{12}}$ can now be calculated from eqs. (172-173) to yield:

$$g_{D_{12}} = D_{12}^I / D_{12}^R$$

or

$$g_{D_{12}} = \left\{ \int_o^1 [g_{E_m} F^R(\eta) + F^I(\eta)]d\eta + (1/3)[(\mu\delta)^3 - 1]\nu_m^R \Lambda^I \right\}$$
$$\cdot \left\{ \int_o^1 [F^R(\eta) - g_{E_m} F^I(\eta)]d\eta + (1/3)[(\mu\delta)^3 - 1]\nu_m^R \Lambda^R \right\} \qquad (175)$$

3.5 Transverse Flexural Loss Tangent

Owing to antisymmetry in loading with respect to the η axis as depicted in fig. 6, shear stresses τ_{yz} again vanish as for the case of the transverse in-plane Young's modulus E_{22}, Section 3.3. Therefore, the total strain energy and damping energies per cycle are given by the eqs. (165 and 166). The loss tangent $g_{D_{22}}$ and the storage stiffness D_{22}^R are obtained by a procedure similar to that described in the first subsection of Section 3.3.

3.6 Twisting Loss Tangent

For a composite layer subjected to a pure twisting torque, all the stress components except τ_{xz} and τ_{yz} vanish. Thus, the strain energy and the damping energy per cycle in the fiber and matrix regions, respectively, are calculated from the following formulas:

$$U^i = \iint_{A_i} (\tau_{xz}^2 + \tau_{yz}^2)\, dx\, dy \,/\, (2\, G_i) \qquad (i=f,m) \qquad (176)$$

$$U_d^i = 2\pi\, g_{G_i}\, U_i \qquad (i=f,m) \qquad (177)$$

where the shear stress components τ_{xz} and τ_{yz} are as given by eqs. (C-19 through C-22) for each typical composite element depicted in fig. 7. With the strain energies and damping energies calculated from eqs. (176 and 177), the loss tangent $g_{D_{66}}$ associated with the twisting stiffness D_{66} is obtained readily from eq. (151).

3.7 Longitudinal Thickness-Shear Loss Tangent

In view of eqs. (97), the strain energies per cycle for the fiber and matrix regions are:

$$U^i = \iint_{A_i} (\tau_{xz}^2+\tau_{yz}^2)dx\, dy/(2\, G_i) + \iint_{A_i} \sigma_z^2\, dx\, dy/(2\, E_i) \qquad (i=f,m) \qquad (178)$$

where the strain components are as given by eqs. (97). According to eq. (147), the damping energies per cycle in the respective fiber and matrix regions are therefore equal to:

$$U_d^i = 2\pi\, g_{G_i} \iint_{A_i} (\tau_{xz}^2+\tau_{yz}^2)dx\, dy/(2\, G_i)$$

$$+ 2\pi\, g_{E_i} \iint_{A_i} \sigma_z^2\, dx\, dy\, /(2\, E_i) \qquad (i=f,m) \qquad (179)$$

The loss tangent $g_{S_{55}}$ associated with the longitudinal thickness-shear stiffness is then calculated according to the general procedure described in Section 3.1 with the help of eq. (151).

3.8 Transverse Thickness-Shear Loss Tangent

The strain energies per cycle for the fiber and matrix regions may be readily calculated from the results of elastic analysis in Section 2.8, eqs. (128, 129, and 135-137), as follows:

$$U^f = U_s^f + U_b^f$$

$$= (9Q_x^2/8G_f)F_1 + \left\{3\lambda' Q_x^2/[4E_m(\mu\delta)^6]\right\}F_3 \qquad (180)$$

$$U^m = U_s^m + U_b^m$$

$$= (3Q_x^2/G_m)\left\{(\mu-1)/(5\mu\delta)+(3/8)F_2\right\}$$

$$+ \left\{3Q_x^2/[4E_m(\mu\delta)^3]\right\}\left[(2/3)(\mu-1)(4\mu^2+\mu+1) + F_4\right] \qquad (181)$$

where the subscripts s and b refer to shear and bending, respectively; F_1 and F_2 are as defined in equations (136 and 137); and F_3 and F_4 are given by the following expressions:

$$F_3 = \int_{-1}^{1} \left\{(\mu-\xi)/[1+(\lambda'-1)(\mu\delta)^{-3}(1-\xi^2)^{3/2}]\right\}^2 (1-\xi^2)^{3/2}\, d\xi \qquad (182)$$

$$F_4 = \int_{-1}^{1} \left\{ (\mu-\xi) / [1+(\lambda'-1)(\mu\delta)^{-3}(1-\xi^2)^{3/2}] \right\}^2$$

$$\cdot \left[(\mu\delta)^3 - (1-\xi^2)^{3/2} \right] d\xi \qquad (183)$$

In view of equations (181 and 182), the damping energies per cycle in the respective fiber and matrix regions are equal to:

$$U_d^f = 2\pi g_{G_f} (9Q_x^2/8G_f) F_1 + 2\pi g_{E_f} \left\{ 3\lambda' Q_x^2 / [4E_m(\mu\delta)^6] \right\} F_3 \qquad (184)$$

$$U_d^m = 2\pi g_{G_m} (3Q_x^2/G_m) \left\{ (\mu-1)/(5\mu\delta) + (3/8) F_2 \right\}$$

$$+ 2\pi g_{E_m} \left\{ 3Q_x^2 / [4E_m(\mu\delta)^3] \right\} [(2/3)(\mu-1)(4\mu^2+\mu+1) + F_4] \qquad (185)$$

Finally, the loss tangent associated with the transverse thickness-shear stiffness is calculated on substitution of equations (180, 181, 184, and 185) into eq. (151). It is noted that Q_x^2, the square of the shear force per unit z-length, cancels and thus the loss tangent is expressed in terms of the loss tangents, moduli ratios, and Poisson's ratios.

This completes the damping analyses for the determinations of the loss tangents associated with all the stiffnesses pertinent to the characterization of the damping behaviors of a single layer of a monofilament composite. The results obtained herein are used in the next section, Section IV, for the construction of the design curves and comparisons of the numerical results with available analytical and experimental data.

SECTION IV

NUMERICAL RESULTS

In this section, numerical results as obtained from the foregoing elastic and damping analyses, Sections II and III, are presented. First, in Section 4.1, the results of the present elastic analyses are compared with some available analytical and experimental results obtained elsewhere as a verification of the present analyses. Secondly, in Section 4.2, property data deduction procedures for some of the constituent materials are briefly described. Then comparisons of the dynamic stiffnesses and their associated loss tangents are made with the limited experimental results which are available. Finally, in Section 4.3, the results of the present analyses are summarized in the form of a set of design curves for boron-epoxy composites, and in a tabulated form for boron-aluminum and glass-epoxy composites. This set of design curves is particularly useful in predicting the elastic and damping behavior of structural elements consisting of one or more layers of monofilament composites (reference 63).

4.1 Comparison with Conventional Micromechanics Results

This section is concerned with the numerical comparisons of the stiffnesses calculated from the present analyses with those obtained elsewhere in order to assess the accuracy of the present analyses. Two aspects of the comparisons to be considered here are:

1. Comparisons of the in-plane and thickness-shear stiffnesses with those obtained from conventional micromechanics analysis where the composite layer consists of many small fibers randomly or regularly distributed throughout the entire cross section; see fig. 1(b).
2. Comparisons of the flexural and twisting stiffnesses with those deduced from the in-plane stiffnesses by the use of eq. (4).

Major Young's modulus E_{11}. - There have been many analytical investigations to determine the major Young's modulus E_{11} (refs. 1,39,47, and 48) ranging from a simple mechanics-of-materials analysis to a more sophisticated elastic analysis. In all cases, however, it was demonstrated that the effect of difference in the Poisson's ratios of the constituent materials is negligibly small. In fact, Hill (ref. 47) showed by a variational method that the rule of mixtures, eq. (11), is the lower bound. Therefore, for all practical design purposes, eq. (11) is deemed sufficiently accurate. Furthermore, experimentally, the published data for Narmco 5505 boron-epoxy composite (reference 64) gave values of E_{11} to be 30.6×10^6 psi in tension and 34.0×10^6 psi in compression; whereas, the value of 30.3×10^6 psi was obtained from eq. (11) by using nominal Young's modulus values of 60×10^6 psi for boron and 0.5×10^6 psi for epoxy.

Major in-plane Poisson's ratio ν_{12}. - Many analytical investigations have shown that the major Poisson's ratio may be predicted by the rule of mixtures, eq. (38), with sufficient accuracy. In particular, Abolin'sh (ref. 53) presented in detail the derivation of eq. (38) where the major Poisson's ratio of the fiber ν_f may be allowed to be transversely isotropic with the plane of isotropy normal to the fiber. However, in his derivation, no

allowance was made for the actual fiber cross-sectional shape. Within the context of mechanics-of-materials theory, Bert showed that eq. (38) holds for circular cross-section fibers (reference 65). Halpin and Tsai (reference 66) devised an interpolation method and applied it to the elastic numerical results in a graphical form obtained previously by Hermans (reference 67) to show that the numerical data can be empirically approximated by eq. (38). As a further verification of eq. (38), the numerical results for ν_{12}, as obtained from the second of eqs. (36), are shown in table I for various fiber volume fractions. It is observed that, for all practical purposes, the rule of mixtures, eq. (38), may be used for estimating the major Poisson's ratio ν_{12}. Unfortunately, comparison with the experimental result (ref. 64) showed that the theory predicted a much lower value of 0.30 against 0.36 for Narmco 5505 boron-epoxy composite with a fiber volume fraction of 0.50. This is attributed mainly to the discrepancies in the nominal constituent-material data used for calculation.

Minor Young's modulus E_{22}. - The minor Young's modulus E_{22} as calculated from the first of eqs. (36) and those obtained by other investigators are plotted against Young's modulus ratio E_f/E_m for various fiber volume fractions for comparison as shown in figure 11. Foye has summarized the results of analytical investigations on the various estimates of the transverse properties of filamentary composites (ref. 40). It was concluded that, in general, the transverse stiffness is relatively insensitive to the types of models chosen. The specific analytical results for E_{22} chosen here for comparison are those due to Tsai (reference 68) and Adams and Doner (ref. 56). In fig. 11, it is observed that the present theory predicts values for E_{22} which are consistently lower than those of Tsai and of Adams

and Doner. However, it must be remembered that in their analyses, a square-array composite model was used. Thus, the free-edge effect was completely eliminated. In the present analysis, a single-layer model was chosen in order to obtain a more realistic representation of the layer property on the micro-scale. Hulbert and Rybicki (reference 69) showed in their recent paper that the free-edge effect for some filamentary composites may range from 9.8% (for boron-epoxy) to 5.0% (for boron-aluminum) at a fiber volume fraction of 0.50. It is believed that this accounts for the lower estimates of the present analysis shown in fig. 11.Chen and Cheng (ref. 38) chose a hexagonal-array model and gave some numerical results for an E glass-epoxy composite and showed that their result from the elastic analysis is well within the previous results obtained by Hashin and Rosen (ref. 35) and Dow and Rosen (reference 70). The present analysis also gave a result that is bounded by the results of the above two references (refs. 35 and 70).

In-plane longitudinal shear stiffness G_{66}. - Adams and Doner (ref. 46) determined the in-plane shear modulus G_{66} using a square-array model and compared their results obtained from an over-relaxation procedure with other analytical results (refs. 35, 38, and 71) and a limited number of experimental results. Excellent agreement was observed between their results and the complex-variable elastic solution of Wilson and Goree (ref. 71), whereas comparison with the analytical work of Chen and Cheng (ref. 38) and that of Hashin and Rosen (ref. 35) showed some discrepancy due to the hexagonal-array model used by these investigators. A fair agreement is observed between Adam and Doner's results and that of experiment; theoretical values being consistenly lower by 5.3% for boron-epoxy, 6.7%

for carbon-epoxy, and 13.5% for glass-epoxy composites. From an engineering design point of view, an explicit formula such as the one given by Hashin and Rosen (ref. 35) would be highly desirable. For this reason, an empirical correction factor Cv_f was introduced in Hashin and Rosen's formula in order to bring their results to coincide with that of Adams and Doner (ref. 46).

Longitudinal flexural stiffness D_{11}. - In eq. (48), it is observed that the ratio $E_{11}^{(b)}/E_{11}$ represents a measure of flexural stiffness efficiency which is less than unity for all realistic values of the parameters. In effect, this means that, unlike those composites containing many small fibers, the longitudinal flexural stiffness D_{11} calculated from eq. (4) using the in-plane major Young's moudlus would be highly unconservative. A lower bound for the equivalent Young's modulus can be estimated readily from a "netting type" analysis in which the contribution of the matrix material to the composite flexural stiffness is completely neglected. This leads to the expression, originally derived by Margolin (reference 72).

$$\left[E_{11}^{(b)}/E_{11}\right]_{\text{Netting Analysis}} \approx (3/4)/(\mu\delta)^2 \qquad (186)$$

In table II are shown the flexural stiffness efficiency, $E_{11}^{(b)}/E_{11}$, for various constituent-material combinations, aspect ratios δ, and volume fractions (reference 73). It is noted that the effect of δ on the flexural stiffness efficiency is much stronger than those of μ and V_f.

Flexural stiffness efficiencies for various constituent-material combinations and fiber volume fractions are plotted as shown in figure 12 for square typical elements, i.e., a square array of fibers. For example,

in the case of a boron-epoxy monofilament composite with a fiber volume fraction of 0.50, conventional theory, eq. (4), predicts a value for flexural stiffness D_{11} that is twice as large as the actual flexural stiffness for a single layer. Also shown in the figure as dashed lines are lower-bound estimates for fiber volume fractions of 0.20 and 0.70. It is seen that the lower-bound estimate, eq. (186), increases in accuracy as the fiber becomes stiffer (large E_f/E_m ratio), and as the fiber volume fraction increases.

Poisson flexural stiffness D_{12}. - The values of Poisson flexural stiffness as calculated from the present analysis, eq. (50), are compared with those calculated from eq. (4) by the use of in-plane stiffnesses and Poisson ratios. Again, it is found that Poisson flexural stiffnesses calculated in a conventional fashion are much greater than those of present analysis as demonstrated in Table III. For all of the composites compared, it is observed that for a low E_f/E_m ratio (≤ 6) and low fiber volume fraction (≤ 0.40), D_{12} as calculated from eq. (4) is in fair agreement, the difference being less than 7%. However, for a high-stiffness-fiber composite such as boron-epoxy, the conventional formula, eq. (4), over-estimates by as much as 40% or more at a fiber volume fraction of 0.60.

Transverse flexural stiffness D_{22}. - In order to assess the transverse flexural stiffness efficiency in an analogous manner as that of longitudinal flexural stiffness, the ratio of the value of D_{22} as obtained from eq. (59) and that obtained from eq. (4) is plotted against the E_f/E_m ratio for various fiber volume fractions as shown in figure 13. It is observed that the conventional estimates from eq. (4) are again on the unconservative side. However, variance in the transverse flexural rigidity

efficiency due to fiber volume fraction is relatively weak. This is perhaps due to the rather insignificant stiffening effect that the fiber has on the transverse in-plane and flexural stiffnesses. For a boron-epoxy composite with fiber volume fractions ranging from 0.4 to 0.6, the stiffening effect, as reflected by the value of E_{22}/E_m, ranges from 2 to 4, whereas in the case of the longitudinal modulus, the values of E_{11}/E_m ranges from 48 to 72!

Twisting stiffness D_{66}. - The torsional problem of a composite layer presented in Section 2.6 is particularized to a simple case of a single typical element and compared with the result obtained by Ely and Zienkiewicz, who solved the problem by the application of the relaxation method (ref. 74). Comparisons of the values of the Prandtl torsion function at the mesh points showed that the present analysis is in good agreement with that of ref. 74; see figure 14. A series of exploratory computer runs indicated that the solution was relatively insensitive to the number of boundary points and the number of terms retained in the series solutions, eq. (80), for the values of parameters used in this example ($G_f/G_m = 10$, $\mu = 2$, $\delta = 1$). In the example shown, 31 equally spaced points on the vertical edge of the cross section and a 31-term series solution were used.

In figure 15 is shown the values of the normalized Dirichlet torsion function Ψ at equally-spaced mesh points of the one-quarter cross section of a composite layer containing three repeating typical elements. In this example, a total of 50 points and 10-term and 20-term series solutions of the respective zeroth and first regions were used. Pertinent data are: $G_f/G_m = 0$, $\mu = 2$, and $\delta = 1$. It is interesting

to note the similarity and symmetry in the Ψ - value in the first and the second quarter-sections. It is also of interest to note the decrease in the Ψ - value in the third quarter-section that is farthest from the origin. This means that for a layer containing many fibers, the torsional rigidity (not the layer twisting stiffness) can be approximated as the number-of-fiber multiples of the torsional rigidity of a single element.

Figure 16 shows the twisting stiffness ratio D_{66}/D_{66}^{m} for various values of fiber volume fractions and shear modulus ratio G_f/G_m.

Comparisons of the twisting stiffnesses for a square single element cross section calculated from eq. (84) and eq. (4) are tabulated as shown in Table IV. It is apparent that a twisting analysis is a must in predicting the layer-twisting stiffness.

Longitudinal thickness-shear stiffness G_{55}. - For a small-fiber composite or parallel laminates consisting of many layers, it is generally accepted that the longitudinal thickness-shear modulus G_{55} is equal to the in-plane longitudinal shear modulus G_{66} (references 75 and 76). However, in the case of a single-layer composite with only a single row of fibers, the longitudinal thickness-shear modulus G_{55} is expected to be greater than the in-plane shear modulus G_{66} due to the shear-stiffening effect of the fiber. Bert used an approximate Jourawski-type shear theory to predict that the ratio G_{55}/G_{66} may vary from 2.86 for boron-aluminum to 37 for boron-epoxy composites with a volume fraction of 0.482 (ref. 73). In the present more refined analysis, this ratio is found to vary from 1.5 for boron-aluminum to 16.2 for boron-epoxy composites with a volume fraction of 0.5.

Numerical results for the longitudinal thickness-shear modulus are summarized as shown in figure 17 for various volume fractions and constituent-material combinations.

Transverse thickness-shear modulus G_{44}. - The transverse thickness-shear modulus G_{44} is plotted against volume fractions for various constituent-material combinations as shown in figure 18. Comparison with the analytical results obtained by Heaton (ref. 75) showed that fair agreement is observed for fiber volume fractions below 0.5, but at higher fiber volume fractions, 0.6 say, the present estimate for boron-epoxy composites gave a 14% higher value for G_{44}. The discrepancy is attributed to the differences in the models chosen for the analyses; Heaton's model being that of a multi-fiber square array.

4.2 Storage Moduli and Associated Loss Tangents.

Prior to evaluations of the dynamic stiffness and damping behavior of a layer of a monofilament composite characterized by nine stiffnesses and a Poisson ratio with their respective associated loss tangents, accurate dynamic constitutive properties of each constituent material must be known. A survey of the literature revealed that numerous experiments have been made to determine damping characteristics of glass (references 77-80), epoxy (ref. 9), and aluminum (references 81-83). However, apparently no such data are available on boron. Because of different experimental techniques and perhaps slight differences in material compositions in the specimens, the damping properties obtained by these investigators do not always correlate with those obtained for the composite specimens. Therefore, it would be necessary to have avail-

able good data for the constituent-material properties for the micro-mechanics prediction of the composite macroscopic properties. However, sometimes this may be difficult to obtain experimentally, for example due to frailty of fibers in the filamentary composites or nonlinear effects (see Appendix D).

In view of this, a scheme for obtaining in-situ constituent material properties from tests on composites may be necessary. Some successful attempts at deducing such constituent-material properties were reported by Papirno and Slepetz (reference 84) and Bert (reference 85) for static properties. Therefore, this deduction procedure was used in the present investigation properties to obtain the dynamic properties of some of the constituents from the test data on filamentary composites when necessary.

To characterize the isotropic behavior of the material completely, two independent moduli and their associated loss tangents must be known. For the subsequent data deduction, it is assumed here that each material behaves elastically in dilatation. With this assumption and the knowledge of the Young's modulus and associated loss tangent, the second pertinent modulus (shear modulus or Poisson's ratio) and its associated loss tangent may be readily obtained.

The dynamic Young's modulus and associated loss tangent for boron, epoxy, E glass, aluminum alloy 2024-T3, and aluminum alloy 6061 are summarized as shown in figures 19-23. Data for E glass (fig. 21) were obtained from ref. 79; for aluminum 2024-T3 (fig. 22), from ref. 81; for aluminum 6061 (fig. 23), from refs. 81 and 8; and curve B for epoxy (fig. 20), from ref. 9.

Curve A for epoxy (fig. 20) was deduced from the experimental data on glass-epoxy filamentary composites by Mazza et al. (reference 86); and the data for boron (fig. 19) were deduced from curve A and the experimental results on boron-epoxy filamentary composites of the same reference.

A quick comparison showed that the prediction of the loss tangent associated with the transverse Young's modulus for glass-epoxy is in good agreement with the experimental results of ref. 9, both varying from 1% to 3% for the frequency range between 20 and 2000 Hz.

The same comparison for boron-epoxy filamentary composites also indicated excellent agreement on the prediction of the loss tangent associated with the transverse Young's modulus; in both cases, ref. 86 and the present analysis, the value of loss tangent varies between 1.6 and 2.0% in the frequency range 20-400 Hz.

Pertinent data for the complete characterization of the constituent properties are summarized in Tables V-IX.

4.3 Design Curves and Tables - Storage Moduli and Associated Loss Tangents Versus Frequency for Various Fiber Volume Fractions

The results of the present analyses are summarized in the form of design curves for a boron-epoxy filamentary composite as shown in figs. 24-33 for the frequency range 50-2000 Hz. and the fiber volume fractions V_f = 0.4, 0.5, and 0.6. In application, the curve A series should be used for better predictions of the composite stiffnesses and associated loss tangents; the Curve B series is included for comparison purposes only.

In Tables X-XXIX are listed all the pertinent dynamic stiffnesses and associated loss tangents for the characterization of the layer properties of boron-aluminum and E glass-epoxy composites for the same ranges of frequency and fiber volume fractions.

V. CONCLUSIONS

Elastic and damping analyses resulting in determination of all pertinent stiffnesses and associated loss tangents for the characterization of the elastic and damping behavior of a monofilament composite were carried out.

The numerical results obtained for the stiffnesses and associated loss tangents compared favorably with some existing analytical and experimental results for some typical filamentary composites, such as, boron-epoxy, boron-aluminum, E glass-epoxy.

The results of the flexural and twisting stiffness analyses showed that these properties cannot be deduced accurately from the in-plane-properties, and, thereby, the necessity for such analyses for a monofilament composite layer.

The assumption of Kimball-Lovell type damping was shown to be equivalent to the elastic-viscoelastic correspondence principle for the case of the in-plane longitudinal stiffness.

The results of this investigation were summarized in a set of design curves for a boron-epoxy composite, and in a set of design data tables for boron-aluminum and E glass-epoxy composites. The former were applied to the problem of predicting resonant frequencies nodal patterns, and damping ratios for laminated boron-epoxy plates

(references 64 and 87) and achieved excellent agreement with available experimental results for six different plates (ref. 14).

Recommendations for future investigation. - For future researches, the following topics are suggested:

1. Experimental characterization of the complete set of dynamic stiffness and damping properties of various filamentary composite materials of technological importance.
2. Analytical investigation of the viscoelastic behavior of composite materials with thermo-mechanical coupling.
3. A unified viscoelastic analysis for filamentary composite.

APPENDIX A

BOUNDARY-POINT LEAST-SQUARE METHOD

Numerous approximate methods are available for the solution of boundary-value problems. To name a few, there are the Rayleigh-Ritz, Galerkin, Kantorovich, finite element, relaxation, and collocation methods. Of these methods, especially with the availability of modern digital computers, probably the boundary-point least-square version (ref. 5) of the collocation method is the most efficient for solution of mixed boundary-value problems, such as those investigated in Section II. The main useful features of the method are:

1. It may be applied to mixed boundary-value problems with relative ease.
2. The assumed solution may be made to satisfy the boundary conditions at a set of sufficiently dense points in the sense of minimizing the square error; hence the solution may be made independent of the number of boundary points chosen.

In general then, the solution is reduced to the satisfaction of a set of overdetermined algebraic simultaneous equations

$$\underset{\sim}{\underset{\sim}{A}}\,\underset{\sim}{X} = \underset{\sim}{B} \tag{A-1}$$

where $\underset{\sim}{\underset{\sim}{A}}$ = m x n coefficient matrix (m > n), $\underset{\sim}{X}$ = n-dimension column vector of unknown coefficients, $\underset{\sim}{B}$ = n-dimension column vector of prescribed

boundary values, m = number of chosen boundary points, and n ≡ number of unknown coefficients.

Then the mean-square-error matrix (E^2) for equation (A-1) is given as

$$E^2 = \tilde{(A\tilde{X}-\tilde{B})}^T \tilde{(A\tilde{X}-\tilde{B})} \tag{A-2}$$

where the superscript T denotes the transpose of the matrix quantity which it follows.

On minimizing equation (A-2) with respect to X, one obtains

$$(\tilde{A}^T\tilde{A})\tilde{X} = (\tilde{A}^T\tilde{B}) \tag{A-3}$$

or

$$\tilde{A}^*\tilde{X} = \tilde{B}^* \tag{A-4}$$

where $\tilde{A}^*$ is an n x n matrix given by

$$\tilde{A}^* = \tilde{A}^T\tilde{A} \tag{A-5}$$

and $\tilde{B}^*$ is an n-dimension column vector given by

$$\tilde{B}^* = \tilde{A}^T\tilde{B} \tag{A-6}$$

Finally, the solution-coefficient vector $\tilde{X}$ that minimizes the square error is obtained readily from equation (A-4) by using a number of standard computer scientific subroutines. However, care must be taken in the choice

of appropriate forms of the stress functions and in the choice of boundary points to avoid any boundary points at which the prescribed boundary values are identically satisfied.

APPENDIX B

MODELS AND MEASURES OF MATERIAL DAMPING

B1. Mathematical Models for Material Damping

Internal friction or damping in materials can be caused by a variety of combinations of fundamental physical mechanisms, depending upon the specific material. For metals, these mechanisms include thermoelasticity on both the micro and macro scales, grain boundary viscosity, point-defect relaxations, eddy-current effects, stress-induced ordering, interstitial impurities, and electronic effects (ref. 7). According to Lazan (ref. 7), little is known about the physical micromechanisms operative in most nonmetallic materials. However, for one important class of these, namely polymers and elastomers, considerable phenomenological data have been obtained. Due to the long-range molecular order associated with their giant molecules, polymers exhibit rheological behavior intermediate between that of a crystalline solid and a simple liquid. Of particular importance is the marked dependence of both stiffness and damping on frequency and temperature.

The purpose of developing a mathematical model for the rheological behavior of a solid is to permit realistic results to be obtained from mathematical analyses of complicated structures under various conditions, such as sinusoidal, random, and transient loading. According to reference 7 , as early as 1784 Coulomb recognized that the mechanisms of damping

operative at low stresses may be different than those at high stresses. Even today, after more than 2500 publications on damping have appeared, major emphasis is placed on linear models of damping for several reasons: they have sufficient accuracy for the low-stress regime and linear analyses are computationally more economical than nonlinear ones.

The simplest mathematical models of rheological systems are single-parameter models: (1) an idealized spring, which exhibits a restoring force linearly proportional to displacement and thus displays no damping whatsoever, and (2) an idealized dashpot, which produces a force linearly proportional to velocity. Obviously, neither of these models are very appropriate to represent the behavior of most real materials.

The next most complicated models of rheological systems are the two-parameter models: (1) the Maxwell model, which consists of a spring and dashpot in mechanical series, as shown schematically in figure B-1(a); and (2) the Kelvin-Voigt model, which is comprised of a spring in parallel with a dashpot, as shown in figure B-1(b). The Maxwell model is a fair approximation to the behavior of a viscoelastic liquid. However, as a model for a viscoelastic solid, it has several very serious drawbacks (ref. 7); there are no means to provide for internal stress and for afterworking. The Kelvin-Voigt model overcomes these deficiencies and is a first approximation to the behavior of a viscoelastic solid. However, it has the following disadvantages (ref. 7): there is no elastic response during application or release of loading, the creep rate approaches zero for long durations of loading, and there is no permanent set irrespective of the loading history.

It should be mentioned that the Kelvin-Voigt model is the simplest one which permits representation as a complex quantity when subjected to sinusoidal motion. To show this, one can write the following differential equation governing the motion of a single-degree-of-freedom system consisting of a sinusoidally excited mass attached to a Kelvin-Voigt element:

$$m\ddot{u} + c\dot{u} + k\,u = \tilde{F}\, e^{i\omega t} \qquad \text{(B-1)}$$

where $m \equiv$ mass, $c \equiv$ viscous damping coefficeint, $k \equiv$ spring rate, $\tilde{F} \equiv$ exciting force amplitude, $\omega \equiv$ circular frequency of exciting force, $u \equiv$ displacement, $i \equiv \sqrt{-1}$, $t \equiv$ time, and a dot denotes a derivative with respect to time. Assuming that sufficient time has passed for the transients to die out,* we can write the steady state solution of equation (B-1) as follows:

$$u = \tilde{u}\, e^{i(\omega t - \varphi)} = \tilde{F}\,[(k - m\omega^2) + i\omega c]^{-1}\, e^{i\omega t} \qquad \text{(B-2)}$$

where $\varphi \equiv$ phase angle between the response (u) and the exciting force, and $\tilde{u} \equiv$ displacement amplitude.

It is noted that the terms containing Kelvin-Voigt coefficients k and $i\omega c$ can be grouped into a single Kelvin-Voigt <u>complex stiffness</u> ($\bar{k}$) as follows:

---

*It can be shown that they do die out for a mechanical system, for which c, m, and k are all positive quantities.

$$\bar{k} = k + i\omega c \tag{B-3}$$

Alternatively, the Kelvin-Voigt element coefficient could have been grouped into a single complex damping coefficient ($\bar{c}$) as follows:

$$\bar{c} = c - (i\ k/\omega) \tag{B-4}$$

The force (F_d) in a dashpot is given by

$$F_d = c\ \dot{u} = i\omega c\tilde{u}e^{i(\omega t - \varphi)} \tag{B-5}$$

The energy dissipated per cycle (U_d) in a dashpot undergoing sinusoidal motion can be calculated as follows:

$$U_d = \oint F_d\ du = \int_0^{2\pi/\omega} F_d\ \dot{u}\ dt = \pi c\omega\tilde{u}^2 \tag{B-6}$$

In 1927, Kimball and Lovell (ref. 22) observed that many *engineering materials exhibited energy losses which were contradictory* to equation (B-6). Specifically, they found that U_d was proportional to $\tilde{u}^2$ but independent of ω, i. e.

$$U_d = C_d'\ \tilde{u}^2 \tag{B-7}$$

Later work by Wegel and Walther (reference 38) also showed that $U_d \propto \tilde{u}^2$ but C_d' was a weak function of ω. Still later, for stresses below the fatigue limit of the material, Lazan (references 7,89) showed that $U_d \propto \tilde{u}^2$ and C_d' was practically independent of ω.

Equating the energy dissipated per cycle in the Kimball-Lovell material, equation (B-7), to that in the dashpot, equation (B-6), one obtains

$$C'_d = \pi c \omega \tag{B-8}$$

To utilize the Kimball-Lovell observation in practical structural dynamic analyses, it was desirable to have an expression for the associated damping force, i.e. an equation analogous to equation (B-5), which governs a dashpot. According to Bishop (reference 90) this was first done by Collar. Combining equations (B-5, B-8), one obtains the following "frequency-dependent damping" relation:

$$F_d = (b/\omega)\, \dot{u} \tag{B-9}$$

where b is a constant given by

$$b = C'_d/\pi \tag{B-10}$$

The kind of damping represented by equation (B-9) has been called frequency-dependent damping, since the usual dashpot coefficient c is now replaced by the quantity b/ω.

For the damper represented by Eq. (B-9), it is convenient to replace k in the undamped system by the Kimball-Lovell <u>complex stiffness</u> (reference 91):

$$\bar{k}' = k + ib \tag{B-11}$$

where it is now noted that both k and b are assumed to be independent of frequency. This representation has been used extensively in aircraft

structural dynamic and flutter analyses (references 92,93).

An alternative to equation (B-11), is to use the concept of a complex damping coefficient, originated by Myklestad (reference 94), in which the spring constant is replaced by

$$\bar{k}'' = C_1 e^{im} \tag{B-12}$$

where C_1 and m are constants.

Although Kimball and Lovell's original work was based on data obtained during steady-state sinusoidal motion, the models represented by equations (B-9, B-11, B-12) have been applied to free vibrations as well (refs. 90, 91 , 95). To alleviate the difficulty of the interpreting of ω in equation (B-9) for the case of free vibration or for multiple-frequency forced vibration, Reid (reference 96) suggested the following form:

$$F_d = b \left| u/\dot{u} \right| \dot{u} \tag{B-13}$$

where the bars denote that the absolute value of the quantity between them is to be used.

In summary, four different versions of material damping have been discussed. In terms of the differential equation for free vibration, they may be written as follows:

$$m\ddot{u} + (b/\omega)\,\dot{u} + ku = 0 \tag{B-14a}$$

$$m\dot{u} + (k + ib)\,u = 0 \tag{B-14b}$$

$$m\ddot{u} + C_1 e^{im} u = 0 \tag{B-14c}$$

$$m\ddot{u} + b \left| u/\dot{u} \right| \dot{u} + ku = 0 \tag{B-14d}$$

The models represented by equations (B-14) have been criticized by many investigators for various reasons:

1. In equation (B-14a), the interpretation of ω is dubious (references 96,98). Milne (reference 97) suggested that it is associated with the imaginary part of the pair of complex roots, but went on to state that there is no clear justification for this interpretation.

2. Equations (B-14b) and (B-14c) are equations with complex coefficients and the meaning of this is not clear (refs. 95, 97). Furthermore, although they have complex exponential solutions, neither the real nor imaginary parts alone are solutions (refs. 97, 98).

3. Equation (B-14d) is a nonlinear differential equation, due to the behavior of $|u/\dot{u}|$ (ref. 97).

4. None of the models represented by equations (B-14) can be simulated, even on a conceptual basis, on an analog computer (refs. 96, 98).

5. The model represented by equation (B-14a) does not meet the Wiener-Paley condition (references 99,100) of causality for physically realizable systems, as was shown in references 98,102-103.

6. Equation (B-14b) fails to give the proper relations of a damping force that is proportional to displacement and in phase with velocity. This can be alleviated by use of a more unwieldy expression proposed in references 104,105.

Incidentally reference 106 claimed that none of the equation (B-14) models result in energy dissipation that is independent of ω (the reason for abandoning the Kelvin-Voigt model). However, an error in this reasoning, which makes it invalid, was pointed out in reference 107.

It can be shown that the sinusoidally forced vibration version of free vibration equations (B-14a,b,c) are exactly equivalent. Probably the most popular form for writing this is as follows:

$$m\ddot{u} + (k + ib)u = \tilde{F}e^{i\omega t} \qquad \text{(B-15)}$$

The major criticism of the use of equation (B-15) is that it results in a conventionally defined magnification factor (see Section B2), corresponding to zero frequency, which is not equal to unity for $g \neq 0$ (ref. 90). This difficulty can be eliminated by redefining the magnification factor as follows:

$$MF' \equiv \tilde{u}/u'_{st} \qquad \text{(B-16)}$$

where

$$u'_{st} \equiv \tilde{F}/k'$$

and k' is the stiffness coefficient associated with the total in-plane force amplitude, i.e.

$$k' \equiv (k^2 + b^2)^{\frac{1}{2}}$$

Thus,

$$MF' = (k^2 + b^2)^{\frac{1}{2}}/[k-m\omega^2)^2 + b^2]^{\frac{1}{2}} = (1 + g^2)^{\frac{1}{2}}/[(1-\omega^2/\omega_n^2)^2 + g^2]^{\frac{1}{2}}$$

The major advantages of using the equation (B-15) model for steady-state vibrational and flutter analyses are as follows:

1. The analysis is considerably simplified in comparison with that for viscous damping, as pointed out in reference 108.

2. The analysis is linear.

3. The complex-modulus concept has long been in common use, especially

in connection with measurement of the damping properties of elastomers, polymers, etc. (reference 107).

4. The complex-stiffness approach has been used very successfully in flutter analysis for approximately three decades (refs. 92,93 ,107 ,109).

In view of these considerations, the complex-stiffness approach is used in the main portion of the present report. However, for completeness and comparison, a number of other more complicated approaches are also discussed in this section.

To overcome some of the deficiencies of the Kelvin-Voigt and Maxwell models, they were combined in various ways to obtain the three-parameter models shown in figure B-1(c) and (d). It can be shown (reference 110) that by properly selecting the values of the coefficients, the two models can be used interchangably. In other words, the model representation is not unique. In fact, both representations have been called the "standard linear solid", "standard linear material," "simple anelastic model", or "standard model of a viscoelastic body" (references 111-114). Unfortunately, few materials have been characterized by the use of the standard linear solid. Perhaps the most extensive characterization has been carried out for flexural vibration of 2024-T4 aluminum alloy: by Granick and Stern (reference 82,115) in air and by Gustafson et al. (ref. 81) in vacuo.

Obviously one can go on from a three-parameter model to a four-parameter one, etc. Continuing this process, one obtains two well-known models (ref. 111): the Kelvin chain, shown in figure B-2(a), and the generalized Maxwell model, shown in figure B-2(b). The behavior of such systems can be written in either differential or integral form, as discussed in detail in reference 111. However, the complexity of

such a model has limited its use both experimentally (in characterizing engineering materials) and analytically (in performing dynamic analyses). Thus, for engineering applications, there is a continuing search for models which are simple, yet represent the behavior of real materials with sufficient accuracy.

A relatively simple model, which is somewhat similar to the generalized Maxwell one, is due to Biot (reference 116); see figure B-2(c). The number of simple Voigt elements in this model is allowed to increase without bound, so that the damping force is represented by the following expression:

$$F_d = g_1 \int_{t_1}^{t} Ei\,[-\epsilon(t-\tau)]\,(du/d\tau)\,d\tau \qquad \text{(B-17)}$$

where τ is a dummy variable; $\epsilon, g_1 \equiv$ parameters, and Ei(u) is the exponential integral

$$Ei(u) \equiv \int_{\infty}^{-u} (e^{-\xi}/\xi)\,d\xi \qquad \text{(B-18)}$$

Caughey (ref. 98) made a detailed study of Biot's model for both free and forced vibration. He showed that for $\omega/\epsilon > 10$, the energy dissipated in Biot's model is within 4% of being independent of frequency (ω) and thus essentially depends only upon the square of the displacement amplitude. Milne (ref. 97) studies the Biot model by means of the convolution integral.

Neubert (reference 117) introduced a variant of the Biot model, in which a different distribution function for the local stiffness-damping ratio is used. Milne (ref. 97) also studied this model via the convolution integral. Milne introduced a new synthesized model of his own. However,

the main conclusion of his investigation was that, for practical engineering purposes, the choice of a rheological model is not critical, provided that the range of constant damping is kept the same and the damping is small.

The linear hereditary theory of material damping was originated in 1876 by Boltzmann (reference 118). In this theory, the energy loss is attributed to the elastic delay by which the deformation lags behind the applied force. It is called a hereditary theory because the instantaneous deformation depends upon all of the stresses applied to the body previously as well as upon the stress at that instant. The damping force is given by

$$F_d = \int_{-\infty}^{t} \Phi(t,\tau)\, u(\tau)\, d\tau \qquad \text{(B-19)}$$

where $t \equiv$ actual time, $\tau \equiv$ an instant of time (dummy variable), $u \equiv$ displacement, and $\Phi \equiv$ hereditary kernel or memory function. Often the hereditary kernel depends upon the difference $(t-\tau)$ only; then equation (B-19) becomes:

$$F_d = \int_{-\infty}^{t} \Phi(t - \tau)\, u(\tau)\, d\tau \qquad \text{(B-20)}$$

It is most advantageous to determine the hereditary kernel from experimental data. It has been found to be a monotonically decreasing function which can be represented mathematically as follows:

$$\Phi(t) = \sum_{i=1}^{n} A_i e^{-\alpha_i t} \qquad \text{(B-21)}$$

Such a system is said to have a heredity of degree n and A_i and α_i

are called heredity constants. Hobbs (ref. 112) has shown that a first-degree hereditary model is equivalent to a simple anelastic model (standard linear solid).

Volterra (reference 119) has presented a method of determining the hereditary kernel from material response to either suddenly applied loading or to sinusoidal excitation. He also presented plots of magnification factor and phase shift versus frequency for a wide range of parameters of a single-degree-of-freedom system with first-degree hereditary damping. For certain combinations of the parameters, the magnification and phase characteristics are quite different from that of a viscously damped system; yet for certain other combinations, the characteristics are quite similar.

Numerous nonlinear mathematical models have been proposed to permit better correspondence between theory and experiment. However, all of them, by their very nonlinear nature, are more complicated to apply in structural dynamic analyses of practical engineering systems. Perhaps the simplest one is damping energy per unit volume and per cycle proportional to stress to a power (ref. 7):

$$U_{dv} = C_d \tilde{\sigma}^m \qquad \text{(B-22)}$$

where C_d and m are material constants and $\tilde{\sigma}$ is the cyclic stress amplitude. It is noted that m = 2 corresponds to the Kimball-Lovell relation (linear theory) discussed previously. It has been found that m varies from 1.8 to 6.0, generally being near 2.0 at low stress amplitudes.

The hysteresis loop associated with the complex-modulus model, equation (B-11), is elliptic in shape; see figure B-3(a). However,

the hysteresis loops determined experimentally have sharp corners at both ends and are nearly linear in the low-stress, low-strain region, as shown in figure B-3(b). According to ref. 7 (page 97), in 1938 Davidenkov proposed a nonlinear mathematical model which results in a similar shape of hysteresis loop. Further work on this class of model has been carried out by Pisarenko (reference 120).

Rosenblueth and Herrera (reference 121) proposed a nonlinear model which eliminates the causality difficulties of the complex-modulus model. Chang and Bieber (reference 122) introduced a nonlinear hysteresis model in which there is no hysteresis damping unless the displacement amplitude exceeds a certain threshold value.

B2. Measures of Material Damping

In this section, various definitions of damping are discussed in the context of a complex-modulus material.

Energy Dissipation Under Steady-State Sinusoidal Vibration. - Energy dissipated per cycle (U_d) in the form of internal frictional heating is one measure of damping. However, this quantity depends upon the size, shape, and dynamic stress distribution (which in turn, depends upon the particular mode of vibration). In view of the above difficulties, the specific damping energy (U_{dv}) is usually considered to be a more basic property of the material, rather than the structure. The U_{dv} is defined as the damping energy per cycle and per unit volume, assuming a uniform dynamic stress distribution throughout the volume considered. Thus, the total damping energy is

$$U_d = \oint_V U_{dv}\, dV \qquad \text{(B-23)}$$

where V ≡ volume. The usual units of U_d are in-lb/cycle and of U_{dv}, in-lb/in^3-cycle.

Resonant Magnification Factor Under Steady-State Sinusoidal Excitation. - The resonant magnification factor (RMF) is defined as the dimensionless ratio of the response at resonance to the excitation, where both the response and the excitation must be specified in the same units (see figure B-4). These quantities may be in units of displacement, velocity, acceleration, or strain. Unfortunately, the resonant magnification factor is dependent upon the structural system configuration as well as upon the damping property of the material, so that it is considered to be a system characteristic, rather than a basic material property.

Incidentally RMF is not applicable to nonlinear systems, since then it depends upon the excitation level. (In a linear system, RMF is independent of the level of excitation.)

Bandwidth of Half-Power Points Under Steady-State Sinusoidal Excitation.- The separation $(\omega_2-\omega_1)$ between the frequencies associated with the half-power points increases with an increase in damping (see figure B-5) and thus can be used as a measure of damping. A more meaningful definition is to normalize by the associated resonant frequency (ω_n), i.e. use the dimensionless bandwidth given by

$$(\omega_2 - \omega_1)/\omega_n \quad .$$

This measure is the basis for determination of damping by the original Kennedy-Pancu method (reference 123).

The quality factor Q is defined as the reciprocal of the dimensionless

bandwidth.

Derivative of Phase Angle with Respect to Frequency, at Resonance. - This measure is the basis for determination of damping by an improvement (reference 124) of the Kennedy-Pancu method.

Loss Tangent Under Steady-State Sinusoidal Excitation. - Applying the complex-stiffness (see Section B1) to the material property representing stiffness, namely the Young's modulus (E), we obtain

$$E \rightarrow E^R(1 + ig) \tag{B-24}$$

Thus, the loss tangent* is defined as follows:

$$g \equiv E^I/E^R \tag{B-25}$$

where $E^I \equiv$ loss modulus** and E^R is called the storage modulus.***

Referring to figure B-6, we obtain the following relation:

$$g = \tan \gamma = E^I/E^R \tag{B-26}$$

or

$$\gamma = \arctan E^I/E^R \tag{B-27}$$

---

*Also known as the "loss coefficient", "loss factor", or "damping factor".

**Also sometimes called the "dissipation modulus."

***Also sometimes called "elastic modulus" or "real modulus."

The quantity γ is called the loss angle and equation (B-26) explains the origin of the term loss tangent for g.

Cyclic Decay of Free Vibrations. - In a linear system, free vibrations decay exponentially (see figure B-7). The larger the damping, the faster is the decay. Thus, the logarithmic decrement δ is defined as follows:

$$\delta \equiv \ell n \ (a_i / a_{i+1}) \qquad \text{(B-28)}$$

where $\ell n \equiv$ natural logarithm.

For a power-law material, eq. (B-22), to have δ independent of amplitude, m must be 2 (see Section B3 for proof). When m=2, the following means of calculating δ is more practical, especially when damping is small:

$$\delta = (1/n) \ \ell n \ (a_i / a_{i+n}) \qquad \text{(B-29)}$$

where n is any arbitrary integer.

Temporal Decay of Free Vibrations. - Another measure associated with the decay of free vibrations is the temporal decay constant v_t, defined as follows (reference 7, foldout opposite p. 35):

$$v_t \equiv (t_2 - t_1)^{-1} \ \ell n \left[u(t_1)/u(t_2) \right] \qquad \text{(B-30)}$$

where t_1 and t_2 are two different values of time, arbitrary except that $t_2 > t_1$ and $(t_2 - t_1)$ must be an integer number of periods of damped vibration. The quantities $u(t_1)$ and $u(t_2)$ are the respective displacements at times t_1 and t_2. It is seen that the usual units for v_t are sec^{-1}.

An alternate way of specifying the temporal decay is the decay rate γ_t, which has units of decibels per second (db/sec) and is defined as follows:

$$\gamma_t \equiv 20\ (t_2 - t_1)^{-1}\ \log\ [u(t_1)/u(t_2)] \qquad \text{(B-31)}$$

or

$$\gamma_t = 20(t_2 - t_1)^{-1}\ \log\ e^{\nu_t(t_2 - t_1)} = (20\ \log\ e)\nu_t \approx 8.68\ \nu_t$$

where log ≡ logarithm to the base 10.

Spatial Attenuation of a Plane Wave in a Slender Bar. - If one propagates a plane, harmonic wave in a slender bar made of a homogeneous, linear material, the wave exhibits exponential decay with axial position (x), analogous to the temporal decay of free vibration (which may be considered as a standing wave). Analogous to the logarithmic decrement (see above), we have the logarithmic attenuation δ_s, defined as follows in terms of amplitudes $a(x_1)$ and $a(x_2)$ at stations x_1 and x_2:

$$\delta_s \equiv \ln\ [a(x_1)/a(x_2)] \qquad \text{(B-32)}$$

Analogous to the temporal decay constant, we define the spatial attenuation constant ν_s as follows:

$$\nu_s \equiv (x_2 - x_1)^{-1}\ \ln\ [a(x_1)/a(x_2)] \qquad \text{(B-33)}$$

The unit of ν_s is in^{-1}.

Finally, analogous to the decay rate, we define the spatial attenuation rate γ_s as follows:

$$\gamma_s \equiv 20(x_2 - x_1)^{-1} \log [a(x_1)/a(x_2)] \approx 8.68\ v_s. \qquad \text{(B-34)}$$

The unit of γ_s is db per unit length.

It should be cautioned that the determination of damping by wave attenuation requires that the cross section of the bar be compact (preferably round or square) and that the largest cross-sectional dimension be very small compared to the wave length of the traveling wave. Furthermore, the two stations along the bar, at which the wave measurements are made, must be: (1) sufficiently far from the point of impact that initial transients have died out and (2) sufficiently far from each other so that a measurable change in amplitude occurs. Kolsky discussed these points in detail in reference 125.

B3. Inter-Relationships Among Various Measures of Damping for Homogeneous Materials

Here we consider a single degree-of-freedom system consisting of a mass supported on a massless spring made of a homogeneous Kimball-Lovell or complex-modulus material. Then the governing differential equation for simple harmonic excitation is equation (B-15), which has the following steady-state solution:

$$u = \tilde{u}\, e^{i(\omega t - \varphi)} \qquad \text{(B-35)}$$

where

$$\tilde{u} \equiv \tilde{F} \left[(k - m\omega^2)^2 + b^2 \right]^{-1/2} \qquad \text{(B-36)}$$

$$\varphi \equiv \arctan \left[b/(k - m\omega^2) \right] \qquad \text{(B-37)}$$

The magnification factor (MF) is defined as follows:

$$MF \equiv \tilde{u}/u_{st} \tag{B-38}$$

where u_{st} is the so-called static displacement, defined as follows:

$$u_{st} \equiv \tilde{F}/k \tag{B-39}$$

Combining equations (B-36, B-38, and B-39), one obtains the following relation:

$$MF = \left\{\left[1 - (\omega/\omega_n)^2\right]^2 + (b/m\omega_n^2)^2\right\}^{-1/2} \tag{B-40}$$

where ω_n is the natural frequency (i.e. the resonant frequency of the undamped system), given by:

$$\omega_n = (k/m)^{1/2} \tag{B-41}$$

The critical material damping coefficient (b_c) is the minimum value of b for which the free vibratory motion is non-oscillatory. It is obtained from the following relationship:

$$(b_c/2m\omega_n)^2 = k/m = \omega_n^2 \tag{B-42}$$

or

$$b_c = 2m\omega_n^2 \tag{B-42}$$

The damping ratio ζ is defined as follows:

$$\zeta \equiv b/b_c \tag{B-43}$$

Combining equations (B-40, B-42, and B-43), one arrives at the following general, dimensionless relationship:

$$MF = \left\{\left[1-(\omega/\omega_n)^2\right]^2 + 4\zeta^2\right\}^{-1/2} \qquad \text{(B-44)}$$

It is seen easily that MF is a function of only two parameters: the frequency ratio (ω/ω_n) and the damping ratio (ζ). It should be mentioned that equation (B-44) is somewhat <u>different</u> than the known relationship for a single-degree-of-freedom Kelvin-Voigt viscously damped system, even though the damping ratio ζ is defined analogously ($\equiv c/c_c$, where $c_c = 2m\omega_n$).

The <u>resonant magnification factor</u> (RMF) is defined as the value of MF at resonance, which is taken here to occur when $\varphi = 90^o$. In view of equation (B-37), this implies that the resonant frequency is ω_n. Thus, at resonance, equation (B-44) reduces to the following simple expression:

$$\boxed{RMF = (2\zeta)^{-1}} \qquad \text{(B-45)}$$

Thus, it is seen that the same simple relationship between the damping ratio and the <u>resonant</u> magnification factor holds as does for a Kelvin-Voigt system. Although the resonant amplitude can be measured accurately, there are problems in measuring the static deflection in complicated structures (due to signal-to-noise ratio limitations of instrumentation). For this reason, in structural dynamics, RMF is seldom used as a measure of damping.

The damping energy, i.e. the energy dissipated per cycle, can be computed as follows:

$$U_d = \oint F_d \, du = \int_0^{2\pi/\omega} F_d \dot{u} \, dt \qquad \text{(B-46)}$$

where F_d is the damping force, given by

$$F_d = (b/\omega)\dot{u} \tag{B-47}$$

Substituting equations (B-35) and (B-47) into equation (B-46) and integrating, we obtain the following result:

$$U_d = \pi b \tilde{u}^2 \tag{B-48}$$

To convert equation (B-48) to the form of equation (B-22), with m=2, it is necessary to divide by the volume and to relate $\tilde{u}$ to $\tilde{\sigma}$. Now the force amplitude is

$$\tilde{F} = A\tilde{\sigma} = k\tilde{u} \tag{B-49}$$

where A ≡ cross-sectional area.

Assuming the spring is a massless and uniform bar, we have

$$k = AE/L \tag{B-50}$$

where L ≡ effective length of spring and E ≡ Young's modulus of the bar. Combining equations (B-48, B-49, B-50), one obtains the following result:

$$U_{dv} = U_d/V = (\pi bL/A)(\tilde{\sigma}/E)^2 \tag{B-51}$$

Comparing the form of equations (B-22) and (B-51), we see that for a Kimball-Lovell material, m = 2 and

$$C_d = \pi bL/AE^2 \tag{B-52}$$

It should be noted that Lazan (reference 7, chap. II) has shown that these results are independent of the stress distribution and the specimen geometry, provided that m = 2.

In view of equations (B-42, B-43, and B-44), equation (B-52) can be expressed in the following more useful form:

$$\boxed{C_d = 2\pi\, \zeta/E} \qquad \text{(B-53)}$$

According to equation (B-48), the damping energy (and thus, excitation power) is proportional to the square of the displacement amplitude u_o (and thus, the MF). Then the power is one half of what it is at resonance when MF = RMF/$\sqrt{2}$. In view of equation (B-45), the half-power magnification factor (HPMF) is related to the damping ratio as follows:

$$\text{HPMF} = \text{RMF}/\sqrt{2} = (2\sqrt{2}\,\zeta)^{-1} \qquad \text{(B-54)}$$

To determine the two sideband frequencies ($\omega = \omega_1$ and ω_2) corresponding to half power, we combine equations (B-44) and (B-54) to obtain the following quadratic expression in ω^2:

$$(2\sqrt{2}\,\zeta)^2 = [1 - (\omega/\omega_n)^2]^2 + 4\zeta^2$$

which has the following positive roots:

$$\omega_{1,2} = \omega_n (1 \pm 2\,\zeta)^{\frac{1}{2}} \qquad \text{(B-55)}$$

It is interesting to note that equation (B-55) is identical to the analogous expression for the lightly damped Kelvin-Voigt system, i.e. $(c/c_c)^2 \ll 1$.

For small damping ($\zeta \ll \frac{1}{2}$),

$$\omega_{1,2} \approx (1 \pm \zeta)\, \omega_n$$

Thus, we get the following relation between the dimensionless bandwidth and the damping ratio ζ:

$$\boxed{(\omega_2-\omega_1)/\omega_n \approx 2\zeta} \qquad \text{(B-56)}$$

In the original Kennedy-Pancu method (reference 123), this relationship is used to determine the damping ratio from the geometry of an experimentally determined Argand plot (a polar-coordinate plot of response amplitude versus phase angle).

In terms of the quality factor Q, equation (B-56) may be rewritten as follows:

$$\boxed{Q \approx (2\zeta)^{-1}} \qquad \text{(B-57)}$$

It is interesting to note that in order for the half-power frequencies to be real, the damping ratio ζ must be no greater than $\sqrt{2}/2 \approx 0.707$. However, this is not a severe limitation for actual structural materials.

The potential energy (strain energy) stored in our single-degree-of-freedom mathematical model is given by:

$$U = \oint F_s \, du \qquad \text{(B-58)}$$

where F_s is the spring force, given by

$$F_s = ku \qquad \text{(B-59)}$$

Thus,

$$U = k\int_0^{\tilde{u}} u \, du = k\tilde{u}^2/2 \qquad \text{(B-60)}$$

Combining equations (B-48) and (B-60), we obtain

$$U_d/U = 2\pi b/k \qquad \text{(B-61)}$$

Using equations (B-41, B-42, B-43), we can rewrite equation (B-61) in the following more useful form:

$$U_d/U = 4\pi\zeta \tag{B-62}$$

or

$$\boxed{\zeta = (1/4\pi)(U_d/U)} \tag{B-63}$$

The loss tangent is defined as follows for the system considered here:

$$g \equiv b/k \tag{B-64}$$

Inserting equations (B-41, B-42, B-43) into equation (B-64) we obtain the following useful relationship:

$$\boxed{g = 2\zeta} \tag{B-65}$$

The following useful relationship, which is sometimes taken as a fundamental definition of damping (ref. 104), is obtained here by combining equations (B-63) and (B-65):

$$\boxed{g = (1/2\pi)(U_d/U)} \tag{B-66}$$

Taking the derivative of phase angle φ with respect to frequency ω, one obtains the following result from equation (B-37):

$$d\varphi/d\omega = 2bm\omega/[(k-m\omega^2)^2+b^2] \tag{B-67}$$

At resonance (subscript R), defined by $\omega=\omega_n \equiv\sqrt{k/m}$, equation (B-67) becomes:

$$(d\varphi/d\omega)_R = 2m\omega_n/b \tag{B-68}$$

Combining equations (B-42, B-43, and B-68), we obtain the following

very useful result:

$$\boxed{\zeta = [\omega_n \ (d\varphi/d\omega)_R]^{-1}} \qquad \text{(B-69)}$$

It is interesting to note that although the MF vs. ω relation, equation (B-44), is different than the corresponding relation for a Kelvin-Voigt viscously damped system, equation (B-69) is identical to its corresponding relationship for a Kelvin-Voigt system. Equation (B-69) is used to determine the damping ratio from an experimentally determined Argand diagram in the improved Kennedy-Pancu method (ref. 124).

The transient solution of the system represented by equation (B-14a) can be written as follows:

$$u' = \tilde{u}\ 'e^{-\zeta\omega_n t} \sin\ (\sqrt{1-\zeta^2}\ \omega_n t - \varphi) \qquad \text{(B-70)}$$

From its definition in equation (B-28), the logarithmic decrement δ can be determined as follows:

$$\delta = \ell n \frac{e^{-\zeta\omega_n t_1}}{e^{-\zeta\omega_n (t_1+T)}} = \ell n\ e^{\zeta\omega_n T} = \zeta\omega_n T \qquad \text{(B-71)}$$

where T is the period of damped oscillation, given by

$$T = (2\pi\zeta/\omega_n)(1-\zeta^2)^{-1/2} \qquad \text{(B-72)}$$

Thus, we now have

$$\boxed{\delta = 2\pi\zeta\ (1-\zeta^2)^{-1/2}} \qquad \text{(B-73)}$$

For small damping ($\zeta^2 << 1$), equation (B-73) can be replaced by the following approximate expression:

$$\boxed{\delta \approx 2\pi\zeta} \qquad \text{(B-74)}$$

Combining equations (B-65) and (B-74), one obtains the following:

$$\boxed{\delta = \pi g} \tag{B-75}$$

In view of equation (B-63) and since the specific energies are given by:

$$U_{dv} \equiv U_d/V, \; U_v \equiv U/V, \tag{B-76}$$

we have

$$\zeta = U_{dv}/4\pi U_s \tag{B-77}$$

However, the specific strain energy is

$$U_v = \tilde{\sigma}^2/2E \tag{B-78}$$

A power-law-damping material is defined by equation (B-22). Combining this relation with equation (B-78), one obtains:

$$\zeta = (E\, C_d/8\pi)\tilde{\sigma}^{m-2} \tag{B-79}$$

Thus, it is clear that ζ is independent of stress amplitude only for a KL (Kimball-Lovell) material (m=2). Then

$$\boxed{\zeta = E\, C_d/8\pi} \tag{B-80}$$

or, in view of equation (B-65),

$$\boxed{g = E\, C_d/4\pi} \tag{B-81}$$

Furthermore, since the logarithmic decrement of a KL material with small damping is approximately proportional to the damping ratio as shown by equation (B-74), the following approximate relation holds:

$$\boxed{\delta \approx E\, C_d/4} \tag{B-82}$$

APPENDIX C

DETAILS OF FORMULAS USED IN SECTION II

C1. Airy Stress Function and the Associated Stress, Strain, and Displacement Components

Some useful formulas pertaining to analyses carried out in Section 2.3 and 2.5 are summarized as follows. See the main text and the list of symbols for the definitions of notations used. It is to be noted that the same formula will apply to fiber as well as matrix regions with appropriate interpretations of the material property values, E and ν, etc., and choices of terms in the series. For example, in the fiber region, terms containing negative powers of ρ must be omitted to prevent a singularity in stress.

Polar stress components. - Stress components σ_r, σ_θ, and $\tau_{r\theta}$ are given by:

$$\sigma_r = a_o\rho^{-2} + 2b_o + 2b_1\rho\cos\theta - 2a_1'\rho^{-3}\cos\theta$$
$$- \sum_{n=2,3,\ldots}^{\infty} [a_n n(n-1)\rho^{n-2} + b_n (n-2)(n+1)\rho^n$$
$$+ a_n' n(n+1)\rho^{-n-2} + b_n' (n+2)(n-1)\rho^{-n}]\cos n\theta \qquad (C\text{-}1)$$

$$\sigma_\theta = -a_o\rho^{-2} + 2\,b_o + 6\,b_1\rho\cos\theta + 2\,a_1'\rho^{-3}\cos\theta$$

$$+\sum_{n=2,3,\ldots}^{\infty}\left[a_n\,n(n-1)\,\rho^{n-2} + b_n(n+2)(n+1)\rho^n + a_n'\,n(n+1)\rho^{-n-2}\right.$$

$$\left. + b_n'\,(n-2)(n-1)\,\rho^{-n}\right]\cos n\,\theta \qquad \text{(C-2)}$$

$$\tau_{r\theta} = 2\,b_1\rho\sin\theta - 2\,a_1'\rho^{-3}\sin\theta$$

$$+\sum_{n=2,3,\ldots}^{\infty}\left[a_n n(n-1)\rho^{n-2} + b_n\,n(n+1)\rho^n\right.$$

$$\left. -a_n'\,n(n+1)\,\rho^{-n-2} - b_n'\,n(n-1)\rho^{-n}\right]\sin n\,\theta \qquad \text{(C-3)}$$

Rectangular stress components. - Stress components σ_x, σ_y, and τ_{xy} are given by:

$$\sigma_x = a_o\rho^{-2}\cos 2\theta + 2\,b_o + 2\,b_1\rho\cos\theta - 2\,a_1'\rho^{-3}\cos 3\theta$$

$$-\sum_{n=2,3,\ldots}^{\infty}\left\{a_n\,n(n-1)\rho^{n-2}\cos(n-2)\theta + b_n(n+1)\rho^n[n\cos(n-2)\theta\right.$$

$$- 2\cos n\,\theta] + a_n'\,n(n+1)\rho^{-n-2}\cos(n+2)\theta$$

$$\left. + b_n'(n-1)\rho^{-n}\,[n\cos(n+2)\,\theta + 2\cos n\,\theta]\right\} \qquad \text{(C-4)}$$

$$\sigma_y = -a_o\rho^{-2}\cos 2\theta + 2\,b_o + 6\,b_1\rho\cos\theta + 2\,a_1'\rho^{-3}\cos 3\,\theta$$

$$+\sum_{n=2,3,\ldots}^{\infty}\left\{a_n\,n\,(n-1)\rho^{n-2}\cos(n-2)\,\theta + b_n(n+1)\rho^n[n\cos(n-2)\,\theta\right.$$

$$+ 2 \cos n\theta] + a_n' n(n+1)\rho^{-n-2} \cos (n+2)\theta$$

$$+ b_n'(n-1)\rho^{-n}[n \cos (n+2)\theta - 2 \cos n\theta] \Big\} \qquad \text{(C-5)}$$

$$\tau_{xy} = a_o\rho^{-2} \sin 2\theta - 2 b_1\rho \sin\theta + 2 a_1'\rho^{-3} \sin\theta (1-4\cos^2\theta)$$

$$+ \sum_{n=2,3,\ldots}^{\infty} [a_n n(n-1)\rho^{n-2} + b_n n(n+1)\rho^n - a_n' n(n+1)\rho^{-n-2}$$

$$+ b_n' n(n-1)\rho^{-n}] \sin (n+2)\theta \qquad \text{(C-6)}$$

Rectangular displacement components. - Displacement components u and v are given by:

$$E (1+\nu)^{-1}(u/R) = -a_o\rho^{-1} \cos\theta + 2 b_o(1-2\nu)\rho \cos\theta$$

$$- b_1\rho^2 [3+4 (1+\nu)] \cos 2\theta + a_1'\rho^{-2} \cos 2\theta$$

$$+ \sum_{n=2,3,\ldots}^{\infty} \Big\{-a_n n\rho^{n-1} \cos (n-1)\theta + b_n\rho^{n+1} [-n \cos (n-1)\theta$$

$$+ 2 (1-2\nu) \cos (n+1)\theta - 2 \sin n\theta \sin\theta]$$

$$+ a_n' n\rho^{-n-1} \cos (n+1)\theta$$

$$+ b_n'\rho^{-n+1} [n \cos (n+1)\theta + 2 (1-2\nu) \cos (n-1)\theta$$

$$+ 2 \sin n\theta \sin\theta] \Big\} \qquad \text{(C-7)}$$

$$E\,(1+\nu)^{-1}(v/R) = -a_o\rho^{-1}\sin\theta + 2\,b_o(1-2\nu)\rho\sin\theta + 4\,b_1\rho^2(1-\nu)\sin 2\theta$$

$$+ a_1'\rho^{-2}\sin 2\,\theta + \sum_{n=2,3,\ldots}^{\infty}\Big\{a_n\,n\rho^{n-1}\sin(n-1)\,\theta$$

$$+ b_n\rho^{n+1}[\,n\sin(n-1)\,\theta + 2\,(1-2\nu)\sin(n+1)\,\theta + 2\sin n\,\theta\cos\theta]$$

$$+ a_n'\,n\rho^{-n-1}\sin(n+1)\,\theta$$

$$+ b_n'\rho^{-n+1}\,[n\sin(n+1)\,\theta - 2\,(1-2\nu)\sin(n-1)\,\theta - 2\sin n\,\theta\cos\theta]\Big\} \qquad (C\text{-}8)$$

C2. Details of Formulas Used in Section 2.6

Dirichlet torsion function $\psi^i(\rho,\theta)$ $(i=f,m)$. - Torsion functions ψ^f and ψ^m that satisfy Laplace equation in the fiber and matrix regions, respectively are assumed to be:

$$\psi^f(\rho,\theta) = a_o + \sum_{k=1,2,\ldots}^{\infty} a_k\rho^k\cos k\,\theta \qquad (C\text{-}9)$$

$$\psi^m(\rho,\theta) = b_o + \sum_{k=1,2,\ldots}^{\infty}(b_k\rho^k + b_{-k}\rho^{-k})\cos k\,\theta \qquad (C\text{-}10)$$

Relationships among fiber-region and matrix-region coefficients a_k and b_k.- For the nth element, the distance of the fiber from the origin is $d = 2(n-1)\mu$. The boundary conditions at the fiber-matrix interface are:

$$\left.\begin{aligned} \lambda\psi^f &= \psi^m + \tfrac{1}{2}(\lambda-1)(\xi^2+\eta^2) \\ d\psi^f/dn &= d\psi^m/dn \end{aligned}\right\} \quad \text{on } C_1 \qquad \text{(C-11)}$$

On the interface C_1, $\rho=1$, hence, equations (C-11) becomes

$$\lambda\left(a_o + \sum_{k=1,2,\ldots}^{\infty} a_k \cos k\theta\right) = b_o + \sum_{k=1,2,\ldots}^{\infty} (b_k + b_{-k}) \cos k\theta$$

$$+ (\tfrac{1}{2})(\lambda-1)(1+d^2+2d\cos\theta) \qquad \text{(C-12)}$$

$$\sum_{k=1,2,\ldots}^{\infty} k\, a_k \cos k\theta = \sum_{k=1,2,\ldots}^{\infty} k\,(b_k - b_{-k}) \cos k\theta \qquad \text{(C-13)}$$

Equating the coefficients of cos k θ in equations (C-12 and 13), we have:

$$\left.\begin{aligned} a_o &= [b_o + (\lambda-1)(1+d^2)/2]/\lambda \\ a_1 &= 2\,b_1/(\lambda+1) + \lambda_1 d \\ a_k &= 2\,b_k/(\lambda+1) \quad (k=2,3,\ldots) \\ b_{-1} &= \lambda_1(b_1-d) \\ b_{-k} &= \lambda_1 b_k \quad (k=2,3,\ldots) \end{aligned}\right\} \qquad \text{(C-14)}$$

where

$$\lambda_1 \equiv (\lambda-1)/(\lambda+1) \qquad \text{(C-15)}$$

Inter-element boundary conditions between the n-th and (n+1)-th elements. - On the inter-face boundary C_2 where $\xi = (2n-1)\mu$, the local coordinate systems $[\rho_{(i)}, \theta_{(i)}], [\xi_{(i)}, \eta_{(i)}]$ $(i=1,2,\ldots n)$ are inter-related as

$$\rho_{(n)} = \rho_{(n+1)} \quad , \quad \theta_{(n)} = \pi - \theta_{(n+1)} \quad , \quad \eta_{(n)} = \eta \quad \xi_{(n)} = \xi - 2(n-1)\mu \tag{C-16}$$

Thus the boundary conditions $\Psi^m_{(n)} = \Psi^m_{(n+1)}$ and $\partial\Psi^m_{(n)}/\partial\xi = \partial\Psi^m_{(n+1)}/\partial\xi$ which warrant the displacement continuity and stress equilibrium on C_2 become, respectively:

$$[b_o^{(n)} - b_o^{(n+1)}] + \sum_{k=1,2,\ldots}^{\infty} [b_k^{(n)} - (-1)^k b_k^{(n+1)}](\rho_{(n)}^k + \lambda_1 \rho_{(n)}^{-k} \cos k\,\theta_{(n)}$$

$$= 2\,\lambda_1(d+\mu)\ \rho_{(n)}^{-1} \cos\theta_{(n)} \tag{C-17}$$

and

$$\sum_{k=1,2,\ldots}^{\infty} k[b_k^{(n)} + (-1)^k b_k^{(n+1)}][\rho_{(n)}^{k-1} \cos(k-1)\,\theta_{(n)} - \lambda_1 \rho_{(n)}^{-k-1} \cos(k+1)\,\theta_{(n)}]$$

$$= 2\lambda_1\mu\ \rho^{-2} \cos 2\,\theta_{(n)} \tag{C-18}$$

Shear stress formulas. - The shear stresses τ_{xz}^i, τ_{yz}^i $(i=f,m)$ in the fiber and matrix regions of the n-th element are calculated from equations (79 and 80) (Section 2.6) as follows:

$$\tau_{xz}^{f}/(\alpha\lambda G_m r) = (\partial\Psi^{f}/\partial\eta) - \eta$$

$$= -\sum_{k=1,2,\ldots}^{\infty} k\, a_k \rho^{k-1} \sin (k-1)\,\theta - \eta \qquad \text{(C-19)}$$

$$\tau_{yz}^{f}/(\alpha\lambda G_m r) = -(\partial\Psi^{f}/\partial\xi) + \xi$$

$$= -\sum_{k=1,2,\ldots}^{\infty} k\, a_k \rho^{k-1} \cos (k-1)\,\theta + \xi \qquad \text{(C-20)}$$

$$\tau_{xz}^{m}/(\alpha G_m r) = (\partial\Psi^{m}/\partial\eta) - \eta$$

$$= -\sum_{k=1,2,\ldots}^{\infty} k\, b_k \left[\rho^{k-1} \sin (k-1)\,\theta + \lambda_1 \rho^{-k-1} \sin (k+1)\,\theta\right]$$

$$+ (\lambda_1 d)\rho^{-2} \sin 2\theta - \eta \qquad \text{(C-21)}$$

$$\tau_{yz}^{m}/(\alpha G_m r) = -(\partial\Psi^{m}/\partial\xi) + \xi$$

$$= -\sum_{k=1,2,\ldots}^{\infty} k\, b_k \left[\rho^{k-1} \cos (k-1)\,\theta - \lambda_1 \rho^{-k-1} \cos (k+1)\,\theta\right]$$

$$+ (\lambda_1 d)\, \rho^{-2} \cos 2\theta + \xi \qquad \text{(C-22)}$$

Torsional rigidity calculations for the nth element. - The torsional rigidity $D_{(n)}$ for the n-th element is calculated from equation (83 and 84) as

$$D_{(n)}/(G_m r^4) = \lambda\,(2\,R_1 - R_2) + (2\,R_3 - R_4) \tag{C-23}$$

where

$$\left.\begin{aligned}
R_1 &= \iint_{R_f} \Psi_f \, d\xi \, d\eta = \pi\, a_o \\
R_2 &= \iint_{R_f} (\xi^2 + \eta^2)\, d\xi \, d\eta = \pi\,[(\tfrac{1}{2}) + d^2] \\
R_3 &= \iint_{R_m} \Psi^m \, d\xi \, d\eta \\
&= b_o\,(4\mu^2\delta - \pi) + b_2\,[(4/3)\,\mu^4\delta\,(1-\delta^2) + \lambda_1(\pi - \arctan\,\delta)] \\
&\quad + 4 \sum_{k=4,6,\ldots}^{\infty} b_k \mu^{k+2}/(k+2)\,(S_1 + \delta^{k+2} S_2) \\
&\quad + 4\,\lambda_1 \sum_{k=4,6,\ldots}^{\infty} b_k\,\mu^{-k+2}/(-k+2)\,(S_3 + \delta^{-k+2} S_4) \\
R_4 &= (4/3)\,\mu^4\delta\,(1+\delta^2) + 4\mu^2\,\delta\,d^2 - \pi\,[(\tfrac{1}{2}) + d^2]
\end{aligned}\right\} \tag{C-24}$$

$$\left.\begin{aligned}
S_1 &= \int_0^{\tan^{-1}\delta} \sec^{k+2}\theta \cos k\,\theta \, d\theta \\
&= \sum_{m=1}^{[(k+2)/2]} (-1)^{m-1} \delta^{2\,m-1}\, C^k_{2(m-1)}/(2\,m-1) \\
S_2 &= \sum_{\tan^{-1}\delta}^{\pi/2} \csc^{k+2}\theta \cos k\,\theta \, d\theta
\end{aligned}\right\}$$

$$= \sum_{m=1}^{[(k+2)/2]} (-1)^{m-1} \delta^{-k+2m-3} C^{k}_{2(m-1)} / (k-2m+3)$$

$$S_3 = \int_0^{\tan^{-1}\delta} \sec^{-k+2}\theta \cos k\theta \, d\theta$$

$$= (k-1)^{-1} \sum_{m=1}^{k-1} \sum_{n=1}^{[(k-m+2)/2]} (-1)^{n+1} 2^{-m} \delta^{2m-1} (1+\delta^2)^{m-k} C^{k-m+1}_{2n-1}$$

$$S_4 = -(k-1)^{-1} \Big[\sum_{m-1}^{k-1} \sum_{n=1}^{[(k-2m+3)/2]} (-1)^{m+n} 2^{2m-1} \delta^{k-2m+2n-1} (1+\delta^2)^{-k+2m-1} C^{k-2m+2}_{2n-1}$$

$$+ \sum_{m=1}^{(k-2)/2} \sum_{n=1}^{[(k-2m+3)/2]} (-1)^{m+n} 2^{2m} \delta^{k-2m+2n-3} (1+\delta^2)^{-k+2m} C^{k-2m+1}_{2(n-1)} \Big] \qquad \text{(C-25)}$$

C3. Details of Formulas Used in Section 2.7

Saint-Venant flexural function $\chi^i(\rho,\theta)$ (i=f,m). - Flexural functions χ^f and χ^m that satisfy the Laplace equation in the respective fiber and matrix regions are assumed in series form as follows:

$$\chi^f(\rho,\theta) = \sum_{k=1,3}^{\infty} a_k \rho^k \cos k\theta$$

$$\chi^m(\rho,\theta) = \sum_{k=1,3}^{\infty} (b_k \rho^k + b_{-k} \rho^{-k}) \cos k\theta \qquad \text{(C-26)}$$

Note that in equations (C-26), coefficients with even-numbered subscripts are zero due to the anti-symmetry condition with respect to the η-axis.

Relationships among fiber-region and matrix-region coefficients, a_k and b_k. - In view of the displacement-continuity and the stress-equilibrium requirements at the fiber-matrix interface, where $\rho = 1$, a_k are related to b_k, on substitution of eq. (C-26) into eqs. (109 and 110), as follows:

$$\left.\begin{aligned} a_k &= b_k + b_{-k} \qquad (k = 1,3,\ldots) \\ \lambda a_k &= b_k - b_{-k} \qquad (k = 5,7,\ldots) \\ \lambda a_1 &= b_1 - b_{-1} - (\lambda - 1)\ (3+2\bar{\nu})/4 \\ \lambda a_3 &= b_z - b_{-z} + (\lambda - 1)/4 \end{aligned}\right\} \qquad \text{(C-27)}$$

Equation (C-27) may be solved for a_k and b_{-k} in terms of b_k to yield:

$$\left.\begin{aligned} a_1 &= 2\ b_1/(\lambda+1) - \lambda_1(3+2\bar{\nu})/4 \\ a_3 &= 2\ b_3/(\lambda+1) + \lambda_1/4 \\ a_k &= 2\ b_k/(\lambda+1) \qquad (k=3,5,\ldots) \\ b_{-1} &= -\lambda_1\ [b_1 + (3+2\bar{\nu})/4] \\ b_{-3} &= -\lambda_1\ [b_3 + (1/4)] \\ b_{-k} &= -\lambda_1 b_k \qquad (k=3,5,\ldots) \end{aligned}\right\} \qquad \text{(C-28)}$$

where λ_1 is as defined in eq. (C-15).

Longitudinal thickness-shear stiffness S_{55}. - In view of notations in eq. (106), the longitudinal thickness-shear stiffness expression, eq. (120), may be written as

$$S_{55}/(E_m r) = 4\ \delta\mu^2[(\lambda'-1)(\pi/4) + 4\ \delta\mu^4/3]/P' \qquad \text{(C-29)}$$

where

$$\left.\begin{aligned}
P' &= (2/3)\ \delta\mu^4\ [\bar{\nu}(\delta^2-1) - 2\ \delta^2] \\
&\quad - (3/\mu^2)\ [(\pi a_1/4) + \iint_{A_m} \xi\ \chi^m\ d\xi\ d\eta] \\
\iint_{A_m} \xi\chi^m d\xi\ d\eta &= -(\pi b_1/4)[\mu^2\ \tan^{-1}\delta - (\pi/4) + \mu^2\delta^2(\delta^{-1} - \tfrac{1}{2}\pi \\
&\quad + \tan^{-1}\delta)] + b_{-3}[2\ (\tfrac{1}{2}\pi - \tan^{-1}\delta) + \tfrac{1}{2}\pi - 2\delta/(1+\delta^2)] \\
&\quad + 4\int_0^{\tan^{-1}\delta} G_1(\theta)\ d\theta + 4\int_{\tan^{-1}\delta}^{\pi/2} G_2(\theta)\ d\theta \\
G_1(\theta) &= (b_1/4)\ \mu^4\ \sec^2\theta + (b_3/6)(\mu\ \sec\theta)^6\ \cos\theta\cos 3\theta \\
&\quad + \sum_{k=5,7,\ldots}^{\infty} b_k\ [(k+3)^{-1}\ (\mu\ \sec\theta)^{k+3} - \lambda_1\ (-k+3)^{-1}(\mu\ \sec\theta)^{-k+3}]\cdot \\
&\quad \cdot\ \cos\theta\ \cos k\theta \\
G_2(\theta) &= (b_1/4)\ (\mu\ \delta\ \csc\theta)^4\ \cos^2\theta + (b_3/6)(\mu\delta\ \csc\theta)^6\ \cos\theta\ \cos 3\theta \\
&\quad + \sum_{k=5,7,\ldots}^{\infty} b_k\ [(k+3)^{-1}\ (\mu\delta\ \csc\theta)^{k+3} - \lambda_1\ (-k+3)^{-1}\ (\mu\delta\ \csc\theta)^{-k+3}]\cdot \\
&\quad \cdot \cos\theta\ \cos k\theta
\end{aligned}\right\} \qquad \text{(C-30)}$$

APPENDIX D

EXPERIMENTAL OBSERVATION ON THE DAMPING BEHAVIOR OF A BORON FIBER

In the damping analysis of a monofilament composite, it was found that the loss tangent $g_{E_{11}}$ associated with the in-plane Young's modulus is related to the volume fractions, stiffness ratio, and the loss tangents of the constituent materials by the equation, [eq. (156)]

$$g_{E_{11}} = (\lambda' V_f g_{E_f} + V_m g_{E_m})/(\lambda' V_f + V_m)$$

In the case of boron-epoxy composite, the stiffness ratio λ' is usually of the order of 120; whereas the loss tangent of boron is expected to be about one-tenth that of epoxy. The complete omission of the contribution of the boron fibers to the damping of the composite will then lead to a composite loss tangent which is unreasonably low.

Unfortunately, so far as known to the authors, no experimental data dealing with the damping behavior of boron material alone are available in the literature. In view of this, a crude exploratory experiment was carried out on an Avco 4.5-mil-diameter boron fiber in order to assess roughly the order of magnitude of damping in the boron material. A boron-fiber cantilever with a concentrated mass attached at its tip was deflected a certain prescribed distance and then released to oscillate in the vertical

plane. The profile of the oscillation was recorded by a 16-mm motion-picture camera (set at 64 frames per second) until the motion of the fiber decays and returns to its initial equilibrium position. The decaying sinusoidal motion of the concentrated mass at the fiber tip is then reconstructed from the frame-by-frame observation of the film. The experiment was repeated several times with different initial deflections.

The logarithmic decrement was obtained from the displacement versus time plots of the fiber tip (figure D-1) and then related to the loss tangent using eq. (B-75) from Appendix B. Averages of several runs were summarized as in figure D-2, where logarithmic decrements δ based on the number of cycles elapsed were calculated for three cases with initial deflections equal to 1.5, 1.0, and 0.5 inch, respectively. These curves show clearly the amplitude dependency of the logarithmic decrement which is attributed mainly to the air damping. In view of the air damping which predominated, the loss tangent at small deflections, as estimated from this experiment, is of the order of 0.02 to 0.05, which is roughly ten times that of the estimated loss tangent for boron in vacuum (see Section IV). It is concluded that, in order to assess the material damping of a boron fiber, the experiment must be carried out in vacuum to eliminate the effects of air damping which is both nonlinear and amplitude-dependent.

APPENDIX E

COMPUTER PROGRAM DOCUMENTATION

The computer program for computing the stiffnesses and the associated loss tangents consists of one lead-in program and ten subroutine programs.

The lead-in program is concerned with the input of the material data, calling of each subprogram, and the output of the computed results.

The input data consist of various pertinent material data such as Young's modulus, shear modulus, Poisson's ratio, and their respective loss tangents for specific frequencies as listed in Tables V-IX.

Each subprogram is concerned with the calculation of a specific stiffness and associated loss tangent based on the input data. For example, subprogram COMPE11 calculates the major Young's modulus E_{11} and the associated loss tangent $g_{E_{11}}$.

Each subprogram is designed to accomplish three functions:

1. Generation of the parameters necessary for solution,
2. Evaluation of the stiffness, and
3. Evaluation of the loss tangent.

The program was written in FORTRAN IV language as prescribed

in IBM System Reference Library Form C-28-6274-3.

A complete listing of the computer program is presented at the end of this report.

REFERENCES

1. Ekvall, J.C.: Structural Behavior of Monofilament Composites. AIAA 6th Structures and Materials Conf., Palm Springs, Calif., Apr. 1965, pp. 250-263.

2. Lekhnitskki, S.G.: Anisotropic Plates, 2nd. ed., (English Translation). Gordon and Breach, N.Y., 1968, p. 41.

3. Ashton, J.E.; Halpin, J.C.; and Petit, P.H.: Primer on Composite Materials: Analysis. Technomic Publishing Company, Inc., Stamford, Conn., 1969, Ch. 3.

4. Chamis, C.C.; and Sendeckyj, G.P.: Critique on Theories Predicting Thermoelastic Properties of Fibrous Composites. J. Composite Matls., vol. 2, no. 3, July 1968, pp. 332-358.

5. Chambers, R.E.; and McGarry, F.J.: Shear Effects in Glass Fiber Reinforced Plastics Laminates. ASTM Bulletin, no. 238, May 1959, pp. 38-41.

6. Khischenko, Yu M.: Effect of Shear on the Modulus of Elasticity of Specimens of Glass Fiber Reinforced Plastics Tested in Transverse Bending. Industrial Laboratory, vol. 30, no. 6, June 1964, pp. 937-939.

7. Lazan, B.J.: Damping of Materials and Members in Structural Mechanics.

Pergamon Press, 1968, Oxford, England.

8. Pottinger, M.G.: Material Damping of Glass Fiber-Epoxy and Boron Fiber-Aluminum Composites. Rept. ARL 70-0237, Aerospace Research Laboratories, Wright-Patterson Air Force Base, Ohio, Oct. 1970 (AD-721191).

9. Schultz, A.B.; and Tsai, S.W.: Dynamic Moduli and Damping Ratios in Fiber-Reinforced Composites. J. Composite Matls., vol. 2, no. 3, July 1968, pp. 368-379.

10. Schultz, A.B.; and Tsai, S.W.: Measurements of Complex Dynamic Moduli for Laminated Fiber-Reinforced Composites. J. Composite Matls., vol. 3, no. 3, July 1969, pp. 434-443.

11. James, W.L.: Calculation of Vibration Damping in Sandwich Construction from Damping Properties of the Cores and Facings. Rept. 1888, Forest Products Laboratory, U.S. Dept. of Agriculture, Madison, Wis., Dec. 1962.

12. Nordby, G.M.; Crisman, W.C.; and Bert, C.W.: Dynamic Elastic, Damping, and Fatigue Characteristics of Fiberglass-Reinforced Sandwich Structure. Rept. USAAVLABS TR 65-60, U.S. Army Aviation Materiel Laboratories, Ft. Eustis, Va., Oct. 1965 (AD-623128).

13. Bert, C.W.; Wilkins, D.J., Jr.; and Crisman, W.C.: Damping in Sandwich Beams with Shear-Flexible Cores. J. Eng. Industry, Trans. ASME, vol. 89B, no. 4, Nov. 1967, pp. 662-670.

14. Clary, R.R.: Vibration Characteristics of Unidirectional Filamentary Composite Material Panels. Composite Materials: Testing and Design (Second Conference), Amer. Soc. Testing & Matls., Spec. Tech. Publ. 497, 1972.

15. Bert, C.W.; Mayberry, B.L.; and Ray, J.D.: Vibration Evaluation of Sandwich Conical Shells with Fiber-Reinforced Composite Facings. Rept. USAAVLABS TR 68-85, U.S. Army Aviation Materiel Laboratories, Ft. Eustis, Va., Dec. 1968 (AD-685318).

16. Ray, J.D.; Bert, C.W.; and Egle, D.M.: The Application of Kennedy-Panchu Method to Experimental Vibration Studies of Complex Shell Structures. Shock and Vib. Bull., Bull. 39, Pt. 3, U.S. Dept. Defense, Jan. 1969, pp. 107-115.

17. Bert, C.W.; and Ray, J.D.: Vibrations of Orthotropic Sandwich Conical Shells with Free Edges. Int. J. Mech. Sci., vol. 11, no. 9, Sept. 1969, pp. 767-779.

18. Richter, H.P.H.: Photographic Method for Measuring Material Damping and Dynamic Young's Modulus at Low Frequencies Applied to a Fiberglass Reinforced Resin Structure. Proc. 18th Ann. Tech. & Mgt. Conf., Reinf. Plastics Div., Soc. Plastics Industry, Inc., 1963, sec. 4-D.

19. Kerr, L.; and Lazan, B.J.: Damping and Fatigue Properties of Sandwich Configuration in Flexure. Rept. ASD TR 61-646, Aeron. Systems Div., Wright-Patterson Air Force Base, Ohio, Nov. 1961 (AD-272016).

20. Hashin, Z.: Complex Moduli of Viscoelastic Composites - I. General Theory and Application to Particulate Composites. Int. J. Solids & Structures, vol. 6, no. 5, May 1970, pp. 539-552.

21. Hashin, Z.: Complex Moduli of Viscoelastic Composites- II. Fiber Reinforced Materials. Int. J. Solids & Structures, vol. 6, no. 6, June 1970, pp. 797-807.

22. Kimball, A.L.; and Lovell, D.E.: Internal Frictions in Solids. Physical Review, ser. 2, vol. 30, 1927, pp. 948-959.

23. Miller, K.D., Jr.; and Breslau, S.M.: Fiber-Reinforced Plastic as a Rocket Structural Material. Jet Propulsion, vol. 26, no. 11, Nov. 1956, pp. 969-972.

24. Rosato, D.V.; and Grove, C.S., Jr.: Filament Winding: Its Development, Manufacture, Applications and Design. John Wiley & Sons, Inc., N.Y. 1964.

25. Outwater, J.O., Jr.: The Mechanics of Plastics Reinforcement in Tension. Modern Plastics, vol. 33, no. 7, March 1956, p. 156ff.

26. Beer, F.: Die Festigkeitseigenschaften Kreuzweisebewehrter Kunstoffe. VDI Zeits., vol. 101, Apr. 1959, pp. 463-468.

27. Brown, R.L., Jr.: Simplified Stress Analysis of Filament Reinforced Plastic Pressure Vessels. Soc. Plastic Engrs. J., vol. 17, 1961, p. 989.

28. Ekvall, J.C.: Elastic Properties of Orthotropic Monofilament Laminates. Paper 61-Av-56, ASME Aviation Conference, Los Angeles, Calif., Mar. 12-16,

29. Greszczuk, L.B.: Theoretical and Experimental Studies on Properties and Behavior of Filamentary Composites. SPI 21st Conference, Chicago, Ill. 1966, sect. 5-B.

30. Nosarev, A.V.: Effect of Fiber Curvature of the Elastic Properties of Unidirectionally Reinforced Plastics (in Russian). Mekhanika Polimerov, vol. 3, 1967, p. 858.

31. Hill, R.: Theory of Mechanical Properties of Fiber-Strengthened Materials: III. Self-Consistent Model. J. Mech. Phys. Solids, vol. 13, Aug. 1965, pp. 189-198.

32. Whitney, J.M.; and Riley, M.B.: Elastic Properties of Fiber Reinforced Composite Materials. AIAA J., vol. 4, no. 9, Sept. 1966, pp. 1537-1542.

33. Sokolnikoff, I.S.: Mathematical Theory of Elasticity, 2nd. ed. McGraw-Hill Book Co., Inc., N.Y., 1956, Chapt. 7.

34. Tsai, S.W.: Structural Behavior of Composite Materials. NASA CR-71, 1964.

35. Hashin, Z.; and Rosen, B.W.: The Elastic Moduli of Fiber Reinforced Materials. J. Appl. Mech., vol. 31, no. 2, June 1964, pp. 233-232; errata, vol. 32, Mar. 1965, p. 219.

36. Wu, T.T.: On the Parametrization of the Elastic Moduli of Two-Phase Materials. J. Appl. Mech., vol. 32, no. 1, Mar. 1965, pp. 211-214.

37. Haener, J.; and Ashbaugh, N.: Three-Dimensional Stress Distribution in a Unidirectional Composite. J. Composite Matls., vol. 1, no. 1,

Jan. 1967, pp. 54-63.

38. Chen, C.H.; and Cheng, S., Mechanical Properties of Fiber Reinforced Composites, J. Composite Matls., vol. 1, no. 1, Jan. 1967, pp. 30-41; errata, vol. 1, no. 2, Apr. 1967, p. 207.

39. Bloom, J.M.; and Wilson, H.B.: Axial Loading of a Unidirectional Composite, J. Composite Matls., vol. 1, no. 3, July 1967, pp. 268-277.

40. Foye, R.L.: An Evaluation of Various Engineering Estimates of the Transverse Properties of Unidirectional Composites. SAMPE, National Symposia, vol. 10, 1966, p. G-31.

41. Foye, R.L.: Structural Composites. Quarterly Progress Reports no. 1 and 2, AFML Contract No. AF 33(615)-5150, 1966.

42. Bolotin, V.V.: Basic Equations of the Theory of Reinforced Media. Polymer Mechanics, vol. 1, no. 2, 1965, pp. 23-30.

43. Herrmann, G.; and Achenbach, J.D.: On Dynamic Theories of Fiber Reinforced Composites. AIAA/ASME 8th Structures, Structural Dynamics and Materials Conference, Palm Springs, Calif., Apr. 1967, pp. 112-118.

44. Chi, S.H.: Bibliography and Tabulation of Damping Properties of Nonmetallic Materials. Rept. WADD-TR-60-140, Wright Air Development Division, Wright-Patterson Air Force Base, Ohio, Sept. 1962.

45. Hashin, Z.: Viscoelastic Fiber Reinforced Materials. AIAA J., vol. 4, no. 8, Aug. 1966, pp. 1411-1417.

46. Adams, D.F.; and Doner, D.R.: Longitudinal Shear Loading of a Unidirectional Composite. J. Composite Matls., vol. 1, no. 1, Jan. 1967, pp. 4-17.

47. Hill, R.: Theory of Mechanical Properties of Fiber-Strengthened Materials: I. Elastic Behavior. J. Mech. Phys. Solids, vol. 12, 1964, pp. 199-212.

48. Bloom, J.M.: Nonconservative Behavior of Composite Materials. Rept. AFML-TR-68-10, Air Force Materials Laboratory, Wright-Patterson AFB, Ohio, Jan. 1968 (AD-666676).

49. Timoshenko, S.; and Goodier, J.N.: Theory of Elasticity, 3rd. ed. McGraw-Hill, New York, 1969, pp. 132-136.

50. Conway, H.D.: The Approximate Analysis of Certain Boundary Value Problems. J. Appl. Mech., vol. 27, no. 2, June 1960, pp. 275-277.

51. Conway, H.D.; and Leissa, A.W.: Application of the Point Matching Method to Shallow Spherical Shell Theory. J. Appl. Mech., vol. 29, no. 4, Dec. 1962, pp. 745-747.

52. Hulbert, L.E.; and Niedenfuhr, F.W.: On the Numerical Solution of Certain Classes of Boundary Value Problems. Presented at the 19th Annual Meeting of the Association for Computing Machinery, Denver, Colo., Aug. 27, 1963.

53. Abolin'sh, D.S.: Compliance Tensor for an Elastic Material Reinforced in One Direction. Polymer Mechanics, vol. 1, no. 4, 1965, pp. 28-32.

54. Hill, R.: Elastic Properties of Reinforced Solids: Some Theoretical Principles. J. Mech. Phys. Solids, vol. 11, 1963, pp. 357-372.

55. Paul, B.: Prediction of Elastic Constants of Multiphase Materials. Trans. AIME, vol. 218, no. 1, Feb. 1960, pp. 36-41.

56. Adams, D.F.; and Doner, D.R.: Transverse Normal Loading of a Unidirectional Composite. J. Composite Matls., vol. 1, no. 2, Apr. 1967, pp. 152-173.

57. Muskhelishivili, N.I.: Some Basic Problems of the Mathematical Theory of Elasticity, 4th ed. P. Noordhoff, Ltd., Groningen, The Netherlands, 1963, sec. 139, pp. 609-626.

58. Timoshenko, S.: Strength of Materials, Part I, 2nd. ed, D. Van Nostrand Co., Inc., New York, 1940, pp. 170-171.

59. Timoshenko, S.: On the Correction for Shear of the Differential Equation for Transverse Vibrations of Prismatic Bars. Philosophical Magazine, ser. 6, vol. 41, 1921, pp. 744-746.

60. Mindlin, R.D.; and Deresiewicz, H.: Timoshenko's Shear Coefficient for Flexural Vibrations of Beams. Proc. 2nd. U.S. Nat. Congr. Appl. Mech., 1954, pp. 175-178.

61. Roark, R.J.: Formulas for Stress and Strains, 3rd. ed., McGraw-Hill Book Company, Inc., New York, 1954, pp. 119-121.

62. Cowper, G.P.: The Shear Coefficient in Timoshenko's Beam Theory. J. Appl. Mech., vol. 33, no. 2, June 1966, pp. 335-340.

63. Bert, C.W.; and Siu, C.C.: Vibration and Damping of Laminated, Composite-Material Plates Including Thickness-Shear Effects. Final Report (Part II), NASA Research Grant NGR-37-003-055, School of Aerospace, Mechanical & Nuclear Engineering, Univ. of Oklahoma, Norman, Okla., Mar. 1972.

64. Hadcock, R.N.: Boron-Epoxy Aircraft Structures, Chap. 24 in Handbook of Fiberglass and Advanced Plastics Composites, edited by G. Lubin. Van Nostrand Reinhold, N.Y., 1969, pp. 628-660.

65. Bert, C.W.: Lecture Notes on Introduction to Analysis and Design of Composite-Material Structures. Univ. of Oklahoma, Jan. 1970.

66. Halpin, J.C.; and Tsai, S.W.: Environmental Factors in Composite Materials Design. AFML-TR-67-423, Air Force Materials Laboratory, Wright-Patterson AFB, Ohio, 1967.

67. Hermans, J.J.: The Elastic Properties of Fiber Reinforced Materials When the Fibers are Aligned. Proc. Konikl. Nederl. Akad. van Wetenschapp., Amsterdam, vol. B70, no. 1, 1967, pp. 1-9.

68. Tsai, S.W.: Mechanics of Composite Materials, Part I - Introduction. AFML-TR-66-149, Part I, Air Force Materials Laboratory, Wright-Patterson AFB, Ohio, June 1966.

69. Hulbert, L.E.; and Rybicki, E.F.: Boundary Point Least Squares Analysis of the Free Edge Effects in Some Unidirectional Fiber Composites. J. Composite Matls., vol. 5, no. 2, April 1971,

pp. 164-175.

70. Dow, N.F.; and Rosen, B.W.: Evaulation of Filament-reinforced Composites for Aerospace Structural Applications. NASA Report CR-207, April 1965.

71. Wilson, H.B., Jr.; and Goree, J.G.: Transverse Shear Loading in an Elastic Matrix Containing Two Elastic Circular Cylindrical Inclusions, Mathematical Studies of Composite Materials III. Rohm and Haas Co. Report S-98, Huntsville, Alabama, June 1966, pp. 30-38.

72. Margolin, G.G.: Elasticity Modulus in the Bending of Thin Specimens of a Unidirectional Glass Reinforced Plastic. Polymer Mechanics, vol. 3, no. 4, 1967, pp. 737-740.

73. Bert, C.W.: Flexural Micromechanics of a Composite Material Containing Large-Diameter Fibers. Presented at the 60th Annual Meeting of the Oklahoma Academy of Science, Norman, Okla., Dec. 1971; to be published in Proceedings, vol. 52, 1972.

74. Ely, J.F.; and Zienkiewicz, O.C.: Torsion of Compound Bars - A Relaxation Solution. International J. Mechanical Sciences, vol. 1, no. 4, July 1960, pp. 356-365.

75. Heaton, M.D.: A Calculation of the Elastic Contants of a Unidirectional Fiber-Reinforced Composite. Brit. J. Appl. Phys. (J. Phys. D.), ser. 2, vol. 1, 1968, pp. 1039-1048.

76. Wu, C.; and Vinson, J.R.: On the Nonlinear Oscillations of Plates Composed of Composite Materials. J. Comp. Matls., vol. 3, no. 3, July 1969, pp. 548-561.

77. Gemant, A: The Measurement of Solid Friction of Plastics. J. Appl. Phys., vol.11, no. 10, Oct. 1940, pp. 647-653.

78. Blum, S.L.: Some Physical Factors Affecting the Internal Damping of Glass. J. Amer. Ceramic Soc., vol. 38, no. 6, June 1955, pp. 205-210.

79. Tamchyna, J.; and V. Zvonar: Static and Dyanmic Properties of Glass-Reinforced Plastics. Polymer Mechanics, vol. 1, no. 1, Jan.-Feb. 1965, pp. 102-105.

80. Masri, S.F.: Cumulative Damages Caused by Shock Excitation. Shock and Vibration Bull., Bull. 35, pt. 3, Jan. 1966, pp. 57-71.

81. Gustafson, A.J.; Mazza, L.T.; Rodgers, R.L.; and McIlwean, E.H.: Development of Test Methods for Measuring Damping of Fiber-Reinforced Materials, USAAVLABS Technical Reprot 70-42, U.S. Army Aviation Materiel Laboratories, Fort Eustis, Va., June 1970.

82. Granick, N.; and Stern, J.E.: Material Damping of Aluminum by a Resonant-Dwell Technique. NASA TN D-2893, Clearing House for Federal Scientific and Technical Information, Springfield, Va., 1965.

83. Bodner, S.R.; and Fraser, A.F.: Vibrations and Wave Propagation in

Aluminum Alloys at Elevated Temperatures. Trans. Soc. Rheology, vol. 6, no. 1, 1962, pp. 157-177.

84. Papirno, R.; and Slepetz, J.: Determination of Matrix and Filament Stress-Strain Properties from Tests Made on Composites, Composite Matls., Paris, Apr. 2-3, 1970), NATO, Advisory Group for Aerospace Res. and Dev., AGARD-CP-83-71, Sept. 1971. AD-732741.

85. Bert, C.W.: Plasticity and Creep Analysis of Filamentary Metal Matrix Composites SC-DR-720055, Sandia Laboratories, Albuquerque, N.M., March 1972.

86. Mazza, L.T.; Paxon, E.B.; and Rodgers, R.L.: Measurement of Damping Coefficients and Dynamic Modulus of Fiber Composites. USAAVLABS-TN-2, (AD-8690 25), U.S. Army Aviation Materiel Laboratories, Fort Eustis, Va., May 1971.

87. Chi, C.C.: Forced Vibration of Laminated Anisotropic Plates Including Thickness-Shear and Damping Effects. Ph.D. dissertation, Univ. of Oklahoma, Norman, Okla., May 1972

88. Wegel, R.L.; and Walther, H.: Internal Dissipation in Solids for Small Cyclic Strains. Physics, vol. 6, 1935, pp. 141-157.

89. Lazan, B.J.: A Study with New Equipment of the Effects of Fatigue Stress on the Damping Capacity and Elasticity of Mild Steel. Trans. Am. Soc. Metals, vol. 42, 1950, pp. 499-549.

90. Bishop, R.E.D.: The Theory of Damping Forces in Vibration Theory. J. Roy. Aeron. Soc., vol. 59, no. 539, Nov. 1955, pp. 738-742.

91. Soroka, W.W.: Note on the Relations Between Viscous and Structural Damping Coefficients. J. Aeron. Sci., vol. 16, no. 7, Jul. 1949, pp. 409-410, 448.

92. Theodorsen, T.; and Garrick, I.E.: Mechanism of Flutter- A Theoretical and Experimental Investigation of the Flutter Problem. NACA TR 685, 1940.

93. Scanlan, R.H.; and Rosenbaum, R.: Introduction to the Study of Aircraft Vibration and Flutter. Macmillan, 1951; Dover, 1968.

94. Myklestad, N.O.: The Concept of Complex Damping. J. Appl. Mech., vol. 19, no. 3, Sep. 1952, pp. 284-286.

95. Lancaster, P.: Free Vibration and Hysteretic Damping. J. Roy. Aeron. Soc., vol. 64, no. 592, Apr. 1960, p. 229.

96. Reid, T.J.: Free Vibration and Hysteretic Damping. J. Roy. Aeron. Soc., vol. 60, no. 544, Apr. 1956, p. 283.

97. Milne, R.D.: A Constructive Theory of Linear Damping. Paper C.4, Symposium on Structural Dynamics, Loughborough Univ. of Technology, Loughborough, England, 1970.

98. Caughey, T.K.: Vibration of Dynamic Systems with Linear Hysteretic Damping (Linear Theory). Proc. 4th. U.S. Nat. Congr. Appl. Mech., vol. 1, 1962, pp. 87-97.

99. Paley, R.E.A.C.; and Wiener, N.: Fourier Transforms in the Complex Domain. Am. Math. Soc. Colloquium Publicat., vol. 19, 1934.

100. Garcia - Moliner, F.; and Thomson, R.: Linear Response Functions and the Phenomenological Equations of Internal Friction. J. Appl. Phys., vol. 37, no. 1, Jan. 1966, pp. 83-89.

101. Fraeijs de Veubeke, B.M.: Influence of Internal Dampikng on Air-Craft Resonance. AGARD Manual on Elasticity, vol. 1, chap. 3, 1960.

102. Crandall, S.H.: Dynamic Response of Systems with Structural Damping. Air, Space, and Instruments (C.S. Draper Anniv. Vol.), S. Lees, ed. McGraw-Hill Book Co., 1963, pp. 183-193.

103. Crandall, S.H.: The Role of Damping in Vibration Theory. J. Sound & Vib., vol. 11, no. 1, Jan. 1970, pp. 3-18.

104. Pinsker, W.: Structural Damping. J. Aeron. Sci., vol. 16, no. 11, Nov. 1949, p. 699.

105. Scanlan, R.H.; and Mendelson, A.: Structural Damping. AIAA J., vol. 1, no. 4, Apr. 1963, pp. 938-939.

106. Naylor, V.D.: Some Fallacies in Modern Damping. J. Sound & Vib., vol. 11, no. 2, Feb. 1970, pp. 278-280.

107. Scanlan, R.H.: Linear Damping Models and Causality in Vibrations. J. Sound & Vib., vol. 13, no. 4, Dec. 1970, pp. 499-509.

108. Bishop, R.E.D.: The Behavior of Damped Linear System in Steady

Oscillation. Aeron. Quart., vol. 7, no. 2, May 1956, pp. 156-168.

109. Cunningham, H.J.: In Defense of Modern Damping Theory in Flutter Analysis. J. Sound & Vib., vol. 14, no. 1, Jan. 1971, pp. 142-144.

110. Bland, D.R.: The Theory of Linear Viscoelasticity. Pergamon Press, 1960, pp. 3-4.

111. Parke, S.: Logarithmic Decrements at High Damping. Brit. J. Appl. Phys., vol. 17, no. 2, Feb. 1966, pp. 271-273.

112. Flugge, W.: Viscoelasiticty. Blaisdell Publishing Company, 1967, p. 14.

113. Hobbs, G.K.: Methods of Treating Damping in Structures. AIAA Paper 71-349, presented at the AIAA/ASME 12th Structures, Structural Dynamics and Materials Conference, Anaheim, Calif., Apr. 19-21, 1971.

114. Huang, T.C.; and Huang, C.C.: Free Vibrations of Viscoelastic Timoshenko Beams. J. Appl. Mech., vol. 38, no. 2, June 1971, pp. 515-521.

115. Granick, N.; and Stern, J.E.: Material Damping of Aluminum by Resonance-Dwell Technique. Shock & Vib. Bull., Bull. 34, Pt. 5, U.S. Dept. Defense, Feb. 1965, pp. 177-195.

116. Biot, M.A.: Linear Thermodynamics and the Mechanics of Solids. Proc. 3rd. U.S. Nat. Congr. Appl. Mech., 1958, pp. 1-18.

117. Neubert, H.K.P.: A Simple Model Representing Internal Damping in Solid Materials. Aeron. Quart., vol. 14, no. 2, May 1963, pp.

187-210.

118. Boltzmann, L.: Zur Theorie der elastische Nachwirkung. Annalen der Physik und Chemie, suppl. 7, 1876, pp. 624-654.

119. Volterra, E.: Vibrations of Elastic Systems Having Hereditary Characteristics. J. Appl. Mech., vol. 17, no. 4, Dec. 1950, pp. 363-371.

120. Pisarenko, G.S.: Vibrations of Elastic Systems Taking Account of Energy Dissipation in the Material. Kiev, 1955; Engl. transl., WADD TR-60-582, Wright Air Development Div., Feb. 1962 (AD-274743).

121. Rosenblueth, E.; and Herrera, I.: On a Kind of Hysteretic Damping. J. Eng. Mech. Div., Proc. ASCE, vol. 90, no. EM4, Aug. 1964, pp. 37-48.

122. Chang, C.S.; and Bieber, R.E.: Synthesis of Structural Damping. AIAA J., vol. 6, no. 4, Apr. 1968, pp. 718-719.

123. Kennedy, C.C.; and Pancu, C.D.P.: Use of Vectors in Vibration Measurement and Analysis. J. Aeron. Sci., vol. 14, no. 11, Nov. 1947, pp. 603-625.

124. Pendered, J.W.; and Bishop, R.E.D.: A Critical Introduction to Some Industrial Resonance Testing Techniques. J. Mech. Eng. Sci., vol. 5, no. 4, Dec. 1963, pp. 345-367.

125. Kolsky, H.: Stress Waves in Solids. Oxford Univ. Press, 1963; Dover, 1963.

TABLE I. COMPARISON OF LONGITUDINAL IN-PLANE POISSON'S RATIO.

E_f/E_m	Longitudinal In-Plane Poisson's Ratio ν_{12}		V_f
	Eq. (30)	Eq. (38)	
120.	0.331	0.322	0.3
	0.317	0.311	0.4
	0.316	0.300	0.5
	0.292	0.288	0.6
5.3	0.286	0.282	0.4
	0.273	0.270	0.5
	0.260	0.258	0.6
24.1	0.299	0.294	0.4
	0.284	0.282	0.5
	0.269	0.268	0.6

TABLE II. LONGITUDINAL FLEXURAL STIFFNESS EFFICIENCY OF MONOFILAMENT COMPOSITES.

Composite	E_f/E_m	δ	μ	V_f	$E_{11}^{(b)}/E_{11}$	
					Eq. (48)	Eq. (142)
Steel-Epoxy	74	1.00	1.11	0.636	0.616	0.608
		1.00	1.06	0.708	0.683	0.677
		0.95	1.11	0.673	0.683	0.677
		0.90	1.11	0.707	0.755	0.750
		0.95	1.06	0.746	0.755	0.750
		0.93	1.16	0.743	0.730	0.725
		1.00	1.00	0.785	0.755	0.750
S glass-Epoxy	24	0.85	1.38	0.482	0.578	0.542
		0.90	1.23	0.572	0.636	0.608
		0.95	1.11	0.673	0.697	0.677
Boron-Epoxy	120	0.85	1.38	0.482	0.549	0.542
		0.90	1.23	0.572	0.614	0.608
		0.95	1.11	0.673	0.681	0.677
Boron-Al.	6	0.85	1.38	0.482	0.678	0.542

TABLE III. COMPARISONS OF POISSON FLEXURAL STIFFNESS FOR COMPOSITES HAVING SQUARE TYPICAL ELEMENTS.

Composite	Fiber Volume Fraction	$[D_{12}]_{eq.\ (50)} / [D_{12}]_{eq.\ (4)}$
Boron-Epoxy	0.4	0.725
	0.5	0.593
	0.6	0.567
Glass-Epoxy	0.4	0.780
	0.5	0.657
	0.6	0.638
Boron-Al.	0.4	0.930
	0.5	0.835
	0.6	0.833

TABLE IV. COMPARISONS OF IN-PLANE LONGITUDINAL SHEAR MODULUS AND EQUIVALENT SHEAR MODULUS AS CALCULATED FROM THE TORSION ANALYSIS.

Composite	G_f/G_m	Fiber volume fraction	Ratio G_{66}/G_m	
			In-Plane	Equivalent in Torsion
Boron-Epoxy	135.	0.4	2.30	25.30
		0.5	3.23	38.98
		0.6	4.67	55.66
E Glass-Epoxy	23.4	0.4	2.16	5.04
		0.5	2.84	7.34
		0.6	3.80	10.13
Boron-Al.	6.7	0.4	1.84	2.01
		0.5	2.22	2.58
		0.6	2.72	3.29

TABLE V. - ELASTIC AND DAMPING PROPERTIES OF BORON

FREQ	K	E	GE	G	GG	RNU	GNU
HZ	1.E6 PSI	1.E6 PSI	PER CENT	1.E6 PSI	PER CENT		PER CENT
5.	0.322E 02	0.562E 02	0.129E 00	0.232E 02	0.160E 00	0.209E 00	-0.179E 00
7.	0.322E 02	0.548E 02	0.130E 00	0.225E 02	0.160E 00	0.216E 00	-0.170E 00
10.	0.322E 02	0.537E 02	0.131E 00	0.219E 02	0.160E 00	0.222E 00	-0.163E 00
20.	0.322E 02	0.523E 02	0.134E 00	0.212E 02	0.163E 00	0.229E 00	-0.158E 00
50.	0.322E 02	0.510E 02	0.136E 00	0.206E 02	0.165E 00	0.236E 00	-0.152E 00
70.	0.322E 02	0.506E 02	0.138E 00	0.204E 02	0.167E 00	0.238E 00	-0.151E 00
100.	0.322E 02	0.503E 02	0.141E 00	0.202E 02	0.170E 00	0.239E 00	-0.153E 00
200.	0.322E 02	0.498E 02	0.146E 00	0.200E 02	0.176E 00	0.242E 00	-0.155E 00
500.	0.322E 02	0.494E 02	0.154E 00	0.198E 02	0.185E 00	0.244E 00	-0.161E 00
700.	0.322E 02	0.493E 02	0.158E 00	0.198E 02	0.190E 00	0.244E 00	-0.164E 00
1000.	0.322E 02	0.492E 02	0.161E 00	0.197E 02	0.193E 00	0.245E 00	-0.167E 00
2000.	0.322E 02	0.490E 02	0.168E 00	0.196E 02	0.202E 00	0.246E 00	-0.172E 00

TABLE VI. - ELASTIC AND DAMPING PROPERTIES OF EPOXY A

FREQ	K	E	GE	G	GG	RNU	GNU
HZ	1.E6 PSI	1.E6 PSI	PER CENT	1.E6 PSI	PER CENT		PER CENT
5.	0.488E 00	0.444E 00	0.160E 01	0.164E 00	0.177E 01	0.348E 00	-0.696E 00
7.	0.488E 00	0.448E 00	0.161E 01	0.166E 00	0.179E 01	0.346E 00	-0.709E 00
10.	0.488E 00	0.452E 00	0.162E 01	0.167E 00	0.180E 01	0.345E 00	-0.723E 00
20.	0.488E 00	0.460E 00	0.165E 01	0.171E 00	0.184E 01	0.342E 00	-0.755E 00
50.	0.488E 00	0.475E 00	0.173E 01	0.177E 00	0.193E 01	0.337E 00	-0.830E 00
70.	0.488E 00	0.480E 00	0.179E 01	0.179E 00	0.200E 01	0.336E 00	-0.873E 00
100.	0.488E 00	0.475E 00	0.183E 01	0.177E 00	0.205E 01	0.337E 00	-0.878E 00
200.	0.488E 00	0.420E 00	0.200E 01	0.154E 00	0.221E 01	0.356E 00	-0.804E 00
500.	0.488E 00	0.364E 00	0.230E 01	0.132E 00	0.250E 01	0.375E 00	-0.761E 00
700.	0.488E 00	0.355E 00	0.252E 01	0.128E 00	0.274E 01	0.378E 00	-0.806E 00
1000.	0.488E 00	0.348E 00	0.263E 01	0.125E 00	0.285E 01	0.381E 00	-0.820E 00
2000.	0.488E 00	0.340E 00	0.310E 01	0.122E 00	0.336E 01	0.383E 00	-0.937E 00

TABLE VII. - ELASTIC AND DAMPING PROPERTIES OF EPOXY B

FREQ	K	E	GE	G	GG	RNU	GNU
HZ	1.E6 PSI	1.E6 PSI	PER CENT	1.E6 PSI	PER CENT		PER CENT
5.	0.244E 00	0.256E 00	0.160E 01	0.965E-01	0.181E 01	0.325E 00	-0.860E 00
7.	0.244E 00	0.290E 00	0.161E 01	0.111E 00	0.185E 01	0.301E 00	-0.105E 01
10.	0.244E 00	0.328E 00	0.162E 01	0.128E 00	0.190E 01	0.275E 00	-0.131E 01
20.	0.244E 00	0.415E 00	0.165E 01	0.170E 00	0.203E 01	0.216E 00	-0.216E 01
50.	0.244E 00	0.490E 00	0.173E 01	0.210E 00	0.222E 01	0.165E 00	-0.350E 01
70.	0.244E 00	0.500E 00	0.179E 01	0.215E 00	0.231E 01	0.158E 00	-0.385E 01
100.	0.244E 00	0.489E 00	0.183E 01	0.209E 00	0.235E 01	0.165E 00	-0.368E 01
200.	0.244E 00	0.420E 00	0.200E 01	0.173E 00	0.247E 01	0.213E 00	-0.269E 01
500.	0.244E 00	0.364E 00	0.230E 01	0.145E 00	0.275E 01	0.251E 00	-0.227E 01
700.	0.244E 00	0.355E 00	0.252E 01	0.141E 00	0.300E 01	0.257E 00	-0.237E 01
1000.	0.244E 00	0.348E 00	0.263E 01	0.137E 00	0.312E 01	0.262E 00	-0.238E 01
2000.	0.244E 00	0.340E 00	0.310E 01	0.134E 00	0.366E 01	0.267E 00	-0.268E 01

TABLE VIII. - ELASTIC AND DAMPING PROPERTIES OF ALU 2224-T3

FREQ	K	E	GE	G	GG	RNU	GNU
HZ	1.E6 PSI	1.E6 PSI	PER CENT	1.E6 PSI	PER CENT		PER CENT
5.	0.106E 02	0.107E 02	0.980E-01	0.402E 01	0.110E 00	0.331E 00	-0.498E-01
7.	0.106E 02	0.107E 02	0.121E 00	0.403E 01	0.136E 00	0.331E 00	-0.617E-01
10.	0.106E 02	0.107E 02	0.150E 00	0.404E 01	0.169E 00	0.330E 00	-0.767E-01
20.	0.106E 02	0.107E 02	0.211E 00	0.405E 01	0.237E 00	0.330E 00	-0.108E 00
50.	0.106E 02	0.108E 02	0.176E 00	0.406E 01	0.198E 00	0.329E 00	-0.907E-01
70.	0.106E 02	0.108E 02	0.142E 00	0.407E 01	0.160E 00	0.329E 00	-0.733E-01
100.	0.106E 02	0.108E 02	0.110E 00	0.407E 01	0.124E 00	0.329E 00	-0.568E-01
200.	0.106E 02	0.108E 02	0.110E 00	0.407E 01	0.124E 00	0.329E 00	-0.568E-01
500.	0.106E 02	0.108E 02	0.340E-01	0.407E 01	0.383E-01	0.329E 00	-0.175E-01
700.	0.106E 02	0.108E 02	0.290E-01	0.407E 01	0.327E-01	0.329E 00	-0.149E-01
1000.	0.106E 02	0.108E 02	0.250E-01	0.407E 01	0.282E-01	0.329E 00	-0.129E-01
2000.	0.106E 02	0.108E 02	0.210E-01	0.406E 01	0.236E-01	0.329E 00	-0.108E-01

TABLE IX. - ELASTIC AND DAMPING PROPERTIES OF E-GLASS

FREQ	K	E	GE	G	GG	RNU	GNU
HZ	1.E6 PSI	1.E6 PSI	PER CENT	1.E6 PSI	PER CENT		PER CENT
5.	0.630E 01	0.107E 02	0.270E 00	0.442E 01	0.333E 00	0.215E 00	-0.356E 00
7.	0.630E 01	0.107E 02	0.265E 00	0.443E 01	0.327E 00	0.215E 00	-0.351E 00
10.	0.630E 01	0.107E 02	0.260E 00	0.443E 01	0.321E 00	0.214E 00	-0.345E 00
20.	0.630E 01	0.108E 02	0.258E 00	0.446E 01	0.318E 00	0.213E 00	-0.346E 00
50.	0.630E 01	0.108E 02	0.260E 00	0.447E 01	0.321E 00	0.212E 00	-0.351E 00
70.	0.630E 01	0.108E 02	0.265E 00	0.448E 01	0.327E 00	0.212E 00	-0.358E 00
100.	0.630E 01	0.108E 02	0.310E 00	0.448E 01	0.383E 00	0.212E 00	-0.419E 00
200.	0.630E 01	0.108E 02	0.310E 00	0.447E 01	0.383E 00	0.212E 00	-0.417E 00
500.	0.630E 01	0.108E 02	0.420E 00	0.444E 01	0.518E 00	0.214E 00	-0.559E 00
700.	0.630E 01	0.107E 02	0.480E 00	0.443E 01	0.592E 00	0.215E 00	-0.635E 00
1000.	0.630E 01	0.107E 02	0.550E 00	0.440E 01	0.678E 00	0.216E 00	-0.720E 00
2000.	0.630E 01	0.105E 02	0.700E 00	0.433E 01	0.860E 00	0.220E 00	-0.888E 00

TABLE X. - IN-PLANE LONGITUDINAL YOUNG'S MODULUS AND ASSOCIATED LOSS TANGENT FOR A BORON-ALUMINUM 2024-T3 MONOFILAMENT COMPOSITE

IDATA 3 RMU 1.401 DELTA 1.000 VF 0.400

*****BORON-ALUMINUM 2024-T3*****

FREQUENCY HERTZ	E11 1.E6 PSI	GE11 PER CENT	EF/EM	E11/EM
0.5000E 01	0.2891E 02	0.1221E 00	0.5252E 01	0.2702E 01
0.7000E 01	0.2835E 02	0.1280E 00	0.5121E 01	0.2649E 01
0.1000E 02	0.2791E 02	0.1354E 00	0.5019E 01	0.2608E 01
0.2000E 02	0.2735E 02	0.1521E 00	0.4888E 01	0.2556E 01
0.5000E 02	0.2689E 02	0.1456E 00	0.4722E 01	0.2489E 01
0.7000E 02	0.2673E 02	0.1390E 00	0.4685E 01	0.2475E 01
0.1000E 03	0.2661E 02	0.1335E 00	0.4657E 01	0.2463E 01
0.2000E 03	0.2641E 02	0.1372E 00	0.4611E 01	0.2445E 01
0.5000E 03	0.2625E 02	0.1244E 00	0.4574E 01	0.2430E 01
0.7000E 03	0.2621E 02	0.1261E 00	0.4565E 01	0.2426E 01
0.1000E 04	0.2617E 02	0.1273E 00	0.4556E 01	0.2423E 01
0.2000E 04	0.2609E 02	0.1315E 00	0.4537E 01	0.2415E 01

TABLE X. - IN-PLANE LONGITUDINAL YOUNG'S MODULUS AND ASSOCIATED LOSS TANGENT FOR A BORON-ALUMINUM 2024-T3 MONOFILAMENT COMPOSITE (CONTINUED)

IDATA 4 RMU 1.253 DELTA 1.000 VF 0.500

*****BORON-ALUMINUM 2024-T3*****

FREQUENCY	E11	GE11	EF/EM	E11/EM
HERTZ	1.E6 PSI	PER CENT		
0.5000E 01	0.3346E 02	0.1240E 00	0.5252E 01	0.3127E 01
0.7000E 01	0.3276E 02	0.1285E 00	0.5121E 01	0.3062E 01
0.1000E 02	0.3221E 02	0.1342E 00	0.5019E 01	0.3010E 01
0.2000E 02	0.3151E 02	0.1471E 00	0.4888E 01	0.2945E 01
0.5000E 02	0.3091E 02	0.1430E 00	0.4722E 01	0.2862E 01
0.7000E 02	0.3071E 02	0.1387E 00	0.4685E 01	0.2844E 01
0.1000E 03	0.3056E 02	0.1355E 00	0.4657E 01	0.2830E 01
0.2000E 03	0.3031E 02	0.1396E 00	0.4611E 01	0.2806E 01
0.5000E 03	0.3011E 02	0.1325E 00	0.4574E 01	0.2788E 01
0.7000E 03	0.3006E 02	0.1348E 00	0.4565E 01	0.2783E 01
0.1000E 04	0.3001E 02	0.1365E 00	0.4556E 01	0.2779E 01
0.2000E 04	0.2991E 02	0.1415E 00	0.4537E 01	0.2769E 01

TABLE X. - IN-PLANE LONGITUDINAL YOUNG'S MODULUS AND ASSOCIATED LOSS TANGENT FOR A BORON-ALUMINUM 2024-T3 MONOFILAMENT COMPOSITE (CONTINUED)

IDATA 5 RMU 1.144 DELTA 1.000 VF 0.600

*****BORON-ALUMINUM 2024-T3*****

FREQUENCY	E11	GE11	EF/EM	E11/EM
HERTZ	1.E6 PSI	PER CENT		
0.5000E 01	0.3801E 02	0.1255E 00	0.5252E 01	0.3552E 01
0.7000E 01	0.3717E 02	0.1290E 00	0.5121E 01	0.3473E 01
0.1000E 02	0.3651E 02	0.1332E 00	0.5019E 01	0.3412E 01
0.2000E 02	0.3566E 02	0.1432E 00	0.4888E 01	0.3333E 01
0.5000E 02	0.3492E 02	0.1409E 00	0.4722E 01	0.3234E 01
0.7000E 02	0.3468E 02	0.1385E 00	0.4685E 01	0.3212E 01
0.1000E 03	0.3450E 02	0.1371E 00	0.4657E 01	0.3195E 01
0.2000E 03	0.3420E 02	0.1415E 00	0.4611E 01	0.3167E 01
0.5000E 03	0.3396E 02	0.1387E 00	0.4574E 01	0.3145E 01
0.7000E 03	0.3390E 02	0.1416E 00	0.4565E 01	0.3139E 01
0.1000E 04	0.3384E 02	0.1436E 00	0.4556E 01	0.3134E 01
0.2000E 04	0.3372E 02	0.1492E 00	0.4537E 01	0.3123E 01

TABLE XI. - IN-PLANE MAJOR POISSON'S RATIO AND ASSOCIATED LOSS TANGENT FOR A BORON-ALUMINUM 2024-T3 MONOFILAMENT COMPOSITE

IDATA 3 RMU 1.401 DELTA 1.000 VF 0.400

*****BORON-ALUMINUM 2024-T3*****

FREQUENCY HERTZ	RNU12	GNU12 PER CENT	RNUF	RNUM
0.5000E 01	0.2822E 00	-0.8809E-01	0.2090E 00	0.3310E 00
0.7000E 01	0.2850E 00	-0.9455E-01	0.2160E 00	0.3310E 00
0.1000E 02	0.2868E 00	-0.1034E 00	0.2220E 00	0.3300E 00
0.2000E 02	0.2896E 00	-0.1238E 00	0.2290E 00	0.3300E 00
0.5000E 02	0.2918E 00	-0.1105E 00	0.2360E 00	0.3290E 00
0.7000E 02	0.2926E 00	-0.9859E-01	0.2380E 00	0.3290E 00
0.1000E 03	0.2930E 00	-0.8820E-01	0.2390E 00	0.3290E 00
0.2000E 03	0.2942E 00	-0.8912E-01	0.2420E 00	0.3290E 00
0.5000E 03	0.2950E 00	-0.6500E-01	0.2440E 00	0.3290E 00
0.7000E 03	0.2950E 00	-0.6425E-01	0.2440E 00	0.3290E 00
0.1000E 04	0.2954E 00	-0.6404E-01	0.2450E 00	0.3290E 00
0.2000E 04	0.2958E 00	-0.6445E-01	0.2460E 00	0.3290E 00

TABLE XI. - IN-PLANE MAJOR POISSON'S RATIO AND ASSOCIATED LOSS TANGENT FOR A BORON-ALUMINUM 2024T3 MONOFILAMENT COMPOSITE (CONTINUED)

IDATA 4 RMU 1.253 DELTA 1.000 VF 0.500

*****BORON-ALUMINUM 2024-T3*****

FREQUENCY	RNU12	GNU12	RNUF	RNUM
HERTZ		PER CENT		
0.5000E 01	0.2700E 00	-0.9984E-01	0.2090E 00	0.3310E 00
0.7000E 01	0.2735E 00	-0.1045E 00	0.2160E 00	0.3310E 00
0.1000E 02	0.2760E 00	-0.1114E 00	0.2220E 00	0.3300E 00
0.2000E 02	0.2795E 00	-0.1285E 00	0.2290E 00	0.3300E 00
0.5000E 02	0.2825E 00	-0.1163E 00	0.2360E 00	0.3290E 00
0.7000E 02	0.2835E 00	-0.1059E 00	0.2380E 00	0.3290E 00
0.1000E 03	0.2840E 00	-0.9730E-01	0.2390E 00	0.3290E 00
0.2000E 03	0.2855E 00	-0.9844E-01	0.2420E 00	0.3290E 00
0.5000E 03	0.2865E 00	-0.7864E-01	0.2440E 00	0.3290E 00
0.7000E 03	0.2865E 00	-0.7843E-01	0.2440E 00	0.3290E 00
0.1000E 04	0.2870E 00	-0.7871E-01	0.2450E 00	0.3290E 00
0.2000E 04	0.2875E 00	-0.7981E-01	0.2460E 00	0.3290E 00

TABLE XI. - IN-PLANE MAJOR POISSON'S RATIO AND ASSOCIATED LOSS TANGENT FOR A BORON-ALUMINUM @)@$-T3 MONOFILAMENT COMPOSITE (CONTINUED)

IDATA 5 RMU 1.144 DELTA 1.000 VF 0.600

*****BORON-ALUMINUM 2024-T3*****

FREQUENCY HERTZ	RNU12	GNU12 PER CENT	RNUF	RNUM
0.5000E 01	0.2578E 00	-0.1127E 00	0.2090E 00	0.3310E 00
0.7000E 01	0.2620E 00	-0.1153E 00	0.2160E 00	0.3310E 00
0.1000E 02	0.2652E 00	-0.1201E 00	0.2220E 00	0.3300E 00
0.2000E 02	0.2694E 00	-0.1335E 00	0.2290E 00	0.3300E 00
0.5000E 02	0.2732E 00	-0.1225E 00	0.2360E 00	0.3290E 00
0.7000E 02	0.2744E 00	-0.1137E 00	0.2380E 00	0.3290E 00
0.1000E 03	0.2750E 00	-0.1070E 00	0.2390E 00	0.3290E 00
0.2000E 03	0.2768E 00	-0.1083E 00	0.2420E 00	0.3290E 00
0.5000E 03	0.2780E 00	-0.9309E-01	0.2440E 00	0.3290E 00
0.7000E 03	0.2780E 00	-0.9344E-01	0.2440E 00	0.3290E 00
0.1000E 04	0.2786E 00	-0.9423E-01	0.2450E 00	0.3290E 00
0.2000E 04	0.2792E 00	-0.9604E-01	0.2460E 00	0.3290E 00

TABLE XII. - IN-PLANE TRANSVERSE YOUNG'S MODULUS AND ASSOCIATED LOSS TANGENT FOR A BORON-ALUMINUM 2024-T3 MONOFILAMENT COMPOSITE

IDATA# 1 RMU# 1.401 DELTA# 1.000 VF# 0.400

*****BORON-ALUMINUM 2024-T3*****

FREQUENCY HERTZ	E22 1.E6 PSI	GE22 PER CENT	RNU12	EF/EM	E22/EM	IKS
0.5000E 01	0.1722E 02	0.1028E 00	0.2863E 00	0.5252E 01	0.1610E 01	0
0.7000E 01	0.1714E 02	0.1225E 00	0.2893E 00	0.5121E 01	0.1602E 01	0
0.1000E 02	0.1705E 02	0.1472E 00	0.2912E 00	0.5019E 01	0.1593E 01	0
0.2000E 02	0.1695E 02	0.1990E 00	0.2943E 00	0.4888E 01	0.1584E 01	0
0.5000E 02	0.1702E 02	0.1697E 00	0.2967E 00	0.4722E 01	0.1576E 01	0
0.7000E 02	0.1698E 02	0.1415E 00	0.2976E 00	0.4685E 01	0.1572E 01	0
0.1000E 03	0.1695E 02	0.1152E 00	0.2981E 00	0.4657E 01	0.1570E 01	0
0.2000E 03	0.1692E 02	0.1160E 00	0.2993E 00	0.4611E 01	0.1566E 01	0
0.5000E 03	0.1689E 02	0.5388E-01	0.3001E 00	0.4574E 01	0.1564E 01	0
0.7000E 03	0.1689E 02	0.5036E-01	0.3001E 00	0.4565E 01	0.1564E 01	0
0.1000E 04	0.1688E 02	0.4758E-01	0.3005E 00	0.4556E 01	0.1563E 01	0
0.2000E 04	0.1686E 02	0.4543E-01	0.3011E 00	0.4537E 01	0.1561E 01	0

TABLE XII. - IN-PLANE TRANSVERSE YOUNG'S MODULUS AND ASSOCIATED LOSS TANGENT FOR A BORON-ALUMINUM 2024-T3 MONOFILAMENT COMPOSITE (CONTINUED)

IDATA# 1 RMU# 1.253 DELTA# 1.000 VF# 0.500

*****BORON-ALUMINUM 2024-T3*****

FREQUENCY HERTZ	E22 1.E6 PSI	GE22 PER CENT	RNU12	EF/EM	E22/EM	IKS
0.5000E 01	0.1978E 02	0.1049E 00	0.2730E 00	0.5252E 01	0.1849E 01	0
0.7000E 01	0.1964E 02	0.1232E 00	0.2767E 00	0.5121E 01	0.1836E 01	0
0.1000E 02	0.1952E 02	0.1459E 00	0.2795E 00	0.5019E 01	0.1824E 01	0
0.2000E 02	0.1937E 02	0.1936E 00	0.2836E 00	0.4888E 01	0.1811E 01	0
0.5000E 02	0.1941E 02	0.1669E 00	0.2865E 00	0.4722E 01	0.1797E 01	0
0.7000E 02	0.1937E 02	0.1413E 00	0.2876E 00	0.4685E 01	0.1793E 01	0
0.1000E 03	0.1933E 02	0.1175E 00	0.2882E 00	0.4657E 01	0.1790E 01	0
0.2000E 03	0.1928E 02	0.1187E 00	0.2900E 00	0.4611E 01	0.1785E 01	0
0.5000E 03	0.1923E 02	0.6262E-01	0.2909E 00	0.4574E 01	0.1781E 01	0
0.7000E 03	0.1923E 02	0.5976E-01	0.2909E 00	0.4565E 01	0.1781E 01	0
0.1000E 04	0.1927E 02	0.5770E-01	0.2923E 00	0.4556E 01	0.1784E 01	0
0.2000E 04	0.1918E 02	0.5611E-01	0.2917E 00	0.4537E 01	0.1776E 01	0

TABLE XII. - IN-PLANE TRANSVERSE YOUNG'S MODULUS AND ASSOCIATED LOSS TANGENT FOR A BORON-ALUMINUM 2024-T3 MONOFILAMENT COMPOSITE (CONTINUED)

IDATA# 1 RMU# 1.144 DELTA# 1.000 VF# 0.600

*****BORON-ALUMINUM 2024-T3*****

FREQUENCY	E22	G22	RNU12	EF/EM	E22/EM	IKS
HERTZ	1.E6 PSI	PER CENT				
0.5000E 01	0.2301E 02	0.1070E 00	0.2602E 00	0.5252E 01	0.2151E 01	0
0.7000E 01	0.2280E 02	0.1238E 00	0.2645E 00	0.5121E 01	0.2131E 01	0
0.1000E 02	0.2262E 02	0.1446E 00	0.2675E 00	0.5019E 01	0.2114E 01	0
0.2000E 02	0.2245E 02	0.1882E 00	0.2720E 00	0.4888E 01	0.2098E 01	0
0.3000E 02	0.2239E 02	0.1641E 00	0.2762E 00	0.4722E 01	0.2073E 01	0
0.7000E 02	0.2231E 02	0.1410E 00	0.2770E 00	0.4685E 01	0.2066E 01	0
0.1000E 03	0.2224E 02	0.1197E 00	0.2780E 00	0.4657E 01	0.2060E 01	0
0.2000E 03	0.2219E 02	0.1212E 00	0.2798E 00	0.4611E 01	0.2055E 01	0
0.5000E 03	0.2211E 02	0.7112E-01	0.2811E 00	0.4574E 01	0.2048E 01	0
0.7000E 03	0.2211E 02	0.6489E-01	0.2811E 00	0.4565E 01	0.2047E 01	0
0.1000E 04	0.2209E 02	0.6717E-01	0.2817E 00	0.4556E 01	0.2046E 01	0
0.2000E 04	0.2207E 02	0.6556E-01	0.2822E 00	0.4537E 01	0.2043E 01	0

TABLE XIII. - IN-PLANE LONGITUDINAL SHEAR MODULUS AND ASSOCIATED LOSS TANGENT FOR A BORON-ALUMINUM 2024-T3 MONOFILAMENT COMPOSITE

IDATA 3 RMU 1.401 DELTA 1.000 VF 0.400

*****BORON-ALUMINUM 2024-T3*****

FREQUENCY HERTZ	G66 1.E6 PSI	GG66 PER CENT	GF/GM	G66/GM	SHAPE
0.5000E 01	0.7177E 01	0.1209E 00	0.5771E 01	0.1785E 01	0.1044E 01
0.7000E 01	0.7143E 01	0.1414E 00	0.5583E 01	0.1772E 01	0.1046E 01
0.1000E 02	0.7113E 01	0.1670E 00	0.5421E 01	0.1761E 01	0.1047E 01
0.2000E 02	0.7073E 01	0.2198E 00	0.5235E 01	0.1746E 01	0.1049E 01
0.5000E 02	0.7039E 01	0.1902E 00	0.5074E 01	0.1734E 01	0.1051E 01
0.7000E 02	0.7036E 01	0.1617E 00	0.5012E 01	0.1729E 01	0.1052E 01
0.1000E 03	0.7019E 01	0.1351E 00	0.4963E 01	0.1725E 01	0.1052E 01
0.2000E 03	0.7002E 01	0.1366E 00	0.4914E 01	0.1720E 01	0.1053E 01
0.5000E 03	0.6985E 01	0.7399E-01	0.4865E 01	0.1716E 01	0.1053E 01
0.7000E 03	0.6985E 01	0.7097E-01	0.4865E 01	0.1716E 01	0.1053E 01
0.1000E 04	0.6977E 01	0.6842E-01	0.4840E 01	0.1714E 01	0.1054E 01
0.2000E 04	0.6955E 01	0.6720E-01	0.4828E 01	0.1713E 01	0.1054E 01

TABLE XIII. - IN-PLANE LONGITUDINAL SHEAR MODULUS AND ASSOCIATED LOSS TANGENT FOR A BORON-ALUMINUM 2024-T3 MONOFILAMENT COMPOSITE (CONTINUED)

IDATA 4 RMU 1.253 DELTA 1.000 VF 0.500

*****BORON-ALUMINUM 2024-T3*****

FREQUENCY	G66	GG66	GF/GM	G66/GM	SHAPE
HERTZ	1.E6 PSI	PER CENT			
0.5000E 01	0.8607E 01	0.1244E 00	0.5771E 01	0.2141E 01	0.1035E 01
0.7000E 01	0.8546E 01	0.1430E 00	0.5583E 01	0.2121E 01	0.1038E 01
0.1000E 02	0.8493E 01	0.1663E 00	0.5421E 01	0.2102E 01	0.1039E 01
0.2000E 02	0.8425E 01	0.2145E 00	0.5235E 01	0.2080E 01	0.1042E 01
0.5000E 02	0.8365E 01	0.1878E 00	0.5074E 01	0.2060E 01	0.1044E 01
0.7000E 02	0.8354E 01	0.1622E 00	0.5012E 01	0.2052E 01	0.1045E 01
0.1000E 03	0.8328E 01	0.1384E 00	0.4963E 01	0.2046E 01	0.1045E 01
0.2000E 03	0.8302E 01	0.1404E 00	0.4914E 01	0.2040E 01	0.1046E 01
0.5000E 03	0.8275E 01	0.8488E-01	0.4865E 01	0.2033E 01	0.1047E 01
0.7000E 03	0.8275E 01	0.8265E-01	0.4865E 01	0.2033E 01	0.1047E 01
0.1000E 04	0.8262E 01	0.8067E-01	0.4840E 01	0.2030E 01	0.1047E 01
0.2000E 04	0.8235E 01	0.8049E-01	0.4828E 01	0.2028E 01	0.1048E 01

TABLE XIII. - IN-PLANE LONGITUDINAL SHEAR MODULUS AND ASSOCIATED LOSS TANGENT FOR A BORON-ALUMINUM 2024-T3 MONOFILAMENT COMPOSITE (CONTINUED)

IDATA 5 RMU 1.144 DELTA 1.000 VF 0.600

*****BORON-ALUMINUM 2024-T3*****

FREQUENCY	G66	GG66	GF/GM	G66/GM	SHAPE
HERTZ	1.E6 PSI	PER CENT			
0.5000E 01	0.1041E 02	0.1284E 00	0.5771E 01	0.2589E 01	0.1026E 01
0.7000E 01	0.1030E 02	0.1450E 00	0.5583E 01	0.2557E 01	0.1029E 01
0.1000E 02	0.1022E 02	0.1656E 00	0.5421E 01	0.2529E 01	0.1032E 01
0.2000E 02	0.1010E 02	0.2083E 00	0.5235E 01	0.2495E 01	0.1035E 01
0.5000E 02	0.1001E 02	0.1850E 00	0.5074E 01	0.2465E 01	0.1037E 01
0.7000E 02	0.9983E 01	0.1628E 00	0.5012E 01	0.2453E 01	0.1038E 01
0.1000E 03	0.9944E 01	0.1423E 00	0.4963E 01	0.2443E 01	0.1039E 01
0.2000E 03	0.9905E 01	0.1448E 00	0.4914E 01	0.2434E 01	0.1040E 01
0.5000E 03	0.9865E 01	0.9734E-01	0.4865E 01	0.2424E 01	0.1041E 01
0.7000E 03	0.9865E 01	0.9601E-01	0.4865E 01	0.2424E 01	0.1041E 01
0.1000E 04	0.9845E 01	0.9469E-01	0.4840E 01	0.2419E 01	0.1041E 01
0.2000E 04	0.9810E 01	0.9567E-01	0.4828E 01	0.2416E 01	0.1042E 01

TABLE XIV. - LONGITUDINAL FLEXURAL STIFFNESS AND ASSOCIATED LOSS TANGENT FOR A BORON-ALUMINUM 2024-T3 MONOFILAMENT COMPOSITE

IDATA 3 RMU 1.401 DELTA 1.000 VF 0.400

*****BORON-ALUMINUM 2024-T3*****

FREQUENCY	D11S	GD11	EF/EM	D11/D11M
HERTZ	1.E6 PSI	PER CENT		
0.5000E 01	0.1766E 02	0.1131E 00	0.5252E 01	0.1650E 01
0.7000E 01	0.1744E 02	0.1253E 00	0.5121E 01	0.1630E 01
0.1000E 02	0.1727E 02	0.1410E 00	0.5019E 01	0.1614E 01
0.2000E 02	0.1706E 02	0.1749E 00	0.4888E 01	0.1594E 01
0.5000E 02	0.1695E 02	0.1576E 00	0.4722E 01	0.1569E 01
0.7000E 02	0.1689E 02	0.1402E 00	0.4685E 01	0.1563E 01
0.1000E 03	0.1684E 02	0.1242E 00	0.4657E 01	0.1559E 01
0.2000E 03	0.1676E 02	0.1264E 00	0.4611E 01	0.1552E 01
0.5000E 03	0.1670E 02	0.8827E-01	0.4574E 01	0.1546E 01
0.7000E 03	0.1669E 02	0.8727E-01	0.4565E 01	0.1545E 01
0.1000E 04	0.1667E 02	0.8637E-01	0.4556E 01	0.1544E 01
0.2000E 04	0.1664E 02	0.8718E-01	0.4537E 01	0.1541E 01

TABLE XIV. - LONGITUDINAL FLEXURAL STIFFNESS AND ASSOCIATED LOSS TANGENT FOR A BORON-ALUMINUM 2024-T3 MONOFILAMENT COMPOSITE (CONTINUED)

IDATA 4 RMU 1.253 DELTA 1.000 VF 0.500

*****BORON-ALUMINUM 2024-T3*****

FREQUENCY HERTZ	D11S 1.E6 PSI	GD11 PER CENT	EF/EM	D11/D11M
0.5000E 01	0.2157E 02	0.1173E 00	0.5252E 01	0.2016E 01
0.7000E 01	0.2124E 02	0.1265E 00	0.5121E 01	0.1985E 01
0.1000E 02	0.2098E 02	0.1384E 00	0.5019E 01	0.1960E 01
0.2000E 02	0.2064E 02	0.1644E 00	0.4888E 01	0.1929E 01
0.5000E 02	0.2041E 02	0.1521E 00	0.4722E 01	0.1890E 01
0.7000E 02	0.2031E 02	0.1396E 00	0.4685E 01	0.1881E 01
0.1000E 03	0.2024E 02	0.1284E 00	0.4657E 01	0.1874E 01
0.2000E 03	0.2012E 02	0.1313E 00	0.4611E 01	0.1863E 01
0.5000E 03	0.2002E 02	0.1047E 00	0.4574E 01	0.1854E 01
0.7000E 03	0.2000E 02	0.1050E 00	0.4565E 01	0.1852E 01
0.1000E 04	0.1998E 02	0.1050E 00	0.4556E 01	0.1850E 01
0.2000E 04	0.1993E 02	0.1074E 00	0.4537E 01	0.1845E 01

TABLE XIV. - LONGITUDINAL FLEXURAL STIFFNESS AND ASSOCIATED LOSS TANGENT FOR A BORON-ALUMINUM 2024-T3 MONOFILAMENT COMPOSITE (CONTINUED)

IDATA 5 RMU 1.144 DELTA 1.000 VF 0.600

*****BORON-ALUMINUM 2024-T3*****

FREQUENCY HERTZ	D11S 1.E6 PSI	GD11 PER CENT	EF/EM	D11/D11M
0.5000E 01	0.2635E 02	0.1207E 00	0.5252E 01	0.2462E 01
0.7000E 01	0.2587E 02	0.1276E 00	0.5121E 01	0.2417E 01
0.1000E 02	0.2549E 02	0.1362E 00	0.5019E 01	0.2382E 01
0.2000E 02	0.2501E 02	0.1556E 00	0.4888E 01	0.2337E 01
0.5000E 02	0.2463E 02	0.1475E 00	0.4722E 01	0.2280E 01
0.7000E 02	0.2449E 02	0.1392E 00	0.4685E 01	0.2267E 01
0.1000E 03	0.2438E 02	0.1320E 00	0.4657E 01	0.2258E 01
0.2000E 03	0.2421E 02	0.1355E 00	0.4611E 01	0.2242E 01
0.5000E 03	0.2407E 02	0.1187E 00	0.4574E 01	0.2229E 01
0.7000E 03	0.2404E 02	0.1200E 00	0.4565E 01	0.2226E 01
0.1000E 04	0.2401E 02	0.1209E 00	0.4556E 01	0.2223E 01
0.2000E 04	0.2394E 02	0.1245E 00	0.4537E 01	0.2216E 01

NGENT FOR

VF 0.400

YEM	D12/D12M
62E 01	0.4024E 00
21E 01	0.4039E 00
19E 01	0.4040E 00
38E 01	0.4056E 00
22E 01	0.4056E 00
35E 01	0.4061E 00
57E 01	0.4062E 00
11E 01	0.4069E 00
74E 01	0.4073E 00
55E 01	0.4073E 00
56E 01	0.4075E 00
37E 01	0.4077E 00

TABLE XV. - POISSON FLEXURAL STIFFNESS AND ASSOCIATED LOSS TANGENT FOR A BORON-ALUMINUM 2024-T3 MONOFILAMENT COMPOSITE (CONTINUED)

IDATA 4 RMU 1.253 DELTA 1.000 VF 0.500

*****BORON-ALUMINUM 2024-T3*****

FREQUENCY HERTZ	D12S 1.E6 PSI	GD12 PER CENT	EF/EM	D12/D12M
0.5000E 01	0.4567E 01	0.1212E-01	0.5252E 01	0.4268E 00
0.7000E 01	0.4594E 01	0.2375E-01	0.5121E 01	0.4294E 00
0.1000E 02	0.4605E 01	0.3777E-01	0.5019E 01	0.4304E 00
0.2000E 02	0.4632E 01	0.6578E-01	0.4888E 01	0.4329E 00
0.5000E 02	0.4685E 01	0.5077E-01	0.4722E 01	0.4338E 00
0.7000E 02	0.4692E 01	0.3592E-01	0.4685E 01	0.4344E 00
0.1000E 03	0.4695E 01	0.2146E-01	0.4657E 01	0.4347E 00
0.2000E 03	0.4706E 01	0.2117E-01	0.4611E 01	0.4358E 00
0.5000E 03	0.4713E 01	-0.1329E-01	0.4574E 01	0.4364E 00
0.7000E 03	0.4712E 01	-0.1586E-01	0.4565E 01	0.4363E 00
0.1000E 04	0.4717E 01	-0.1831E-01	0.4556E 01	0.4367E 00
0.2000E 04	0.4720E 01	-0.2077E-01	0.4537E 01	0.4371E 00

TABLE XV. - POISSON FLEXURAL STIFFNESS AND ASSOCIATED LOSS TANGENT FOR A BORON-ALUMINUM 2024-T3 MONOFILAMENT COMPOSITE (CONTINUED)

IDATA 5 RMU 1.144 DELTA 1.000 VF 0.600

*****BORON-ALUMINUM 2024-T3*****

FREQUENCY HERTZ	D12S 1.E6 PSI	GD12 PER CENT	EF/EM	D12/D12M
0.5000E 01	0.4946E 01	0.8237E-03	0.5252E 01	0.4622E 00
0.7000E 01	0.4987E 01	0.1364E-01	0.5121E 01	0.4661E 00
0.1000E 02	0.5011E 01	0.2870E-01	0.5019E 01	0.4683E 00
0.2000E 02	0.5050E 01	0.5801E-01	0.4888E 01	0.4720E 00
0.5000E 02	0.5118E 01	0.4326E-01	0.4722E 01	0.4739E 00
0.7000E 02	0.5128E 01	0.2823E-01	0.4685E 01	0.4749E 00
0.1000E 03	0.5132E 01	0.1334E-01	0.4657E 01	0.4752E 00
0.2000E 03	0.5149E 01	0.1305E-01	0.4611E 01	0.4768E 00
0.5000E 03	0.5160E 01	-0.2250E-01	0.4574E 01	0.4777E 00
0.7000E 03	0.5158E 01	-0.2522E-01	0.4565E 01	0.4776E 00
0.1000E 04	0.5165E 01	-0.2791E-01	0.4556E 01	0.4782E 00
0.2000E 04	0.5170E 01	-0.3059E-01	0.4537E 01	0.4787E 00

TABLE XVI. - TRANSVERSE FLEXURAL STIFFNESS AND ASSOCIATED LOSS TANGENT FOR A BORON-ALUMINUM 2024-T3 MONOFILAMENT COMPOSITE

IDATA 1 RMU 1.401 DELTA 1.000 VF 0.400

*****BORON-ALUMINUM 2024-T3*****

FREQUENCY	D22S	GD22	EF/EM	D22/D22M	IKS
HERTZ	1.E6 PSI	PER CENT			
0.5000E 01	0.1235E 02	0.1061E 00	0.5252E 01	C.1150E 01	0
0.7000E 01	0.1230E 02	0.1278E 00	0.5121E 01	C.1152E 01	0
0.1000E 02	0.1222E 02	0.1552E 00	0.5019E 01	C.1142E 01	0
0.2000E 02	0.1215E 02	0.2125E 00	0.4888E 01	C.1140E 01	0
0.5000E 02	0.1224E 02	0.1797E 00	0.4722E 01	C.1130E 01	0
0.7000E 02	0.1218E 02	0.1484E 00	0.4685E 01	C.1128E 01	0
0.1000E 03	0.1217E 02	0.1192E 00	0.4657E 01	C.1130E 01	0
0.2000E 03	0.1210E 02	0.1169E 00	0.4611E 01	C.1126E 01	0
0.5000E 03	0.1210E 02	0.4921E-01	0.4574E 01	C.1124E 01	0
0.7000E 03	0.1209E 02	0.4501E-01	0.4565E 01	C.1124E 01	0
0.1000E 04	0.1207E 02	0.4272E-01	0.4556E 01	C.1122E 01	0
0.2000E 04	0.1205E 02	0.4039E-01	0.4537E 01	C.1120E 01	0

TABLE XVI. - TRANSVERSE FLEXURAL STIFFNESS AND ASSOCIATED LOSS TANGENT FOR A BORON-ALUMINUM 2024-T3 MONOFILAMENT COMPOSITE (CONTINUED)

IDATA 2 RML 1.253 DELTA 1.000 VF 0.500

*****BORON-ALUMINUM 2024-T3*****

FREQUENCY	D22S	CD22	EF/EM	C22/D22M	IKS
HERTZ	1.E6 PSI	PER CENT			
0.5000E 01	0.1521E 02	0.1077E 00	0.5252E 01	0.1420E 01	0
0.7000E 01	0.1512E 02	0.1283E 00	0.5121E 01	0.1406E 01	0
0.1000E 02	0.1503E 02	0.1540E 00	0.5019E 01	0.1404E 01	0
0.2000E 02	0.1490E 02	0.2077E 00	0.4886E 01	0.1392E 01	0
0.5000E 02	0.1492E 02	0.1773E 00	0.4722E 01	0.1380E 01	0
0.7000E 02	0.1482E 02	0.1481E 00	0.4685E 01	0.1381E 01	0
0.1000E 03	0.1480E 02	0.1207E 00	0.4657E 01	0.1380E 01	0
0.2000E 03	0.1486E 02	0.1217E 00	0.4611E 01	0.1372E 01	0
0.5000E 03	0.1478E 02	0.5720E-01	0.4574E 01	0.1370E 01	0
0.7000E 03	0.1478E 02	0.5360E-01	0.4565E 01	0.1370E 01	0
0.1000E 04	0.1480E 02	0.5067E-01	0.4556E 01	0.1373E 01	0
0.2000E 04	0.1468E 02	0.4858E-01	0.4537E 01	0.1365E 01	0

TABLE XVI. - TRANSVERSE FLEXURAL STIFFNESS AND ASSOCIATED LOSS TANGENT FOR A BORON-ALUMINUM 2024-T3 MONOFILAMENT COMPOSITE (CONTINUED)

ICATA 3 RMU 1.144 DELTA 1.000 VF 0.600

*****BORON-ALUMINUM 2024-T3*****

FREQUENCY HERTZ	D22S 1.E6 PSI	GD22 PER CENT	EF/EM	D22/D22M	IKS
0.5000E 01	0.1892E 02	0.1086E 00	0.5252E 01	0.1764E 01	0
0.7000E 01	0.1873E 02	0.1287E 00	0.5121E 01	0.1750E 01	0
0.1000E 02	0.1860E 02	0.1530E 00	0.5019E 01	0.1732E 01	0
0.2000E 02	0.1844E 02	0.2036E 00	0.4888E 01	0.1729E 01	0
0.5000E 02	0.1835E 02	0.1751E 00	0.4722E 01	0.1702E 01	0
0.7000E 02	0.1835E 02	0.1478E 00	0.4685E 01	0.1700E 01	0
0.1000E 03	0.1834E 02	0.1223E 00	0.4657E 01	0.1691E 01	0
0.2000E 03	0.1830E 02	0.1237E 00	0.4611E 01	0.1686E 01	0
0.5000E 03	0.1820E 02	0.6367E-01	0.4574E 01	0.1682E 01	0
0.7000E 03	0.1818E 02	0.6057E-01	0.4565E 01	0.1681E 01	0
0.1000E 04	0.1817E 02	0.5796E-01	0.4556E 01	0.1680E 01	0
0.2000E 04	0.1816E 02	0.5655E-01	0.4537E 01	0.1675E 01	0

TABLE XVII. - TWISTING STIFFNESS AND ASSOCIATED LOSS TANGENT FOR A BORON-ALUMINUM 2024-T3 MONOFILAMENT COMPOSITE

IDATA# 1 RMU# 1.401 DELTA# 1.000 VF# 0.400

*****BORON-ALUMINUM 2024-T3*****

FREQUENCY	D66S	GD66	GF/GM	D66/D66M	RTK	IKS
HERTZ	1.E6 PSI	PER CENT				
0.5000E 01	0.7387E 01	0.1378E 00	0.5771E 01	0.1837E 01	0.1406E 00	0
0.7000E 01	0.7298E 01	0.1492E 00	0.5583E 01	0.1811E 01	0.1406E 00	0
0.1000E 02	0.7189E 01	0.1641E 00	0.5421E 01	0.1779E 01	0.1406E 00	0
0.2000E 02	0.7087E 01	0.1976E 00	0.5235E 01	0.1750E 01	0.1406E 00	0
0.5000E 02	0.6995E 01	0.1807E 00	0.5074E 01	0.1723E 01	0.1406E 00	0
0.7000E 02	0.6989E 01	0.1636E 00	0.5012E 01	0.1717E 01	0.1406E 00	0
0.1000E 03	0.7424E 01	0.1477E 00	0.4953E 01	0.1824E 01	0.1406E 00	0
0.2000E 03	0.6766E 01	0.1509E 00	0.4914E 01	0.1662E 01	0.1406E 00	0
0.5000E 03	0.6866E 01	0.1137E 00	0.4865E 01	0.1687E 01	0.1406E 00	0
0.7000E 03	0.6866E 01	0.1136E 00	0.4865E 01	0.1687E 01	0.1406E 00	0
0.1000E 04	0.6804E 01	0.1127E 00	0.4840E 01	0.1672E 01	0.1406E 00	0
0.2000E 04	0.6793E 01	0.1150E 00	0.4828E 01	0.1673E 01	0.1406E 00	0

TABLE XVII. - TWISTING STIFFNESS AND ASSOCIATED LOSS TANGENT FOR A BORON-ALUMINUM 2024-T3 MONOFILAMENT COMPOSITE (CONTINUED)

IDATA# 2 RMU# 1.253 DELTA# 1.000 VF# 0.500

*****BORON-ALUMINUM 2024-T3*****

FREQUENCY	D66S	GD66	GF/GM	D66/D66M	RTK	IKS
HERTZ	1.E6 PSI	PER CENT				
0.5000E 01	0.9376E 01	0.1449E 00	0.5771E 01	0.2332E 01	0.1406E 00	0
0.7000E 01	0.9197E 01	0.1526E 00	0.5593E 01	0.2282E 01	0.1406E 00	0
0.1000E 02	0.9033E 01	0.1628E 00	0.5421E 01	0.2236E 01	0.1406E 00	0
0.2000E 02	0.8844E 01	0.1869E 00	0.5235E 01	0.2184E 01	0.1406E 00	0
0.5000E 02	0.8679E 01	0.1759E 00	0.5074E 01	0.2138E 01	0.1406E 00	0
0.7000E 02	0.8740E 01	0.1647E 00	0.5012E 01	0.2147E 01	0.1406E 00	0
0.1000E 03	0.8577E 01	0.1546E 00	0.4963E 01	0.2107E 01	0.1406E 00	0
0.2000E 03	0.8517E 01	0.1585E 00	0.4914E 01	0.2093E 01	0.1406E 00	0
0.5000E 03	0.8467E 01	0.1353E 00	0.4865E 01	0.2080E 01	0.1406E 00	0
0.7000E 03	0.8467E 01	0.1367E 00	0.4865E 01	0.2080E 01	0.1406E 00	0
0.1000E 04	0.8430E 01	0.1370E 00	0.4840E 01	0.2071E 01	0.1406E 00	0
0.2000E 04	0.8406E 01	0.1413E 00	0.4828E 01	0.2070E 01	0.1406E 00	0

TABLE XVII. - TWISTING STIFFNESS AND ASSOCIATED LOSS TANGENT FOR A BORON-ALUMINUM 2024-T3 MONOFILAMENT COMPOSITE (CONTINUED)

IDATA# 3 RMU# 1.144 DELTA# 1.000 VF# 0.600

*****BORON-ALUMINUM 2024-T3*****

FREQUENCY	D66S	GD66	GF/GM	D66/D66M	RTK	IKS
HERTZ	1.E6 PSI	PER CENT				
0.5000E 01	0.1178E 02	0.1493E 00	0.5771E 01	0.2930E 01	0.1406E 00	0
0.7000E 01	0.1150E 02	0.1547E 00	0.5583E 01	0.2853E 01	0.1406E 00	0
0.1000E 02	0.1126E 02	0.1620E 00	0.5421E 01	0.2788E 01	0.1406E 00	0
0.2000E 02	0.1095E 02	0.1800E 00	0.5235E 01	0.2704E 01	0.1406E 00	0
0.5000E 02	0.1076E 02	0.1728E 00	0.5074E 01	0.2650E 01	0.1406E 00	0
0.7000E 02	0.1067E 02	0.1653E 00	0.5012E 01	0.2621E 01	0.1406E 00	0
0.1000E 03	0.1058E 02	0.1590E 00	0.4963E 01	0.2600E 01	0.1406E 00	0
0.2000E 03	0.1050E 02	0.1634E 00	0.4914E 01	0.2581E 01	0.1406E 00	0
0.5000E 03	0.1042E 02	0.1493E 00	0.4865E 01	0.2561E 01	0.1406E 00	0
0.7000E 03	0.1042E 02	0.1517E 00	0.4865E 01	0.2561E 01	0.1406E 00	0
0.1000E 04	0.1038E 02	0.1528E 00	0.4840E 01	0.2550E 01	0.1406E 00	0
0.2000E 04	0.1034E 02	0.1584E 00	0.4828E 01	0.2546E 01	0.1406E 00	0

TABLE XVIII. - LONGITUDINAL THICKNESS-SHEAR MODULUS AND ASSOCIATED LOSS TANGENT FOR A BORON-ALUMINUM 2024-T3 MONOFILAMENT COMPOSITE

IDATA 1 RMU 1.401 DELTA 1.000 VF 0.400

*****ECRON-ALUMINUM 2024-T3*****

FREQUENCY	G55	GG55	GF/GM	G55/GM	SHAPE	IKS
HERTZ	1.E6 PSI	PER CENT				
0.5000E 01	0.9254E 01	0.1542E 00	0.5771E 01	0.2302E 01	0.4752E 00	0
0.7000E 01	0.8926E 01	0.1570E 00	0.5583E 01	0.2215E 01	0.4724E 00	0
0.1000E 02	0.8928E 01	0.1612E 00	0.5421E 01	0.2210E 01	0.4706E 00	0
0.2000E 02	0.8918E 01	0.1740E 00	0.5235E 01	0.2202E 01	0.4678E 00	0
0.5000E 02	0.8753E 01	0.1703E 00	0.5074E 01	0.2156E 01	0.4656E 00	0
0.7000E 02	0.8710E 01	0.1658E 00	0.5012E 01	0.2140E 01	0.4648E 00	0
0.1000E 03	0.8580E 01	0.1623E 00	0.4963E 01	0.2108E 01	0.4644E 00	0
0.2000E 03	0.8547E 01	0.1670E 00	0.4914E 01	0.2100E 01	0.4633E 00	0
0.5000E 03	0.8490E 01	0.1592E 00	0.4865E 01	0.2086E 01	0.4625E 00	0
0.7000E 03	0.8490E 01	0.1623E 00	0.4865E 01	0.2086E 01	0.4625E 00	0
0.1000E 04	0.8311E 01	0.1637E 00	0.4840E 01	0.2042E 01	0.4621E 00	0
0.2000E 04	0.8217E 01	0.1701E 00	0.4828E 01	0.2024E 01	0.4617E 00	0

TABLE XVIII. - LONGITUDINAL THICKNESS-SHEAR MODULUS AND ASSOCIATED LOSS TANGENT FOR A BORON-ALUMINUM 2024-T3 MONOFILAMENT COMPOSITE (CONTINUED)

IDATA 2 RMU 1.253 DELTA 1.000 VF 0.500

*****BORON-ALUMINUM 2024-T3*****

FREQUENCY	G55	GG55	GF/GM	G55/GM	SHAPE	IKS
HERTZ	1.E6 PSI	PER CENT				
0.5000E 01	0.1401E 02	0.1570E 00	0.5771E 01	0.3485E 01	0.4877E 00	0
0.7000E 01	0.1339E 02	0.1584E 00	0.5583E 01	0.3323E 01	0.4841E 00	0
0.1000E 02	0.1289E 02	0.1606E 00	0.5421E 01	0.3191E 01	0.4815E 00	0
0.2000E 02	0.1290E 02	0.1688E 00	0.5235E 01	0.3185E 01	0.4780E 00	0
0.5000E 02	0.1260E 02	0.1678E 00	0.5074E 01	0.3104E 01	0.4750E 00	0
0.7000E 02	0.1246E 02	0.1664E 00	0.5012E 01	0.3062E 01	0.4739E 00	0
0.1000E 03	0.1243E 02	0.1659E 00	0.4963E 01	0.3053E 01	0.4734E 00	0
0.2000E 03	0.1239E 02	0.1772E 00	0.4914E 01	0.3044E 01	0.4719E 00	0
0.5000E 03	0.1223E 02	0.1711E 00	0.4865E 01	0.3005E 01	0.4709E 00	0
0.7000E 03	0.1222E 02	0.1751E 00	0.4865E 01	0.3002E 01	0.4709E 00	0
0.1000E 04	0.1217E 02	0.1771E 00	0.4846E 01	0.2990E 01	0.4704E 00	0
0.2000E 04	0.1201E 02	0.1847E 00	0.4826E 01	0.2958E 01	0.4699E 00	0

TABLE XVIII. - LONGITUDINAL THICKNESS-SHEAR MODULUS AND ASSOCIATED LOSS TANGENT FOR A BORON-ALUMINUM 2024-T3 MONOFILAMENT COMPOSITE (CONTINUED)

IDATA 3 RML 1.144 DELTA 1.0CC VF 0.600

*****BORON-ALUMINUM 2024-T3******

FREQUENCY	G55	GG55	GF/GM	G55/GM	SHAPE	IKS
HERTZ	1.E6 PSI	PER CENT				
0.5000E 01	0.1616E 02	0.1580E 00	0.5771E 01	C.4021E 01	0.5003E 00	0
0.7000E 01	0.1613E 02	0.1589E 00	0.5583E 01	C.4003E 01	0.4959E 00	0
C.1000E 02	0.1612E 02	0.1604E 00	0.5421E 01	C.3991E 01	0.4926E 00	0
C.2000E 02	0.1573E 02	0.1670E 00	0.5235E 01	C.3885E 01	0.4883E 00	0
C.5000E 02	0.1528E 02	0.1669E 00	C.5074E 01	C.3764E 01	0.4844E 00	0
0.7000E 02	0.1486E 02	0.1666E 00	0.5012E 01	C.3652E 01	0.4832E 00	0
0.1000E 03	0.1466E 02	0.1671E 00	0.4963E 01	C.3603E 01	0.4825E 00	0
0.2000E 03	0.1465E 02	0.1742E 00	0.4914E 01	C.3600E 01	0.4807E 00	0
C.5000E 03	0.1447E 02	0.1762E 00	0.4865E 01	C.3555E 01	0.4795E 00	0
C.7000E 03	0.1446E 02	0.1800E 00	0.4865E 01	C.3554E 01	0.4795E 00	0
C.1000E 04	0.1433E 02	0.1845E 00	0.4840E 01	C.3520E 01	0.4789E 00	0
0.2000E 04	0.1424E 02	0.1952E 00	0.4826E 01	C.3508E 01	0.4783E 00	0

TABLE XIX. - TRANSVERSE THICKNESS-SHEAR MODULUS AND ASSOCIATED LOSS TANGENT FOR A BORON-ALUMINUM 2024-T3 MONOFILAMENT COMPOSITE

IDATA 3 RMU 1.401 DELTA 1.000 VF 0.400

*****BORON-ALUMINUM 2024-T3*****

FREQUENCY	G44	GG44	GF/GM	G44/GM	SHAPE
HERTZ	1.E6 PSI	PER CENT			
0.5000E 01	0.7951E 01	0.2529E-01	0.5771E 01	0.1978E 01	0.8484E 00
0.7000E 01	0.7896E 01	0.2528E-01	0.5583E 01	0.1959E 01	0.8485E 00
0.1000E 02	0.7848E 01	0.2548E-01	0.5421E 01	0.1943E 01	0.8486E 00
0.2000E 02	0.7788E 01	0.2677E-01	0.5235E 01	0.1923E 01	0.8488E 00
0.5000E 02	0.7735E 01	0.2670E-01	0.5074E 01	0.1905E 01	0.8489E 00
0.7000E 02	0.7725E 01	0.2633E-01	0.5012E 01	0.1898E 01	0.8490E 00
0.1000E 03	0.7703E 01	0.2607E-01	0.4963E 01	0.1893E 01	0.8490E 00
0.2000E 03	0.7679E 01	0.2686E-01	0.4914E 01	0.1887E 01	0.8490E 00
0.5000E 03	0.7656E 01	0.2635E-01	0.4865E 01	0.1881E 01	0.8491E 00
0.7000E 03	0.7656E 01	0.2691E-01	0.4865E 01	0.1881E 01	0.8491E 00
0.1000E 04	0.7644E 01	0.2722E-01	0.4840E 01	0.1878E 01	0.8491E 00
0.2000E 04	0.7619E 01	0.2833E-01	0.4828E 01	0.1877E 01	0.8491E 00

TABLE XIX. - TRANSVERSE THICKNESS-SHEAR MODULUS AND ASSOCIATED LOSS TANGENT FOR A BORON-ALUMINUM 2024-T3 MONOFILAMENT COMPOSITE (CONTINUED)

IDATA 4 RMU 1.253 DELTA 1.000 VF 0.500

*****BORON-ALUMINUM 2024-T3*****

FREQUENCY	G44	GG44	GF/GM	G44/GM	SHAPE
HERTZ	1.E6 PSI	PER CENT			
0.5000E 01	0.9427E 01	0.2441E-01	0.5771E 01	0.2345E 01	0.8484E 00
0.7000E 01	0.9334E 01	0.2500E-01	0.5583E 01	0.2316E 01	0.8485E 00
0.1000E 02	0.9254E 01	0.2547E-01	0.5421E 01	0.2291E 01	0.8486E 00
0.2000E 02	0.9153E 01	0.2650E-01	0.5235E 01	0.2260E 01	0.8488E 00
0.5000E 02	0.9066E 01	0.2638E-01	0.5074E 01	0.2233E 01	0.8489E 00
0.7000E 02	0.9045E 01	0.2651E-01	0.5012E 01	0.2222E 01	0.8490E 00
0.1000E 03	0.9010E 01	0.2686E-01	0.4963E 01	0.2214E 01	0.8490E 00
0.2000E 03	0.8975E 01	0.2784E-01	0.4914E 01	0.2205E 01	0.8490E 00
0.5000E 03	0.8939E 01	0.2909E-01	0.4865E 01	0.2196E 01	0.8491E 00
0.7000E 03	0.8939E 01	0.2988E-01	0.4865E 01	0.2196E 01	0.8491E 00
0.1000E 04	0.8921E 01	0.3037E-01	0.4840E 01	0.2192E 01	0.8491E 00
0.2000E 04	0.8890E 01	0.3182E-01	0.4828E 01	0.2190E 01	0.8491E 00

TABLE XIX. - TRANSVERSE THICKNESS-SHEAR MODULUS AND ASSOCIATED LOSS TANGENT FOR A BORON-ALUMINUM 2024-T3 MONOFILAMENT COMPOSITE (CONTINUED)

IDATA 5 RMU 1.144 DELTA 1.000 VF 0.600

*****BORON-ALUMINUM 2024-T3*****

FREQUENCY HERTZ	G44 1.E6 PSI	GG44 PER CENT	GF/GM	G44/GM	SHAPE
0.5000E 01	0.1133E 02	0.2329E-01	0.5771E 01	0.2817E 01	0.8484E 00
0.7000E 01	0.1117E 02	0.2431E-01	0.5583E 01	0.2772E 01	0.8485E 00
0.1000E 02	0.1104E 02	0.2541E-01	0.5421E 01	0.2733E 01	0.8486E 00
0.2000E 02	0.1086E 02	0.2769E-01	0.5235E 01	0.2686E 01	0.8488E 00
0.5000E 02	0.1074E 02	0.2678E-01	0.5074E 01	0.2645E 01	0.8489E 00
0.7000E 02	0.1070E 02	0.2616E-01	0.5012E 01	0.2628E 01	0.8490E 00
0.1000E 03	0.1064E 02	0.2578E-01	0.4963E 01	0.2615E 01	0.8490E 00
0.2000E 03	0.1059E 02	0.2667E-01	0.4914E 01	0.2602E 01	0.8490E 00
0.5000E 03	0.1054E 02	0.2624E-01	0.4865E 01	0.2589E 01	0.8491E 00
0.7000E 03	0.1054E 02	0.2685E-01	0.4865E 01	0.2589E 01	0.8491E 00
0.1000E 04	0.1051E 02	0.2722E-01	0.4840E 01	0.2582E 01	0.8491E 00
0.2000E 04	0.1047E 02	0.2846E-01	0.4828E 01	0.2579E 01	0.8491E 00

TABLE XX. - IN-PLANE LONGITUDINAL YOUNG'S MODULUS AND ASSOCIATED LOSS TANGENT FOR AN E GLASS-EPOXY MONOFILAMENT COMPOSITE

IDATA 3 RMU 1.401 DELTA 1.000 VF 0.400

*****E GLASS-EPOXY A*****

FREQUENCY HERTZ	E11 1.E6 PSI	GE11 PER CENT	EF/EM	E11/EM
0.5000E 01	0.4548E 01	0.3479E 00	0.2410E 02	0.1024E 02
0.7000E 01	0.4550E 01	0.3444E 00	0.2388E 02	0.1016E 02
0.1000E 02	0.4553E 01	0.3410E 00	0.2367E 02	0.1007E 02
0.2000E 02	0.4597E 01	0.3415E 00	0.2348E 02	0.9994E 01
0.5000E 02	0.4606E 01	0.3509E 00	0.2274E 02	0.9698E 01
0.7000E 02	0.4609E 01	0.3603E 00	0.2250E 02	0.9603E 01
0.1000E 03	0.4606E 01	0.4040E 00	0.2274E 02	0.9698E 01
0.2000E 03	0.4573E 01	0.4031E 00	0.2571E 02	0.1089E 02
0.5000E 03	0.4540E 01	0.5104E 00	0.2967E 02	0.1247E 02
0.7000E 03	0.4494E 01	0.5767E 00	0.3014E 02	0.1266E 02
0.1000E 04	0.4490E 01	0.6467E 00	0.3075E 02	0.1290E 02
0.2000E 04	0.4405E 01	0.8111E 00	0.3088E 02	0.1296E 02

TABLE XX. - IN-PLANE LONGITUDINAL YOUNG'S MODULUS AND ASSOCIATED LOSS TANGENT FOR AN E GLASS-EPOXY MONOFILAMENT COMPOSITE (CONTINUED)

IDATA 4 RNU 1.253 DELTA 1.000 VF 0.500

*****E GLASS-EPOXY A*****

FREQUENCY HERTZ	E11 1.E6 PSI	GE11 PER CENT	EF/EM	E11/EM
0.5000E 01	0.5575E 01	0.3229E 00	0.2410E 02	0.1256E 02
0.7000E 01	0.5577E 01	0.3190E 00	0.2388E 02	0.1245E 02
0.1000E 02	0.5579E 01	0.3151E 00	0.2367E 02	0.1234E 02
0.2000E 02	0.5633E 01	0.3148E 00	0.2348E 02	0.1224E 02
0.3000E 02	0.5640E 01	0.3219E 00	0.2274E 02	0.1187E 02
0.7000E 02	0.5643E 01	0.3298E 00	0.2250E 02	0.1176E 02
0.1000E 03	0.5640E 01	0.3740E 00	0.2274E 02	0.1187E 02
0.2000E 03	0.5613E 01	0.3732E 00	0.2571E 02	0.1336E 02
0.5000E 03	0.5585E 01	0.4812E 00	0.2967E 02	0.1534E 02
0.7000E 03	0.5530E 01	0.5454E 00	0.3014E 02	0.1558E 02
0.1000E 04	0.5527E 01	0.6155E 00	0.3075E 02	0.1588E 02
0.2000E 04	0.5423E 01	0.7752E 00	0.3088E 02	0.1595E 02

TABLE XX. - IN-PLANE LONGITUDINAL YOUNG'S MODULUS AND ASSOCIATED LOSS TANGENT FOR AN E GLASS-EPOXY MONOFILAMENT COMPOSITE (CONTINUED)

IDATA 5 RMU 1.144 DELTA 1.000 VF 0.600

*****E GLASS-EPOXY A*****

FREQUENCY	E11	GE11	EF/EM	E11/EM
HERTZ	1.E6 PSI	PER CENT		
0.5000E 01	0.6599E 01	0.3058E 00	0.2410E 02	0.1486E 02
0.7000E 01	0.6600E 01	0.3015E 00	0.2388E 02	0.1473E 02
0.1000E 02	0.6602E 01	0.2972E 00	0.2367E 02	0.1461E 02
0.2000E 02	0.6665E 01	0.2964E 00	0.2348E 02	0.1449E 02
0.5000E 02	0.6671E 01	0.3019E 00	0.2274E 02	0.1404E 02
0.7000E 02	0.6673E 01	0.3089E 00	0.2250E 02	0.1390E 02
0.1000E 03	0.6671E 01	0.3533E 00	0.2274E 02	0.1404E 02
0.2000E 03	0.6649E 01	0.3527E 00	0.2571E 02	0.1583E 02
0.5000E 03	0.6627E 01	0.4613E 00	0.2967E 02	0.1821E 02
0.7000E 03	0.6563E 01	0.5241E 00	0.3014E 02	0.1849E 02
0.1000E 04	0.6560E 01	0.5941E 00	0.3075E 02	0.1885E 02
0.2000E 04	0.6437E 01	0.7507E 00	0.3088E 02	0.1893E 02

TABLE XXI. - IN-PLANE MAJOR POISSON'S RATIO AND ASSOCIATED LOSS TANGENT FOR AN E GLASS-EPOXY MONOFILAMENT COMPOSITE

IDATA 3 RMU 1.401 DELTA 1.000 VF 0.400

*****E GLASS-EPOXY A*****

FREQUENCY	RNU12	GNU12	RNUF	RNUM
HERTZ		PER CENT		
0.5000E 01	0.2948E 00	-0.5968E 00	0.2150E 00	0.3480E 00
0.7000E 01	0.2936E 00	-0.6041E 00	0.2150E 00	0.3460E 00
0.1000E 02	0.2926E 00	-0.6124E 00	0.2140E 00	0.3450E 00
0.2000E 02	0.2904E 00	-0.6350E 00	0.2130E 00	0.3420E 00
0.5000E 02	0.2870E 00	-0.6884E 00	0.2120E 00	0.3370E 00
0.7000E 02	0.2864E 00	-0.7205E 00	0.2120E 00	0.3360E 00
0.1000E 03	0.2870E 00	-0.7423E 00	0.2120E 00	0.3370E 00
0.2000E 03	0.2984E 00	-0.6940E 00	0.2120E 00	0.3560E 00
0.5000E 03	0.3106E 00	-0.7053E 00	0.2140E 00	0.3750E 00
0.7000E 03	0.3128E 00	-0.7590E 00	0.2150E 00	0.3780E 00
0.1000E 04	0.3150E 00	-0.7926E 00	0.2160E 00	0.3810E 00
0.2000E 04	0.3178E 00	-0.9234E 00	0.2200E 00	0.3830E 00

TABLE XXI. - IN-PLANE MAJOR POISSON'S RATIO AND ASSOCIATED LOSS TANGENT FOR AN E GLASS-EPOXY MONOFILAMENT COMPOSITE (CONTINUED)

IDATA 4 RMU 1.253 DELTA 1.000 VF 0.500

*****E GLASS-EPOXY A*****

FREQUENCY	RNU12	GNU12	RNUF	RNUM
HERTZ		PER CENT		
0.5000E 01	0.2815E 00	-0.5661E 00	0.2150E 00	0.3480E 00
0.7000E 01	0.2805E 00	-0.5717E 00	0.2150E 00	0.3460E 00
0.1000E 02	0.2795E 00	-0.5782E 00	0.2140E 00	0.3450E 00
0.2000E 02	0.2775E 00	-0.5979E 00	0.2130E 00	0.3420E 00
0.3000E 02	0.2745E 00	-0.6449E 00	0.2120E 00	0.3370E 00
0.7000E 02	0.2740E 00	-0.6736E 00	0.2120E 00	0.3360E 00
0.1000E 03	0.2745E 00	-0.7006E 00	0.2120E 00	0.3370E 00
0.2000E 03	0.2840E 00	-0.6595E 00	0.2120E 00	0.3560E 00
0.3000E 03	0.2945E 00	-0.6876E 00	0.2140E 00	0.3750E 00
0.7000E 03	0.2965E 00	-0.7440E 00	0.2150E 00	0.3780E 00
0.1000E 04	0.2985E 00	-0.7838E 00	0.2160E 00	0.3810E 00
0.2000E 04	0.3015E 00	-0.9191E 00	0.2200E 00	0.3830E 00

TABLE XXI. - IN-PLANE MAJOR POISSON'S RATIO AND ASSOCIATED LOSS TANGENT FOR AN E GLASS-EPOXY MONOFILAMENT COMPOSITE (CONTINUED)

IDATA 5 RMU 1.144 DELTA 1.000 VF 0.600

*****E GLASS-EPOXY A*****

FREQUENCY	RNU12	GNU12	RNUF	RNUM
HERTZ		PER CENT		
0.5000E 01	0.2682E 00	-0.5324E 00	0.2150E 00	0.3480E 00
0.7000E 01	0.2674E 00	-0.5362E 00	0.2150E 00	0.3460E 00
0.1000E 02	0.2664E 00	-0.5408E 00	0.2140E 00	0.3450E 00
0.2000E 02	0.2646E 00	-0.5574E 00	0.2130E 00	0.3420E 00
0.5000E 02	0.2620E 00	-0.5974E 00	0.2120E 00	0.3370E 00
0.7000E 02	0.2616E 00	-0.6225E 00	0.2120E 00	0.3360E 00
0.1000E 03	0.2620E 00	-0.6551E 00	0.2120E 00	0.3370E 00
0.2000E 03	0.2696E 00	-0.6214E 00	0.2120E 00	0.3560E 00
0.5000E 03	0.2784E 00	-0.6678E 00	0.2140E 00	0.3750E 00
0.7000E 03	0.2802E 00	-0.7273E 00	0.2150E 00	0.3780E 00
0.1000E 04	0.2820E 00	-0.7740E 00	0.2160E 00	0.3810E 00
0.2000E 04	0.2852E 00	-0.9143E 00	0.2200E 00	0.3830E 00

TABLE XXII. - IN-PLANE TRANSVERSE YOUNG'S MODULUS AND ASSOCIATED LOSS TANGENT FOR AN E GLASS-EPOXY MONOFILAMENT COMPOSITE

IDATA# 1 RMU# 1.401 DELTA# 1.000 VF# 0.400

*****E GLASS-EPOXY A*****

FREQUENCY	E22	GE22	RNU12	EF/EM	E22/EM	IKS
HERTZ	1.E6 PSI	PER CENT				
0.5000E 01	0.8450E 00	0.1550E 01	0.2994E 00	0.2410E 02	0.1903E 01	0
0.7000E 01	0.8508E 00	0.1559E 01	0.2981E 00	0.2388E 02	0.1899E 01	0
0.1000E 02	0.8584E 00	0.1568E 01	0.2971E 00	0.2367E 02	0.1899E 01	0
0.2000E 02	0.8710E 00	0.1597E 01	0.2947E 00	0.2348E 02	0.1894E 01	0
0.5000E 02	0.8958E 00	0.1672E 01	0.2910E 00	0.2274E 02	0.1886E 01	0
0.7000E 02	0.9045E 00	0.1730E 01	0.2904E 00	0.2250E 02	0.1884E 01	0
0.1000E 03	0.8962E 00	0.1770E 01	0.2911E 00	0.2274E 02	0.1887E 01	0
0.2000E 03	0.8059E 00	0.1940E 01	0.3033E 00	0.2571E 02	0.1919E 01	0
0.5000E 03	0.7106E 00	0.2241E 01	0.3167E 00	0.2967E 02	0.1952E 01	0
0.7000E 03	0.6951E 00	0.2457E 01	0.3193E 00	0.3014E 02	0.1958E 01	0
0.1000E 04	0.6831E 00	0.2567E 01	0.3215E 00	0.3075E 02	0.1963E 01	0
0.2000E 04	0.6690E 00	0.3028E 01	0.3248E 00	0.3088E 02	0.1968E 01	0

TABLE XXII. - IN-PLANE TRANSVERSE YOUNG'S MODULUS AND ASSOCIATED LOSS TANGENT FOR AN E GLASS-EPOXY MONOFILAMENT COMPOSITE (CONTINUED)

IDATA# 1 RMU# 1.253 DELTA# 1.000 VF# 0.500

*****E GLASS-EPOXY A*****

FREQUENCY	E22	GE22	RNU12	EF/EM	E22/EM	IKS
HERTZ	1.E6 PSI	PER CENT				
0.5000E 01	0.1019E 01	0.1522E 01	0.2844E 00	0.2410E 02	0.2295E 01	0
0.7000E 01	0.1028E 01	0.1531E 01	0.2837E 00	0.2388E 02	0.2295E 01	0
0.1000E 02	0.1037E 01	0.1539E 01	0.2827E 00	0.2367E 02	0.2295E 01	0
0.2000E 02	0.1052E 01	0.1567E 01	0.2805E 00	0.2348E 02	0.2287E 01	0
0.5000E 02	0.1080E 01	0.1640E 01	0.2770E 00	0.2274E 02	0.2273E 01	0
0.7000E 02	0.1091E 01	0.1695E 01	0.2767E 00	0.2250E 02	0.2274E 01	0
0.1000E 03	0.1082E 01	0.1737E 01	0.2774E 00	0.2274E 02	0.2278E 01	0
0.2000E 03	0.9763E 00	0.1906E 01	0.2877E 00	0.2571E 02	0.2324E 01	0
0.5000E 03	0.8632E 00	0.2206E 01	0.2989E 00	0.2967E 02	0.2371E 01	0
0.7000E 03	0.8420E 00	0.2421E 01	0.3006E 00	0.3014E 02	0.2372E 01	0
0.1000E 04	0.8209E 00	0.2532E 01	0.3015E 00	0.3075E 02	0.2359E 01	0
0.2000E 04	0.8117E 00	0.2986E 01	0.3064E 00	0.3088E 02	0.2387E 01	0

TABLE XXII. - IN-PLANE TRANSVERSE YOUNG'S MODULUS AND ASSOCIATED LOSS TANGENT FOR AN E GLASS-EPOXY MONOFILAMENT COMPOSITE (CONTINUED)

IDATA# 1 RMU# 1.144 DELTA# 1.000 VF# 0.600

*****E GLASS-EPOXY A*****

FREQUENCY	E22	GE22	RNU12	EF/EM	E22/EM	IKS
HERTZ	1.E6 PSI	PER CENT				
0.5000E 01	0.1265E 01	0.1492E 01	0.2698E 00	0.2410E 02	0.2850E 01	0
0.7000E 01	0.1281E 01	0.1499E 01	0.2699E 00	0.2388E 02	0.2859E 01	0
0.1000E 02	0.1289E 01	0.1508E 01	0.2686E 00	0.2367E 02	0.2851E 01	0
0.2000E 02	0.1296E 01	0.1536E 01	0.2686E 00	0.2348E 02	0.2817E 01	0
0.5000E 02	0.1345E 01	0.1604E 01	0.2639E 00	0.2274E 02	0.2832E 01	0
0.7000E 02	0.1356E 01	0.1659E 01	0.2637E 00	0.2250E 02	0.2825E 01	0
0.1000E 03	0.1345E 01	0.1701E 01	0.2642E 00	0.2274E 02	0.2833E 01	0
0.2000E 03	0.1215E 01	0.1869E 01	0.2722E 00	0.2571E 02	0.2894E 01	0
0.5000E 03	0.1078E 01	0.2169E 01	0.2822E 00	0.2967E 02	0.2963E 01	0
0.7000E 03	0.1056E 01	0.2381E 01	0.2842E 00	0.3014E 02	0.2975E 01	0
0.1000E 04	0.1041E 01	0.2489E 01	0.2865E 00	0.3075E 02	0.2992E 01	0
0.2000E 04	0.1017E 01	0.2940E 01	0.2897E 00	0.3088E 02	0.2992E 01	0

TABLE XXIII. - IN-PLANE LONGITUDINAL SHEAR MODULUS AND ASSOCIATED LOSS TANGENT FOR AN E GLASS-EPOXY MONOFILAMENT COMPOSITE

IDATA 3 RMU 1.401 DELTA 1.000 VF 0.400

*****E GLASS-EPOXY A*****

FREQUENCY	G66	GG66	GF/GM	G66/GM	SHAPE
HERTZ	1.E6 PSI	PER CENT			
0.5000E 01	0.3579E 00	0.1678E 01	0.2695E 02	0.2182E 01	0.1053E 01
0.7000E 01	0.3621E 00	0.1695E 01	0.2669E 02	0.2181E 01	0.1052E 01
0.1000E 02	0.3641E 00	0.1704E 01	0.2653E 02	0.2180E 01	0.1052E 01
0.2000E 02	0.3724E 00	0.1740E 01	0.2608E 02	0.2178E 01	0.1050E 01
0.5000E 02	0.3846E 00	0.1821E 01	0.2525E 02	0.2173E 01	0.1047E 01
0.7000E 02	0.3887E 00	0.1885E 01	0.2503E 02	0.2172E 01	0.1047E 01
0.1000E 03	0.3847E 00	0.1937E 01	0.2531E 02	0.2173E 01	0.1047E 01
0.2000E 03	0.3376E 00	0.2101E 01	0.2903E 02	0.2192E 01	0.1056E 01
0.5000E 03	0.2918E 00	0.2396E 01	0.3364E 02	0.2211E 01	0.1065E 01
0.7000E 03	0.2834E 00	0.2630E 01	0.3461E 02	0.2214E 01	0.1066E 01
0.1000E 04	0.2770E 00	0.2741E 01	0.3520E 02	0.2216E 01	0.1068E 01
0.2000E 04	0.2704E 00	0.3235E 01	0.3549E 02	0.2217E 01	0.1070E 01

TABLE XXIII. - IN-PLANE LONGITUDINAL SHEAR MODULUS AND ASSOCIATED LOSS TANGENT FOR AN E GLASS-EPOXY MONOFILAMENT COMPOSITE (CONTINUED)

IDATA 4 RMU 1.253 DELTA 1.000 VF 0.500

*****E GLASS-EPOXY A*****

FREQUENCY HERTZ	G66 1.E6 PSI	GG66 PER CENT	GF/GM	G66/GM	SHAPE
0.5000E 01	0.4709E 00	0.1643E 01	0.2695E 02	0.2872E 01	0.1043E 01
0.7000E 01	0.4763E 00	0.1660E 01	0.2669E 02	0.2869E 01	0.1043E 01
0.1000E 02	0.4789E 00	0.1668E 01	0.2653E 02	0.2868E 01	0.1042E 01
0.2000E 02	0.4896E 00	0.1702E 01	0.2608E 02	0.2863E 01	0.1040E 01
0.5000E 02	0.5053E 00	0.1780E 01	0.2525E 02	0.2855E 01	0.1038E 01
0.7000E 02	0.5106E 00	0.1843E 01	0.2503E 02	0.2852E 01	0.1038E 01
0.1000E 03	0.5054E 00	0.1895E 01	0.2531E 02	0.2855E 01	0.1038E 01
0.2000E 03	0.4450E 00	0.2059E 01	0.2903E 02	0.2890E 01	0.1045E 01
0.5000E 03	0.3858E 00	0.2357E 01	0.3364E 02	0.2923E 01	0.1053E 01
0.7000E 03	0.3749E 00	0.2589E 01	0.3461E 02	0.2929E 01	0.1054E 01
0.1000E 04	0.3665E 00	0.2700E 01	0.3520E 02	0.2932E 01	0.1056E 01
0.2000E 04	0.3580E 00	0.3188E 01	0.3549E 02	0.2934E 01	0.1058E 01

TABLE XXIII. - IN-PLANE LONGITUDINAL SHEAR MODULUS AND ASSOCIATED LOSS TANGENT FOR AN E GLASS-EPOXY MONOFILAMENT COMPOSITE (CONTINUED)

IDATA 5 RMU 1.144 DELTA 1.000 VF 0.600

*****E GLASS-EPOXY A*****

FREQUENCY HERTZ	G66 1.E6 PSI	GG66 PER CENT	GF/GM	G66/GM	SHAPE
0.5000E 01	0.6344E 00	0.1597E 01	0.2695E 02	0.3868E 01	0.1034E 01
0.7000E 01	0.6414E 00	0.1613E 01	0.2669E 02	0.3864E 01	0.1033E 01
0.1000E 02	0.6448E 00	0.1620E 01	0.2653E 02	0.3861E 01	0.1032E 01
0.2000E 02	0.6589E 00	0.1652E 01	0.2608E 02	0.3853E 01	0.1031E 01
0.5000E 02	0.6792E 00	0.1726E 01	0.2525E 02	0.3838E 01	0.1029E 01
0.7000E 02	0.6861E 00	0.1786E 01	0.2503E 02	0.3833E 01	0.1029E 01
0.1000E 03	0.6794E 00	0.1839E 01	0.2531E 02	0.3839E 01	0.1029E 01
0.2000E 03	0.6009E 00	0.2004E 01	0.2903E 02	0.3902E 01	0.1035E 01
0.5000E 03	0.5232E 00	0.2304E 01	0.3364E 02	0.3963E 01	0.1041E 01
0.7000E 03	0.5087E 00	0.2533E 01	0.3461E 02	0.3974E 01	0.1042E 01
0.1000E 04	0.4976E 00	0.2643E 01	0.3520E 02	0.3981E 01	0.1044E 01
0.2000E 04	0.4860E 00	0.3124E 01	0.3549E 02	0.3994E 01	0.1046E 01

TABLE XXIV. - LONGITUDINAL FLEXURAL STIFFNESS AND ASSOCIATED LOSS TANGENT FOR AN E GLASS-EPOXY MONOFILAMENT COMPOSITE

IDATA 3 RMU 1.401 DELTA 1.000 VF 0.400

*****E GLASS-EPOXY A*****

FREQUENCY	D11S	GD11	EF/EM	D11/D11M
HERTZ	1.E6 PSI	PER CENT		
0.5000E 01	0.2012E 01	0.5186E 00	0.2410E 02	0.4532E 01
0.7000E 01	0.2015E 01	0.5183E 00	0.2388E 02	0.4499E 01
0.1000E 02	0.2019E 01	0.5179E 00	0.2367E 02	0.4467E 01
0.2000E 02	0.2041E 01	0.5238E 00	0.2348E 02	0.4437E 01
0.5000E 02	0.2054E 01	0.5480E 00	0.2274E 02	0.4323E 01
0.7000E 02	0.2058E 01	0.5663E 00	0.2250E 02	0.4287E 01
0.1000E 03	0.2054E 01	0.6078E 00	0.2274E 02	0.4323E 01
0.2000E 03	0.2007E 01	0.6096E 00	0.2571E 02	0.4779E 01
0.5000E 03	0.1960E 01	0.7158E 00	0.2967E 02	0.5384E 01
0.7000E 03	0.1937E 01	0.7968E 00	0.3014E 02	0.5456E 01
0.1000E 04	0.1931E 01	0.8676E 00	0.3075E 02	0.5548E 01
0.2000E 04	0.1893E 01	0.1065E 01	0.3088E 02	0.5569E 01

TABLE XXIV. - LONGITUDINAL FLEXURAL STIFFNESS AND ASSOCIATED LOSS TANGENT FOR AN E GLASS-EPOXY MONOFILAMENT COMPOSITE (CONTINUED)

IDATA 4 RML 1.253 DELTA 1.000 VF 0.500

*****E GLASS-EPOXY A*****

FREQUENCY	D11S	GD11	EF/EM	D11/D11M
HERTZ	1.E6 PSI	PER CENT		
0.5000E 01	0.2895E 01	0.4252E 00	0.2410E 02	0.6520E 01
0.7000E 01	0.2898E 01	0.4232E 00	0.2388E 02	0.6469E 01
0.1000E 02	0.2901E 01	0.4213E 00	0.2367E 02	0.6418E 01
0.2000E 02	0.2931E 01	0.4243E 00	0.2348E 02	0.6372E 01
0.5000E 02	0.2942E 01	0.4406E 00	0.2274E 02	0.6194E 01
0.7000E 02	0.2946E 01	0.4541E 00	0.2250E 02	0.6138E 01
0.1000E 03	0.2942E 01	0.4967E 00	0.2274E 02	0.6194E 01
0.2000E 03	0.2901E 01	0.4962E 00	0.2571E 02	0.6906E 01
0.5000E 03	0.2858E 01	0.6022E 00	0.2967E 02	0.7851E 01
0.7000E 03	0.2827E 01	0.6749E 00	0.3014E 02	0.7964E 01
0.1000E 04	0.2822E 01	0.7452E 00	0.3075E 02	0.8109E 01
0.2000E 04	0.2768E 01	0.9244E 00	0.3088E 02	0.8141E 01

TABLE XXIV. - LONGITUDINAL FLEXURAL STIFFNESS AND ASSOCIATED LOSS TANGENT FOR AN E GLASS-EPOXY MONOFILAMENT COMPOSITE (CONTINUED)

IDATA 5 RMU 1.144 DELTA 1.000 VF 0.600

*****E GLASS-EPOXY A*****

FREQUENCY HERTZ	D11S 1.E6 PSI	GD11 PER CENT	EF/EM	D11/D11M
0.5000E 01	0.3971E 01	0.3676E 00	0.2410E 02	0.8944E 01
0.7000E 01	0.3974E 01	0.3645E 00	0.2388E 02	0.8870E 01
0.1000E 02	0.3976E 01	0.3614E 00	0.2367E 02	0.8797E 01
0.2000E 02	0.4016E 01	0.3626E 00	0.2348E 02	0.8731E 01
0.5000E 02	0.4026E 01	0.3738E 00	0.2274E 02	0.8476E 01
0.7000E 02	0.4029E 01	0.3842E 00	0.2250E 02	0.8394E 01
0.1000E 03	0.4026E 01	0.4277E 00	0.2274E 02	0.8476E 01
0.2000E 03	0.3990E 01	0.4267E 00	0.2571E 02	0.9500E 01
0.5000E 03	0.3953E 01	0.5336E 00	0.2967E 02	0.1086E 02
0.7000E 03	0.3913E 01	0.6014E 00	0.3014E 02	0.1102E 02
0.1000E 04	0.3908E 01	0.6715E 00	0.3075E 02	0.1123E 02
0.2000E 04	0.3834E 01	0.8396E 00	0.3088E 02	0.1128E 02

TABLE XXV. - POISSON FLEXURAL STIFFNESS AND ASSOCIATED LOSS TANGENT FOR AN E GLASS-EPOXY MONOFILAMENT COMPOSITE

IDATA 3 RMU 1.401 DELTA 1.000 VF 0.400

*****E GLASS-EPOXY A*****

FREQUENCY HERTZ	D12S 1.E6 PSI	GD12 PER CENT	EF/EM	D12/D12M
0.5000E 01	0.1964E 00	0.8239E 00	0.2410E 02	0.4424E 00
0.7000E 01	0.1970E 00	0.8229E 00	0.2388E 02	0.4397E 00
0.1000E 02	0.1980E 00	0.8199E 00	0.2367E 02	0.4381E 00
0.2000E 02	0.1996E 00	0.8195E 00	0.2348E 02	0.4339E 00
0.5000E 02	0.2029E 00	0.8264E 00	0.2274E 02	0.4271E 00
0.7000E 02	0.2044E 00	0.8424E 00	0.2250E 02	0.4257E 00
0.1000E 03	0.2029E 00	0.8672E 00	0.2274E 02	0.4271E 00
0.2000E 03	0.1899E 00	0.1093E 01	0.2571E 02	0.4521E 00
0.5000E 03	0.1742E 00	0.1400E 01	0.2967E 02	0.4787E 00
0.7000E 03	0.1715E 00	0.1557E 01	0.3014E 02	0.4831E 00
0.1000E 04	0.1697E 00	0.1637E 01	0.3075E 02	0.4876E 00
0.2000E 04	0.1672E 00	0.1955E 01	0.3088E 02	0.4917E 00

TABLE XXV. - POISSON FLEXURAL STIFFNESS AND ASSOCIATED LOSS TANGENT FOR AN E GLASS-EPOXY MONOFILAMENT COMPOSITE (CONTINUED)

IDATA 4 RMU 1.253 DELTA 1.000 VF 0.500

*****E GLASS-EPOXY A*****

FREQUENCY HERTZ	D12S 1.E6 PSI	GD12 PER CENT	EF/EM	D12/D12M
0.5000E 01	0.2157E 00	0.8698E 00	0.2410E 02	0.4858E 00
0.7000E 01	0.2165E 00	0.8704E 00	0.2388E 02	0.4833E 00
0.1000E 02	0.2176E 00	0.8694E 00	0.2367E 02	0.4814E 00
0.2000E 02	0.2195E 00	0.8722E 00	0.2348E 02	0.4771E 00
0.5000E 02	0.2233E 00	0.8864E 00	0.2274E 02	0.4701E 00
0.7000E 02	0.2250E 00	0.9065E 00	0.2250E 02	0.4688E 00
0.1000E 03	0.2233E 00	0.9263E 00	0.2274E 02	0.4701E 00
0.2000E 03	0.2078E 00	0.1146E 01	0.2571E 02	0.4947E 00
0.5000E 03	0.1897E 00	0.1438E 01	0.2967E 02	0.5211E 00
0.7000E 03	0.1866E 00	0.1595E 01	0.3014E 02	0.5257E 00
0.1000E 04	0.1845E 00	0.1670E 01	0.3075E 02	0.5303E 00
0.2000E 04	0.1820E 00	0.1986E 01	0.3080E 02	0.5352E 00

TABLE XXV. - POISSON FLEXURAL STIFFNESS AND ASSOCIATED LOSS TANGENT FOR AN E GLASS-EPOXY MONOFILAMENT COMPOSITE (CONTINUED)

IDATA 5 RMU 1.144 DELTA 1.000 VF 0.600

*****E GLASS-EPOXY A*****

FREQUENCY	D12S	GD12	EF/EM	D12/D12M
HERTZ	1.E6 PSI	PER CENT		
0.5000E 01	0.2470E 00	0.9097E 00	0.2410E 02	0.5564E 00
0.7000E 01	0.2481E 00	0.9121E 00	0.2388E 02	0.5539E 00
0.1000E 02	0.2493E 00	0.9132E 00	0.2367E 02	0.5516E 00
0.2000E 02	0.2516E 00	0.9194E 00	0.2348E 02	0.5470E 00
0.5000E 02	0.2563E 00	0.9411E 00	0.2274E 02	0.5395E 00
0.7000E 02	0.2583E 00	0.9653E 00	0.2250E 02	0.5381E 00
0.1000E 03	0.2563E 00	0.9793E 00	0.2274E 02	0.5395E 00
0.2000E 03	0.2370E 00	0.1192E 01	0.2571E 02	0.5643E 00
0.5000E 03	0.2154E 00	0.1466E 01	0.2967E 02	0.5917E 00
0.7000E 03	0.2118E 00	0.1620E 01	0.3014E 02	0.5966E 00
0.1000E 04	0.2093E 00	0.1688E 01	0.3075E 02	0.6015E 00
0.2000E 04	0.2067E 00	0.2000E 01	0.3088E 02	0.6080E 00

TABLE XXVI. - TRANSVERSE FLEXURAL STIFFNESS AND ASSOCIATED LOSS TANGENT FOR AN E GLASS-EPOXY MONOFILAMENT COMPOSITE

IDATA 1 RMU 1.401 DELTA 1.000 VF 0.400

*****E GLASS-EPOXY A*****

FREQUENCY	D22S	GD22	EF/EM	D22/D22M	IKS
HERTZ	1.E6 PSI	PER CENT			
0.5000E 01	0.5070E 00	0.1650E 01	0.2410E 02	0.1153E 01	0
0.7000E 01	0.5100E 00	0.1662E 01	0.2388E 02	0.1151E 01	0
0.1000E 02	0.5150E 00	0.1671E 01	0.2367E 02	0.1151E 01	0
0.2000E 02	0.5251E 00	0.1708E 01	0.2348E 02	0.1150E 01	0
0.5000E 02	0.5370E 00	0.1788E 01	0.2274E 02	0.1148E 01	0
0.7000E 02	0.5430E 00	0.1851E 01	0.2250E 02	0.1134E 01	0
0.1000E 03	0.5370E 00	0.1892E 01	0.2274E 02	0.1143E 01	0
0.2000E 03	0.4840E 00	0.2062E 01	0.2571E 02	0.1163E 01	0
0.5000E 03	0.4270E 00	0.2362E 01	0.2967E 02	0.1188E 01	0
0.7000E 03	0.4172E 00	0.2589E 01	0.3014E 02	0.1190E 01	0
0.1000E 04	0.4100E 00	0.2696E 01	0.3075E 02	0.1182E 01	0
0.2000E 04	0.4020E 00	0.3179E 01	0.3088E 02	0.1195E 01	0

TABLE XXVI. - TRANSVERSE FLEXURAL STIFFNESS AND ASSOCIATED LOSS TANGENT FOR AN E GLASS-EPOXY MONOFILAMENT COMPOSITE (CONTINUED)

ICATA 2 RMU 1.253 DELTA 1.000 VF 0.500

*****E GLASS-EPOXY A*****

FREQUENCY	D22S	GD22	EF/EM	D22/D22M	IKS
HERTZ	1.E6 PSI	PER CENT			
0.5000E 01	0.7340E 00	0.1641E 01	0.241CE 02	C.1650E 01	0
0.7000E 01	0.7400E 00	0.1653E 01	0.2388E 02	0.1650E 01	0
0.1000E 02	0.7464E 00	0.1663E 01	0.2367E 02	C.1650E 01	0
0.2000E 02	0.7586E 00	0.1694E 01	0.2348E C2	C.1648E C1	0
0.5000E 02	0.7791E 00	0.1776E 01	0.2274E 02	C.1635E C1	0
0.7000E 02	0.7873E C0	0.1838E 01	C.225CE C2	C.1636E 01	0
C.1000E 03	0.7800E 00	0.1881E 01	0.2274E 02	C.1640E 01	0
0.2000E 03	0.7048E 00	C.2050E 01	0.2571E 02	C.1675E C1	0
C.5000E 03	0.6244E 00	0.2348E 01	0.2967E C2	C.1720E C1	0
0.7000E 03	0.6073E 00	0.2574E 01	0.3014E C2	C.1712E 01	0
C.1000E 04	0.5915E 00	0.2683E 01	0.3075E C2	0.1699E C1	0
0.2000E 04	0.5860E 00	0.3163E 01	0.3C8EE 02	C.1723E 01	0

TABLE XXVI. - TRANSVERSE FLEXURAL STIFFNESS AND ASSOCIATED LOSS TANGENT FOR AN E GLASS-EPOXY MONOFILAMENT COMPOSITE (CONTINUED)

IDATA 3 RMU 1.144 DELTA 1.000 VF 0.600

*****E GLASS-EPOXY A*****

FREQUENCY	D22S	GD22	EF/EM	D22/D22M	IKS
HERTZ	1.E6 PSI	PER CENT			
0.5000E 01	0.9648E 00	0.1631E 01	0.2410E 02	0.2162E 01	0
0.7000E 01	0.9725E 00	0.1643E 01	0.2388E 02	0.2175E 01	0
0.1000E 02	0.9799E 00	0.1652E 01	0.2367E 02	0.2178E 01	0
0.2000E 02	0.9850E 00	0.1683E 01	0.2348E 02	0.2144E 01	0
0.5000E 02	0.1023E 01	0.1764E 01	0.2274E 02	0.2153E 01	0
0.7000E 02	0.1031E 01	0.1825E 01	0.2250E 02	0.2143E 01	0
0.1000E 03	0.1022E 01	0.1868E 01	0.2274E 02	0.2159E 01	0
0.2000E 03	0.9250E 00	0.2036E 01	0.2571E 02	0.2192E 01	0
0.5000E 03	0.8190E 00	0.2335E 01	0.2967E 02	0.2245E 01	0
0.7000E 03	0.8040E 00	0.2559E 01	0.3014E 02	0.2260E 01	0
0.1000E 04	0.7912E 00	0.2668E 01	0.3075E 02	0.2273E 01	0
0.2000E 04	0.7722E 00	0.3146E 01	0.3088E 02	0.2273E 01	0

TABLE XXVII. - TWISTING STIFFNESS AND ASSOCIATED LOSS TANGENT FOR AN E GLASS-EPOXY MONOFILAMENT COMPOSITE

IDATA# 1 RMU# 1.401 DELTA# 1.000 VF# 0.400

*****E GLASS-EPOXY A*****

FREQUENCY	D66S	GD66	GF/GM	D66/D66M	RTK	IKS
HERTZ	1.E6 PSI	PER CENT				
0.5000E 01	0.9332E 00	0.5447E 00	0.2695E 02	0.5690E 01	0.1406E 00	0
0.7000E 01	0.9356E 00	0.5443E 00	0.2669E 02	0.5636E 01	0.1406E 00	0
0.1000E 02	0.9326E 00	0.5414E 00	0.2653E 02	0.5585E 01	0.1406E 00	0
0.2000E 02	0.9445E 00	0.5484E 00	0.2608E 02	0.5524E 01	0.1406E 00	0
0.5000E 02	0.9548E 00	0.5717E 00	0.2525E 02	0.5394E 01	0.1406E 00	0
0.7000E 02	0.9573E 00	0.5895E 00	0.2503E 02	0.5348E 01	0.1406E 00	0
0.1000E 03	0.9511E 00	0.6417E 00	0.2531E 02	0.5373E 01	0.1406E 00	0
0.2000E 03	0.9336E 00	0.6356E 00	0.2903E 02	0.6062E 01	0.1406E 00	0
0.5000E 03	0.9110E 00	0.7591E 00	0.3364E 02	0.6901E 01	0.1406E 00	0
0.7000E 03	0.9024E 00	0.8462E 00	0.3491E 02	0.7050E 01	0.1406E 00	0
0.1000E 04	0.8977E 00	0.9319E 00	0.3520E 02	0.7182E 01	0.1406E 00	0
0.2000E 04	0.8825E 00	0.1150E 01	0.3549E 02	0.7233E 01	0.1406E 00	0

TABLE XXVII. - TWISTING STIFFNESS AND ASSOCIATED LOSS TANGENT FOR AN E GLASS-EPOXY MONOFILAMENT COMPOSITE (CONTINUED)

IDATA# 3 RMU# 1.253 DELTA# 1.000 VF# 0.500

*****E GLASS-EPOXY A*****

FREQUENCY	D66S	GD66	GF/GM	D66/D66M	RTK	IKS
HERTZ	1.E6 PSI	PER CENT				
0.5000E 01	0.1367E 01	0.4568E 00	0.2695E 02	0.8336E 01	0.1406E 00	0
0.7000E 01	0.1371E 01	0.4542E 00	0.2669E 02	0.8260E 01	0.1406E 00	0
0.1000E 02	0.1372E 01	0.4503E 00	0.2653E 02	0.8213E 01	0.1406E 00	0
0.2000E 02	0.1362E 01	0.4525E 00	0.2608E 02	0.7962E 01	0.1406E 00	0
0.5000E 02	0.1391E 01	0.4681E 00	0.2525E 02	0.7859E 01	0.1406E 00	0
0.7000E 02	0.1394E 01	0.4811E 00	0.2503E 02	0.7789E 01	0.1406E 00	0
0.1000E 03	0.1393E 01	0.5350E 00	0.2531E 02	0.7869E 01	0.1406E 00	0
0.2000E 03	0.1374E 01	0.5301E 00	0.2903E 02	0.8920E 01	0.1406E 00	0
0.5000E 03	0.1350E 01	0.6573E 00	0.3354E 02	0.1022E 02	0.1406E 00	0
0.7000E 03	0.1345E 01	0.7390E 00	0.3461E 02	0.1050E 02	0.1406E 00	0
0.1000E 04	0.1334E 01	0.8243E 00	0.3520E 02	0.1067E 02	0.1406E 00	0
0.2000E 04	0.1312E 01	0.1027E 01	0.3549E 02	0.1075E 02	0.1406E 00	0

TABLE XXVII. - TWISTING STIFFNESS AND ASSOCIATED LOSS TANGENT FOR AN E GLASS-EPOXY MONOFILAMENT COMPOSITE (CONTINUED)

IDATA# 3 RMU# 1.144 DELTA# 1.000 VF# 0.600

*****E GLASS-EPOXY A*****

FREQUENCY	D66S	GD66	GF/GM	D66/D66M	RTK	IKS
HERTZ	1.E6 PSI	PER CENT				
0.5000E 01	0.1897E 01	0.4138E 00	0.2695E 02	0.1157E 02	0.1406E 00	0
0.7000E 01	0.1901E 01	0.4099E 00	0.2669E 02	0.1145E 02	0.1406E 00	0
0.1000E 02	0.1902E 01	0.4053E 00	0.2653E 02	0.1139E 02	0.1406E 00	0
0.2000E 02	0.1916E 01	0.4062E 00	0.2608E 02	0.1121E 02	0.1406E 00	0
0.5000E 02	0.1924E 01	0.4170E 00	0.2525E 02	0.1087E 02	0.1406E 00	0
0.7000E 02	0.1929E 01	0.4277E 00	0.2503E 02	0.1078E 02	0.1406E 00	0
0.1000E 03	0.1929E 01	0.4824E 00	0.2531E 02	0.1090E 02	0.1406E 00	0
0.2000E 03	0.1910E 01	0.4787E 00	0.2903E 02	0.1240E 02	0.1406E 00	0
0.5000E 03	0.1886E 01	0.5083E 00	0.3364E 02	0.1429E 02	0.1406E 00	0
0.7000E 03	0.1873E 01	0.6869E 00	0.3461E 02	0.1463E 02	0.1406E 00	0
0.1000E 04	0.1866E 01	0.7728E 00	0.3520E 02	0.1492E 02	0.1406E 00	0
0.2000E 04	0.1835E 01	0.9682E 00	0.3549E 02	0.1504E 02	0.1406E 00	0

TABLE XXVIII. - LONGITUDINAL THICKNESS-SHEAR MODULUS AND ASSOCIATED LOSS TANGENT FOR AN E GLASS-EPOXY MONOFILAMENT COMPOSITE

IDATA 1 RMU 1.401 DELTA 1.000 VF 0.400

*****E GLASS-EPOXY A*****

FREQUENCY	G55	GG55	GF/GM	G55/GM	SHAPE	IKS
HERTZ	1.E6 PSI	PER CENT				
0.5000E 01	0.8372E 00	0.3058E 00	0.2695E 02	0.5105E 01	0.4627E 00	0
0.7000E 01	0.8398E 00	0.3300E 00	0.2669E 02	0.5059E 01	0.4639E 00	0
0.1000E 02	0.8355E 00	0.3241E 00	0.2653E 02	0.5003E 01	0.4648E 00	0
0.2000E 02	0.8547E 00	0.3213E 00	0.2608E 02	0.4998E 01	0.4670E 00	0
0.5000E 02	0.8823E 00	0.3249E 00	0.2525E 02	0.4985E 01	0.4704E 00	0
0.7000E 02	0.8902E 00	0.3249E 00	0.2503E 02	0.4973E 01	0.4710E 00	0
0.1000E 03	0.8829E 00	0.3312E 00	0.2531E 02	0.4988E 01	0.4704E 00	0
0.2000E 03	0.8167E 00	0.3870E 00	0.2903E 02	0.5303E 01	0.4591E 00	0
0.5000E 03	0.7371E 00	0.5199E 00	0.3364E 02	0.5584E 01	0.4472E 00	0
0.7000E 03	0.7400E 00	0.5939E 00	0.3461E 02	0.5781E 01	0.4451E 00	0
0.1000E 04	0.7576E 00	0.6799E 00	0.3526E 02	0.6061E 01	0.4430E 00	0
0.2000E 04	0.7453E 00	0.8621E 00	0.3549E 02	0.6109E 01	0.4403E 00	0

TABLE XXVIII. - LONGITUDINAL THICKNESS-SHEAR MODULUS AND ASSOCIATED LOSS TANGENT FOR AN E GLASS-EPOXY MONOFILAMENT COMPOSITE (CONTINUED)

ICATA 2 RML 1.253 DELTA 1.000 VF 0.500

*****E GLASS-EPOXY A*****

FREQUENCY	G55	GG55	GF/GM	G55/GM	SHAPE	IKS
HERTZ	1.E6 PSI	PER CENT				
0.5000E 01	0.1310E 01	0.3342E 00	0.2695E 02	0.7985E 01	0.4760E 00	0
0.7000E 01	0.1296E 01	0.3283E 00	0.2669E 02	0.7809E 01	0.4770E 00	0
0.1000E 02	0.1345E 01	0.3223E 00	0.2653E 02	0.8053E 01	0.4780E 00	0
0.2000E 02	0.1335E 01	0.3194E 00	0.2608E 02	0.7808E 01	0.4800E 00	0
0.5000E 02	0.1367E 01	0.3226E 00	0.2525E 02	0.7725E 01	0.4831E 00	0
0.7000E 02	0.1388E 01	0.3288E 00	0.2503E 02	0.7753E 01	0.4836E 00	0
0.1000E 03	0.1386E 01	0.3847E 00	0.2531E 02	0.7831E 01	0.4831E 00	0
0.2000E 03	0.1279E 01	0.3847E 00	0.2903E 02	0.8303E 01	0.4735E 00	0
0.5000E 03	0.1183E 01	0.5188E 00	0.3364E 02	0.8964E 01	0.4630E 00	0
0.7000E 03	0.1167E 01	0.5928E 00	0.3461E 02	0.9121E 01	0.4610E 00	0
0.1000E 04	0.1165E 01	0.6788E 00	0.3520E 02	0.9320E 01	0.4590E 00	0
0.2000E 04	0.1292E 01	0.8609E 00	0.3549E 02	0.1059E 02	0.4561E 00	0

TABLE XXVIII. - LONGITUDINAL THICKNESS-SHEAR MODULUS AND ASSOCIATED LOSS TANGENT FOR AN E GLASS-EPOXY MONOFILAMENT COMPOSITE (CONTINUED)

IDATA 3 RMU 1.144 DELTA 1.00C VF 0.600

*****E GLASS-EPOXY A*****

FREQUENCY	GSS	GGSS	GF/GM	GSS/GM	SHAPE	IKS
HERTZ	1.E6 PSI	PER CENT				
0.5C00E 01	0.1796E 01	0.3336E 00	C.2695E 02	0.1095E 02	0.4895E 00	0
C.7C00E 01	0.1775E 01	0.3276E 00	0.2665E C2	C.1069E 02	0.4903E 00	0
C.1C00E 02	0.1792E 01	0.3217E 00	0.2653E 02	C.1073E 02	0.4914E 00	0
0.2000E 02	0.1821E 01	0.3187E 00	0.2608E 02	C.1065E 02	0.4932E 00	0
0.5C00E 02	0.1832E 01	0.3218E 00	0.2525E 02	C.1035E 02	0.4959E 00	0
C.7C00E 02	0.1842E 01	0.3279E 00	0.2503E 02	C.1029E 02	0.4963E 00	0
C.1C00E 03	0.1807E 01	0.3839E 00	0.2531E 02	C.1021E 02	0.4959E 00	0
C.2CC0E 03	0.1714E 01	0.3836E 00	0.2903E 02	C.1113E C2	0.4881E 00	0
0.5000E C3	0.1602E 01	0.5184E 00	C.3364E 02	C.1214E 02	0.4791E 00	0
C.7CC0E 03	0.1576E 01	0.5924E 00	0.3461E C2	C.1231E C2	0.4773E 00	0
C.1C00E 04	0.1550E C1	0.6784E 00	0.352CE C2	0.1240E 02	0.4755E 00	0
C.2C00E 04	0.1560E 01	0.8605E 00	0.3549E C2	0.1279E 02	0.4722E 00	0

TABLE XXIX. - TRANSVERSE THICKNESS-SHEAR MODULUS AND ASSOCIATED LOSS TANGENT FOR AN E GLASS-EPOXY MONOFILAMENT COMPOSITE

IDATA 3 RMU 1.401 DELTA 1.000 VF 0.400

*****E GLASS-EPOXY A*****

FREQUENCY	G44	GG44	GF/GM	G44/GM	SHAPE
HERTZ	1.E6 PSI	PER CENT			
0.5000E 01	0.4450E 00	0.1508E 00	0.2695E 02	0.2713E 01	0.8489E 00
0.7000E 01	0.4498E 00	0.1534E 00	0.2669E 02	0.2710E 01	0.8488E 00
0.1000E 02	0.4521E 00	0.1555E 00	0.2653E 02	0.2707E 01	0.8488E 00
0.2000E 02	0.4620E 00	0.1597E 00	0.2608E 02	0.2702E 01	0.8487E 00
0.5000E 02	0.4760E 00	0.1733E 00	0.2525E 02	0.2689E 01	0.8486E 00
0.7000E 02	0.4807E 00	0.1812E 00	0.2503E 02	0.2686E 01	0.8485E 00
0.1000E 03	0.4761E 00	0.1872E 00	0.2531E 02	0.2690E 01	0.8486E 00
0.2000E 03	0.4221E 00	0.1659E 00	0.2903E 02	0.2741E 01	0.8490E 00
0.5000E 03	0.3688E 00	0.1407E 00	0.3364E 02	0.2794E 01	0.8494E 00
0.7000E 03	0.3587E 00	0.1506E 00	0.3461E 02	0.2803E 01	0.8495E 00
0.1000E 04	0.3511E 00	0.1563E 00	0.3520E 02	0.2809E 01	0.8496E 00
0.2000E 04	0.3429E 00	0.1904E 00	0.3549E 02	0.2811E 01	0.8497E 00

TABLE XXIX. - TRANSVERSE THICKNESS-SHEAR MODULUS AND ASSOCIATED LOSS TANGENT FOR AN E GLASS-EPOXY MONOFILAMENT COMPOSITE (CONTINUED)

IDATA 4 RMU 1.253 DELTA 1.000 VF 0.500

*****E GLASS-EPOXY A*****

FRECUENCY	G44	GG44	GF/GM	G44/GM	SHAPE
HERTZ	1.E6 PSI	PER CENT			
0.5000E 01	0.5870E 00	0.6074E-01	0.2695E 02	0.3579E 01	0.8489E 00
0.7000E 01	0.5930E 00	0.6114E-01	0.2669E 02	0.3572E 01	0.8488E 00
0.1000E 02	0.5958E 00	0.6162E-01	0.2653E 02	0.3568E 01	0.8488E 00
0.2000E 02	0.6084E 00	0.6275E-01	0.2608E 02	0.3558E 01	0.8487E 00
0.5000E 02	0.6257E 00	0.7001E-01	0.2525E 02	0.3535E 01	0.8486E 00
0.7000E 02	0.6316E 00	0.7396E-01	0.2503E 02	0.3528E 01	0.8485E 00
0.1000E 03	0.6259E 00	0.8050E-01	0.2531E 02	0.3536E 01	0.8486E 00
0.2000E 03	0.5589E 00	0.6283E-01	0.2903E 02	0.3629E 01	0.8490E 00
0.5000E 03	0.4921E 00	0.8951E-01	0.3364E 02	0.3728E 01	0.8494E 00
0.7000E 03	0.4792E 00	0.1045E 00	0.3461E 02	0.3744E 01	0.8495E 00
0.1000E 04	0.4695E 00	0.1222E 00	0.3520E 02	0.3756E 01	0.8496E 00
0.2000E 04	0.4587E 00	0.1544E 00	0.3549E 02	0.3760E 01	0.8497E 00

TABLE XXIX. - TRANSVERSE THICKNESS-SHEAR MODULUS AND ASSOCIATED LOSS TANGENT FOR AN E GLASS-EPOXY MONOFILAMENT COMPOSITE

IDATA 5 RMU 1.144 DELTA 1.000 VF 0.600

*****E GLASS-EPOXY A*****

FREQUENCY	G44	GG44	GF/GM	G44/GM	SHAPE
HERTZ	1.E6 PSI	PER CENT			
0.5000E 01	0.8239E 00	0.6026E-01	0.2695E 02	0.5024E 01	0.8489E 00
0.7000E 01	0.8317E 00	0.5859E-01	0.2669E 02	0.5010E 01	0.8488E 00
0.1000E 02	0.8351E 00	0.5694E-01	0.2653E 02	0.5001E 01	0.8488E 00
0.2000E 02	0.8516E 00	0.5591E-01	0.2608E 02	0.4980E 01	0.8487E 00
0.5000E 02	0.8733E 00	0.5418E-01	0.2525E 02	0.4934E 01	0.8486E 00
0.7000E 02	0.8807E 00	0.5456E-01	0.2503E 02	0.4920E 01	0.8485E 00
0.1000E 03	0.8737E 00	0.6415E-01	0.2531E 02	0.4936E 01	0.8486E 00
0.2000E 03	0.7895E 00	0.7908E-01	0.2903E 02	0.5127E 01	0.8490E 00
0.5000E 03	0.7039E 00	0.1298E 00	0.3364E 02	0.5333E 01	0.8494E 00
0.7000E 03	0.6869E 00	0.1492E 00	0.3461E 02	0.5367E 01	0.8495E 00
0.1000E 04	0.6739E 00	0.1682E 00	0.3520E 02	0.5391E 01	0.8496E 00
0.2000E 04	0.6588E 00	0.2074E 00	0.3549E 02	0.5400E 01	0.8497E 00

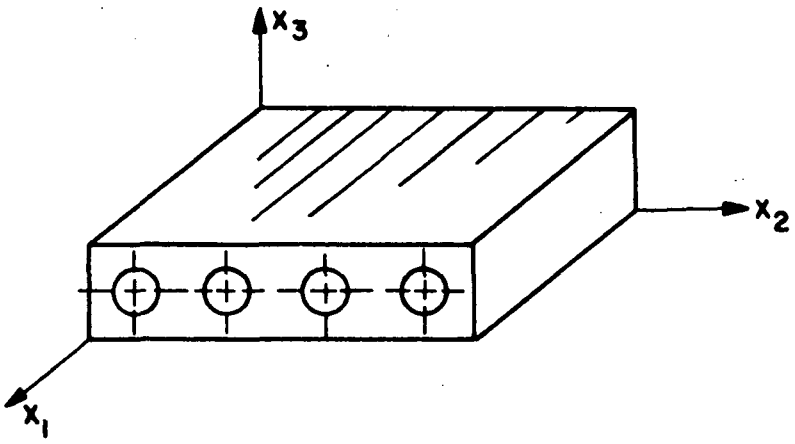

(a) Monofilament composite

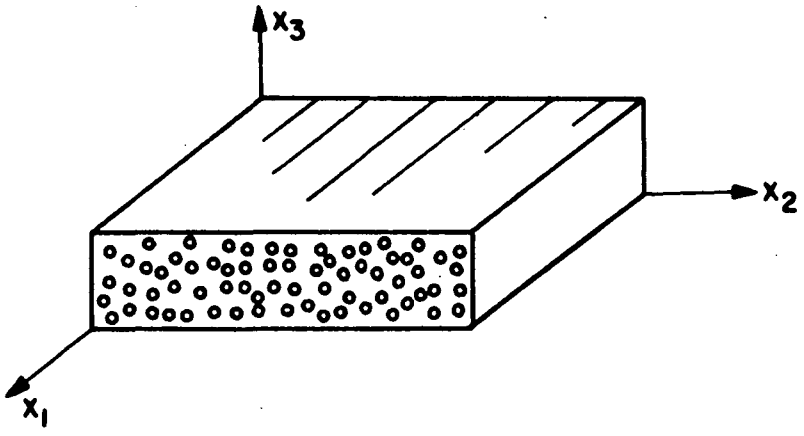

(b) Composite with randomly distributed filaments

Figure 1. Filamentary composites.

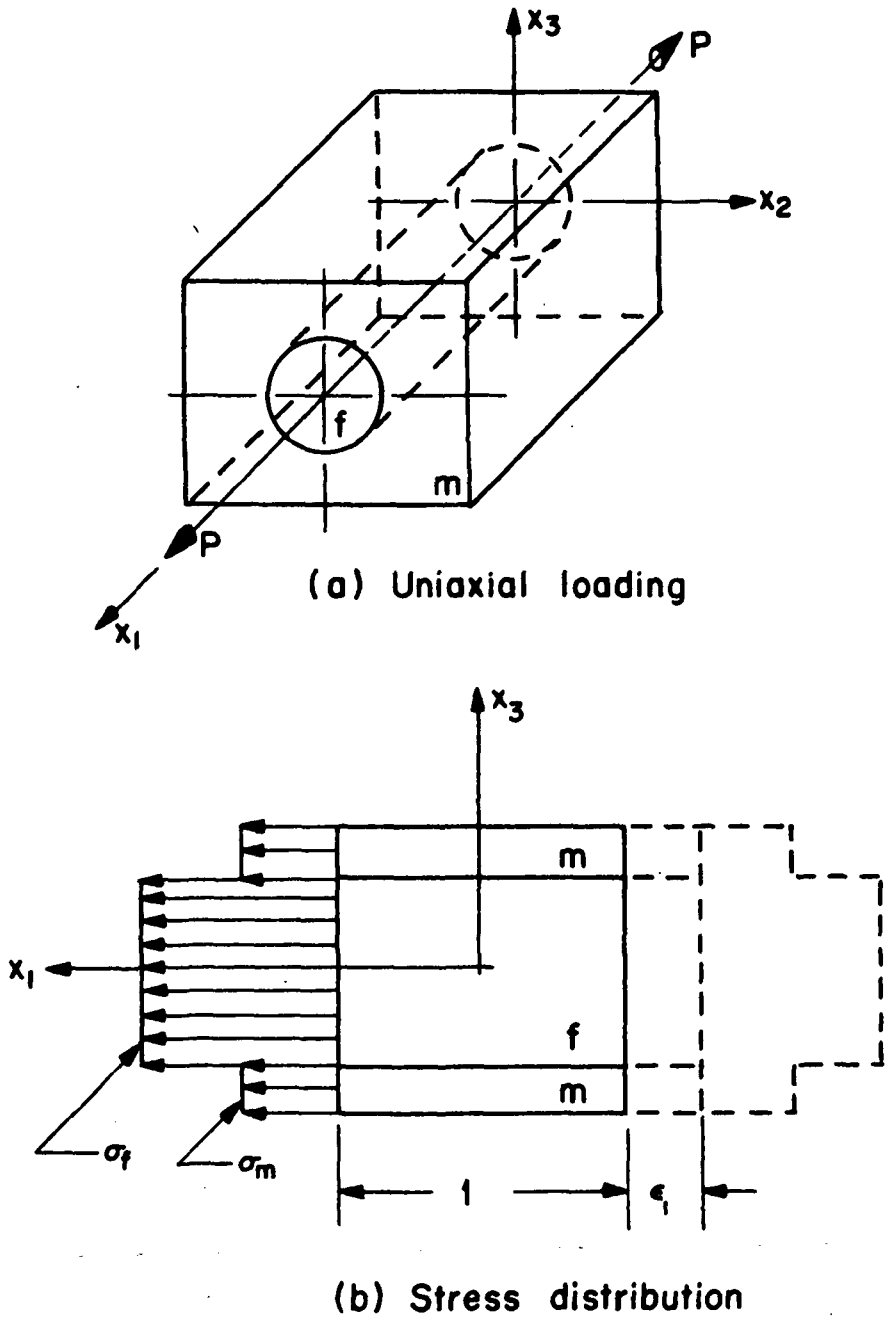

Figure 2. Uniaxial loading of a typical composite element in the longitudinal direction.

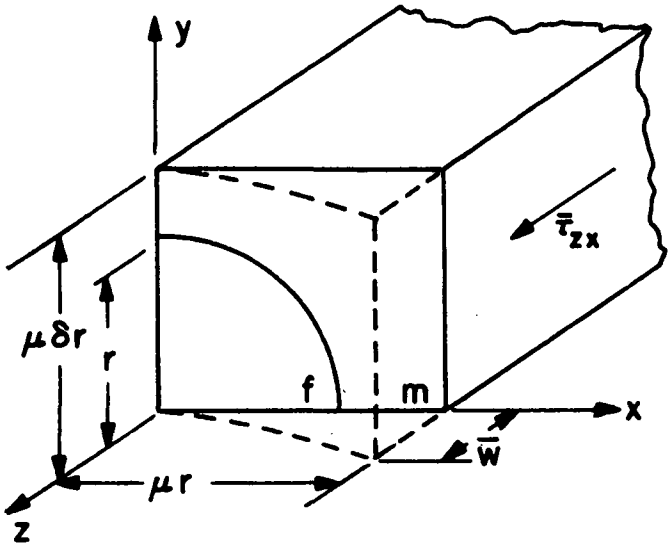

Figure 3. Longitudinal shear loading of a typical composite element.

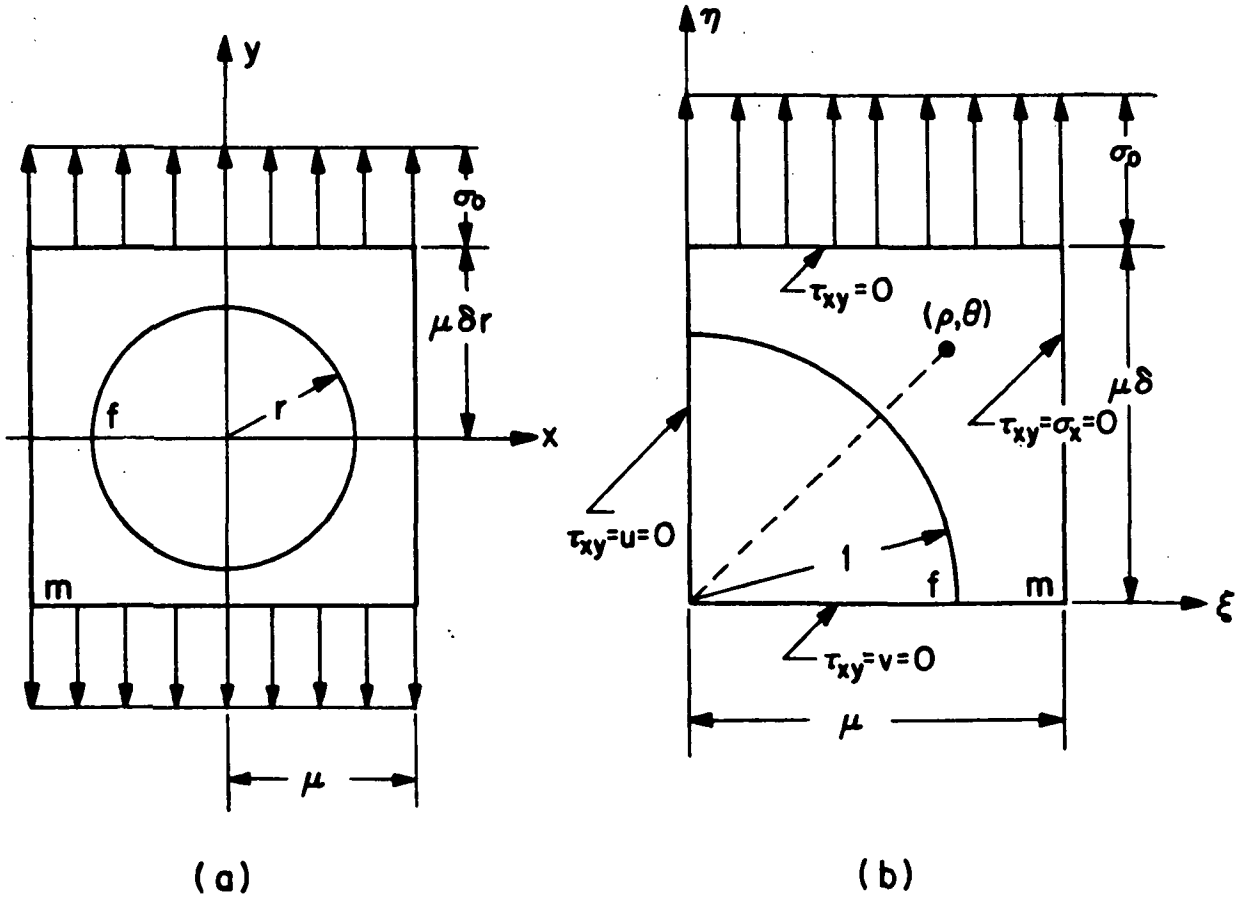

Figure 4. Transverse tension loading of a typical composite element.

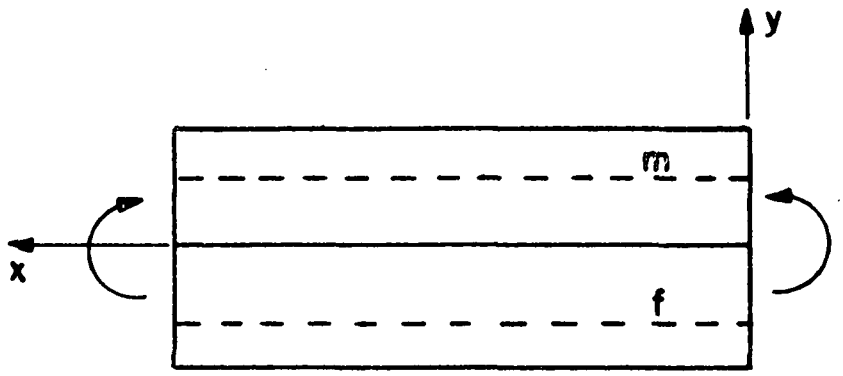

(a) Pure bending of a typical element

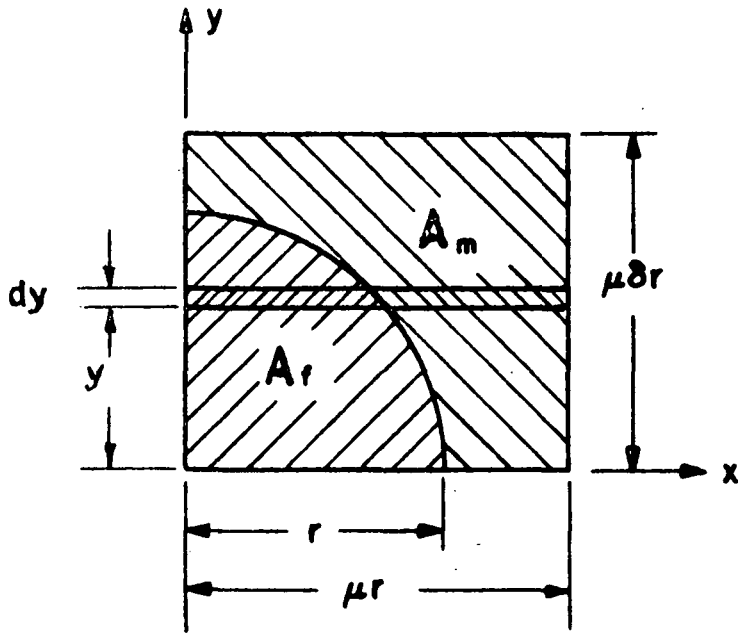

(b) One-quarter cross section

Figure 5. Longitudinal flexural loading of a typical monofilament composite element.

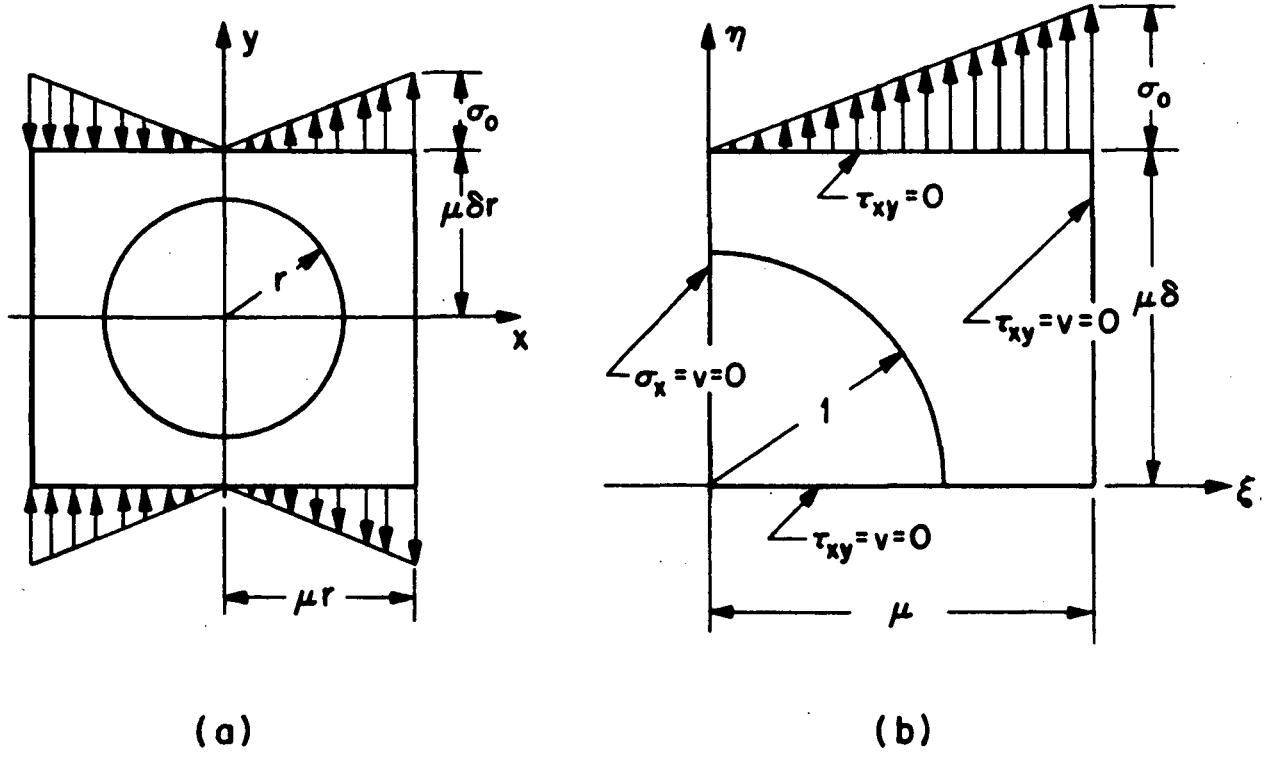

Figure 6. Transverse flexural loading of a typical monofilament composite element.

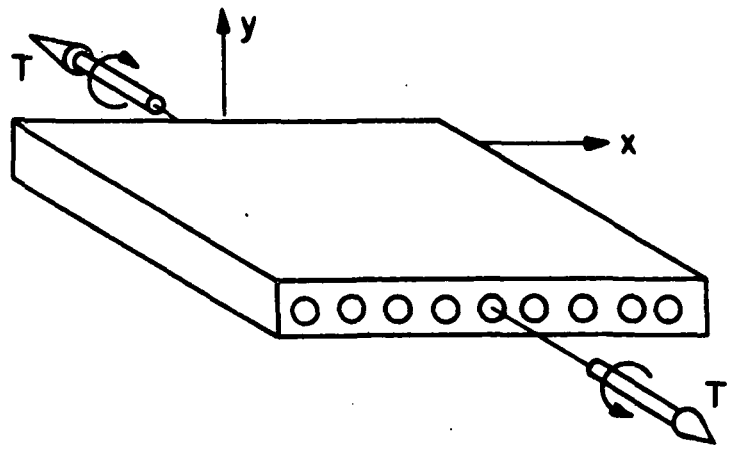

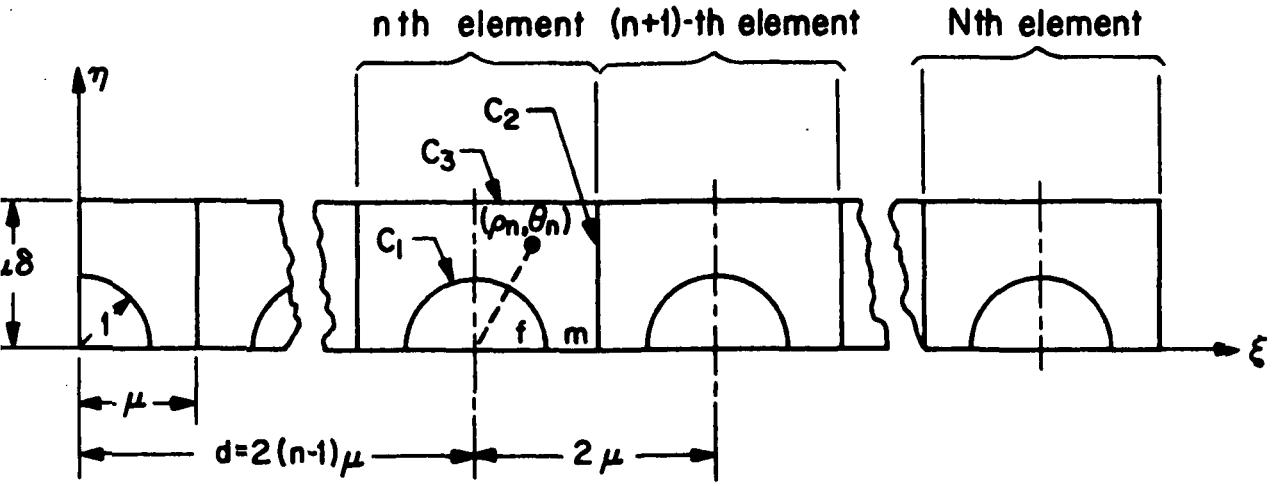

Figure 7. Torsional loading of a monofilament composite layer.

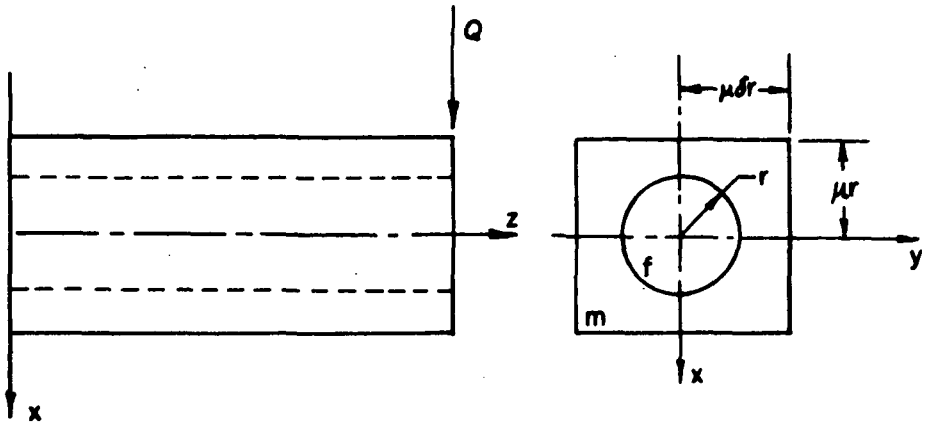

(a) Tip loading of a monofilament beam

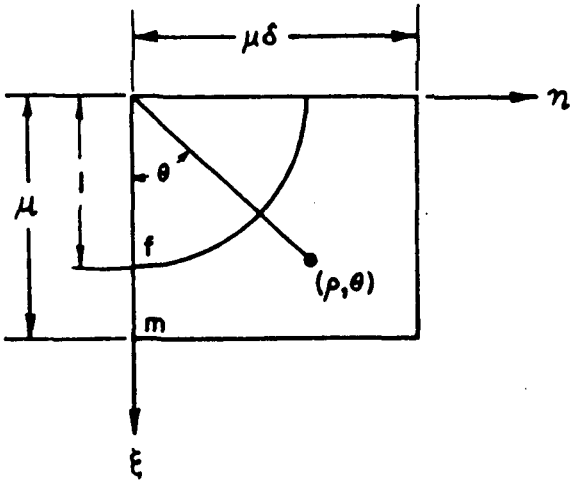

(b) Cross-sectional view

Figure 8. Tip loading of a monofilament composite element.

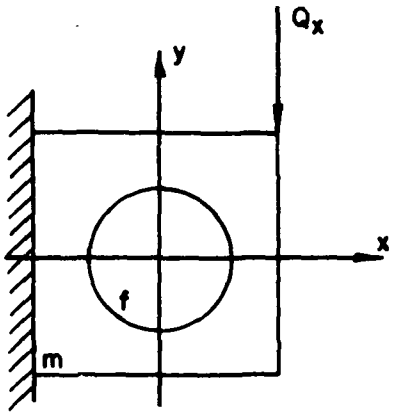

(a) Transverse thickness-shear loading

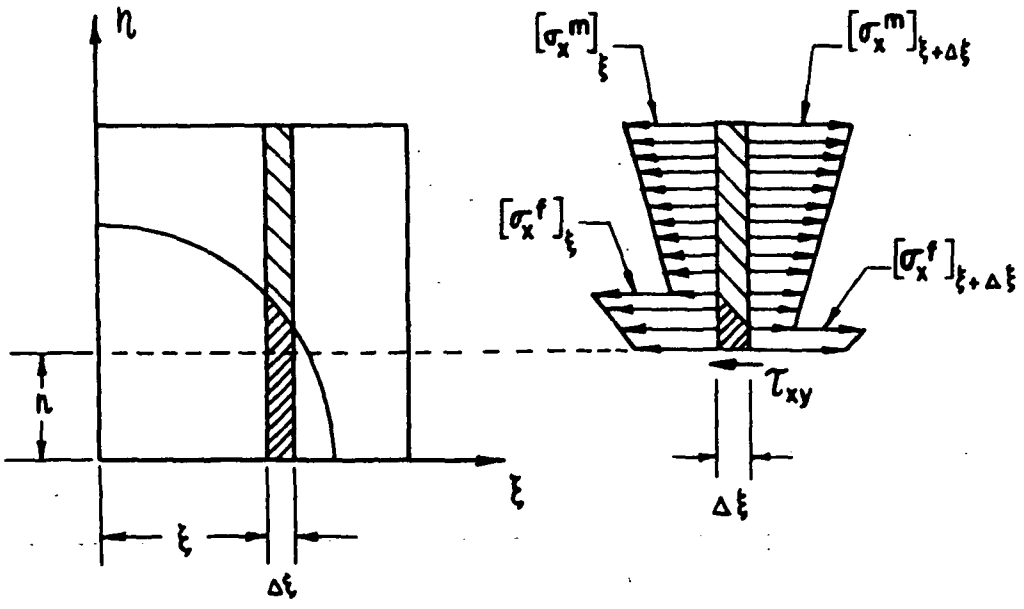

(b) Equilibrium of stresses in a typical strip

Figure 9. Transverse thickness-shear loading of a monofilament composite element.

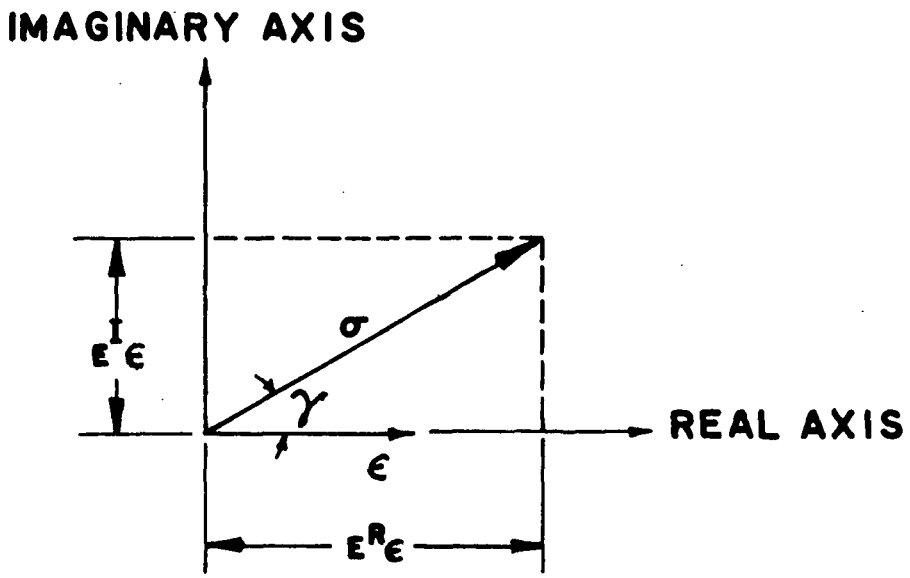

Figure 10. Concept of complex moduli and loss angle.

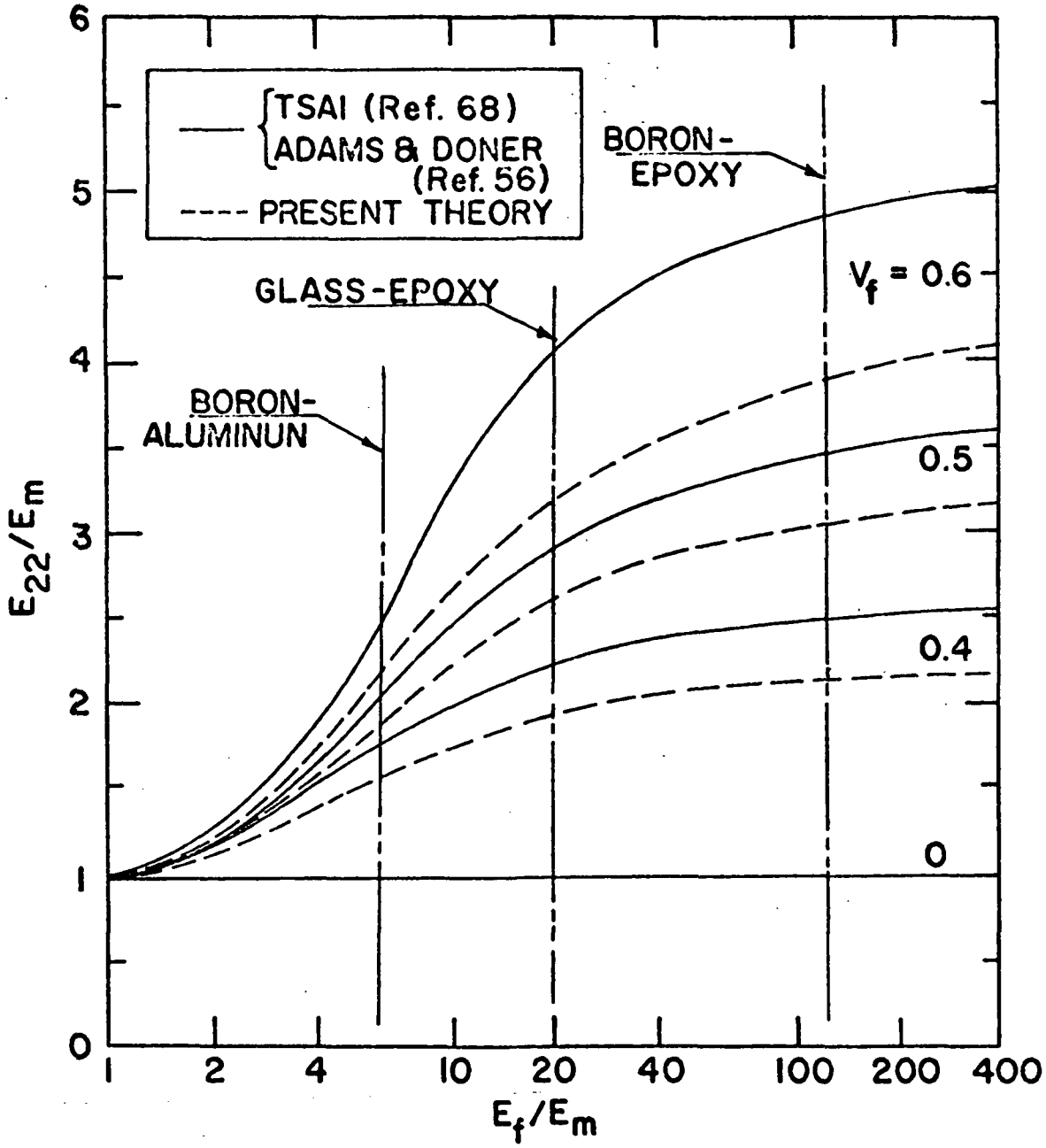

Figure 11. Transverse Young's modulus.

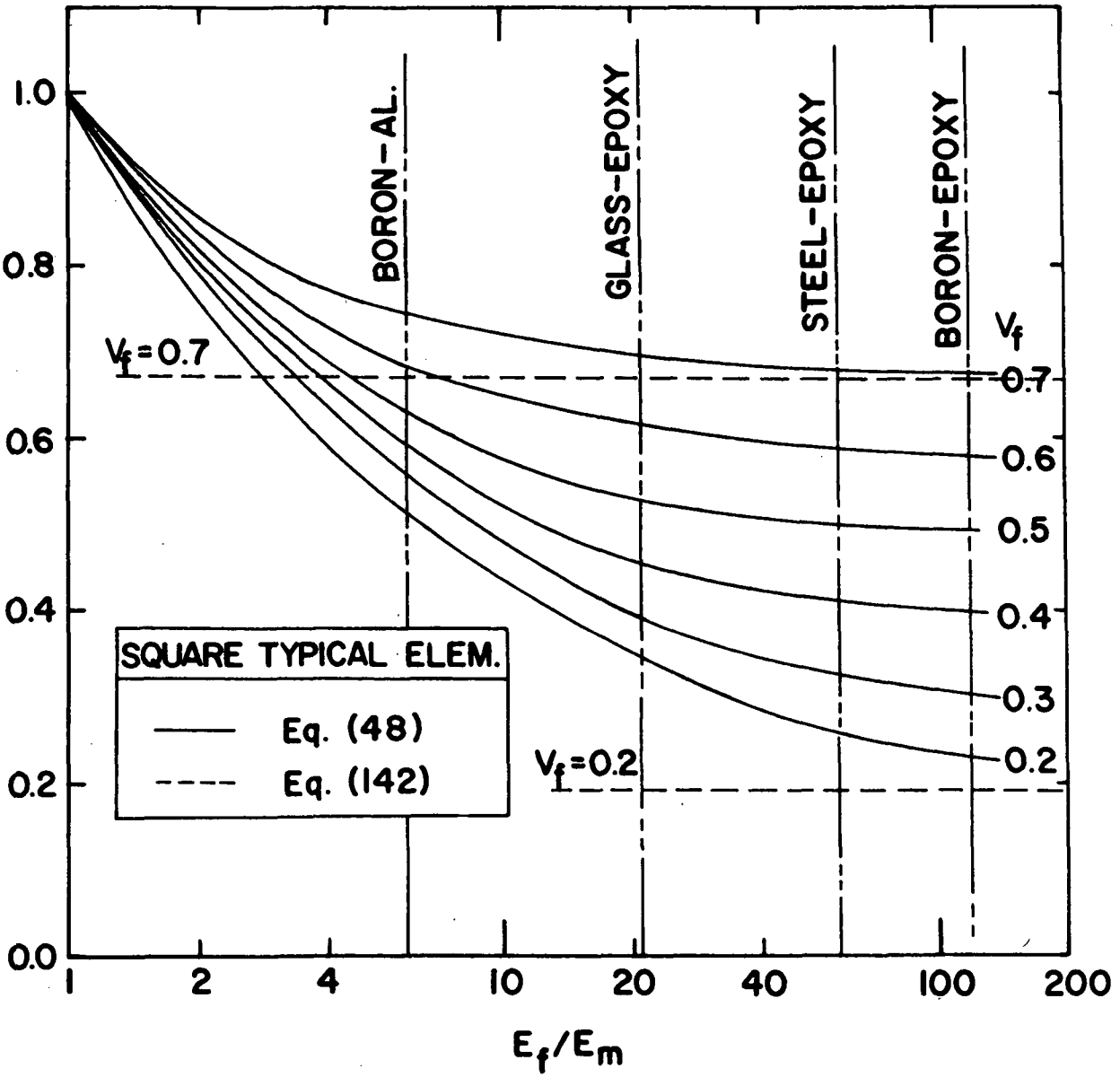

Figure 12. Flexural stiffness efficiency.

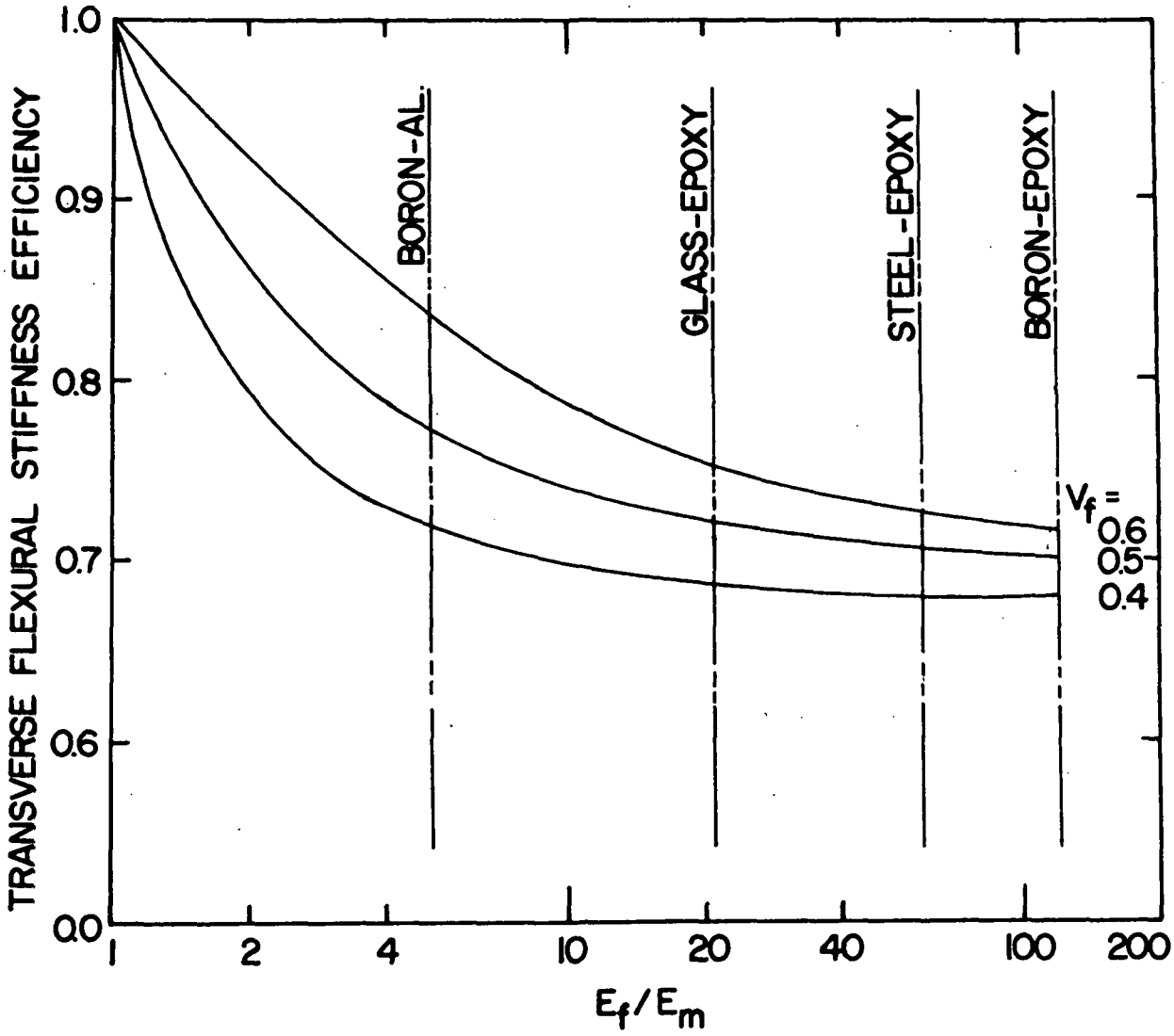

Figure 13. Transverse flexural stiffness efficiency.

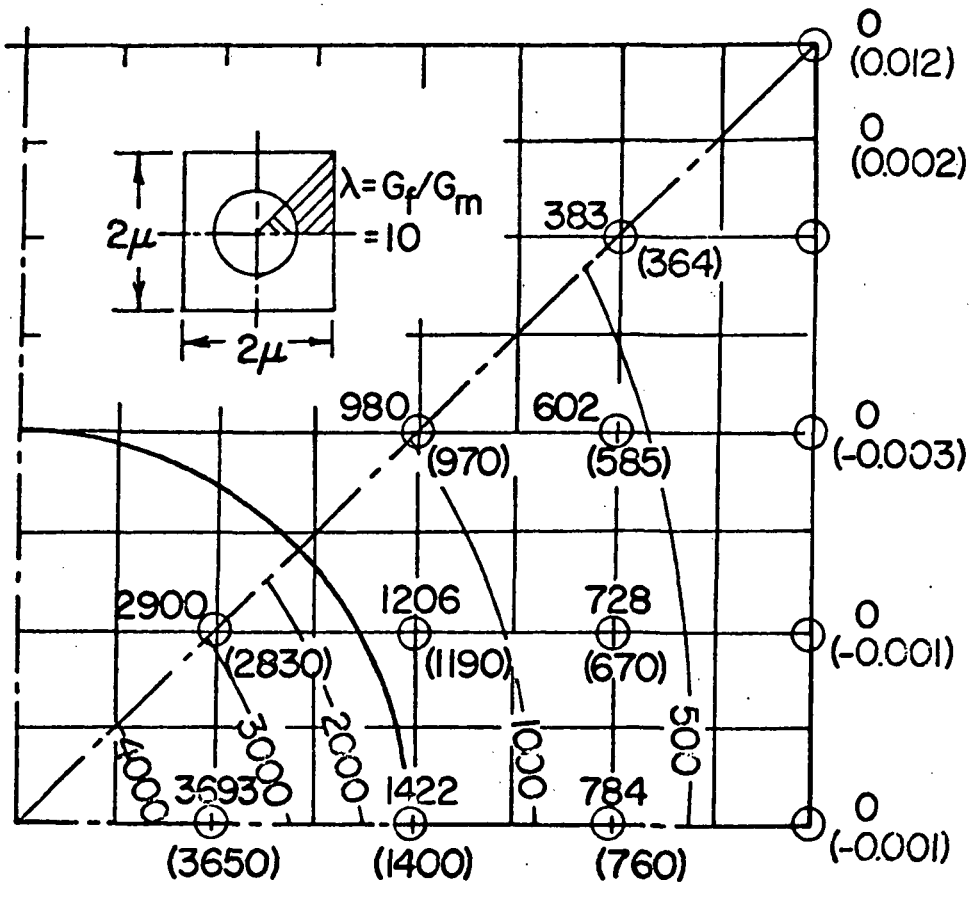

Figure 14. Comparisons of Prandtl torsion function ($\phi x 10^4$) of a square matrix with a circular insert.

Remarks: Numbers at the mesh points denote the values of $\phi x 10^4$ obtained by Ely and Zienkiewics (ref. 75) and those from the point-matching method (in parentheses).

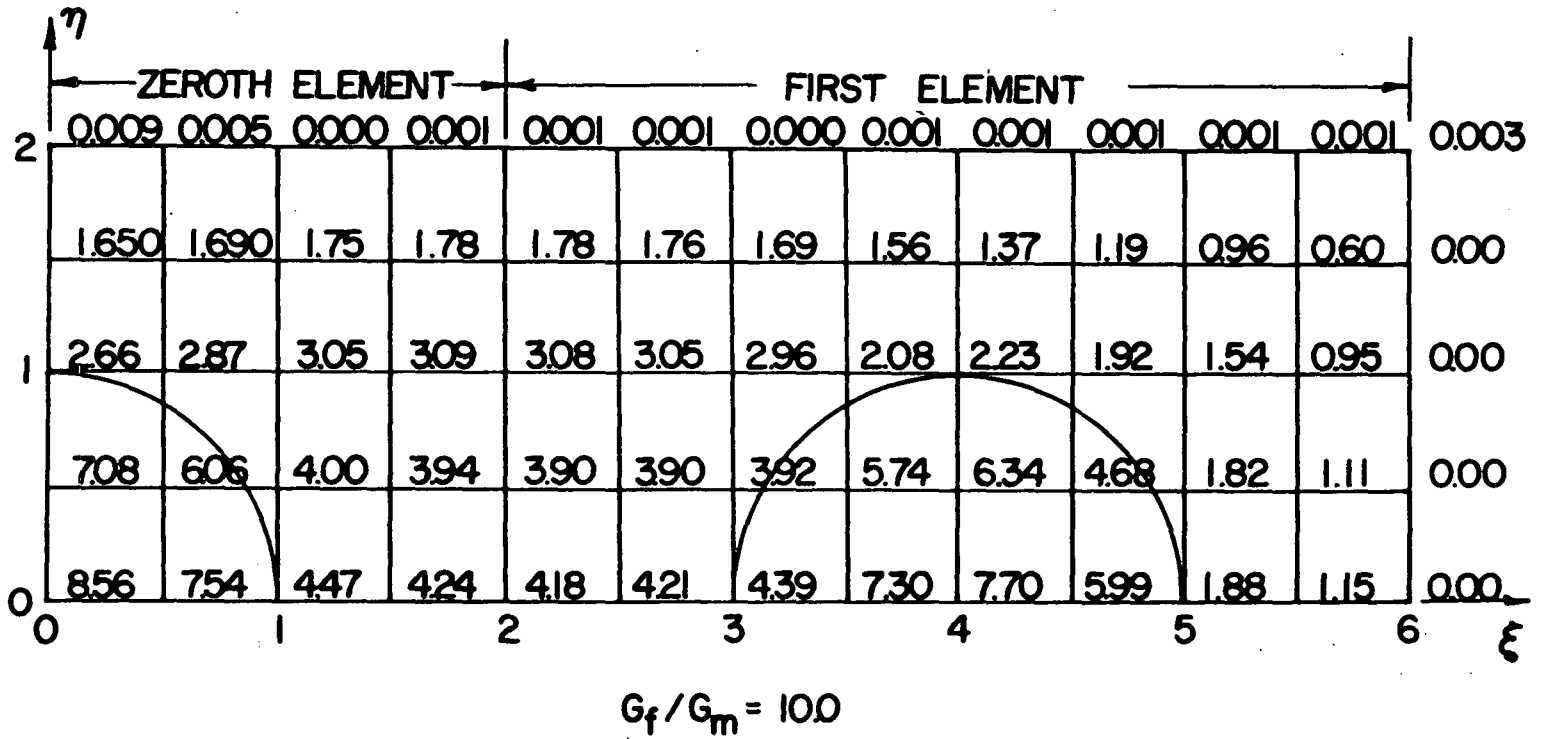

Figure 15. Values of normalized Prandtl torsion function for a three-element model.

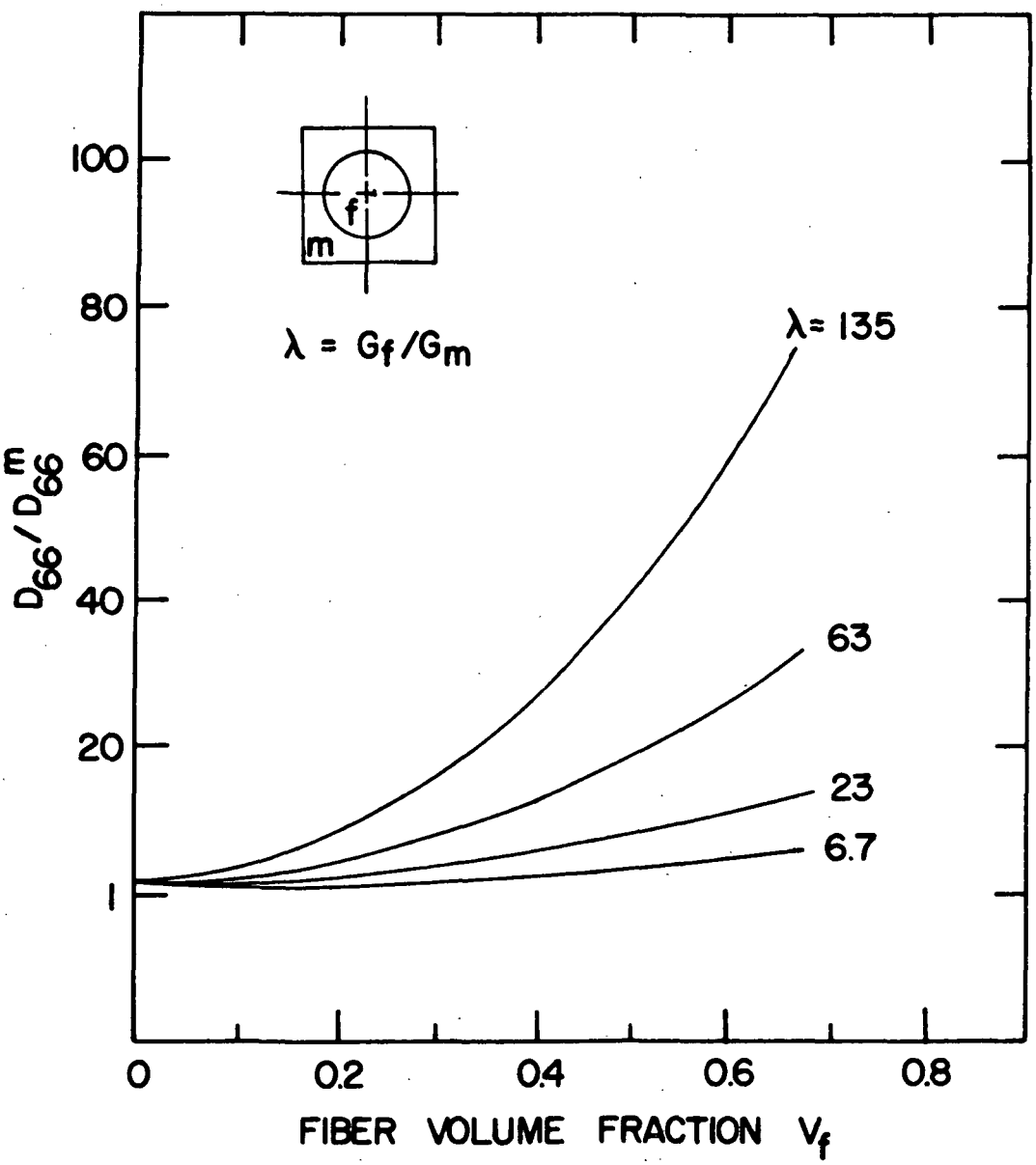

Figure 16. Twisting stiffness versus fiber volume fraction

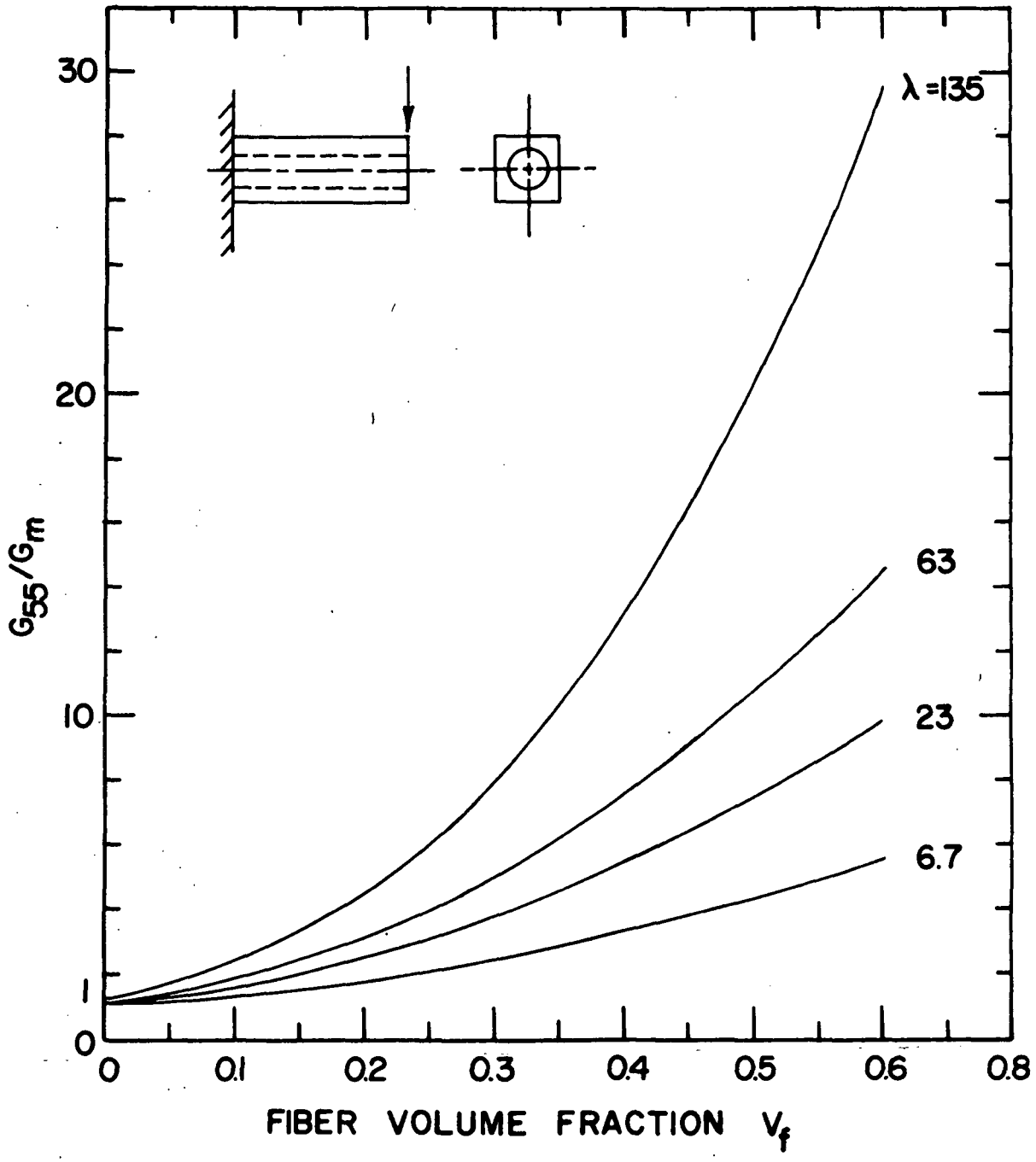

Figure 17. Longitudinal thickness-shear modulus.

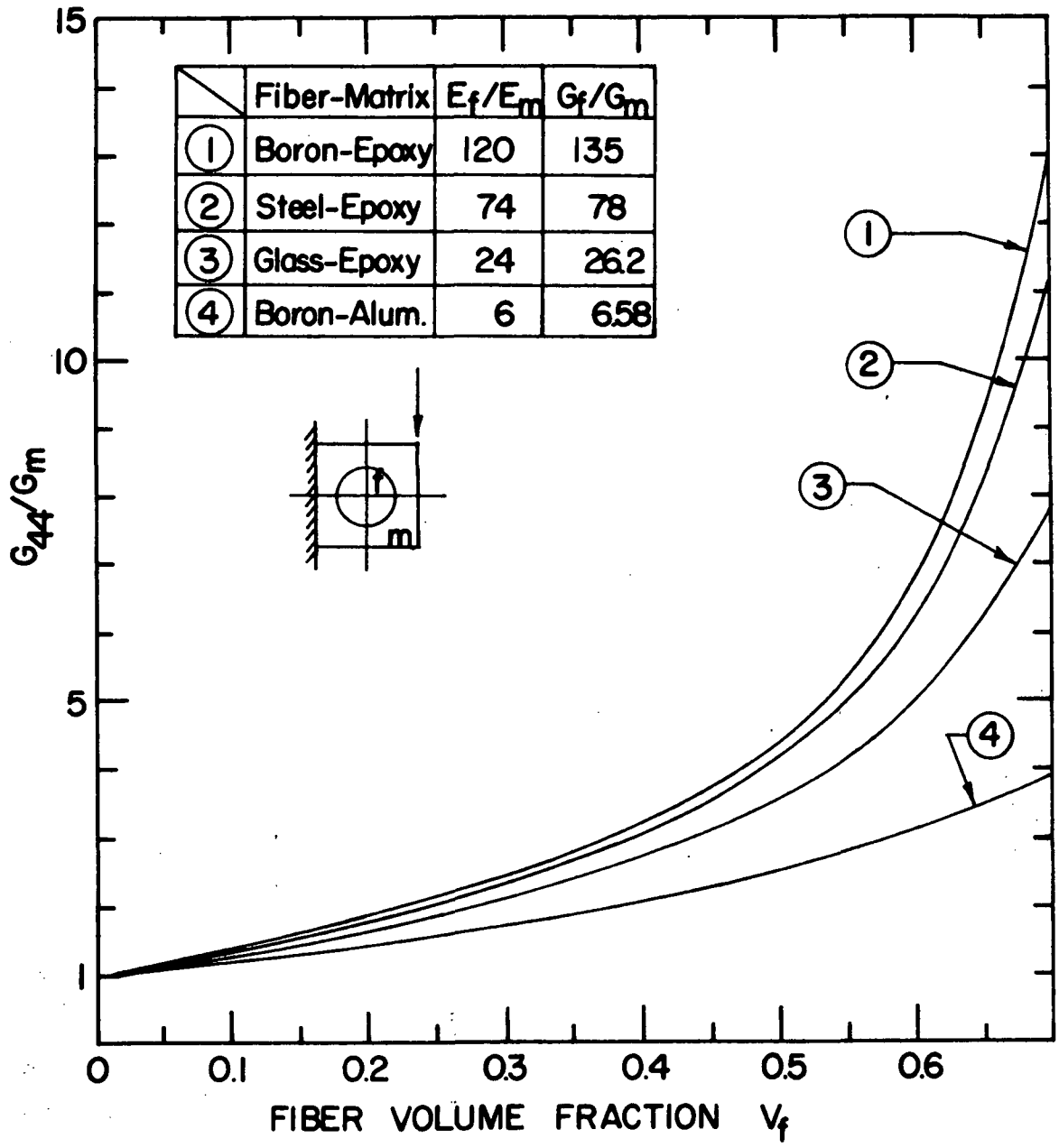

Figure 18. Transverse thickness-shear modulus.

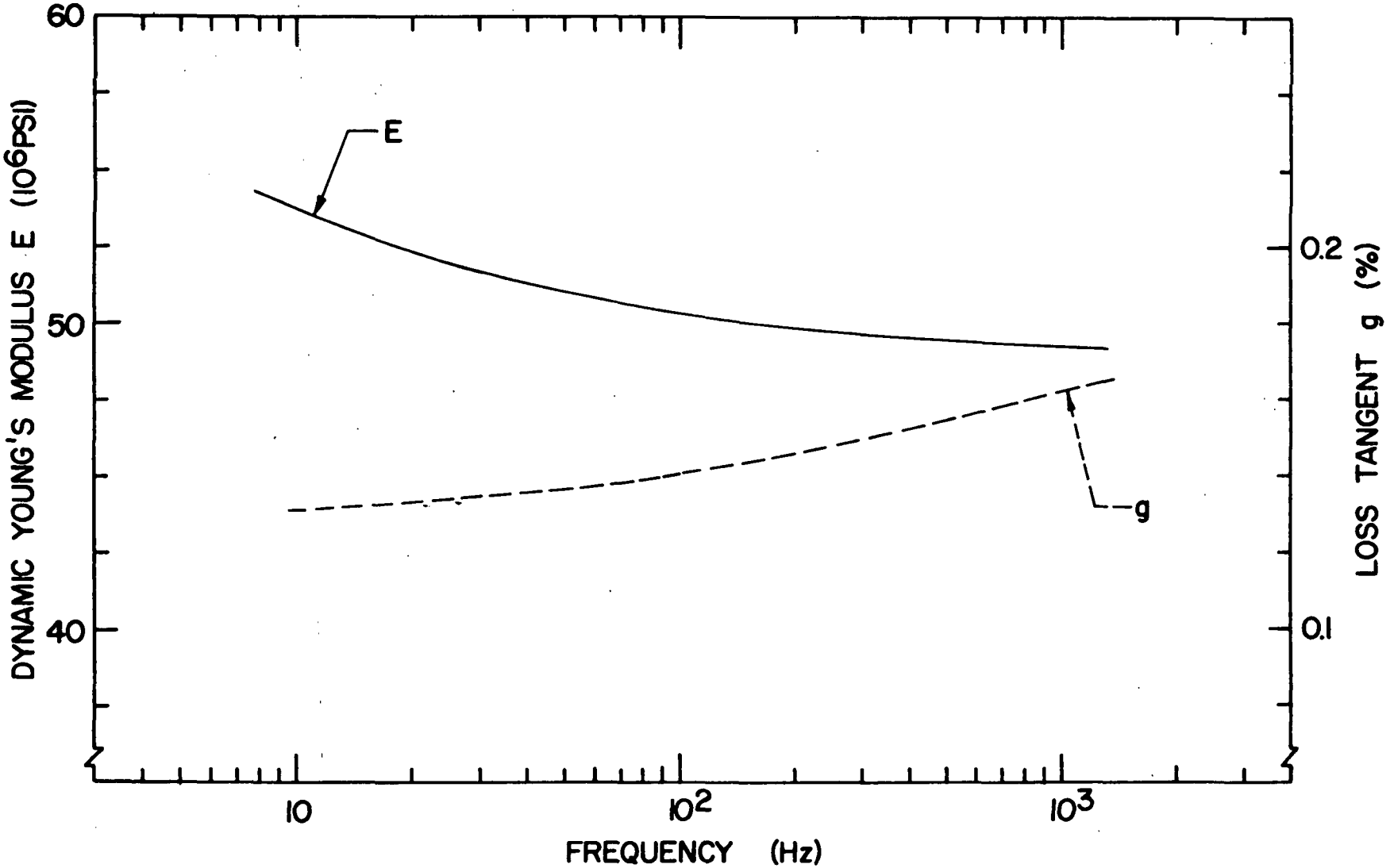

Figure 19. Dynamic Young's modulus and associated loss tangent for boron.

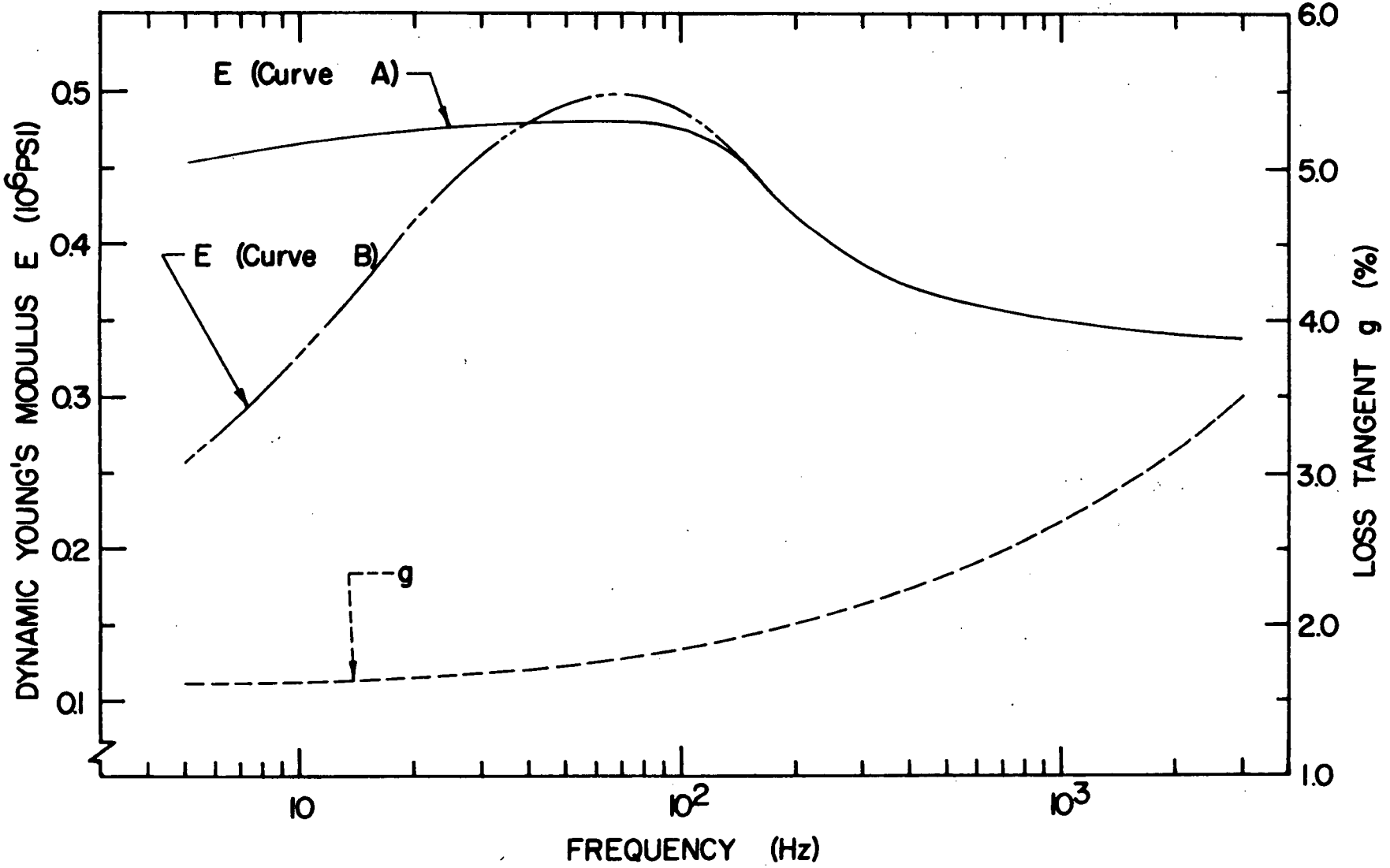

Figure 20. Dynamic Young's modulus and associated loss tangent for epoxy.

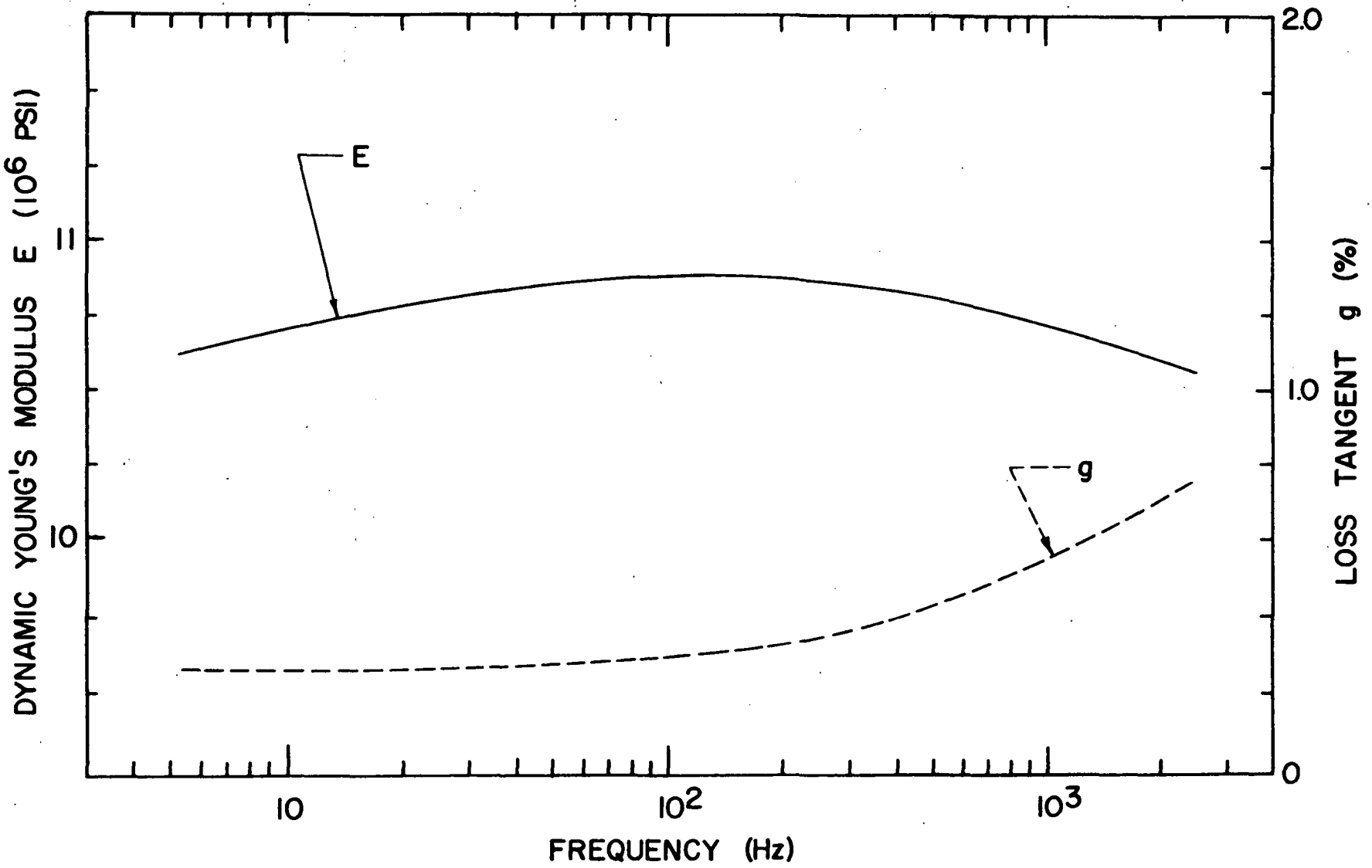

Figure 21. Dynamic Young's modulus and associated loss tangent for E-glass.

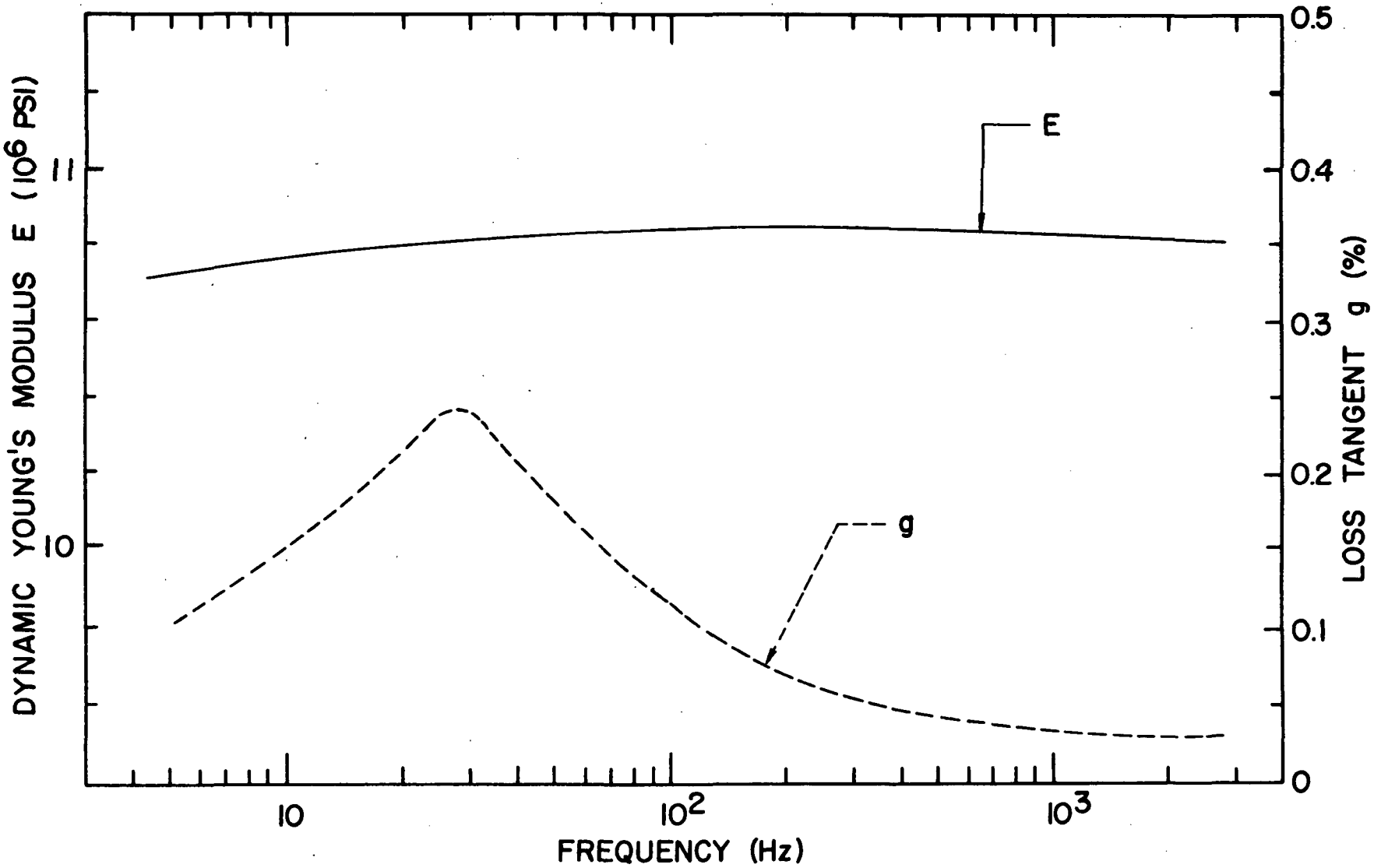

Figure 22. Dynamic Young's modulus and associated loss tangent for aluminum 2024-T3.

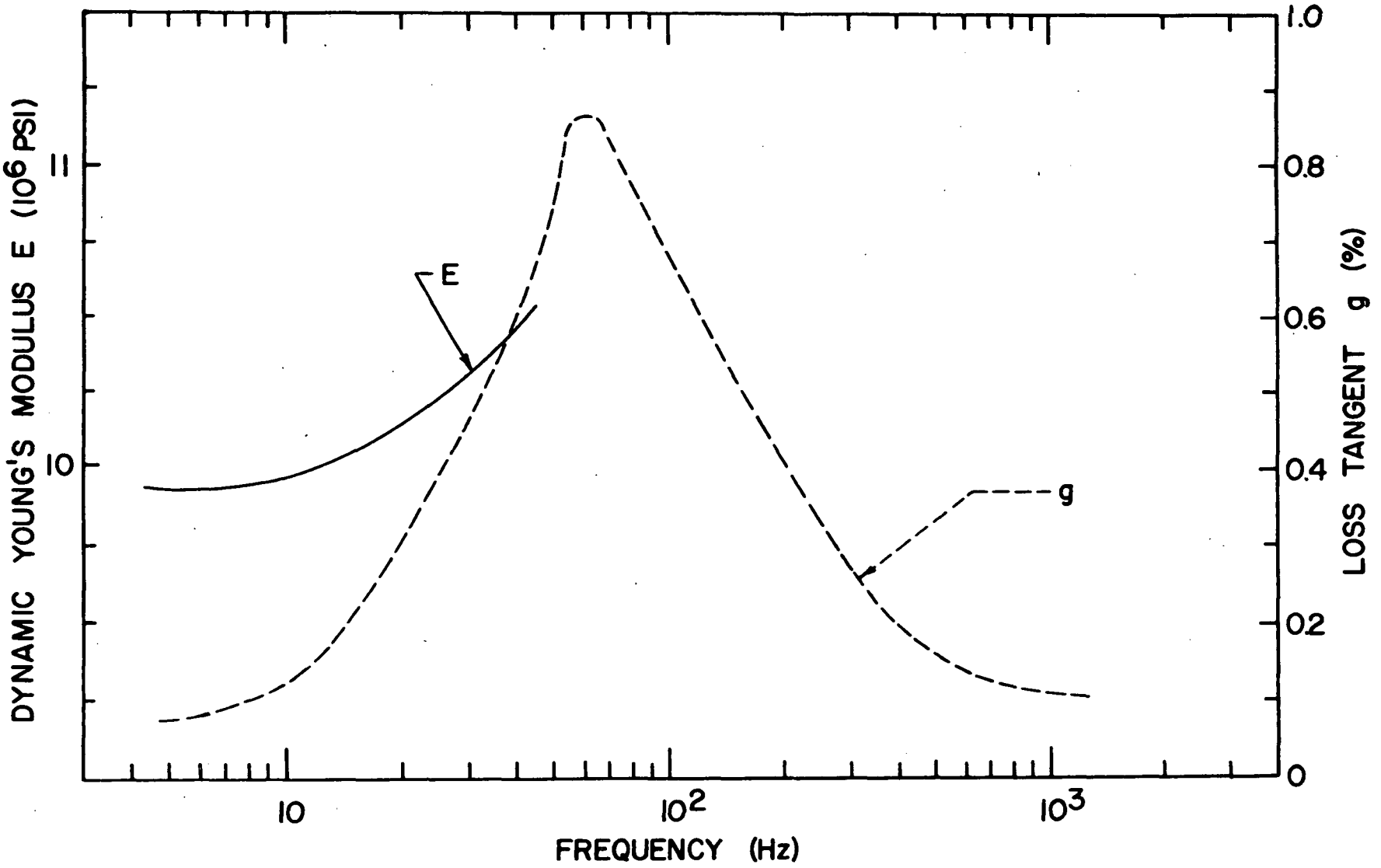

Figure 23. Dynamic Young's modulus and associated loss tangent for aluminum 6061.

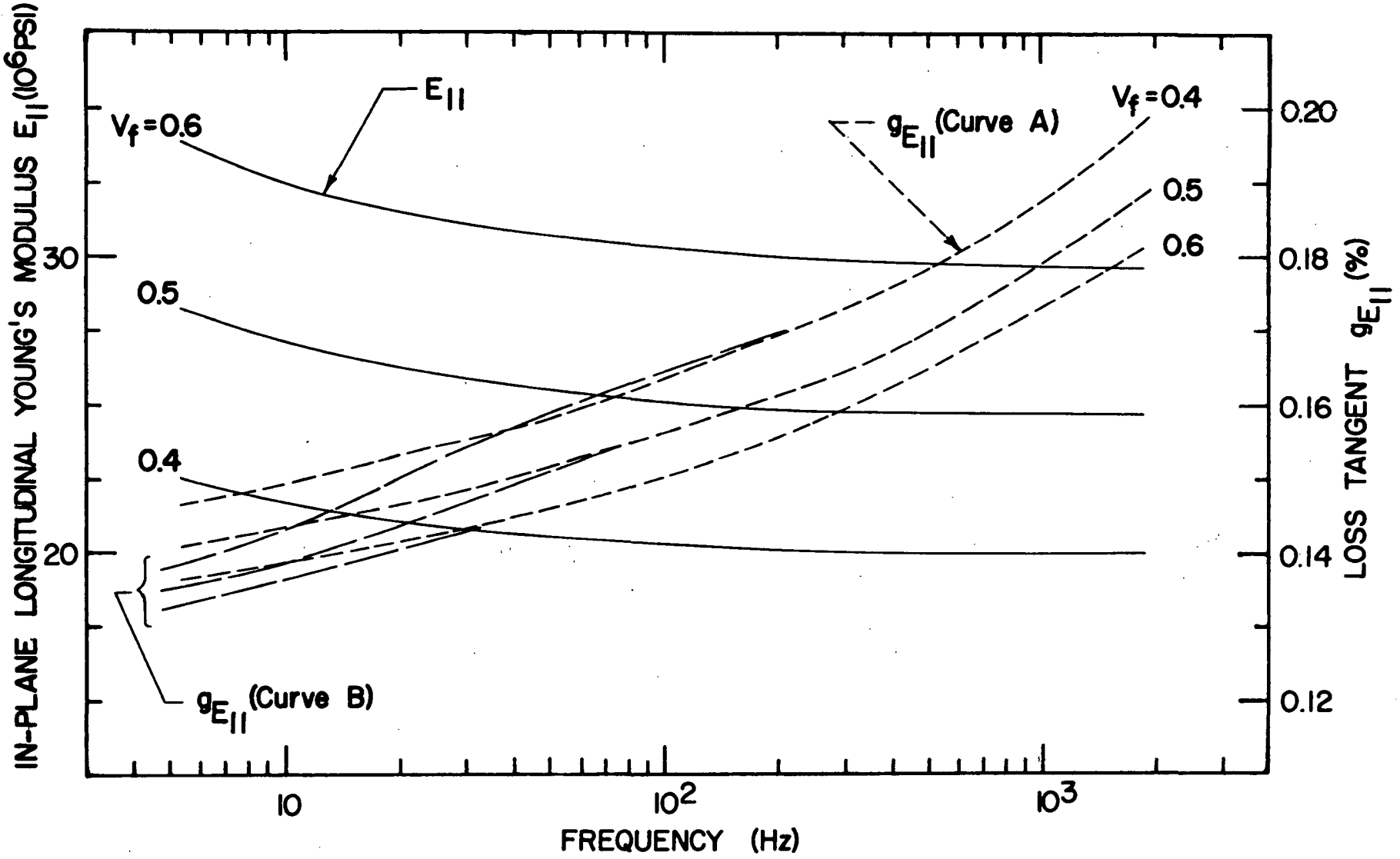

Figure 24. In-plane longitudinal Young's modulus and associated loss tangent for a boron-epoxy monofilament composite.

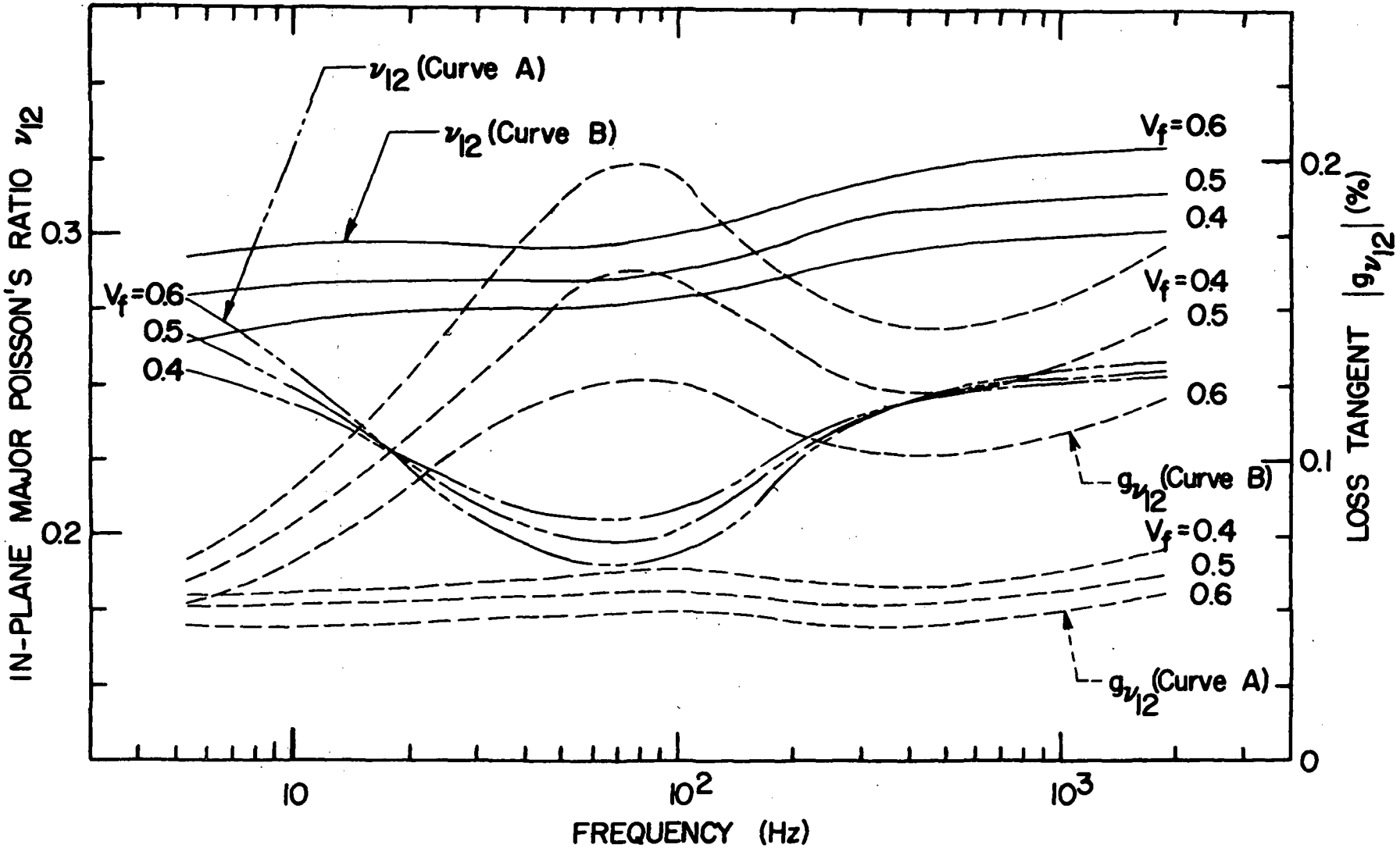

Figure 25. In-plane major Poisson's ratio and associated loss tangent for a boron-epoxy monofilament composite.

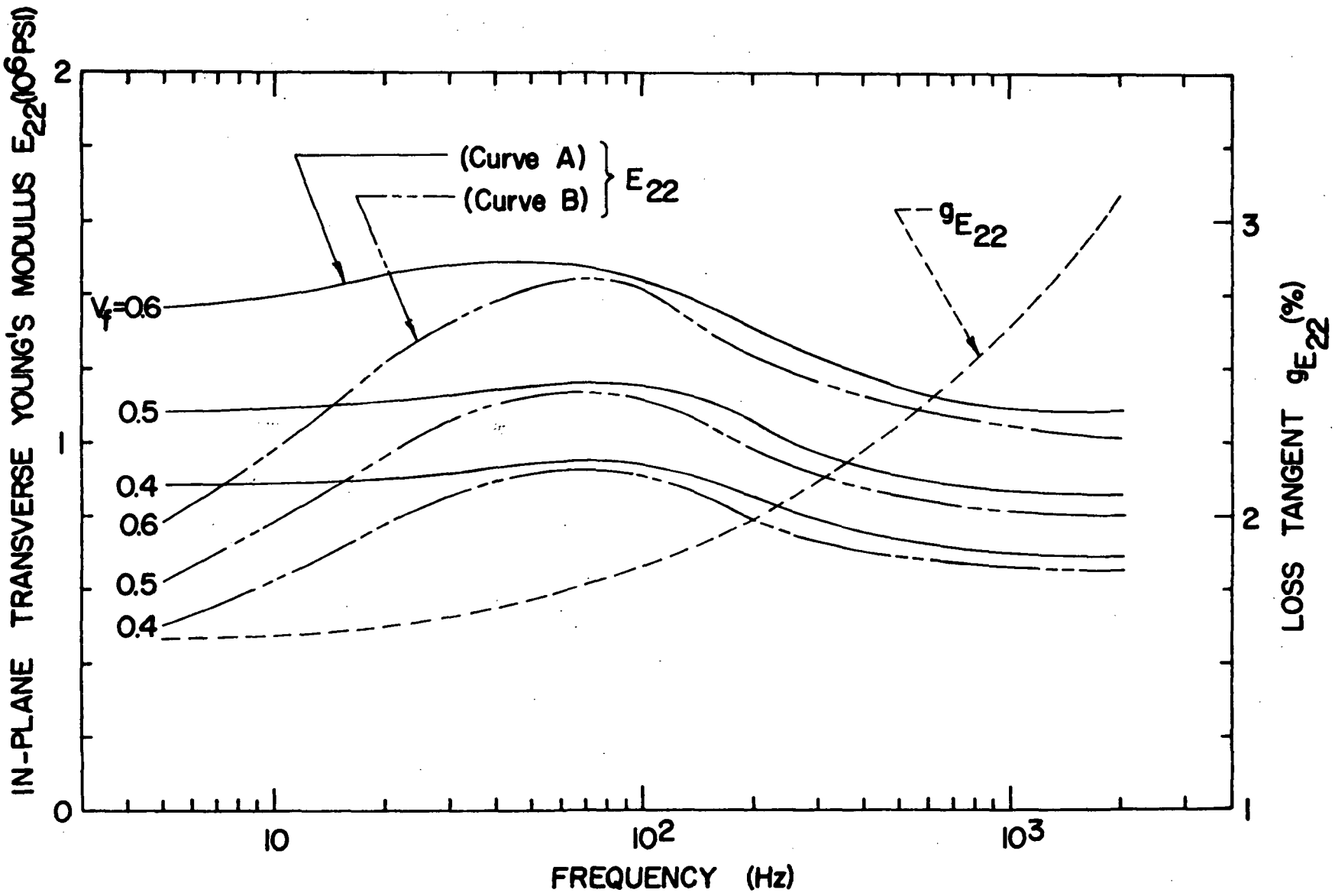

Figure 26. In-plane transverse Young's modulus and associated loss tangent for a boron-epoxy monofilament composites.

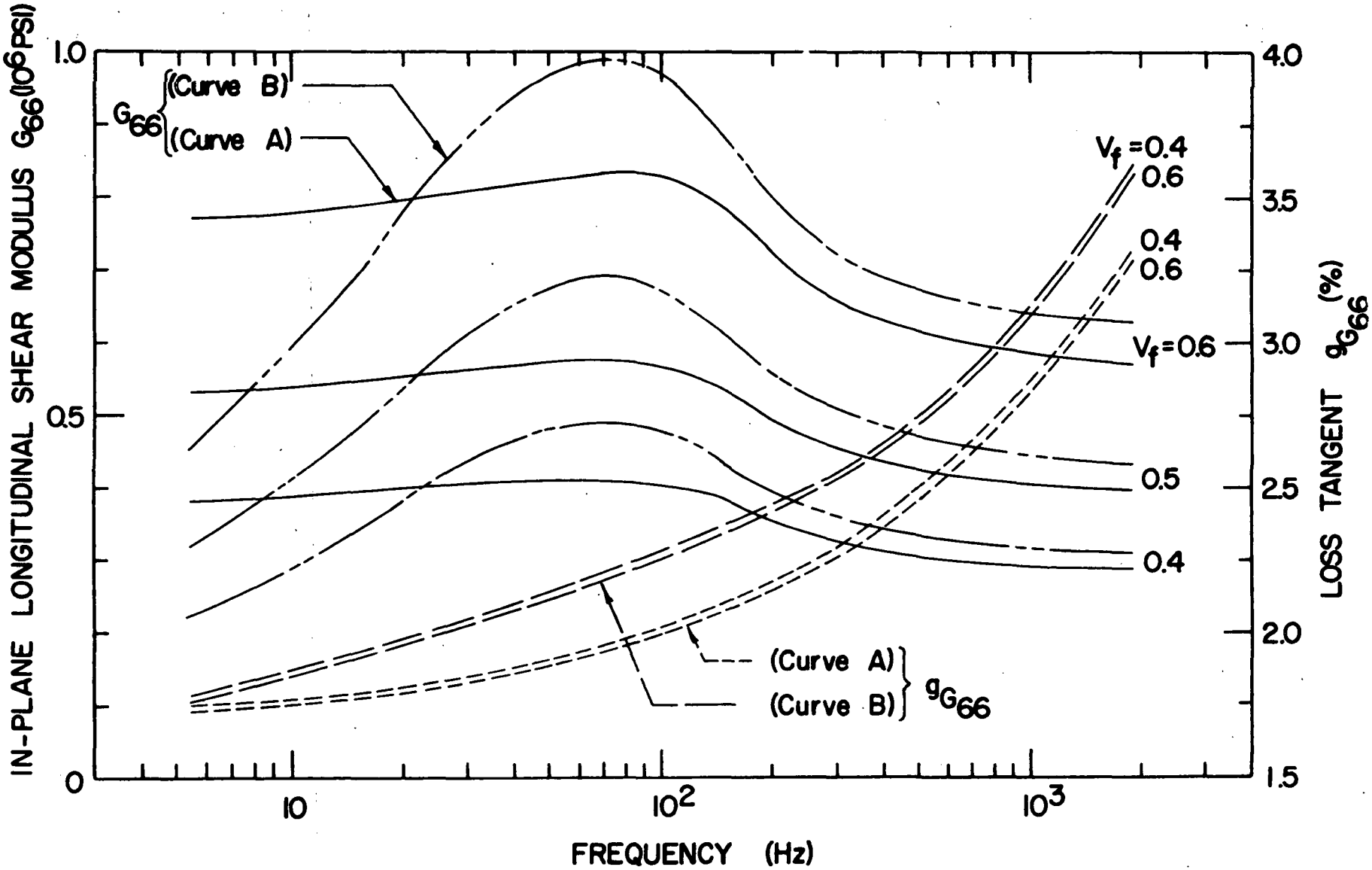

Figure 27. In-plane longitudinal shear modulus and associated loss tangent for a boron-epoxy monofilament composite.

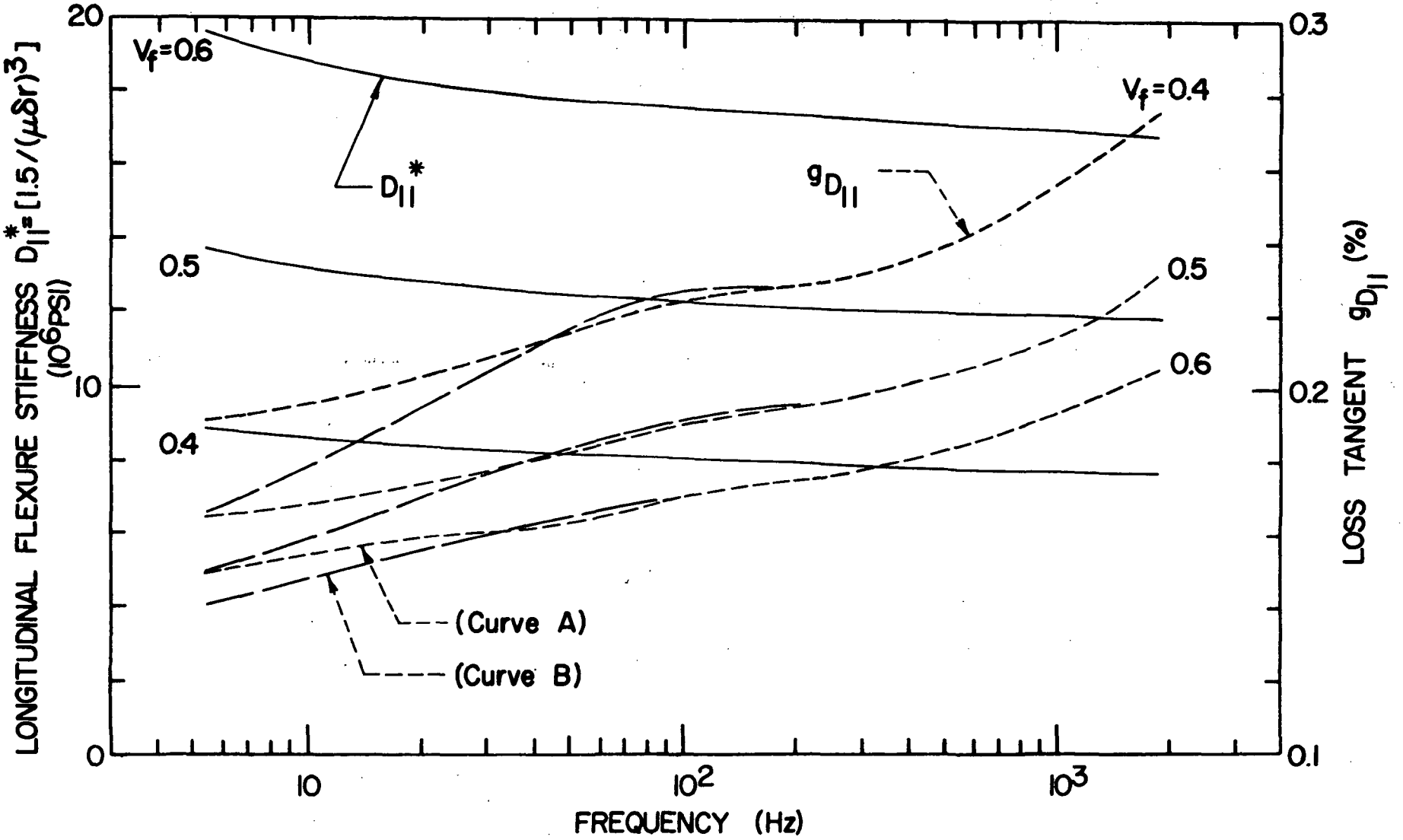

Figure 28. Longitudinal flexural stiffness and associated loss tangent for a boron-epoxy monofilament composite.

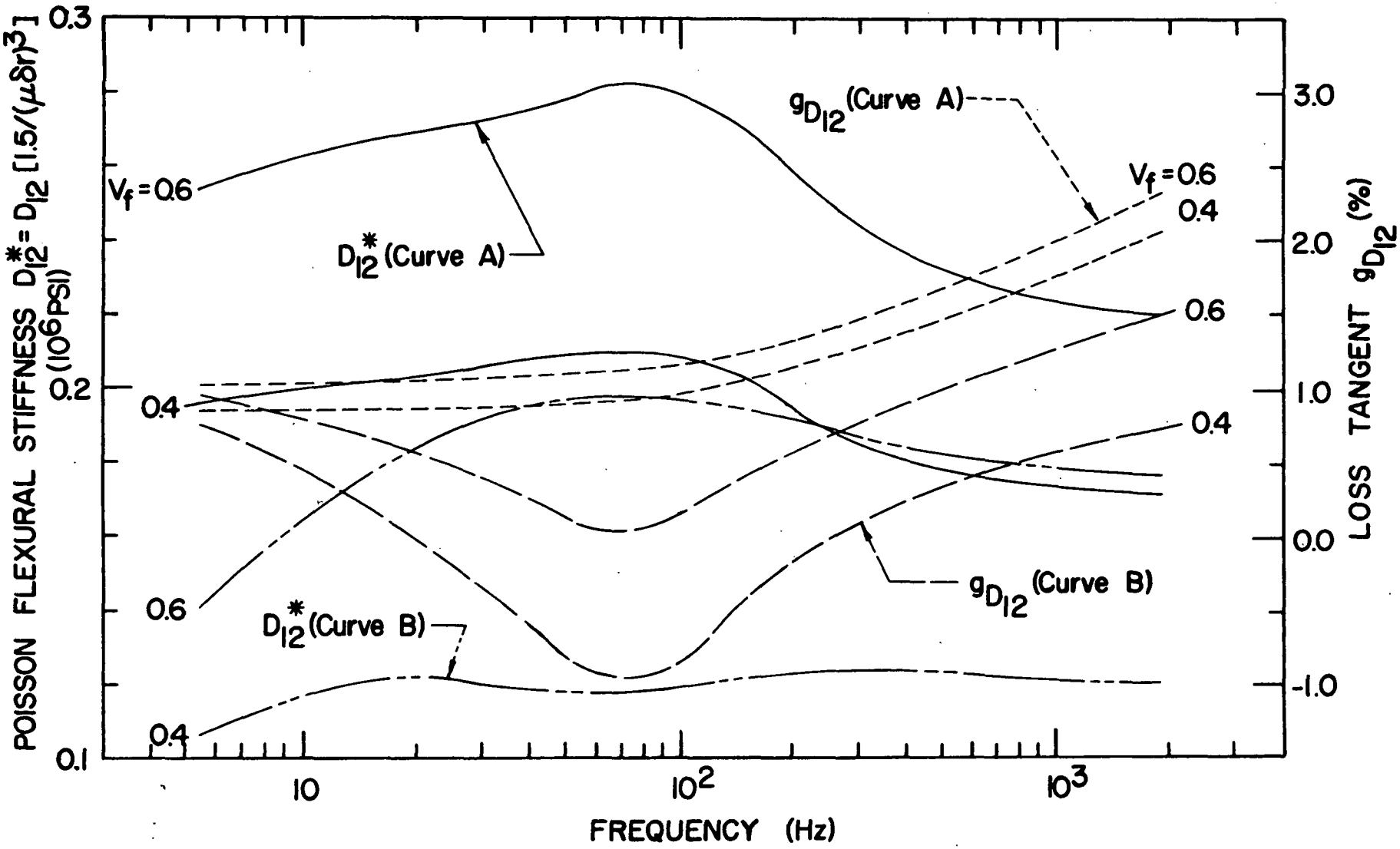

Figure 29. Poisson flexural stiffness and associated loss tangent for a boron-epoxy monofilament composite.

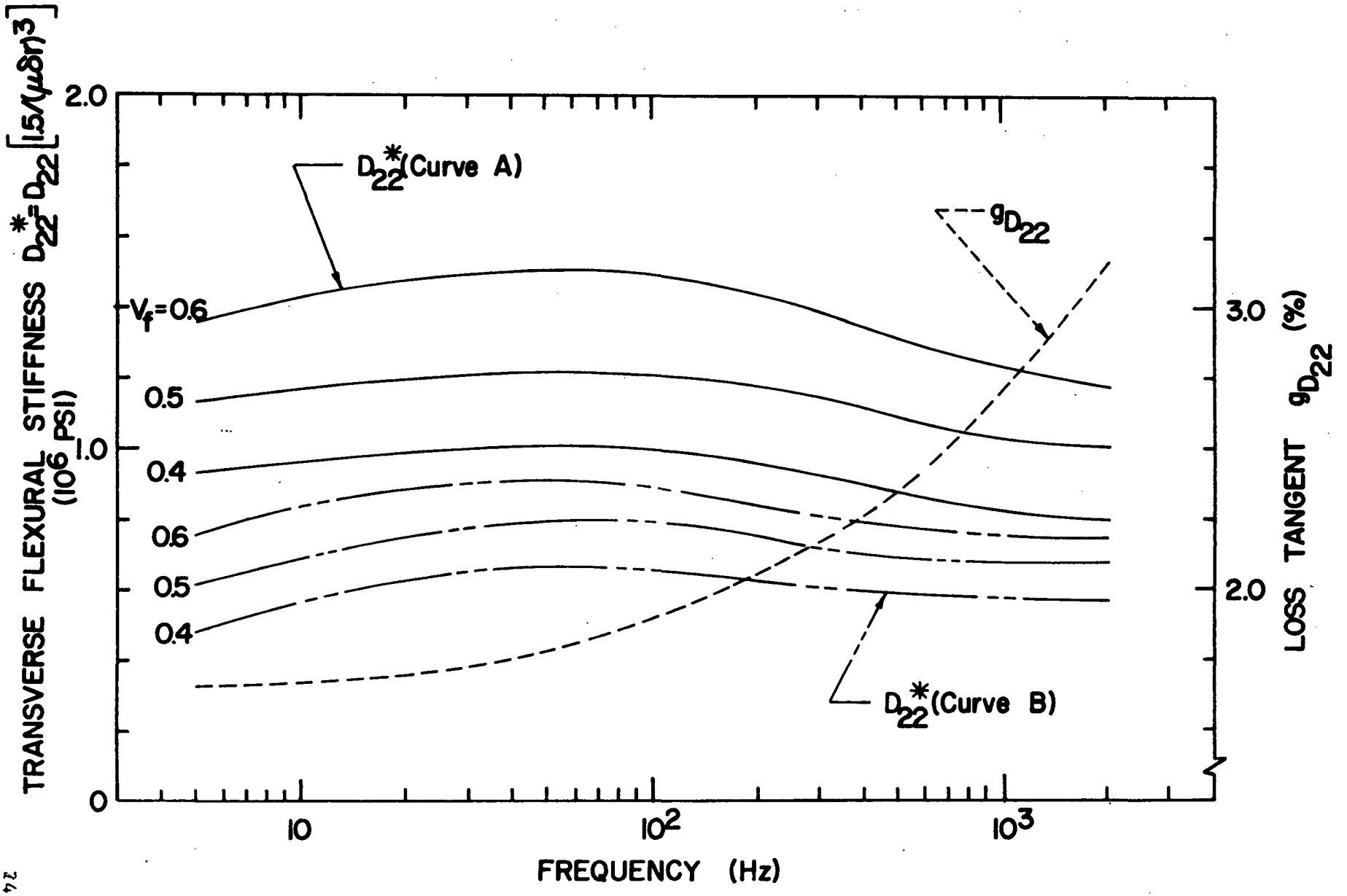

Figure 30. Transverse flexural stiffness and associated loss tangent for a boron-epoxy monofilament composite.

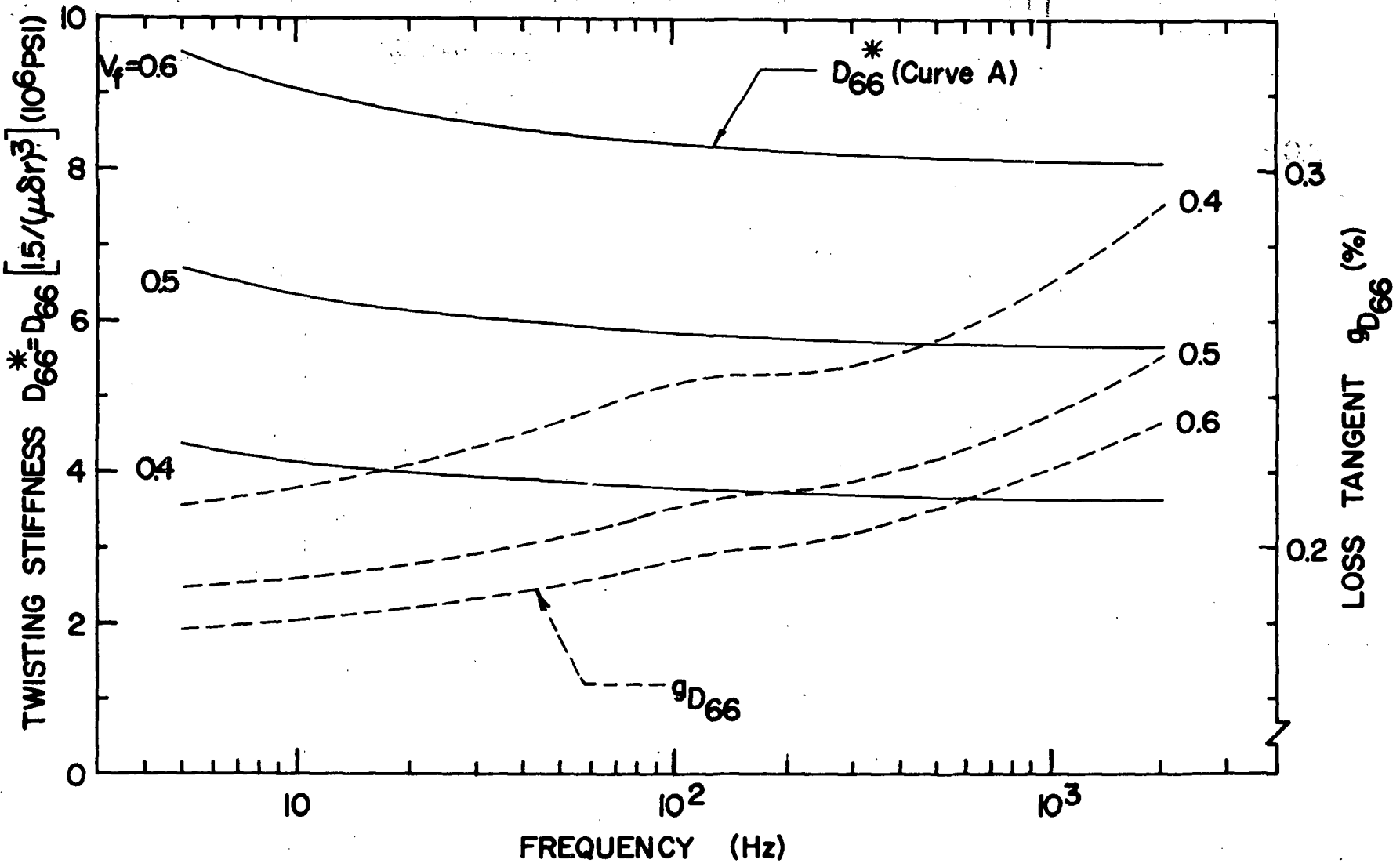

Figure 31. Twisting stiffness and associated loss tanget for a boron-epoxy monofilament composite.

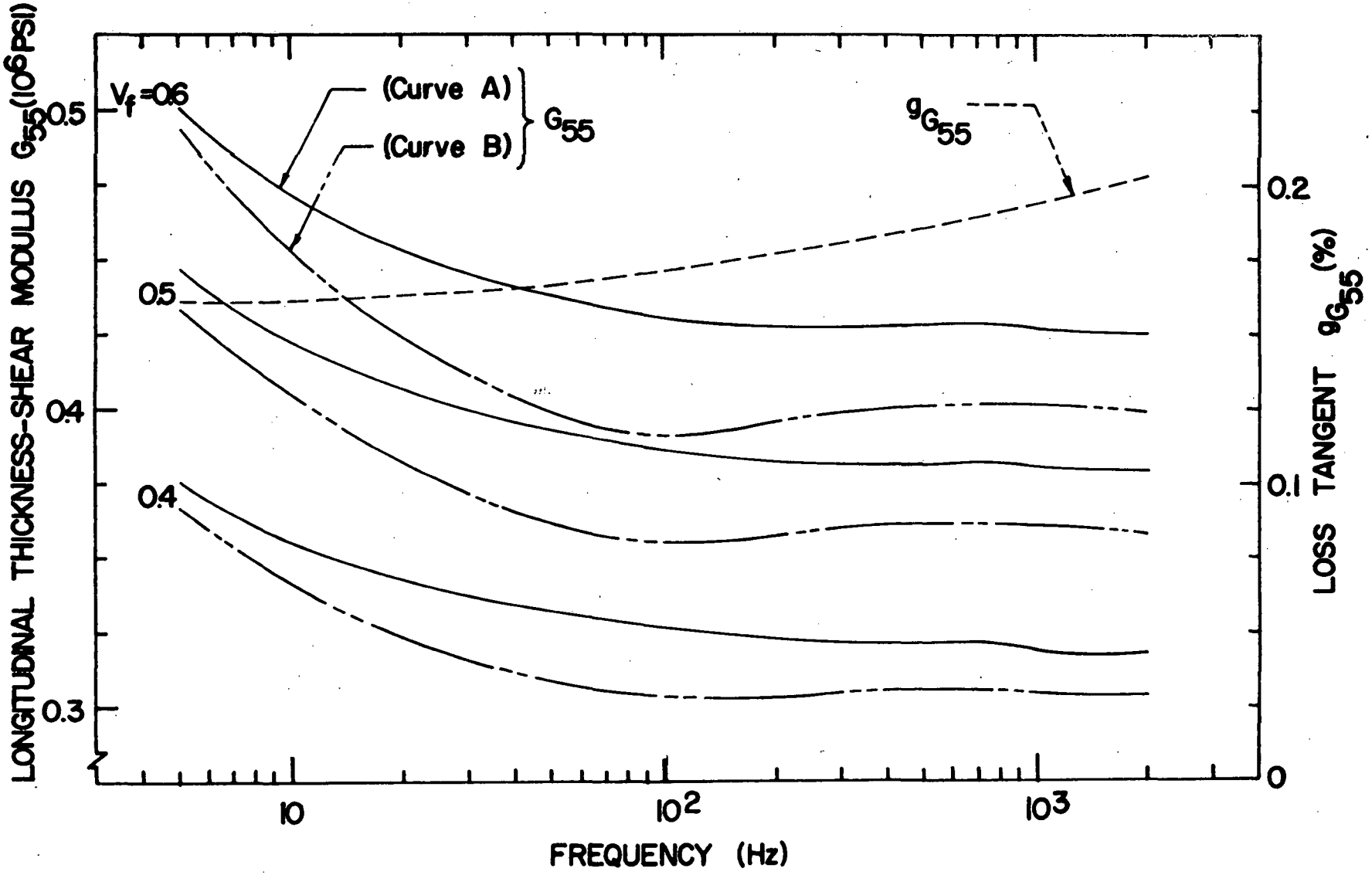

Figure 32. Longitudinal thickness-shear stiffness and associated loss tangent for a boron-epoxy monofilament composite.

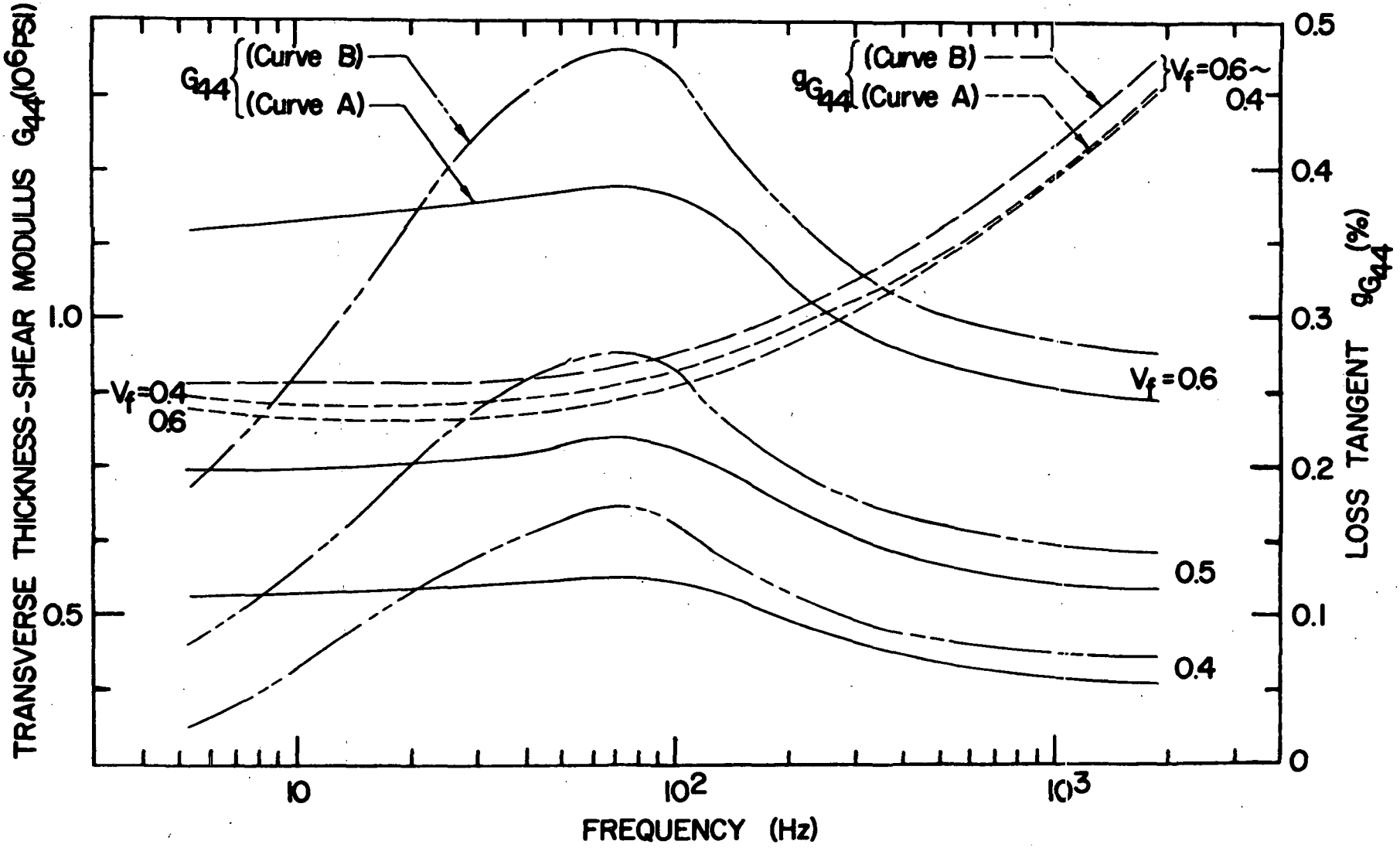

Figure 33. Transverse thickness-shear modulus and associated loss tangent for a boron-epoxy monofilament composite.

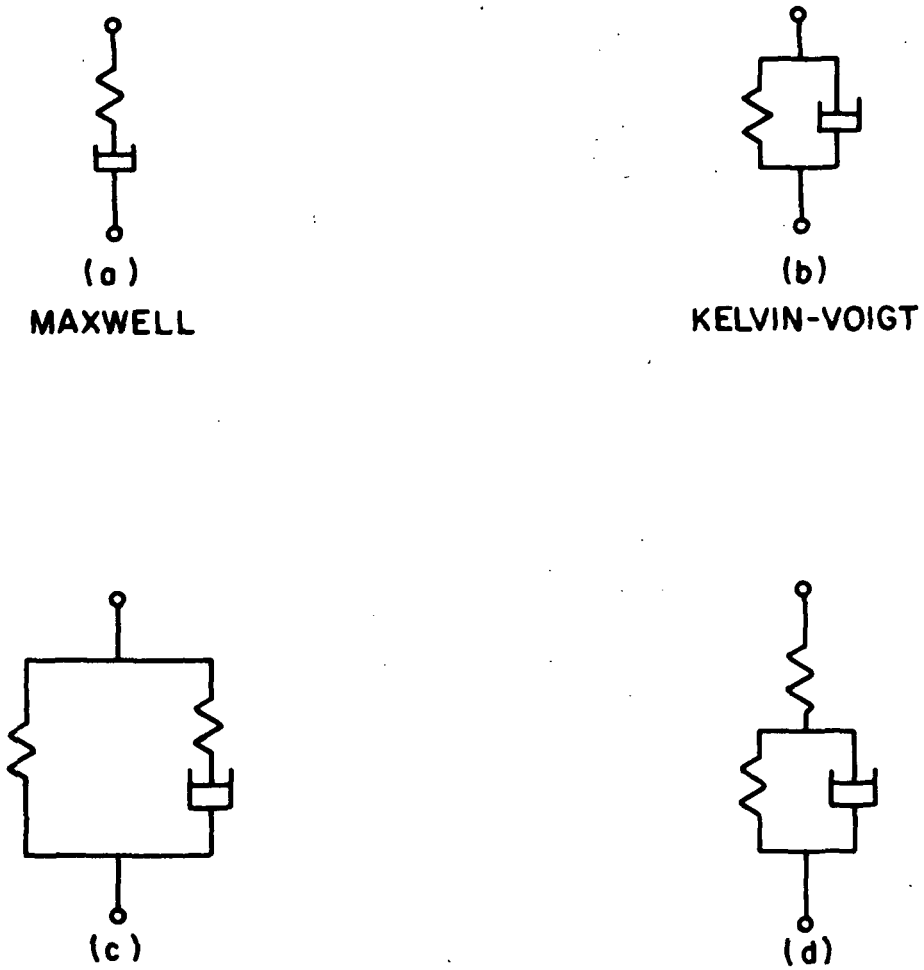

Figure B-1. Two-and three-parameter viscoelastic models.

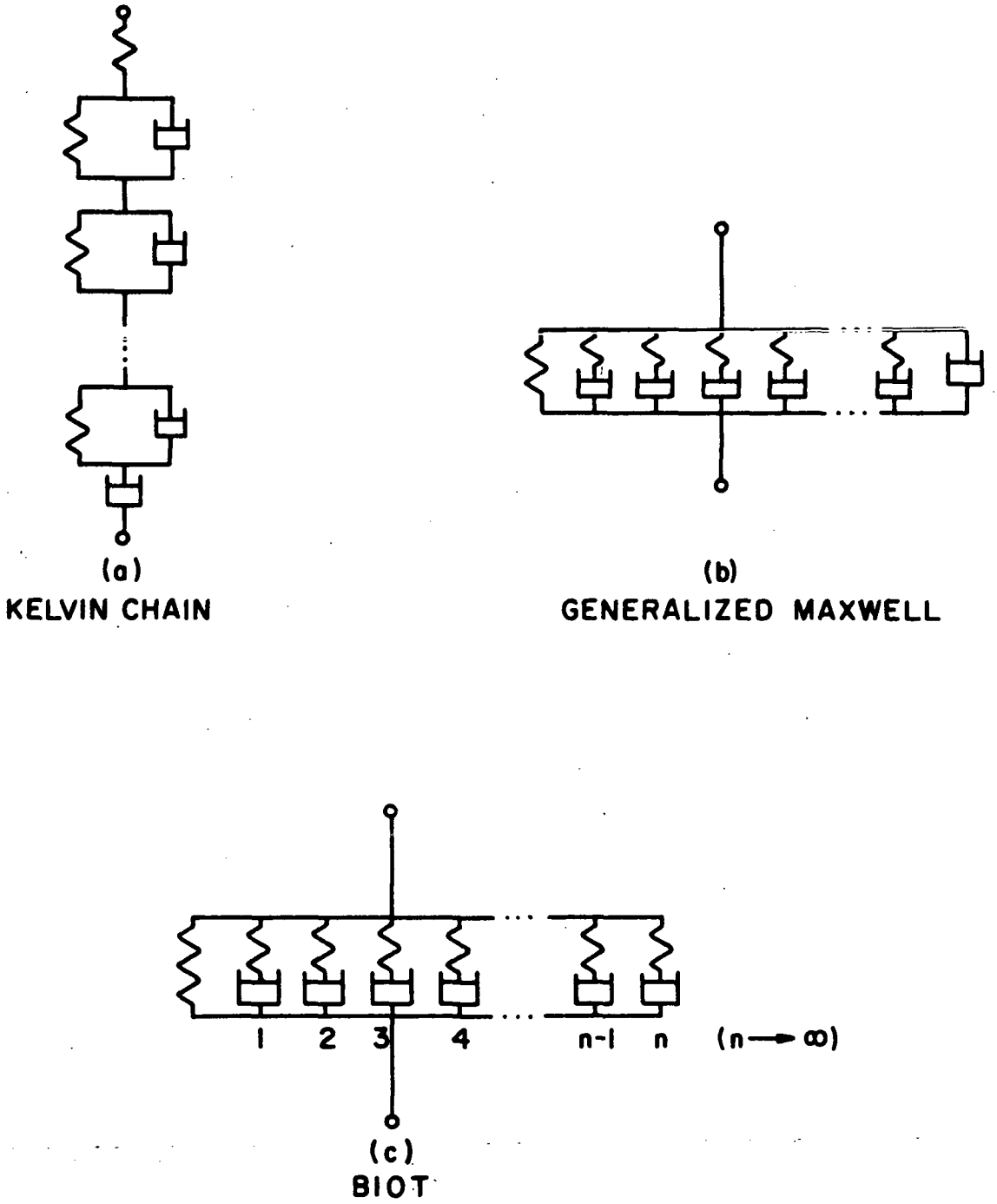

Figure B-2. Many-element viscoelastic models.

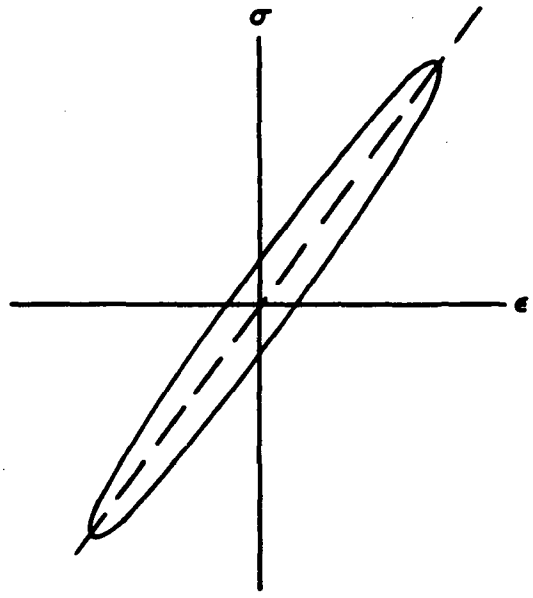

(a) ELLIPTICAL HYSTERESIS LOOP

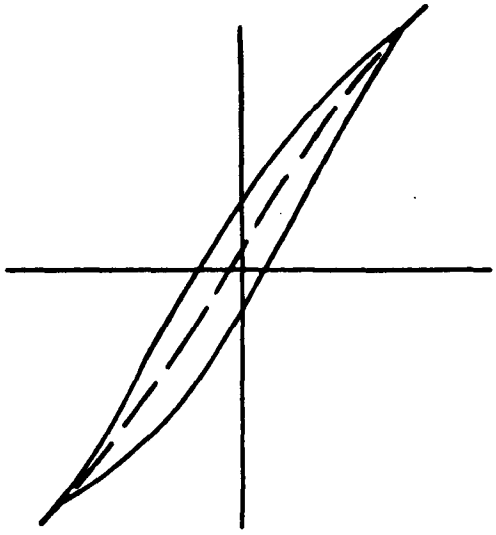

(b) POINTED-END, STRAIGHT-SIDED HYSTERESIS LOOP

Figure B-3. Hysteresis-loop shapes.

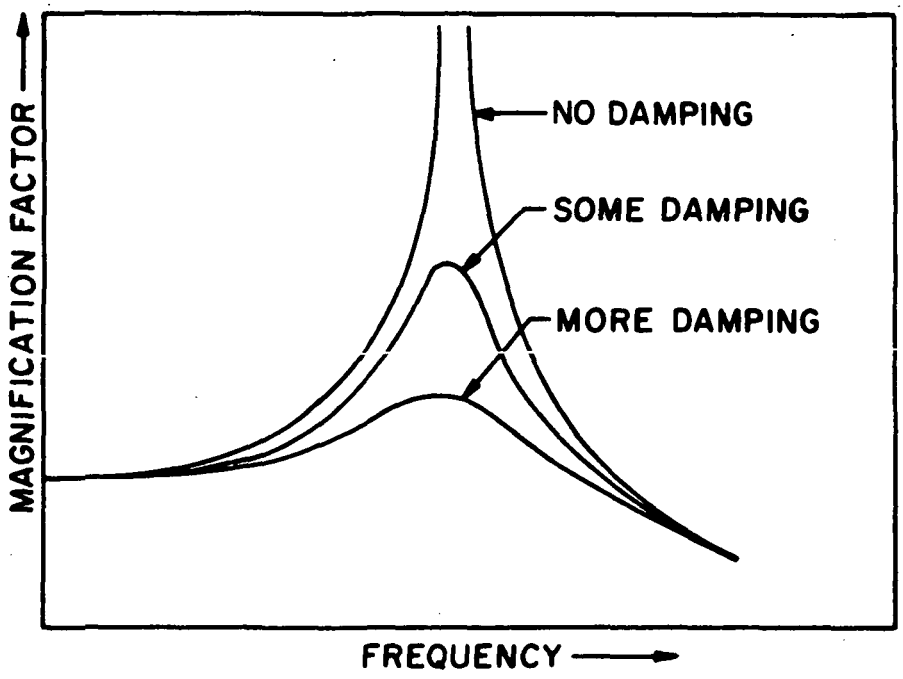

Figure B-4. Effect of damping on magnification factor. (Not drawn to scale).

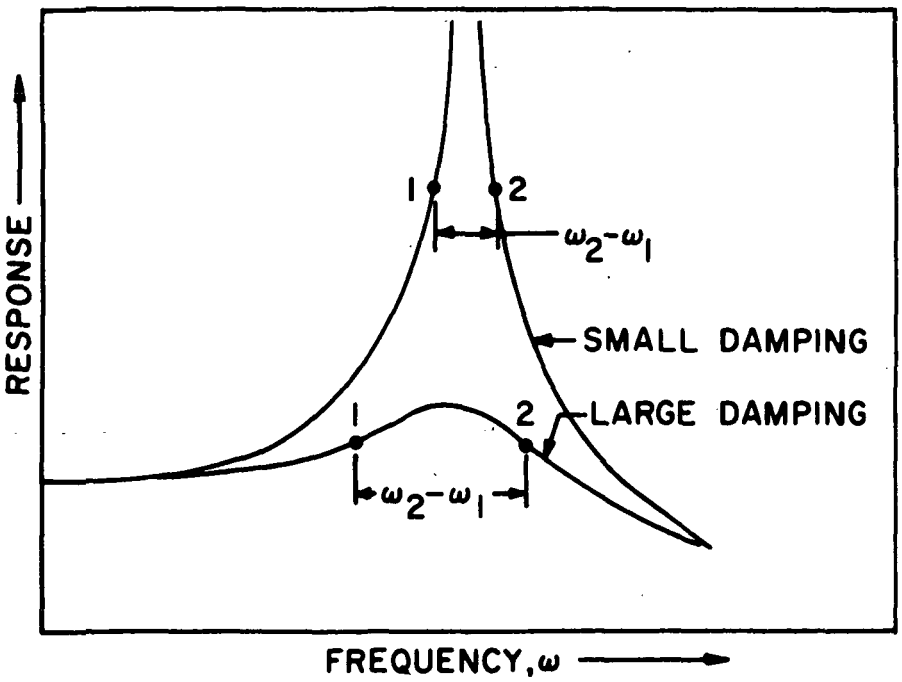

Figure B-5. Effect of damping on half-power-point frequency separation (ω_2-ω_1). (Not drawn to scale).

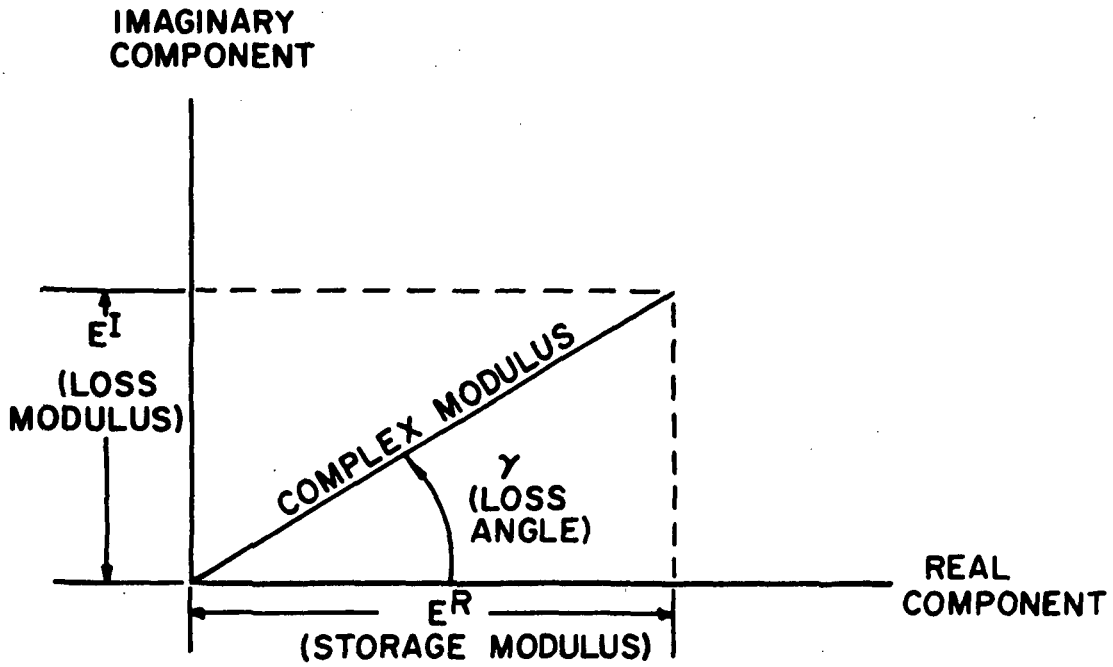

Figure B-6. Concept of complex modulus and loss angle.

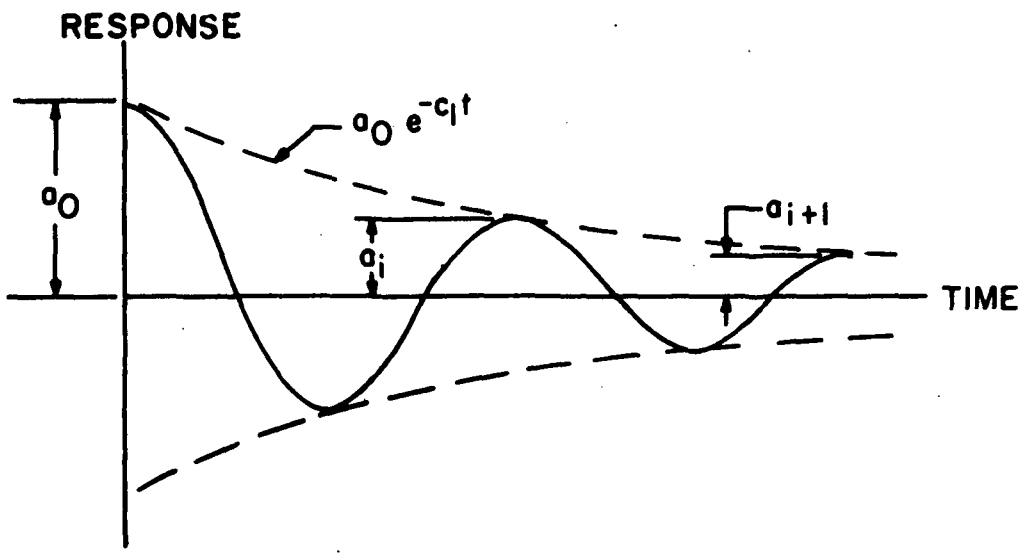

Figure B-7. Exponential decay. (Not drawn to scale).

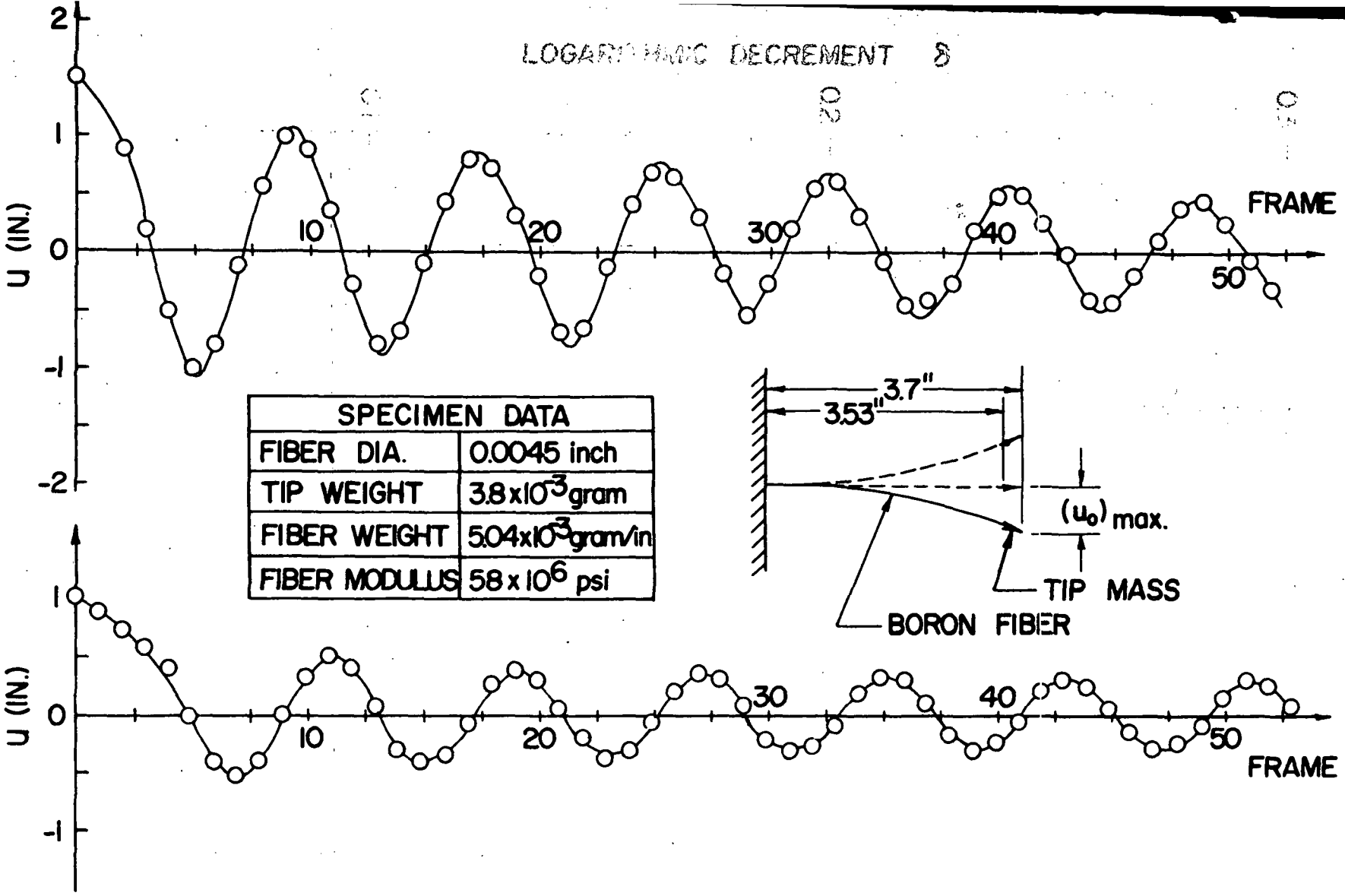

Figure D-1. Logarithmic decay of freely vibrating boron fiber with tip-mass.

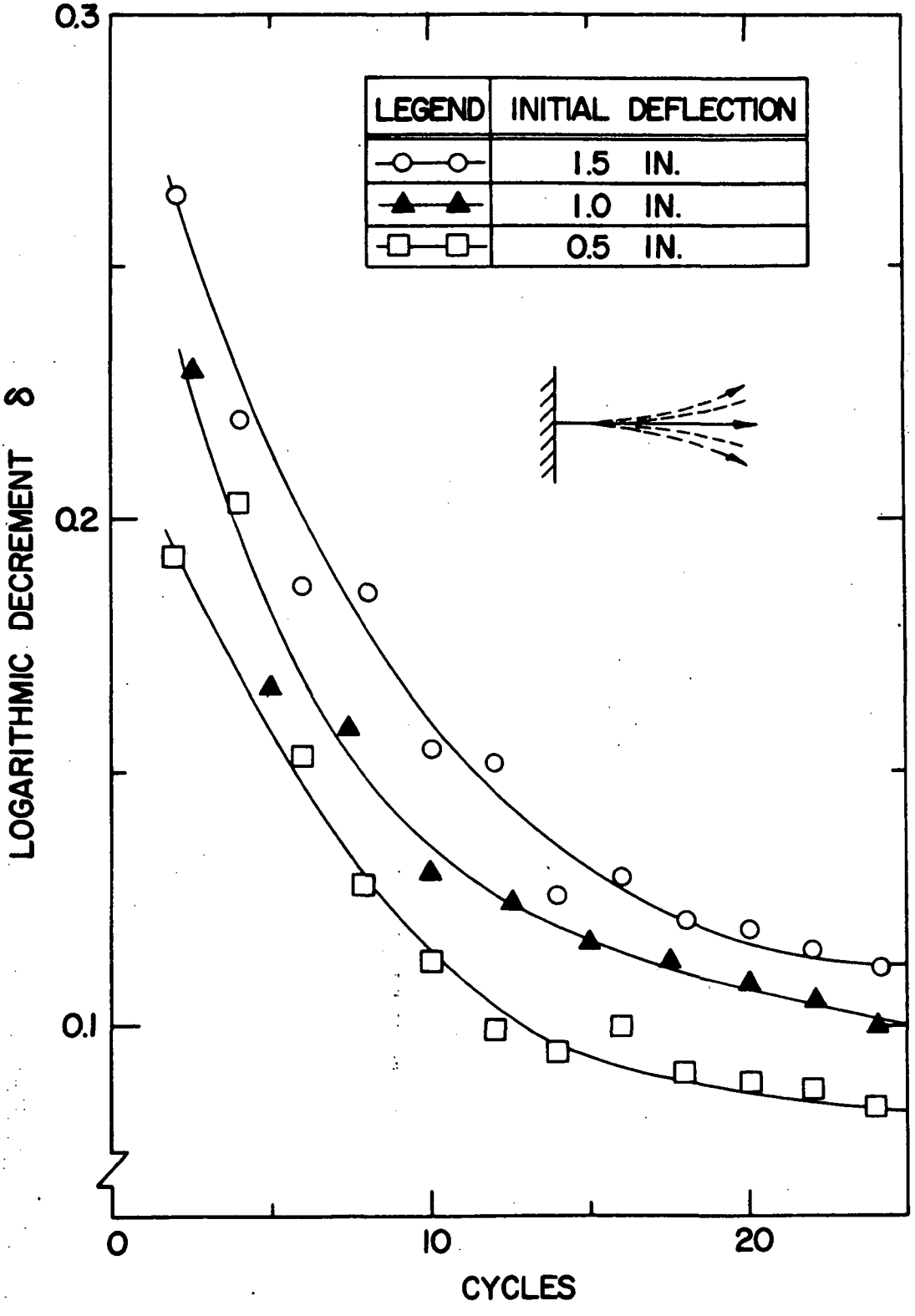

Figure D-2. Logarithmic decrement versus cycles for an AVCO boron fiber.

COMPUTER PROGRAM LISTING

```
C       *****LEAD-IN FOR COMPE11*****
        DIMENSION FMT2%20,6<,FNT2%20<
        COMMON RMU,DELTA,AMDA,AMDAP,AMDA1,AMDA2,EF,GEF,GF,GGF,RNUF,GNJF,
       1    EM,GEM,GM,GGM,RNUM,GNUM,RPI,VF,VM,E11S,DATA%128,8<,E11,GE11,
       2    RNU12,GNU12,AMDA3
C       ***DATA INPUT
        READ %5,2000< FMT2
 2000   FORMAT %20A4<
        CALL GIVEN
C       *READ GEOMETRICAL PARAMETERS RMU AND DELTA
        IDATA#1
        RPI#3.1415927
  700   READ %5,106< RMU,DELTA
  106   FORMAT %2F10.3<
        IF %RMU< 999,999,800
  800   CONTINUE
        VF#RPI/%4.0*RMU**2*DELTA<
        VM#1.0-VF
        IBEG#1
        IEND#6
        IINC#1
        DO 31 IJK#IBEG,IEND,IINC
        IF %IJK-5< 50,50,51
   50   NBEG#12*%IJK-1<&1
        NEND#NBEG&11
        NINC#1
        GO TO 52
   51   NBEG#61
        NEND#NBEG&3
   52   CONTINUE
        WRITE %6,107< IDATA,RMU,DELTA,VF
  107   FORMAT %1H1,////////////,28X,@IDATA#@,I3,@      RMU#@,F7.3,
       1@      DELTA#@,F7.3,@      VF#@,F7.3,////<
        DO 2222 LMN#1,20
 2222   FNT2%LMN<#FMT2%LMN,IJK<
        WRITE %6,FNT2<
```

```
      IF %IJK-5< 53,53,54
   53 CONTINUE
      WRITE %6,330<
  330 FORMAT %15X,13H   FREQUENCY ,18H            E11     ,
     1    18H            GE11    ,18H          EF/EM    ,
     2    18H          E11/EM    ,//<
      WRITE %6,331<
  331 FORMAT %15X,13H     HERTZ    ,18H          1.E6 PSI ,
     1    18H         PER CENT ,///<
      GO TO 55
   54 WRITE %6,332<
  332 FORMAT %27X,20H        FIBER         <
      WRITE %6,333<
  333 FORMAT %27X,20H  VOLUME FRACTION    ,20H         EF/EM        ,
     1    20H          E11/EM     ,///<
   55 CONTINUE
      DO 30 I#NBEG,NEND,NINC
      II#I&64
      FREQ#DATA%I,1<
      EF#DATA%I,3<
      GEF#DATA%I,4<
      GF#DATA%I,5<
      GGF#DATA%I,6<
      RNUF#DATA%I,7<
      GNUF#DATA%I,8<
      EM#DATA%II,3<
      GEM#DATA%II,4<
      GM#DATA%II,5<
      GGM#DATA%II,6<
      RNUM#DATA%II,7<
      GNUM#DATA%II,8<
      AMDA#GF/GM
      AMDAP#EF/EM
      AMDA1#%AMDA-1.0</%AMDA&1.0<
      AMDA2#%AMDA*%1.0-2.0*RNUM<-%1.0-2.0*RNUF<</%AMDA&1.0-2.0*RNUF<
      ALPHA#AMDA*%3.0-4.0*RNUM&1.0</%3.0-4.0*RNUF&AMDA<
```

```
      BETA#4.0*AMDA*%1.0-RNUM</%AMDA-1.0<
      GAMMA#BETA-1.0
      CALL COMPE11
      GO TO %81,81,81,81,81,82<,IJK
   81 WRITE %6,109< FREQ,E11,GE11,AMDAP,E11S
  109 FORMAT %15X,E13.4,4E18.4<
      GO TO 83
   82 WRITE %6,110< VF,AMDAP,E11S
  110 FORMAT %32X,F7.3,11X,E13.4,8X,E13.4<
   83 CONTINUE
   30 CONTINUE
   31 CONTINUE
      IDATA#IDATA&1
      GO TO 700
  999 STOP
      END
C
C
C     ***SUBROUTINE GIVEN***
      SUBROUTINE GIVEN
      DIMENSION FMT1%20,6<,FNT1%20<
      COMMON RMU,DELTA,AMDA,AMDAP,AMDA1,AMDA2,EF,GEF,GF,GGF,RNUF,GNUF,
     1   EM,GEM,GM,GGM,RNUM,GNUM,RPI,VF,VM,E11S,DATA%128,8<,E11,GE11,
     2   RNU12,GNU12,AMDA3
      READ%5,1< FMT1
    1 FORMAT %20A4<
      READ %5,100< %%DATA%I,J<,J#1,8<,I#1,128<
  100 FORMAT %8E10.3<
      IBEG#1
      IEND#6
      IINC#1
      DO 30 I#IBEG,IEND,IINC
      DO 1111 JK#1,20
 1111 FNT1%JK<#FMT1%JK,I<
      WRITE %6,FNT1<
      GO TO %71,72,73,74,75,76<,I
```

```
 71 JBEG#1
    GO TO 77
 72 JBEG#65
    GO TO 77
 73 JBEG#77
    GO TO 77
 74 JBEG#89
    GO TO 77
 75 JBEG#37
 77 JEND#JBEG&11
    WRITE %6,150<
    WRITE %6,151<
    WRITE %6,107< %%DATA%J,K<,K#1,8<,J#JBEG,JEND<
    GO TO 78
 76 CONTINUE
    WRITE %6,152<
    WRITE %6,153<
    WRITE %6,154< %DATA%61,N<,N#3,7,2<
    WRITE %6,155< %DATA%62,N<,N#3,7,2<
    WRITE %6,156< %DATA%63,N<,N#3,7,2<
    WRITE %6,157< %DATA%127,N<,N#3,7,2<
    WRITE %6,158< %DATA%128,N<,N#3,7,2<
150 FORMAT %15X,8H    FREQ,11H       K     ,11H       E     ,
   111H      GE     ,11H       G     ,11H      GG     ,11H      RNU    ,
   211H      GNU    ,/<
151 FORMAT %15X,8H      HZ ,11H  1.E6 PSI ,11H  1.E6 PSI ,
   111H  PER CENT ,11H  1.E6 PSI ,11H  PER CENT ,11X,
   311H  PER CENT ,///<
107 FORMAT %15X,F8.0,7E11.3<
152 FORMAT %25X,16H    MATERIAL     ,16H           E      ,
   116H           G      ,16H           RNU     ,/<
153 FORMAT %41X,16H        1.E6 PSI ,16H        1.E6 PSI ,///<
154 FORMAT %25X,16H       BORON      ,3E16.4,/<
155 FORMAT %25X,16H       STEEL      ,3E16.4,/<
156 FORMAT %25X,16H      E-GLASS     ,3E16.4,/<
157 FORMAT %25X,16H       EPOXY      ,3E16.4,/<
```

```
  158 FORMAT %25X,16H      ALUMINUM    ,3E16.4,/<
   78 CONTINUE
   30 CONTINUE
      RETURN
      END
C
C
C     *****SUBROUTINE COMPE11*****
      SUBROUTINE COMPE11
      COMMON RMU,DELTA,AMDA,AMDAP,AMDA1,AMDA2,EF,GEF,GF,GGF,RNUF,GNUF,
     1    EM,GEM,GM,GGM,RNUM,GNUM,RPI,VF,VM,E11S,DATA%128,8<,E11,GE11,
     2    RNU12,GNU12,AMDA3
      E11#EF*VF&EM*VM
      GE11#%EF*VF*GEF&EM*VM*GEM</E11
      E11S#E11/EM
      RETURN
      END
C
C
C     *****DATA DECK FOR HEADING - COMPE11*****
%46X,@*****BORON-EPOXY A*****@,///<
%46X,@*****BORON-EPOXY B*****@,///<
%41X,@*****BORON-ALUMINUM 2024-T3*****@,///<
%45X,@*****E GLASS-EPOXY A*****@,///<
%45X,@*****E GLASS-EPOXY B*****@,///<
%32X,@*****LONGITUDINAL IN-PLANE STIFFNESS E11/EM*****@,///<
%1H1,////////////,31X,@DATA 1  ELASTIC AND DAMPING PROPERTIES OF BORON@,///<
%1H1,////////////,30X,@DATA 2  ELASTIC AND DAMPING PROPERTIES OF EPOXY A@,///<
%1H1,////////////,30X,@DATA 3  ELASTIC AND DAMPING PROPERTIES OF EPOXY B@,///<
%1H1,////////////,30X,@DATA 4  ELASTIC AND DAMPING PROPERTIES OF ALJ 2224@,///<
%1H1,////////////,29X,@DATA 5  ELASTIC AND DAMPING PROPERTIES OF E-GLASS@,///<
%1H1,////////////,33X,@NOMINAL ELASTIC PROPERTIES OF SELECTED MATERIALS@,///<
C
C
C     *****DATA DECK FOR CONSTITUENT-MATERIAL PROPERTIES*****
 0.500E 01 0.322E 02 0.562E 02 0.129E 00 0.232E 02 0.160E 00 0.209E 00-0.179E 00
```

0.700E 01 0.322E 02 0.548E 02 0.130E 00 0.225E 02 0.160E 00 0.216E 00-0.170E 00
0.100E 02 0.322E 02 0.537E 02 0.131E 00 0.219E 02 0.160E 00 0.222E 00-0.163E 00
0.200E 02 0.322E 02 0.523E 02 0.134E 00 0.212E 02 0.163E 00 0.229E 00-0.158E 00
0.500E 02 0.322E 02 0.510E 02 0.136E 00 0.206E 02 0.165E 00 0.236E 00-0.152E 00
0.700E 02 0.322E 02 0.506E 02 0.138E 00 0.204E 02 0.167E 00 0.238E 00-0.151E 00
0.100E 03 0.322E 02 0.503E 02 0.141E 00 0.202E 02 0.170E 00 0.239E 00-0.153E 00
0.200E 03 0.322E 02 0.498E 02 0.146E 00 0.200E 02 0.176E 00 0.242E 00-0.155E 00
0.500E 03 0.322E 02 0.494E 02 0.154E 00 0.198E 02 0.185E 00 0.244E 00-0.161E 00
0.700E 03 0.322E 02 0.493E 02 0.158E 00 0.198E 02 0.190E 00 0.244E 00-0.164E 00
0.100E 04 0.322E 02 0.492E 02 0.161E 00 0.197E 02 0.193E 00 0.245E 00-0.167E 00
0.200E 04 0.322E 02 0.490E 02 0.168E 00 0.196E 02 0.202E 00 0.246E 00-0.172E 00
0.500E 01 0.322E 02 0.562E 02 0.129E 00 0.232E 02 0.160E 00 0.209E 00-0.179E 00
0.700E 01 0.322E 02 0.548E 02 0.130E 00 0.225E 02 0.160E 00 0.216E 00-0.170E 00
0.100E 02 0.322E 02 0.537E 02 0.131E 00 0.219E 02 0.160E 00 0.222E 00-0.163E 00
0.200E 02 0.322E 02 0.523E 02 0.134E 00 0.212E 02 0.163E 00 0.229E 00-0.158E 00
0.500E 02 0.322E 02 0.510E 02 0.136E 00 0.206E 02 0.165E 00 0.236E 00-0.152E 00
0.700E 02 0.322E 02 0.506E 02 0.138E 00 0.204E 02 0.167E 00 0.238E 00-0.151E 00
0.100E 03 0.322E 02 0.503E 02 0.141E 00 0.202E 02 0.170E 00 0.239E 00-0.153E 00
0.200E 03 0.322E 02 0.498E 02 0.146E 00 0.200E 02 0.176E 00 0.242E 00-0.155E 00
0.500E 03 0.322E 02 0.494E 02 0.154E 00 0.198E 02 0.185E 00 0.244E 00-0.161E 00
0.700E 03 0.322E 02 0.493E 02 0.158E 00 0.198E 02 0.190E 00 0.244E 00-0.164E 00
0.100E 04 0.322E 02 0.492E 02 0.161E 00 0.197E 02 0.193E 00 0.245E 00-0.167E 00
0.200E 04 0.322E 02 0.490E 02 0.168E 00 0.196E 02 0.202E 00 0.246E 00-0.172E 00
0.500E 01 0.322E 02 0.562E 02 0.129E 00 0.232E 02 0.160E 00 0.209E 00-0.179E 00
0.700E 01 0.322E 02 0.548E 02 0.130E 00 0.225E 02 0.160E 00 0.216E 00-0.170E 00
0.100E 02 0.322E 02 0.537E 02 0.131E 00 0.219E 02 0.160E 00 0.222E 00-0.163E 00
0.200E 02 0.322E 02 0.523E 02 0.134E 00 0.212E 02 0.163E 00 0.229E 00-0.158E 00
0.500E 02 0.322E 02 0.510E 02 0.136E 00 0.206E 02 0.165E 00 0.236E 00-0.152E 00
0.700E 02 0.322E 02 0.506E 02 0.138E 00 0.204E 02 0.167E 00 0.238E 00-0.151E 00
0.100E 03 0.322E 02 0.503E 02 0.141E 00 0.202E 02 0.170E 00 0.239E 00-0.153E 00
0.200E 03 0.322E 02 0.498E 02 0.146E 00 0.200E 02 0.176E 00 0.242E 00-0.155E 00
0.500E 03 0.322E 02 0.494E 02 0.154E 00 0.198E 02 0.185E 00 0.244E 00-0.161E 00
0.700E 03 0.322E 02 0.493E 02 0.158E 00 0.198E 02 0.190E 00 0.244E 00-0.164E 00
0.100E 04 0.322E 02 0.492E 02 0.161E 00 0.197E 02 0.193E 00 0.245E 00-0.167E 00
0.200E 04 0.322E 02 0.490E 02 0.168E 00 0.196E 02 0.202E 00 0.246E 00-0.172E 00
0.500E 01 0.630E 01 0.107E 02 0.270E 00 0.442E 01 0.333E 00 0.215E 00-0.356E 00

0.700E 01 0.630E 01 0.107E 02 0.265E 00 0.443E 01 0.327E 00 0.215E 00-0.351E 00
0.100E 02 0.630E 01 0.107E 02 0.260E 00 0.443E 01 0.321E 00 0.214E 00-0.345E 00
0.200E 02 0.630E 01 0.108E 02 0.258E 00 0.446E 01 0.318E 00 0.213E 00-0.346E 00
0.500E 02 0.630E 01 0.108E 02 0.260E 00 0.447E 01 0.321E 00 0.212E 00-0.351E 00
0.700E 02 0.630E 01 0.108E 02 0.265E 00 0.448E 01 0.327E 00 0.212E 00-0.358E 00
0.100E 03 0.630E 01 0.108E 02 0.310E 00 0.448E 01 0.383E 00 0.212E 00-0.419E 00
0.200E 03 0.630E 01 0.108E 02 0.310E 00 0.447E 01 0.383E 00 0.212E 00-0.417E 00
0.500E 03 0.630E 01 0.108E 02 0.420E 00 0.444E 01 0.518E 00 0.214E 00-0.559E 00
0.700E 03 0.630E 01 0.107E 02 0.480E 00 0.443E 01 0.592E 00 0.215E 00-0.635E 00
0.100E 04 0.630E 01 0.107E 02 0.550E 00 0.440E 01 0.678E 00 0.216E 00-0.720E 00
0.200E 04 0.630E 01 0.105E 02 0.700E 00 0.433E 01 0.860E 00 0.220E 00-0.888E 00
0.500E 01 0.630E 01 0.107E 02 0.270E 00 0.442E 01 0.333E 00 0.215E 00-0.356E 00
0.700E 01 0.630E 01 0.107E 02 0.265E 00 0.443E 01 0.327E 00 0.215E 00-0.351E 00
0.100E 02 0.630E 01 0.107E 02 0.260E 00 0.443E 01 0.321E 00 0.214E 00-0.345E 00
0.200E 02 0.630E 01 0.108E 02 0.258E 00 0.446E 01 0.318E 00 0.213E 00-0.346E 00
0.500E 02 0.630E 01 0.108E 02 0.260E 00 0.447E 01 0.321E 00 0.212E 00-0.351E 00
0.700E 02 0.630E 01 0.108E 02 0.265E 00 0.448E 01 0.327E 00 0.212E 00-0.358E 00
0.100E 03 0.630E 01 0.108E 02 0.310E 00 0.448E 01 0.383E 00 0.212E 00-0.419E 00
0.200E 03 0.630E 01 0.108E 02 0.310E 00 0.447E 01 0.383E 00 0.212E 00-0.417E 00
0.500E 03 0.630E 01 0.108E 02 0.420E 00 0.444E 01 0.518E 00 0.214E 00-0.559E 00
0.700E 03 0.630E 01 0.107E 02 0.480E 00 0.443E 01 0.592E 00 0.215E 00-0.635E 00
0.100E 04 0.630E 01 0.107E 02 0.550E 00 0.440E 01 0.678E 00 0.216E 00-0.720E 00
0.200E 04 0.630E 01 0.105E 02 0.700E 00 0.433E 01 0.860E 00 0.220E 00-0.888E 00
0.000E 00 0.333E 02 0.600E 02 0.000E 00 0.250E 02 0.000E 00 0.200E 00 0.000E 00
0.000E 00 0.250E 02 0.300E 02 0.000E 00 0.116E 02 0.000E 00 0.300E 00 0.000E 00
0.000E 00 0.631E 01 0.106E 02 0.000E 00 0.434E 01 0.000E 00 0.220E 00 0.000E 00
0.000E 00 0.333E 02 0.600E 02 0.000E 00 0.250E 02 0.000E 00 0.200E 00 0.000E 00
0.500E 01 0.488E 00 0.444E 00 0.160E 01 0.164E 00 0.177E 01 0.348E 00-0.696E 00
0.700E 01 0.488E 00 0.448E 00 0.161E 01 0.166E 00 0.179E 01 0.346E 00-0.709E 00
0.100E 02 0.488E 00 0.452E 00 0.162E 01 0.167E 00 0.180E 01 0.345E 00-0.723E 00
0.200E 02 0.488E 00 0.460E 00 0.165E 01 0.171E 00 0.184E 01 0.342E 00-0.755E 00
0.500E 02 0.488E 00 0.475E 00 0.173E 01 0.177E 00 0.193E 01 0.337E 00-0.830E 00
0.700E 02 0.488E 00 0.480E 00 0.179E 01 0.179E 00 0.200E 01 0.336E 00-0.873E 00
0.100E 03 0.488E 00 0.475E 00 0.183E 01 0.177E 00 0.205E 01 0.337E 00-0.878E 00
0.200E 03 0.488E 00 0.420E 00 0.200E 01 0.154E 00 0.221E 01 0.356E 00-0.804E 00
0.500E 03 0.488E 00 0.364E 00 0.230E 01 0.132E 00 0.250E 01 0.375E 00-0.761E 00

0.700E 03 0.488E 00 0.355E 00 0.252E 01 0.128E 00 0.274E 01 0.378E 00-0.806E 00
0.100E 04 0.488E 00 0.348E 00 0.263E 01 0.125E 00 0.285E 01 0.381E 00-0.820E 00
0.200E 04 0.488E 00 0.340E 00 0.310E 01 0.122E 00 0.336E 01 0.383E 00-0.937E 00
0.500E 01 0.244E 00 0.256E 00 0.160E 01 0.965E-01 0.181E 01 0.325E 00-0.860E 00
0.700E 01 0.244E 00 0.290E 00 0.161E 01 0.111E 00 0.185E 01 0.301E 00-0.105E 01
0.100E 02 0.244E 00 0.328E 00 0.162E 01 0.128E 00 0.190E 01 0.275E 00-0.131E 01
0.200E 02 0.244E 00 0.415E 00 0.165E 01 0.170E 00 0.203E 01 0.216E 00-0.216E 01
0.500E 02 0.244E 00 0.490E 00 0.173E 01 0.210E 00 0.222E 01 0.165E 00-0.350E 01
0.700E 02 0.244E 00 0.500E 00 0.179E 01 0.215E 00 0.231E 01 0.158E 00-0.385E 01
0.100E 03 0.244E 00 0.489E 00 0.183E 01 0.209E 00 0.235E 01 0.155E 00-0.368E 01
0.200E 03 0.244E 00 0.420E 00 0.200E 01 0.173E 00 0.247E 01 0.213E 00-0.269E 01
0.500E 03 0.244E 00 0.364E 00 0.230E 01 0.145E 00 0.275E 01 0.251E 00-0.227E 01
0.700E 03 0.244E 00 0.355E 00 0.252E 01 0.141E 00 0.300E 01 0.257E 00-0.237E 01
0.100E 04 0.244E 00 0.348E 00 0.263E 01 0.137E 00 0.312E 01 0.262E 00-0.238E 01
0.200E 04 0.244E 00 0.340E 00 0.310E 01 0.134E 00 0.366E 01 0.267E 00-0.268E 01
0.500E 01 0.106E 02 0.107E 02 0.980E-01 0.402E 01 0.110E 00 0.331E 00-0.498E-01
0.700E 01 0.106E 02 0.107E 02 0.121E 00 0.403E 01 0.136E 00 0.331E 00-0.617E-01
0.100E 02 0.106E 02 0.107E 02 0.150E 00 0.404E 01 0.169E 00 0.330E 00-0.767E-01
0.200E 02 0.106E 02 0.107E 02 0.211E 00 0.405E 01 0.237E 00 0.330E 00-0.108E 00
0.500E 02 0.106E 02 0.108E 02 0.176E 00 0.406E 01 0.198E 00 0.329E 00-0.907E-01
0.700E 02 0.106E 02 0.108E 02 0.142E 00 0.407E 01 0.160E 00 0.329E 00-0.733E-01
0.100E 03 0.106E 02 0.108E 02 0.110E 00 0.407E 01 0.124E 00 0.329E 00-0.568E-01
0.200E 03 0.106E 02 0.108E 02 0.110E 00 0.407E 01 0.124E 00 0.329E 00-0.568E-01
0.500E 03 0.106E 02 0.108E 02 0.340E-01 0.407E 01 0.383E-01 0.329E 00-0.175E-01
0.700E 03 0.106E 02 0.108E 02 0.290E-01 0.407E 01 0.327E-01 0.329E 00-0.149E-01
0.100E 04 0.106E 02 0.108E 02 0.250E-01 0.407E 01 0.282E-01 0.329E 00-0.129E-01
0.200E 04 0.106E 02 0.108E 02 0.210E-01 0.406E 01 0.236E-01 0.329E 00-0.108E-01
0.500E 01 0.488E 00 0.444E 00 0.160E 01 0.164E 00 0.177E 01 0.348E 00-0.696E 00
0.700E 01 0.488E 00 0.448E 00 0.161E 01 0.166E 00 0.179E 01 0.346E 00-0.709E 00
0.100E 02 0.488E 00 0.452E 00 0.162E 01 0.167E 00 0.180E 01 0.345E 00-0.723E 00
0.200E 02 0.488E 00 0.460E 00 0.165E 01 0.171E 00 0.184E 01 0.342E 00-0.755E 00
0.500E 02 0.488E 00 0.475E 00 0.173E 01 0.177E 00 0.193E 01 0.337E 00-0.830E 00
0.700E 02 0.488E 00 0.480E 00 0.179E 01 0.179E 00 0.200E 01 0.336E 00-0.873E 00
0.100E 03 0.488E 00 0.475E 00 0.183E 01 0.177E 00 0.205E 01 0.337E 00-0.878E 00
0.200E 03 0.488E 00 0.420E 00 0.200E 01 0.154E 00 0.221E 01 0.356E 00-0.804E 00
0.500E 03 0.488E 00 0.364E 00 0.230E 01 0.132E 00 0.250E 01 0.375E 00-0.761E 00

```
 0.700E 03 0.488E 00 0.355E 00 0.252E 01 0.128E 00 0.274E 01 0.378E 00-0.806E 00
 0.100E 04 0.488E 00 0.348E 00 0.263E 01 0.125E 00 0.285E 01 0.381E 00-0.820E 00
 0.200E 04 0.488E 00 0.340E 00 0.310E 01 0.122E 00 0.336E 01 0.383E 00-0.937E 00
 0.500E 01 0.244E 00 0.256E 00 0.160E 01 0.965E-01 0.181E 01 0.325E 00-0.860E 00
 0.700E 01 0.244E 00 0.290E 00 0.161E 01 0.111E 00 0.185E 01 0.301E 00-0.105E 01
 0.100E 02 0.244E 00 0.328E 00 0.162E 01 0.128E 00 0.190E 01 0.275E 00-0.131E 01
 0.200E 02 0.244E 00 0.415E 00 0.165E 01 0.170E 00 0.203E 01 0.216E 00-0.216E 01
 0.500E 02 0.244E 00 0.490E 00 0.173E 01 0.210E 00 0.222E 01 0.165E 00-0.350E 01
 0.700E 02 0.244E 00 0.500E 00 0.179E 01 0.215E 00 0.231E 01 0.158E 00-0.385E 01
 0.100E 03 0.244E 00 0.489E 00 0.183E 01 0.209E 00 0.235E 01 0.165E 00-0.368E 01
 0.200E 03 0.244E 00 0.420E 00 0.200E 01 0.173E 00 0.247E 01 0.213E 00-0.269E 01
 0.500E 03 0.244E 00 0.364E 00 0.230E 01 0.145E 00 0.275E 01 0.251E 00-0.227E 01
 0.700E 03 0.244E 00 0.355E 00 0.252E 01 0.141E 00 0.300E 01 0.257E 00-0.237E 01
 0.100E 04 0.244E 00 0.348E 00 0.263E 01 0.137E 00 0.312E 01 0.262E 00-0.238E 01
 0.200E 04 0.244E 00 0.340E 00 0.310E 01 0.134E 00 0.366E 01 0.267E 00-0.268E 01
 0.000E 00 0.556E 00 0.500E 00 0.000E 00 0.185E 00 0.000E 00 0.350E 00 0.000E 00
 0.000E 00 0.556E 00 0.500E 00 0.000E 00 0.185E 00 0.000E 00 0.350E 00 0.000E 00
 0.000E 00 0.556E 00 0.500E 00 0.000E 00 0.185E 00 0.000E 00 0.350E 00 0.000E 00
 0.000E 00 0.980E 01 0.100E 02 0.000E 00 0.375E 01 0.000E 00 0.330E 00 0.000E 00
C
C C
C      *****DATA DECK FOR GEOMETRICAL PARAMETERS*****
      1.982      1.000                                                    0.20
      1.772      1.000                                                    0.25
      1.618      1.000                                                    0.3
      1.498      1.000                                                    0.35
      1.401      1.000                                                    0.40
      1.321      1.000                                                    0.45
      1.253      1.000                                                    0.50
      1.195      1.000                                                    0.55
      1.144      1.000                                                    0.60
      1.099      1.000                                                    0.65
      1.059      1.000                                                    0.70
      0.000      0.000                                                    SENTRY
      1.023      1.000                                                    0.75
```

```
C       *****LEAD-IN FOR COMNU12*****
        DIMENSION FMT2%20,6<,FNT2%20<
        COMMON RMU,DELTA,AMDA,AMDAP,AMDA1,AMDA2,EF,GEF,GF,GGF,RNUF,GNUF,
       1    FM,GEM,GM,GGM,RNUM,GNUM,RPI,VF,VM,E11S,DATA%128,8<,E11,GE11,
       2    RNU12,GNU12,AMDA3
C       ***DATA INPUT
        READ %5,2000< FMT2
 2000 FORMAT %20A4<
        CALL GIVEN
C       *READ GEOMETRICAL PARAMETERS RMU AND DELTA
        IDATA#1
        RPI#3.1415927
  700 READ %5,106< RMU,DELTA
  106 FORMAT %2F10.3<
        IF %RMU< 999,999,800
  800 CONTINUE
        VF#RPI/%4.0*RMU**2*DELTA<
        VM#1.0-VF
        IBEG#1
        IEND#6
        IINC#1
        DO 31 IJK#IBEG,IEND,IINC
        IF %IJK-5< 50,50,51
   50 NBEG#12*%IJK-1<&1
        NEND#NBEG&11
        NINC#1
        GO TO 52
   51 NBEG#61
        NEND#NBEG&3
   52 CONTINUE
        WRITE %6,107< IDATA,RMU,DELTA,VF
  107 FORMAT %1H1,////////////,28X,@IDATA#@,I3,@      RMU#@,F7.3,
      1@      DELTA#@,F7.3,@      VF#@,F7.3,/////<
        DO 2222 LMN#1,20
 2222 FNT2%LMN<#FMT2%LMN,IJK<
        WRITE %6,FNT2<
```

```
      IF %IJK-5< 53,53,54
   53 CONTINUE
      WRITE %6,330<
  330 FORMAT %15X,13H    FREQUENCY ,18H            RNU12     ,
     1    18H            GNU12     ,18H             RNUF     ,
     2    18H             RNUM     ,//<
      WRITE %6,331<
  331 FORMAT %15X,13H      HERTZ     ,18X,18H          PER CENT ,//<
      GO TO 55
   54 WRITE %6,332<
  332 FORMAT %27X,20H         FIBER          <
      WRITE %6,333<
  333 FORMAT %27X,20H   VOLUME FRACTION    ,20H       RNUF/RNUM      ,
     1    20H           RNU12        ,//<
   55 CONTINUE
      DO 30 I#NBEG,NEND,NINC
      II#I&64
      FREQ#DATA%I,1<
      EF#DATA%I,3<
      GEF#DATA%I,4<
      GF#DATA%I,5<
      GGF#DATA%I,6<
      RNUF#DATA%I,7<
      GNUF#DATA%I,8<
      EM#DATA%II,3<
      GEM#DATA%II,4<
      GM#DATA%II,5<
      GGM#DATA%II,6<
      RNUM#DATA%II,7<
      GNUM#DATA%II,8<
      AMDA#GF/GM
      AMDAP#EF/EM
      AMDA1#%AMDA-1.0</%AMDA&1.0<
      AMDA2#%AMDA*%1.0-2.0*RNUM<-%1.0-2.0*RNUF<</%AMDA&1.0-2.0*RNUF<
      AMDA3#RNUF/RNUM
      ALPHA#AMDA*%3.0-4.0*RNUM&1.0</%3.0-4.0*RNUF&AMDA<
```

```
      BETA#4.0*AMDA*%1.0-RNUM</%AMDA-1.0<
      GAMMA#BETA-1.0
      CALL COMNU12
      GO TO %81,81,81,81,81,82<,IJK
   81 WRITE %6,109< FREQ,RNU12,GNU12,RNUF,RNUM
  109 FORMAT %15X,E13.4,4E18.4<
      GO TO 83
   82 WRITE %6,110< VF,AMDA3,RNU12
  110 FORMAT %32X,F7.3,11X,E13.4,8X,E13.4<
   83 CONTINUE
   30 CONTINUE
   31 CONTINUE
      IDATA#IDATA&1
      GO TO 700
  999 STOP
      END
C
C
C     *****SUBROUTINE GIVEN*****
C
C
C     *****SUBROUTINE COMNU12*****
      SUBROUTINE COMNU12
      COMMON RMU,DELTA,AMDA,AMDAP,AMDA1,AMDA2,EF,GEF,GF,GGF,RNUF,GNUF,
     1   EM,GEM,GM,GGM,RNUM,GNUM,RPI,VF,VM,E11S,DATA%128,8<,E11,GE11,
     2   RNU12,GNU12,AMDA3
      RNU12#RNUF*VF&RNUM*VM
      GNU12#%RNUF*VF*GNUF&RNUM*VM*GNUM</RNU12
      RETURN
      END
C
C
C     *****DATA DECK FOR HEADING - COMNU12*****
C
C
%46X,@*****BORON-EPOXY A*****@,///<
```

```
%46X,@*****BORON-EPOXY B*****@,///<
%41X,@*****BORON-ALUMINUM 2024-T3*****@,///<
%45X,@*****E GLASS-EPOXY A*****@,///<
%45X,@*****E GLASS-EPOXY B*****@,///<
%31X,@*****LONGITUDINAL IN-PLANE POISSON RATIO RNU12*****@,///<
%1H1,////////////,31X,@DATA 1  ELASTIC AND DAMPING PROPERTIES OF BORON@,///<
%1H1,////////////,30X,@DATA 2  ELASTIC AND DAMPING PROPERTIES OF EPOXY A@,///<
%1H1,////////////,30X,@DATA 3  ELASTIC AND DAMPING PROPERTIES OF EPOXY B@,///<
%1H1,////////////,30X,@DATA 4  ELASTIC AND DAMPING PROPERTIES OF ALU 2224@,///<
%1H1,////////////,29X,@DATA 5  ELASTIC AND DAMPING PROPERTIES OF E-GLASS@,///<
%1H1,////////////,33X,@NOMINAL ELASTIC PROPERTIES OF SELECTED MATERIALS@,///<
```

```
IN FOR COMPE22*****
FMT2%20,6<,FNT2%20<
,DELTA,AMDA,AMDAP,RPI,ALPHA,BETA,GAMMA,EF,GEF,GF,GGF,
UF,EM,GEM,GM,GGM,RNUM,GNUM,A%39<,B%39<,ANP%19<,BNP%19<,
0<,ETA%20,20<,IKS,E22,GE22,RNU12,VF,VM,VAVS%21<,EYBAR,
22S,DATA%128,8<
00< FMT2
A4<
PUT

ETRICAL PARAMETERS RMU AND DELTA

927
5< RMU,DELTA
10.3<
99,999,800


0*RMU**2*DELTA<









IBEG,IEND,IINC
 50,50,51
JK-1<&1
11



3


07< IDATA,RMU,DELTA,VF
```

```
 107 FORMAT %1H1,////////////,28X,@IDATA#@,I3,@      RMU#@,F7.3,
    1@      DELTA#@,F7.3,@      VF#@,F7.3,////<
     DO 2222 LMN#1,20
2222 FNT2%LMN<#FMT2%LMN,IJK<
     WRITE %6,FNT2<
     IF %IJK-5< 53,53,54
  53 CONTINUE
     WRITE %6,330<
 330 FORMAT %15X,13H   FREQUENCY ,13H       E22     ,13H      GE22     ,
    113H     RNU12     ,13H     EF/EM     ,13H     E22/EM    ,7H    IKS ,/<
     WRITE %6,331<
 331 FORMAT %15X,13H      HERTZ    ,13H     1.E6 PSI ,13H     PER CENT ,//<
     GO TO 55
  54 WRITE %6,332<
 332 FORMAT %27X,20H        FIBER          <
     WRITE %6,333<
 333 FORMAT %27X,20H  VOLUME FRACTION    ,20H        EF/EM          ,
    1    20H        E22/EM         ,//<
  55 CONTINUE
     DO 30 I#NBEG,NEND,NINC
     II#I&64
     FREQ#DATA%I,1<
     EF#DATA%I,3<
     GEF#DATA%I,4<
     GF#DATA%I,5<
     GGF#DATA%I,6<
     RNUF#DATA%I,7<
     GNUF#DATA%I,8<
     EM#DATA%II,3<
     GEM#DATA%II,4<
     GM#DATA%II,5<
     GGM#DATA%II,6<
     RNUM#DATA%II,7<
     GNUM#DATA%II,8<
     AMDA#GF/GM
     AMDAP#EF/EM
```

```
      AMDA2#%AMDA*%1.0-2.0*RNUM<-%1.0-2.0*RNUF<</%AMDA&1.0-2.0*RNUF<
      ALPHA#AMDA*%3.0-4.0*RNUM&1.0</%3.0-4.0*RNUF&AMDA<
      BETA#4.0*AMDA*%1.0-RNUM</%AMDA-1.0<
      GAMMA#BETA-1.0
      CALL COMPE22
      GO TO %81,81,81,81,81,82<,IJK
   81 WRITE %6,109< FREQ,E22,GE22,RNU12,AMDAP,E22S,IKS
  109 FORMAT %15X,6E13.4,I5<
      GO TO 83
   82 WRITE %6,110< VF,AMDAP,E22S
  110 FORMAT %32X,F7.3,11X,E13.4,8X,E13.4<
   83 CONTINUE
   30 CONTINUE
   31 CONTINUE
      IDATA#IDATA&1
      GO TO 700
  999 STOP
      END
C
C
C     *****SUBROUTINE GIVEN*****
C
C
C     ***PT400 ***
      SUBROUTINE PT400
      COMMON RMU,DELTA,AMDA,AMDAP,RPI,ALPHA,BETA,GAMMA,EF,GEF,GF,GGF,
     1   RNUF,GNUF,EM,GEM,GM,GGM,RNUM,GNUM,A%39<,B%39<,ANP%19<,BNP%19<,
     2   XI%20,20<,ETA%20,20<,IKS,E22,GE22,RNU12,VF,VM,VAVS%21<,EYBAR,
     3   AMDA2,E22S,DATA%128,8<
      H#RMU/20.0
      V#RMU*DELTA/20.0
      DO 30 I#1,20
      RI#I
      DO 31 J#1,20
      RJ#J
      Y#RMU*DELTA-%RI-0.5<*V
```

```
      X#%RJ-0.5<*H
      XI%I,J<#X
      ETA%I,J<#Y
   31 CONTINUE
   30 CONTINUE
      RETURN
      END
C
CC
C     *****SUBROUTINE COMPE22*****
      SUBROUTINE COMPE22
      DIMENSION CCC%78,39<,C%39,39<,BB%78<
      COMMON RMU,DELTA,AMDA,AMDAP,RPI,ALPHA,BETA,GAMMA,EF,GEF,GF,GGF,
     1    RNUF,GNUF,EM,GEM,GM,GGM,RNUM,GNUM,A%39<,B%39<,ANP%19<,BNP%19<,
     2    XI%20,20<,ETA%20,20<,IKS,E22,GE22,RNU12,VF,VM,VAVS%21<,EYBAR,
     3    AMDA2,E22S,DATA%128,8<
      V#RMU*DELTA/20.0
      H#RMU/20.0
      AREA#V*H
      Y#RMU*DELTA
      DO 30 I#1,20
      II#I&20
      RI#I
      X#RI*H
      ROH#SQRT%X**2&Y**2<
      TETA#ATAN%Y/X<
      BB%I<#1.0
      BB%II<#0.0
      CCC%I,1<#2.0*%1.0-AMDA2*COS%2.0*TETA</%ROH*ROH<<
      CCC%II,1<#2.0*AMDA2*SIN%2.0*TETA</%ROH*ROH<
      T1#1.0
      T2#-2.0/%GAMMA*ROH*ROH<
      T3#%2.0/%ROH*ROH<-3.0/%ROH**4<</GAMMA
      CCC%I,2<#2.0*%T1&T2*COS%2.0*TETA<&T3*COS%4.0*TETA<<
      T4#2.0*ROH*ROH
      T5#2.0*%ROH*ROH-1.0/%GAMMA*ROH*ROH<<
```

```
      T6#%%GAMMA*%1.0-ALPHA<-3.0</%ROH**4<&2.0/%ROH*ROH<</GAMMA
      CCC%I,21<#3.0*%T4&T5*COS%2.0*TETA<&T6*COS%4.0*TETA<<
      CCC%II,2<#2.0*%-T3*SIN%4.0*TETA<<
      CCC%II,21<#3.0*%-T6*SIN%4.0*TETA<<
      DO 33 J#3,20
      N#2*%J-1<
      JJ#J&19
      RN#N
      COSNT#COS%RN*TETA<
      COSM2#COS%%RN-2.0<*TETA<
      COSP2#COS%%RN&2.0<*TETA<
      SINM2#SIN%%RN-2.0<*TETA<
      SINP2#SIN%%RN&2.0<*TETA<
      ROHN#ROH**N
      ROHM2#ROHN/%ROH*ROH<
      ROHP2#ROHN*ROH*ROH
      P1#ROHM2
      P2#-2.0/%ROHN*GAMMA<
      P3#%RN/ROHN-%RN&1.0</%ROHP2<</GAMMA
      CCC%I,J<#RN*%RN-1.0<*%P1*COSM2&P2*COSNT&P3*COSP2<
      Q1#RN*ROHN
      Q2#2.0*%ROHN-%RN-1.0</%ROHN*GAMMA<<
      Q3#%%GAMMA*%1.0-ALPHA<-%RN*RN-1.0<</ROHP2&RN*%RN-1.0</ROHN</GAMMA
      CCC%I,JJ<#%RN&1.0<*%Q1*COSM2&Q2*COSNT&Q3*COSP2<
      R1#ROHM2
      R2#-P3
      CCC%II,J<#RN*%RN-1.0<*%R1*SINM2&R2*SINP2<
      S1#ROHN*RN
      S2#-Q3
      CCC%II,JJ<#%RN&1.0<*%S1*SINM2&S2*SINP2<
   33 CONTINUE
   30 CONTINUE
      X#RMU
      DO 31 I#41,59
      II#I&19
      RI#I-40
```

```
Y#RMU*DELTA-RI*V
ROH#SQRT%X**2&Y**2<
TETA#ATAN%Y/X<
BB%I<#0.0
BB%II<#0.0
CCC%I,1<#2.0*%1.0&AMDA2*COS%2.0*TETA</%ROH*ROH<<
CCC%II,1<#2.0*AMDA2*SIN%2.0*TETA</%ROH*ROH<
T1#-1.0
T2#-2.0/%GAMMA*ROH*ROH<
T3#-%2.0/%ROH*ROH<-3.0/%ROH**4<<
T4#-2.0*ROH*ROH
T5#2.0*%ROH*ROH-1.0/%GAMMA*ROH*ROH<<
T6#-%%GAMMA*%1.0-ALPHA<-%3.0<</%ROH**4<&2.0/%ROH*ROH<<
CCC%I,21<#3.0*%T4&T5*COS%2.0*TETA<&T6*COS%4.0*TETA<<
CCC%II,2<#2.0*T3*SIN%4.0*TETA<
CCC%II,21<#3.0*T6*SIN%4.0*TETA<
DO 34 J#3,20
N#2*%J-1<
JJ#J&19
RN#N
COSNT#COS%RN*TETA<
COSM2#COS%%RN-2.0<*TETA<
COSP2#COS%%RN&2.0<*TETA<
SINM2#SIN%%RN-2.0<*TETA<
SINP2#SIN%%RN&2.0<*TETA<
ROHN#ROH**N
ROHM2#ROHN/%ROH*ROH<
ROHP2#ROHN*ROH*ROH
P1#ROHM2
P2#2.0/%ROHN*GAMMA<
P3#%RN/ROHN-%RN&1.0</ROHP2</GAMMA
CCC%I,J<#-RN*%RN-1.0<*%P1*COSM2&P2*COSNT&P3*COSP2<
Q1#RN*ROHN
Q2#2.0*%-ROHN&%RN-1.0</%ROHN*GAMMA<<
Q3#%%GAMMA*%1.0-ALPHA<-%RN*RN-1.0<</ROHP2&RN*%RN-1.0</ROHN</GAMMA
```

```
      CCC%I,JJ<#-%RN&1.0<**%Q1*COSM2&Q2*COSNT&Q3*COSP2<
      R1#ROHM2
      R2#-P3
      CCC%II,J<#RN*%RN-1.0<**%R1*SINM2&R2*SINP2<
      S1#ROHN*RN
      S2#-Q3
      CCC%II,JJ<#%RN&1.0<**%S1*SINM2&S2*SINP2<
   34 CONTINUE
   31 CONTINUE
      CALL ATA%CCC,C<
      CALL ATB%CCC,BB,B<
      CALL SIMQ%C,B,39,KS<
      IKS#KS
C     ***COMPUTE FIBER REGION COEFFICIENTS A%40<,ANP%19<,AND BNP%19<
      A%1<#2.0*AMDA*%1.0-RNUM</%AMDA&1.0-2.0*RNUF<*B%1<
      DO 32 I#2,20
      N#2*%I-1<
      II#I&19
      RN#N
      J#I-1
      A%I<#%BETA/GAMMA<*B%I<&%%RN&1.0</RN<*%BETA/GAMMA-ALPHA<*B%II<
      A%II<#ALPHA*B%II<
      ANP%J<#-%%RN-1.0</GAMMA<*B%I<&%%%1.0-ALPHA<-%RN*RN-1.0</GAMMA<
     1    /RN<*B%II<
      BNP%J<#%RN*B%I<&%RN&1.0<*B%II<</GAMMA
   32 CONTINUE
      CALL E22NU
      RETURN
      END
C
C
C     ***SUBROUTINE E22NU***
      SUBROUTINE E22NU
      COMMON RMU,DELTA,AMDA,AMDAP,RPI,ALPHA,BETA,GAMMA,EF,GEF,GF,GGF,
     1    RNUF,GNUF,EM,GEM,GM,GGM,RNUM,GNUM,A%39<,B%39<,ANP%19<,BNP%19<,
     2    XI%20,20<,ETA%20,20<,IKS,E22,GE22,RNU12,VF,VM,VAVS%21<,EYBAR,
```

```
  3    AMDA2,E22S,DATA%128,8<
     AREA#%RMU**2<*DELTA/400.0
     E11#EF*VF&EM*VM
     CALL VAVG
     SUMZ#0.0
     SUMSF#0.0
     SUMSM#0.0
     SUMTF#0.0
     SUMTM#0.0
     DO 30 I#1,20
     DO 31 J#1,20
     CALL SIGMA%XI%I,J<,ETA%I,J<,SIGX,SIGY,TAUXY<
     ROH#SQRT%XI%I,J<**2&ETA%I,J<**2<
     IF %ROH-1.0< 50,50,51
50   CONTINUE
     TERM1#%1.0-RNUF<*%SIGX**2&SIGY**2<-2.0*RNUF*SIGX*SIGY
     SUMSF#SUMSF&TERM1
     TERM2#TAUXY*TAUXY
     SUMTF#SUMTF&TERM2
     TERMZ#RNUF*%SIGX&SIGY<
     GO TO 52
51   CONTINUE
     TERM3#%1.0-RNUM<*%SIGX**2&SIGY**2<-2.0*RNUM*SIGX*SIGY
     SUMSM#SUMSM&TERM3
     TERM4#TAUXY*TAUXY
     SUMTM#SUMTM&TERM4
     TERMZ#RNUM*%SIGX&SIGY<
52   CONTINUE
     SUMZ#SUMZ&TERMZ
31   CONTINUE
30   CONTINUE
     USF#SUMSF/%4.0*GF<
     UTF#SUMTF/%2.0*GF<
     USM#SUMSM/%4.0*GM<
     UTM#SUMTM/%2.0*GM<
     SZBAR#SUMZ/400.0
```

```
      E22#E11/%E11*EYBAR&SZBAR*SZBAR<
      E22S#E22/EM
      RNU12#SZBAR
      UDF#2.0*RPI*%GEF*USF&GGF*UTF<
      UDM#2.0*RPI*%GEM*USM&GGM*UTM<
      U#USF&USM&UTF&UTM
      GE22#%UDF&UDM</%2.0*RPI*U<
      RETURN
      END
C
C
C     ***SUBROUTINE VAVG***
      SUBROUTINE VAVG
      COMMON RMU,DELTA,AMDA,AMDAP,RPI,ALPHA,BETA,GAMMA,EF,GEF,GF,GGF,
     1   RNUF,GNUF,EM,GEM,GM,GGM,RNUM,GNUM,A%39<,B%39<,ANP%19<,BNP%19<,
     2   XI%20,20<,ETA%20,20<,IKS,E22,GE22,RNU12,VF,VM,VAVS%21<,EYBAR,
     3   AMDA2,E22S,DATA%128,8<
      Y#RMU*DELTA
      DO 30 I#1,21
      RI#I
      X#%RI-1.0<*%RMU/20.0<
      ROH#SQRT%X**2&Y**2<
      IF %I-1< 50,50,51
   50 TETA#0.5*RPI
      GO TO 52
   51 TETA#ATAN%Y/X<
   52 CONTINUE
      SUM#0.0
      DO 31 J#2,20
      JJ#J&19
      JJJ#J-1
      N#2*%J-1<
      RN#N
      ROHN#ROH**N
      ROHM1#ROHN/ROH
      ROHP1#ROHN*ROH
```

```
      SINM1#SIN%%RN-1.0<*TETA<
      SINNT#SIN%RN*TETA<
      SINP1#SIN%%RN&1.0<*TETA<
      TERM1#B%J<*RN*ROHM1*SINM1
      TERM2#B%JJ<*ROHP1*%RN*SINM1&2.0*%1.0-2.0*RNUM<*SINP1
     1    &2.0*SINNT*COS%TETA<<
      TERM3#ANP%JJJ<*RN*SINP1/ROHP1
      TERM4#%BNP%JJJ</ROHM1<*%RN*SINP1-2.0*%1.0-2.0*RNUM<*SINM1
     1    -2.0*SINNT*COS%TETA<<
      SUM#SUM&TERM1&TERM2&TERM3&TERM4
   31 CONTINUE
      SUM#SUM&2.0*B%1<*%%1.0-2.0*RNUM<*ROH-AMDA2/ROH<*SIN%TETA<
      VAVS%I<#SUM
   30 CONTINUE
      SUM#0.0
      DO 32 I#1,21
      SUM#SUM&VAVS%I<
   32 CONTINUE
      EYBAR#SUM*%1.0&RNUM</%EM*21.0*RMU*DELTA<
      RETURN
      END
C
C
C     ***SUBROUTINE SIGMA%X,Y,SIGX,SIGY,TAUXY<***
      SUBROUTINE SIGMA%X,Y,SIGX,SIGY,TAUXY<
      COMMON RMU,DELTA,AMDA,AMDAP,RPI,ALPHA,BETA,GAMMA,EF,GEF,GF,GGF,
     1    RNUF,GNUF,EM,GEM,GM,GGM,RNUM,GNUM,A%39<,B%39<,ANP%19<,BNP%19<,
     2    XI%20,20<,ETA%20,20<,IKS,E22,GE22,RNU12,VF,VM,VAVS%21<,EYBAR,
     3    AMDA2,E22S,DATA%128,8<
      IF %X< 49,50,51
   49 TETA#ATAN%Y/X<&RPI
      GO TO 52
   50 TETA#0.5*RPI
      GO TO 52
   51 TETA#ATAN%Y/X<
   52 CONTINUE
```

```
      ROH#SQRT%X**2&Y**2<
      IF %ROH< 53,53,54
   53 SIGX#2.0*%A%1<-A%2<<
      SIGY#2.0*%A%1<&A%2<<
      TAUXY#0.0
      RETURN
   54 CONTINUE
      IF %ROH-1.0< 55,55,56
   55 CONTINUE
      SUM1#0.0
      SUM2#0.0
      SUM3#0.0
      DO 30 I#3,20
      II#I&19
      N#2*%I-1<
      RN#N
      ROHN#ROH**N
      ROHM2#ROHN/%ROH*ROH<
      ROHP2#ROHN*ROH*ROH
      COSNT#COS%RN*TETA<
      COSM2#COS%%RN-2.0<*TETA<
      COSP2#COS%%RN&2.0<*TETA<
      P1#RN*%RN-1.0<*ROHM2*COSM2
      P2#%RN&1.0<*ROHN*%RN*COSM2-2.0*COSNT<
      TERM1#-%A%I<*P1&A%II<*P2<
      TERM2#A%I<*P1&A%II<*%RN&1.0<*ROHN*%RN*COSM2&2.0*COSNT<
      SUM1#SUM1&TERM1
      SUM2#SUM2&TERM2
      TERM3#%A%I<*RN*%RN-1.0<*ROHM2&A%II<*RN*%RN&1.0<*ROHN<*
     1    SIN%%RN-2.0<*TETA<
      SUM3#SUM3&TERM3
   30 CONTINUE
      SIGX#SUM1&2.0*A%1<&A%2<*%-2.0<&A%21<**%-3.0*ROH*ROH*%2.0-2.0
     1    *COS%2.0*TETA<<<
      SIGY#SUM2&2.0*A%1<&A%2<*%2.0<&A%21<**%3.0*ROH*ROH*%2.0&2.0*COS
     1    %2.0*TETA<<<
```

```
      TAUXY#SUM3
      RETURN
   56 CONTINUE
      SUM1#0.0
      SUM2#0.0
      SUM3#0.0
      DO 31 I#3,20
      N#2*%I-1<
      II#I&19
      J#I-1
      RN#N
      ROHN#ROH**N
      ROHM2#ROHN/%ROH*ROH<
      ROHP2#ROHN*ROH*ROH
      COSNT#COS%RN*TETA<
      COSP2#COS%%RN&2.0<*TETA<
      COSM2#COS%%RN-2.0<*TETA<
      P1#RN*%RN-1.0<*ROHM2*COSM2
      P2#%RN&1.0<*ROHN*%RN*COSM2-2.0*COSNT<
      P3#RN*%RN&1.0<*COSP2/ROHP2
      P4#%RN-1.0<*%RN*COSP2&2.0*COSNT</ROHN
      TERM1#%B%I<*P1&B%II<*P2&ANP%J<*P3&BNP%J<*P4<
      Q1#P1
      Q2#%RN&1.0<*ROHN*%RN*COSM2&2.0*COSNT<
      Q3#P3
      Q4#%RN-1.0<*%RN*COSP2-2.0*COSNT</ROHN
      TERM2#B%I<*Q1&B%II<*Q2&ANP%J<*Q3&BNP%J<*Q4
      R1#RN*%RN-1.0<*ROHM2
      R2#RN*%RN&1.0<*ROHN
      R3#RN*%RN&1.0</ROHP2
      R4#RN*%RN-1.0</ROHN
      TERM3#%B%I<*R1&B%II<*R2<*SIN%%RN-2.0<*TETA<
     1    -%ANP%J<*R3&BNP%J<*R4<*SIN%%RN&2.0<*TETA<
      SUM1#SUM1&TERM1
      SUM2#SUM2&TERM2
      SUM3#SUM3&TERM3
```

```
   31 CONTINUE
      SIGX#-SUM1&2.0*B%1<*%1.0&AMDA2*COS%2.0*TETA</%ROH*ROH<<
     1    -2.0*B%2<-3.0*B%21<*ROH*ROH*%2.0<*%1.0-COS%2.0*TETA<<
     2    -6.0*ANP%1<*COS%4.0*TETA</%ROH**4<-BNP%1<*%2.0*COS%4.0*TETA<
     3    &2.0*COS%2.0*TETA<<
      SIGY#SUM2&2.0*B%1<*%1.0-AMDA2*COS%2.0*TETA</%ROH*ROH<<
     1    &2.0*B%2<&3.0*B%21<*ROH*ROH*2.0*%1.0&COS%2.0*TETA<<
     2   &6.0*ANP%1<*COS%4.0*TETA</%ROH**4<
     3    &BNP%1<*%2.0*COS%4.0*TETA<-2.0*COS%2.0*TETA<</%ROH*ROH<
      TAUXY#SUM3&2.0*AMDA2*B%1<*SIN%2.0*TETA</%ROH*ROH<
     1    -6.0*ANP%1<*SIN%4.0*TETA</%ROH**4<
     2    -2.0*BNP%1<*SIN%4.0*TETA</%ROH*ROH<
      RETURN
      END
C
C
C     *** SUBROUTINE ATA %A,B<***
      SUBROUTINE ATA %A,B<
      DIMENSION A%78,39<, B%39,39<
      DO 30 I#1,39
      DO 31 J#1,39
      B%I,J<#0.0
      DO 32 M#1,78
      B%I,J<#B%I,J<&A%M,I<*A%M,J<
   32 CONTINUE
   31 CONTINUE
   30 CONTINUE
      RETURN
      END
C
C
C     *** SUBROUTINE ATB%A,B,C,<***
      SUBROUTINE ATB%A,B,C<
      DIMENSION A%78,39<,B%78<,C%39<
      DO 30 I#1,39
      C%I<#0.0
```

```
      DO 31 J#1,78
      C%I<#C%I<&A%J,I<*B%J<
   31 CONTINUE
   30 CONTINUE
      RETURN
      END
C
C
C     *****DATA DECK FOR HEADING - COMPE22*****
C
C
%46X,@*****BORON-EPOXY A*****@,///<
%46X,@*****BORON-EPOXY B*****@,///<
%41X,@*****BORON-ALUMINUM 2024-T3*****@,///<
%45X,@*****E GLASS-EPOXY A*****@,///<
%45X,@*****E GLASS-EPOXY B*****@,///<
%34X,@*****TRANSVERSE IN-PLANE STIFFNESS E22/EM*****@,///<
%1H1,////////////,31X,@DATA 1  ELASTIC AND DAMPING PROPERTIES OF BORON@,///<
%1H1,////////////,30X,@DATA 2  ELASTIC AND DAMPING PROPERTIES OF EPJXY A@,///<
%1H1,////////////,30X,@DATA 3  ELASTIC AND DAMPING PROPERTIES OF EPOXY B@,///<
%1H1,////////////,30X,@DATA 4  ELASTIC AND DAMPING PROPERTIES OF ALJ 2224@,///<
%1H1,////////////,29X,@DATA 5  ELASTIC AND DZMPING PROPERTIES OF E-GLASS@,///<
%1H1,////////////,33X,@NOMINAL ELASTIC PROPERTIES OF SELECTED MATERIALS@,///<
```

```
C       *****LEAD-IN FOR COMPG66*****
        DIMENSION FMT2%20,6<,FNT2%20<
C       ***DATA INPUT
        COMMON RMU,DELTA,AMDA,AMDAP,AMDA1,AMDA2,EF,GEF,GF,GGF,RNUF,GNUF,
       1    EM,GEM,GM,GGM,RNUM,GNUM,RPI,VF,VM,E11S,DATA%128,8<,G66,G66S,
       2    GG66,SHAPE
        READ %5,2000< FMT2
 2000 FORMAT %20A4<
        CALL GIVEN
C       *READ GEOMETRICAL PARAMETERS RMU AND DELTA
        IDATA#1
        RPI#3.1415927
  700 READ %5,106< RMU,DELTA
  106 FORMAT %2F10.3<
        IF %RMU< 999,999,800
  800 CONTINUE
        VF#RPI/%4.0*RMU**2*DELTA<
        VM#1.0-VF
        IBEG#1
        IEND#6
        IINC#1
        DO 31 IJK#IBEG,IEND,IINC
        IF %IJK-5< 50,50,51
   50 NBEG#12*%IJK-1<&1
        NEND#NBEG&11
        NINC#1
        GO TO 52
   51 NBEG#61
        NEND#NBEG&3
        NINC#1
   52 CONTINUE
        WRITE %6,107< IDATA,RMU,DELTA,VF
  107 FORMAT %1H1,////////////,28X,@IDATA#@,I3,@      RMU#@,F7.3,
      1@      DELTA#@,F7.3,@      VF#@,F7.3,/////<
        DO 2222 LMN#1,20
 2222 FNT2%LMN<#FMT2%LMN,IJK<
```

```
      WRITE %6,FNT2<
      IF %IJK-5< 53,53,54
   53 CONTINUE
      WRITE %6,330<
  330 FORMAT %15X,14H     FREQUENCY ,14H         G66     ,14H         GG66    ,
     1    14H        GF/GM    ,14H        G66/GM   ,14H        SHAPE    ,/<
      WRITE %6,331<
  331 FORMAT %15X,14H       HERTZ    ,14H      1.E6 PSI ,
     1    14H      PER CENT ,//<
      GO TO 55
   54 WRITE %6,332<
  332 FORMAT %15X,12H         FIBER<
      WRITE %6,333<
  333 FORMAT %15X,20H  VOLUME FRACTION    ,21H                GF/GM    ,
     1    21H                G66/GM   ,21H                SHAPE    ,//<
   55 CONTINUE
      DO 30 I#NBEG,NEND,NINC
      II#I&64
      FREQ#DATA%I,1<
      EF#DATA%I,3<
      GEF#DATA%I,4<
      GF#DATA%I,5<
      GGF#DATA%I,6<
      RNUF#DATA%I,7<
      GNUF#DATA%I,8<
      EM#DATA%II,3<
      GEM#DATA%II,4<
      GM#DATA%II,5<
      GGM#DATA%II,6<
      RNUM#DATA%II,7<
      GNUM#DATA%II,8<
      AMDA#GF/GM
      AMDAP#EF/EM
      AMDA1#%AMDA-1.0</%AMDA&1.0<
      AMDA2#%AMDA*%1.0-2.0*RNUM<-%1.0-2.0*RNUF<</%AMDA&1.0-2.0*RNUF<
      ALPHA#AMDA*%3.0-4.0*RNUM&1.0</%3.0-4.0*RNUF&AMDA<
```

```
      BETA#4.0*AMDA*%1.0-RNUM</%AMDA-1.0<
      GAMMA#BETA-1.0
      CALL COMPG66
      GO TO %81,81,81,81,81,82<,IJK
   81 WRITE %6,109< FREQ,G66,GG66,AMDA,G66S,SHAPE
  109 FORMAT %15X,6E14.4<
      GO TO 83
   82 WRITE %6,110< VF,AMDA,G66S,SHAPE
  110 FORMAT%15X,E15.4,5X,3E21.4<
   83 CONTINUE
   30 CONTINUE
   31 CONTINUE
      IDATA#IDATA&1
      GO TO 700
  999 STOP
      END
C
C
C     *****SUBROUTINE GIVEN*****
C
C
C     *****SUBROUTINE COMPG66*****
      SUBROUTINE COMPG66
      COMMON RMU,DELTA,AMDA,AMDAP,AMDA1,AMDA2,EF,GEF,GF,GGF,RNUF,GNUF,
     1   EM,GEM,GM,GGM,RNUM,GNUM,RPI,VF,VM,E11S,DATA%128,8<,G66,G66S,
     2   GG66,SHAPE
      GGF#GGF/100.0
      GGM#GGM/100.0
      RNUBA#RNUF*VF&RNUM*VM
      SHAPE#10.0*%1.0&RNUBA</%12.0&1.0*RNUBA<
      A#%1.0&VF<*GF&VM*GM
      B#%1.0&VF<*GF*GGF&VM*GM*GGM
      C#GF*VM&GM*%1.0&VF<
      D#GF*VM*GGF&GM*%1.0&VF<*GGM
      BC#B*C
      AD#A*D
```

```
      IF %AMDA-60.0< 50,50,52
   52 CVF#1.0&%VF-0.4<
      GO TO 53
   50 IF %AMDA-10.0< 54,54,55
   55 CVF#1.0&0.5*%VF-0.4<
      GO TO 53
   54 CVF#1.0&0.25*%VF-0.4<
   53 CONTINUE
      G66#%GM/%C**2&D**2<<*%A*C&B*D-GGM*%B*C-A*D<<*CVF
      GG66#%%BC-AD<&GGM*%A*C&B*D<</%A*C&B*D-GGM*%B*C-A*D<<*100.0
      G66S#G66/GM
      RETURN
      END
C
C
C
C
C     *****DATA DECK FOR HEADING - COMPG66*****
C
C
%46X,@*****BORON-EPOXY A*****@,///<
%46X,@*****BORON-EPOXY B*****@,///<
%41X,@*****BORON-ALUMINUM 2024-T3*****@,///<
%45X,@*****E GLASS-EPOXY A*****@,///<
%45X,@*****E GLASS-EPOXY B*****@,///<
%30X,@*****LONGITUDINAL IN-PLANE SHEAR MODULUS G66/GM*****@,///<
%1H1,////////////,31X,@DATA 1  ELASTIC AND DAMPING PROPERTIES OF BORON@,///<
%1H1,////////////,30X,@DATA 2  ELASTIC AND DAMPING PROPERTIES OF EPOXY A@,///<
%1H1,////////////,30X,@DATA 3  ELASTIC AND DAMPING PROPERTIES OF EPOXY B@,///<
%1H1,////////////,30X,@DATA 4  ELASTIC AND DAMPING PROPERTIES OF ALU 2224@,///<
%1H1,////////////,29X,@DATA 5  ELASTIC AND DAMPING PROPERTIES OF E-GLASS@,///<
%1H1,////////////,33X,@NOMINAL ELASTIC PROPERTIES OF SELECTED MATERIALS@,///<
```

```
C       *****LEAD-IN FOR COMPD11*****
        DIMENSION FMT2%20,6<,FNT2%20<
        COMMON RMU,DELTA,AMDA,AMDAP,AMDA1,AMDA2,EF,GEF,GF,GGF,RNU=,GNU=,
       1    EM,GEM,GM,GGM,RNUM,GNUM,RPI,VF,VM,E11S,DATA%128,8<,D11S,GD11,
       2    D11SM
C       ***DATA INPUT
        READ %5,2000< FMT2
 2000 FORMAT %20A4<
        CALL GIVEN
C       *READ GEOMETRICAL PARAMETERS RMU AND DELTA
        IDATA#1
        RPI#3.1415927
  700 READ %5,106< RMU,DELTA
  106 FORMAT %2F10.3<
        IF %RMU< 999,999,800
  800 CONTINUE
        VF#RPI/%4.0*RMU**2*DELTA<
        VM#1.0-VF
        IBEG#1
        IEND#6
        IINC#1
        DO 31 IJK#IBEG,IEND,IINC
        IF %IJK-5< 50,50,51
   50 NBEG#12*%IJK-1<&1
        NEND#NBEG&11
        NINC#1
        GO TO 52
   51 NBEG#61
        NEND#NBEG&3
   52 CONTINUE
        WRITE %6,107< IDATA,RMU,DELTA,VF
  107 FORMAT %1H1,////////////,28X,@IDATA#@,I3,@      RMU#@,F7.3,
      1@      DELTA#@,F7.3,@      VF#@,F7.3,////<
        DO 2222 LMN#1,20
 2222 FNT2%LMN<#FMT2%LMN,IJK<
        WRITE %6,FNT2<
```

```
      IF %IJK-5< 53,53,54
   53 CONTINUE
      WRITE %6,330<
  330 FORMAT %15X,13H   FREQUENCY ,18H            D11S    ,
     1    18H            GD11    ,18H          EF/EM    ,
     2    18H          D11/D11M ,//<
      WRITE %6,331<
  331 FORMAT %15X,13H     HERTZ    ,18H          1.E6 PSI ,
     1    18H          PER CENT ,///<
      GO TO 55
   54 WRITE %6,332<
  332 FORMAT %27X,20H        FIBER         <
      WRITE %6,333<
  333 FORMAT %27X,20H  VOLUME FRACTION    ,20H          EF/EM        ,
     1    20H         D11/D11M     ,///<
   55 CONTINUE
      DO 30 I#NBEG,NEND,NINC
      II#I&64
      FREQ#DATA%I,1<
      EF#DATA%I,3<
      GEF#DATA%I,4<
      GF#DATA%I,5<
      GGF#DATA%I,6<
      RNUF#DATA%I,7<
      GNUF#DATA%I,8<
      EM#DATA%II,3<
      GEM#DATA%II,4<
      GM#DATA%II,5<
      GGM#DATA%II,6<
      RNUM#DATA%II,7<
      GNUM#DATA%II,8<
      AMDA#GF/GM
      AMDAP#EF/EM
      AMDA1#%AMDA-1.0</%AMDA&1.0<
      AMDA2#%AMDA*%1.0-2.0*RNUM<-%1.0-2.0*RNUF<</%AMDA&1.0-2.0*RNUF<
      ALPHA#AMDA*%3.0-4.0*RNUM&1.0</%3.0-4.0*RNUF&AMDA<
```

```
      BETA#4.0*AMDA*%1.0-RNUM</%AMDA-1.0<
      GAMMA#BETA-1.0
      CALL D1GD1
      GO TO %81,81,81,81,81,82<,IJK
   81 WRITE %6,109< FREQ,D11S,GD11,AMDAP,D11SM
  109 FORMAT %15X,E13.4,4E18.4<
      GO TO 83
   82 WRITE %6,110< VF,AMDAP,D11SM
  110 FORMAT %32X,F7.3,11X,E13.4,8X,E13.4<
   83 CONTINUE
   30 CONTINUE
   31 CONTINUE
      IDATA#IDATA&1
      GO TO 700
  999 STOP
      END
C
C
C     *****SUBROUTINE GIVEN*****
C
C
C     ***SUBROUTINE D1GD1***
      SUBROUTINE D1GD1
      COMMON RMU,DELTA,AMDA,AMDAP,AMDA1,AMDA2,EF,GEF,GF,GGF,RNUF,GNUF,
     1   EM,GEM,GM,GGM,RNUM,GNUM,RPI,VF,VM,E11S,DATA%128,8<,D11S,GD11,
     2   D11SM
      D11S#EM&%EF-EM<*3.0*RPI/%16.0*RMU**4*DELTA**3<
      GD11#%%EF*GEF-EM*GEM<*RPI/32.0&EM*GEM*RMU**4*DELTA**3/6.0</
     1%%EF-EM<*RPI/32.0&EM*RMU**4*DELTA**3/6.0<
      D11SM#D11S/EM
      RETURN
      END
C
C
C     *****DATA DECK FOR HEADING- COMPD11*****
C
```

```
C
%46X,@*****BORON-EPOXY A*****@,///<
%46X,@*****BORON-EPOXY B*****@,///<
%41X,@*****BORON-ALUMINUM 2024-T3*****@,///<
%45X,@*****E GLASS-EPOXY A*****@,///<
%45X,@*****E GLASS-EPOXY B*****@,///<
%31X,@*****LONGITUDINAL FLEXURAL STIFFNESS D11/D11M***@,///<
%1H1,////////////,31X,@DATA 1  ELASTIC AND DAMPING PROPERTIES OF BORON@,///<
%1H1,////////////,30X,@DATA 2  ELASTIC AND DAMPING PROPERTIES OF EPOXY A@,///<
%1H1,////////////,30X,@DATA 3  ELASTIC AND DAMPING PROPERTIES OF EPOXY B@,///<
%1H1,////////////,30X,@DATA 4  ELASTIC AND DAMPING PROPERTIES OF ALU 2224@,///<
%1H1,////////////,29X,@DATA 5  ELASTIC AND DAMPING PROPERTIES OF E-G_ASS@,///<
%1H1,////////////,33X,@NOMINAL ELASTIC PROPERTIES OF SELECTED MATERIALS@,///<
```

```
C       *****LEAD-IN FOR COMPD12*****
        DIMENSION FMT2%20,6<,FNT2%20<
        COMMON RMU,DELTA,AMDA,AMDAP,AMDA1,AMDA2,EF,GEF,GF,GGF,RNUF,GNUF,
       1    EM,GEM,GM,GGM,RNUM,GNUM,RPI,VF,VM,E11S,DATA%128,8<,D11S,GD11,
       2    D11SM,D12S,D12SM,GD12
C       ***DATA INPUT***
        READ %5,2000< FMT2
 2000 FORMAT %20A4<
        CALL GIVEN
C       *READ GEOMETRICAL PARAMETERS RMU AND DELTA
        IDATA#1
        RPI#3.1415927
  700 READ %5,106< RMU,DELTA
  106 FORMAT %2F10.3<
        IF %RMU< 999,999,800
  800 CONTINUE
        VF#RPI/%4.0*RMU**2*DELTA<
        VM#1.0-VF
        IBEG#1
        IEND#6
        IINC#1
        DO 31 IJK#IBEG,IEND,IINC
        IF %IJK-5< 50,50,51
   50 NBEG#12*%IJK-1<&1
        NEND#NBEG&11
        NINC#1
        GO TO 52
   51 NBEG#61
        NEND#NBEG&3
        NINC#1
   52 CONTINUE
        WRITE %6,107< IDATA,RMU,DELTA,VF
  107 FORMAT %1H1,/////////////,28X,@IDATA#@,I3,@      RMU#@,F7.3,
      1@      DELTA#@,F7.3,@      VF#@,F7.3,////<
        DO 2222 LMN#1,20
 2222 FNT2%LMN<#FMT2%LMN,IJK<
```

```
      WRITE %6,FNT2<
      IF %IJK-5< 53,53,54
   53 CONTINUE
      WRITE %6,330<
  330 FORMAT %15X,13H   FREQUENCY ,18H            D12S    ,
     1    18H            GD12    ,18H          EF/EM    ,
     2    18H          D12/D12M ,//<
      WRITE %6,331<
  331 FORMAT %15X,13H      HERTZ    ,18H          1.E6 PSI ,
     1    18H          PER CENT ,///<
      GO TO 55
   54 WRITE %6,332<
  332 FORMAT %27X,20H        FIBER         <
      WRITE %6,333<
  333 FORMAT %27X,20H  VOLUME FRACTION    ,20H          EF/EM        ,
     1    20H         D12/D12M     ,///<
   55 CONTINUE
      DO 30 I#NBEG,NEND,NINC
      II#I&64
      FREQ#DATA%I,1<
      EF#DATA%I,3<
      GEF#DATA%I,4<
      GF#DATA%I,5<
      GGF#DATA%I,6<
      RNUF#DATA%I,7<
      GNUF#DATA%I,8<
      EM#DATA%II,3<
      GEM#DATA%II,4<
      GM#DATA%II,5<
      GGM#DATA%II,6<
      RNUM#DATA%II,7<
      GNUM#DATA%II,8<
      AMDA#GF/GM
      AMDAP#EF/EM
      AMDA1#%AMDA-1.0</%AMDA&1.0<
      AMDA2#%AMDA*%1.0-2.0*RNUM<-%1.0-2.0*RNUF<</%AMDA&1.0-2.0*RNUF<
```

```
      ALPHA#AMDA*%3.0-4.0*RNUM&1.0</%3.0-4.0*RNUF&AMDA<
      BETA#4.0*AMDA*%1.0-RNUM</%AMDA-1.0<
      GAMMA#BETA-1.0
      CALL D12GD
      GO TO %81,81,81,81,81,82<,IJK
   81 WRITE %6,109< FREQ,D12S,GD12,AMDAP,D12SM
  109 FORMAT %15X,E13.4,4E18.4<
      GO TO 83
   82 WRITE %6,110< VF,AMDAP,D12SM
  110 FORMAT %32X,F7.3,11X,E13.4,8X,E13.4<
   83 CONTINUE
   30 CONTINUE
   31 CONTINUE
      IDATA#IDATA&1
      GO TO 700
  999 STOP
      END
C
C
C     *****SUBROUTINE GIVEN*****
C
C
C     ***SUBROUTINE D12GD***
      SUBROUTINE D12GD
      EXTERNAL FREAL,FIMAG
      COMMON RMU,DELTA,AMDA,AMDAP,AMDA1,AMDA2,EF,GEF,GF,GGF,RNUF,GNUF,
     1    EM,GEM,GM,GGM,RNUM,GNUM,RPI,VF,VM,E11S,DATA%128,8<,D11S,GD11,
     2    D11SM,D12S,D12SM,GD12
      GEF#GEF/100.0
      GNUF#GNUF/100.0
      GEM#GEM/100.0
      GNUM#GNUM/100.0
      AMDAD#%1.0-RNUM**2*%1.0-GNUM**2<<**2&%2.0*RNUM**2*GNUM<**2
      AMDAR#%%1.0-GEM*GNUM<-%1.0&GEM*GNUM<*RNUM**2*%1.0&GNUM**2<</AMDAD
      AMDAI#%%GEM&GNUM<&%GNUM-GEM<*RNUM**2*%1.0&GNUM**2<</AMDAD
      CALL QG5%0.0,1.0,FREAL,FR<
```

```
      CALL  QG5%0.0,1.0,FIMAG,FI<
      D12S#3.0*EM/%%RMU*DELTA<**3<*%FR-GEM*FI&%%RMU*DELTA<**3-1.0<
     1    *RNUM*AMDAR/3.0<
      D12SI#3.0*EM/%%RMU*DELTA<**3<*%GEM*FR&FI&%%RMU*DELTA<**3-1.0<
     1    *RNUM*AMDAI/3.0<
      GD12#D12SI/D12S
       GD12#GD12*100.0
      D12SM#D12S/EM
      RETURN
      END
C
C
C     ***FUNCTION FREAL%X<
      FUNCTION FREAL%X<
      COMMON RMU,DELTA,AMDA,AMDAP,AMDA1,AMDA2,EF,GEF,GF,GGF,RNUF,GNUF,
     1    EM,GEM,GM,GGM,RNUM,GNUM,RPI,VF,VM,E11S,DATA%128,8<,D11S,GD11,
     2    D11SM,D12S,D12SM,GD12
      Y#1.0-X**2
      YY#SQRT%Y<
      A#EM&%EF-EM<*YY/RMU
      B#EM*GEM&%EF*GEF-EM*GEM<*Y/RMU
      R#RMU*EF*EM*%1.0-GEF*GEM<
      RR#RMU*EF*EM*%GEF&GEM<
      S#RMU*EF-%EF-EM<*YY
      SS#RMU*EF*GEF-%EF*GEF-EM*GEM<*YY
      C#%R*S&RR*SS</%S**2&SS**2<
      D#%RR*S-R*SS</%S**2&SS**2<
      P#RNUM&%RNUF-RNUM<*YY/RMU
      Q#RNUM*GNUM&%RNUF*GNUF-RNUM*GNUM<*YY/RMU
      T#%A*C-B*D<*P-%A*D&B*C<*Q
      TT#%A*D&B*C<*P&%A*C-B*D<*Q
      U#FM*%A-%P**2-Q**2<*C&D*P*Q-GEM*%B-%P**2-Q**2<*D-2.0*C*P*Q<<
      UU#EM*%B-%P**2-Q**2<*D-2.0*C*P*Q&GEM*%A-%P**2-Q**2<*C&D*P*Q<<
      FREAL#%%T*U&TT*UU</%U**2&UU**2<<*X**2
      RETURN
      END
```

```
C
C
C       *FUNCTION FIMAG%X<
        FUNCTION FIMAG%X<
        COMMON RMU,DELTA,AMDA,AMDAP,AMDA1,AMDA2,EF,GEF,GF,GGF,RNUF,GNUF,
       1    EM,GEM,GM,GGM,RNUM,GNUM,RPI,VF,VM,E11S,DATA%128,8<,D11S,GD11,
       2    D11SM,D12S,D12SM,GD12
        Y#1.0-X**2
        YY#SQRT%Y<
        A#EM&%EF-EM<*YY/RMU
        B#EM*GEM&%EF*GEF-EM*GEM<*Y/RMU
        R#RMU*EF*EM*%1.0-GEF*GEM<
        RR#RMU*EF*EM*%GEF&GEM<
        S#RMU*EF-%EF-EM<*YY
        SS#RMU*EF*GEF-%EF*GEF-EM*GEM<*YY
        C#%R*S&RR*SS<//%S**2&SS**2<
        D#%RR*S-R*SS<//%S**2&SS**2<
        P#RNUM&%RNUF-RNUM<*YY/RMU
        Q#RNUM*GNUM&%RNUF*GNUF-RNUM*GNUM<*YY/RMU
        T#%A*C-B*D<*P-%A*D&B*C<*Q
        TT#%A*D&B*C<*P&%A*C-B*D<*Q
        U#EM*%A-%P**2-Q**2<*C&D*P*Q-GEM*%B-%P**2-Q**2<*D-2.0*C*P*Q<<
        UU#EM*%B-%P**2-Q**2<*D-2.0*C*P*Q&GEM*%A-%P**2-Q**2<*C&D*P*Q<<
        FIMAG#%%TT*U-T*UU<//%U**2&UU**2<<*X**2
        RETURN
        END
C
C
C       ***SUBROUTINE QG5%XL,XU,FCT,Y<***
        SUBROUTINE QG5%XL,XU,FCT,Y<
        A#0.5*%XU&XL<
        B#XU-XL
        C#.4530899*B
        Y#.1184634*%FCT%A&C<&FCT%A-C<<
        C#.2692347*B
        Y#Y&.2393143*%FCT%A&C<&FCT%A-C<<
```

```
      Y#B*%Y&.2844444*FCT%A<<
      RETURN
      END
C
C
C     *****DATA DECK FOR HEADING - COMPD12*****
C
C
%46X,'*****BORON-EPOXY A*****',///<
%46X,'*****BORON-EPOXY B*****',///<
%41X,'*****BORON-ALUMINUM 2024-T3*****',///<
%45X,'*****E GLASS-EPOXY A*****',///<
%45X,'*****E GLASS-EPOXY B*****',///<
%33X,'*****POISSON FLEXURAL STIFFNESS D12/D12M*****',///<
%1H1,////////////,31X,'DATA 1  ELASTIC AND DAMPING PROPERTIES OF BORON',///<
%1H1,////////////,30X,'DATA 2  ELASTIC AND DAMPING PROPERTIES OF EPOXY A',///<
%1H1,////////////,30X,'DATA 3  ELASTIC AND DAMPING PROPERTIES OF EPOXY B',///<
%1H1,////////////,30X,'DATA 4  ELASTIC AND DAMPING PROPERTIES OF ALJ 2224',///<
%1H1,////////////,29X,'DATA 5  ELASTIC AND DAMPING PROPERTIES OF E-GLASS',///<
%1H1,////////////,33X,'NOMINAL ELASTIC PROPERTIES OF SELECTED MATERIALS',///<
```

```
C       *****LEAD-IN FOR COMPD22*****
        DIMENSION FMT2%20,6<,FNT2%20<
        COMMON RMU,DELTA,RPI,AMDA,AMDAP,AMDA1,AMDA2,ALPHA,BETA,GAMMA,
       1    EF,GEF,GF,GGF,RNUF,GNUF,EM,GEM,GM,GGM,RNUM,GNUM,A%38<,B%38<,
       2    XI%20,20<,ETA%20,20<,IKS,ANP%19<,BNP%19<,D22S,GD22,VF,VM,D22SM,
       3    DATA%128,8<,XXX%3,3<,YYY%3,3<
C       ***DATA INPUT
        READ %5,2000< FMT2
 2000   FORMAT %20A4<
        CALL GIVEN
C       *READ GEOMETRICAL PARAMETERS RMU AND DELTA
        IDATA#1
        RPI#3.1415927
  700   READ %5,106< RMU,DELTA
  106   FORMAT %2F10.3<
        IF %RMU< 999,999,800
  800   CONTINUE
        CALL PT400
        CALL PT9
        CALL TRND2
        VF#RPI/%4.0*RMU**2*DELTA<
        VM#1.0-VF
        IBEG#1
        IBEG#3
        IEND#4
        IINC#1
        DO 31 IJK#IBEG,IEND,IINC
        IF %IJK-5< 50,50,51
   50   NBEG#12*%IJK-1<&1
        NEND#NBEG&11
        NINC#1
        GO TO 52
   51   NBEG#61
        NEND#NBEG&3
        NINC#1
   52   CONTINUE
```

```
      WRITE %6,107< IDATA,RMU,DELTA,VF
  107 FORMAT %1H1,////////////,28X,@IDATA#@,I3,@      RMU#@,F7.3,
     1@      DELTA#@,F7.3,@      VF#@,F7.3,////<
      DO 2222 LMN#1,20
 2222 FNT2%LMN<#FMT2%LMN,IJK<
      WRITE %6,FNT2<
      IF %IJK-5< 53,53,54
   53 CONTINUE
      WRITE %6,330<
  330 FORMAT %15X,13H    FREQUENCY ,13H       D22S    ,13H      GD22     ,
     113H      EF/EM    ,13H     D22/D22M ,7H    IKS ,//<
      WRITE %6,331<
  331 FORMAT %15X,13H      HERTZ    ,13H     1.E6 PSI ,13H     PER CENT ,///<
      GO TO 55
   54 WRITE %6,332<
  332 FORMAT %27X,20H         FIBER          <
      WRITE %6,333<
  333 FORMAT %27X,20H  VOLUME FRACTION    ,20H         EF/EM          ,
     1    20H       D22/D22M       ,///<
   55 CONTINUE
      DO 30 I#NBEG,NEND,NINC
      II#I&64
      FREQ#DATA%I,1<
      EF#DATA%I,3<
      GEF#DATA%I,4<
      GF#DATA%I,5<
      GGF#DATA%I,6<
      RNUF#DATA%I,7<
      GNUF#DATA%I,8<
      EM#DATA%II,3<
      GEM#DATA%II,4<
      GM#DATA%II,5<
      GGM#DATA%II,6<
      RNUM#DATA%II,7<
      GNUM#DATA%II,8<
      AMDA#GF/GM
```

```
      AMDAP#EF/EM
      AMDA1#%AMDA-1.0</%AMDA&1.0<
      AMDA2#%AMDA*%1.0-2.0*RNUM<-%1.0-2.0*RNUF<</%AMDA&1.0-2.0*RNUF<
      ALPHA#AMDA*%3.0-4.0*RNUM&1.0</%3.0-4.0*RNUF&AMDA<
      BETA#4.0*AMDA*%1.0-RNUM</%AMDA-1.0<
      GAMMA#BETA-1.0
      CALL COMPD22
      GO TO %81,81,81,81,81,82<,IJK
   81 WRITE %6,109< FREQ,D22S,GD22,AMDAP,D22SM,IKS
  109 FORMAT %15X,5E13.4,I5<
      GO TO 83
   82 WRITE %6,110< VF,AMDAP,D22SM
  110 FORMAT %32X,F7.3,11X,E13.4,8X,E13.4<
   83 CONTINUE
   30 CONTINUE
   31 CONTINUE
      IDATA#IDATA&1
      GO TO 700
  999 STOP
      END
C
C
C     *****SUBROUTINE GIVEN*****
C
C
C     *****SUBROUTINE GIVEN*****
C
C
C     ***SUBROUTINE PT400***
      SUBROUTINE PT400
      COMMON RMU,DELTA,RPI,AMDA,AMDAP,AMDA1,AMDA2,ALPHA,BETA,GAMMA,
     1   EF,GEF,GF,GGF,RNUF,GNUF,EM,GEM,GM,GGM,RNUM,GNUM,A%38<,B%38<,
     2   XI%20,20<,ETA%20,20<,IKS,ANP%19<,BNP%19<,D22S,GD22,VF,VM,D22SM,
     3   DATA%128,8<,XXX%3,3<,YYY%3,3<
      H#RMU/20.0
      V#RMU*DELTA/20.0
```

```
      DO 30 I#1,20
      RI#I
      DO 31 J#1,20
      RJ#J
      XI%I,J<#%RJ-0.5<*H
      ETA%I,J<#RMU*DELTA-%RI-0.5<*V
   31 CONTINUE
   30 CONTINUE
      RETURN
      END
C
C
C     *****SUBROUTINE COMPD22*****
      SUBROUTINE COMPD22
      DIMENSION CCC%78,38<,CC%38,38<,C%38,38<,BB%78<
      COMMON RMU,DELTA,RPI,AMDA,AMDAP,AMDA1,AMDA2,ALPHA,BETA,GAMMA,
     1    EF,GEF,GF,GGF,RNUF,GNUF,EM,GEM,GM,GGM,RNUM,GNUM,A%38<,B%38<,
     2    XI%20,20<,ETA%20,20<,IKS,ANP%19<,BNP%19<,D22S,GD22,VF,VM,D22SM,
     3    DATA%128,8<,XXX%3,3<,YYY%3,3<
      V#RMU*DELTA/20.0
      H#RMU/20.0
      AREA#V*H
      Y#RMU*DELTA
      DO 30 I#1,20
      II#I&20
      RI#I
      X#RI*H
      ROH#SQRT%X**2&Y**2<
      TETA#ATAN%Y/X<
      BB%I<#X/RMU
      BB%II<#0.0
      DO 33 J#1,19
      N#2*J&1
      JJ#J&19
      RN#N
      COSNT#COS%RN*TETA<
```

```
      COSM2#COS%%RN-2.0<*TETA<
      COSP2#COS%%RN&2.0<*TETA<
      SINM2#SIN%%RN-2.0<*TETA<
      SINP2#SIN%%RN&2.0<*TETA<
      ROHN#ROH**N
      ROHM2#ROHN/%ROH*ROH<
      ROHP2#ROHN*ROH*ROH
      P1#ROHM2
      P2#-2.0/%GAMMA*ROHN<
      P3#%RN/ROHN-%RN&1.0</ROHP2</GAMMA
      CCC%I,J<#RN*%RN-1.0<*%P1*COSM2&P2*COSNT&P3*COSP2<
      Q1#RN*ROHN
      Q2#2.0*%ROHN-%RN-1.0</%ROHN*GAMMA<<
      Q3#%%GAMMA*%1.0-ALPHA<-%RN*RN-1.0<</ROHP2&RN*%RN-1.0</ROHN</GAMMA
      CCC%I,JJ<#%RN&1.0<*%Q1*COSM2&Q2*COSNT&Q3*COSP2<
      R1#ROHM2
      R2#-P3
      CCC%II,J<#RN*%RN-1.0<*%R1*SINM2&R2*SINP2<
      S1#ROHN*RN
      S2#-Q3
      CCC%II,JJ<#%RN&1.0<*%S1*SINM2&S2*SINP2<
   33 CONTINUE
   30 CONTINUE
      X#RMU
      DO 31 I#41,59
      II#I&19
      RI#I-40
      Y#RMU*DELTA-RI*V
      ROH#SQRT%X**2&Y**2<
      TETA#ATAN%Y/X<
      BB%I<#0.0
      BB%II<#0.0
      DO 34 J#1,19
      JJ#J&19
      N#2*J&1
      RN#N
```

```
      COSNT#COS%RN*TETA<
      COSM2#COS%%RN-2.0<*TETA<
      COSP2#COS%%RN&2.0<*TETA<
      SINM2#SIN%%RN-2.0<*TETA<
      SINP2#SIN%%RN&2.0<*TETA<
      ROHN#ROH**N
      ROHM2#ROHN/%ROH*ROH<
      ROHP2#ROHN*ROH*ROH
      P1#-ROHM2
      P2#-2.0/%ROHN*GAMMA<
      P3#-%RN/ROHN-%RN&1.0</ROHP2</GAMMA
      CCC%I,J<#RN*%RN-1.0<*%P1*COSM2&P2*COSNT&P3*COSP2<
      Q1#-RN*ROHN
      Q2#2.0*%ROHN-%RN-1.0</%ROHN*GAMMA<<
      Q3#-%%GAMMA*%1.0-ALPHA<-%RN*RN-1.0<</ROHP2&RN*%RN-1.0</ROHN</GAMMA
      CCC%I,JJ<#%RN&1.0<*%Q1*COSM2&Q2*COSNT&Q3*COSP2<
      R1#-P1
      R2#P3
      CCC%II,J<#RN*%RN-1.0<*%R1*SINM2&R2*SINP2<
      S1#ROHN*RN
      S2#Q3
      CCC%II,JJ<#%RN&1.0<*%S1*SINM2&S2*SINP2<
   34 CONTINUE
   31 CONTINUE
      CALL ATA%CCC,C<
      CALL ATB%CCC,BB,B<
      CALL SIMQ%C,B,38,KS<
      IKS#KS
C     ***COMPUTE A%38<,ANP%19<,BNP%19<.
      DO 32 I#1,19
      N#2*I&1
      II#I&19
      RN#N
      A%I<#%BETA/GAMMA<*B%I<&%%RN&1.0</RN<*%BETA/GAMMA-ALPHA<*B%II<
      A%II<#ALPHA*B%II<
      ANP%I<#-%RN-1.0<*B%I</GAMMA&%%1.0-ALPHA<-%RN*RN-1.0</GAMMA<
```

```
     1    *B%II</RN
          BNP%I<#%RN*B%I<&%RN&1.0<*B%II<</GAMMA
     32 CONTINUE
          CALL D2GD2
          RETURN
          END
C
C
          SUBROUTINE D2GD2
          EXTERNAL FUNC
          COMMON RMU,DELTA,RPI,AMDA,AMDAP,AMDA1,AMDA2,ALPHA,BETA,GAMMA,
     1    EF,GEF,GF,GGF,RNUF,GNUF,EM,GEM,GM,GGM,RNUM,GNUM,A%38<,B%38<,
     2    XI%20,20<,ETA%20,20<,IKS,ANP%19<,BNP%19<,D22S,GD22,VF,VM,D22SM,
     3    DATA%128,8<,XXX%3,3<,YYY%3,3<
          XL#ATAN%DELTA<
          XU#0.5*RPI
          CALL SQG5%XL,XU,FUNC,FUN<
          D22S#%RMU*RMU</%3.0*FUN<
          D22SM#D22S/EM
          AREA#%RMU**2<*DELTA/400.0
          SUMSF#0.0
          SUMSM#0.0
          SUMTF#0.0
          SUMTM#0.0
          DO 30 I#1,19
          DO 31 J#1,19
          CALL STRES%XI%I,J<,ETA%I,J<,SIGX,SIGY,TAUXY<
          ROH#SQRT%XI%I,J<**2&ETA%I,J<**2<
          IF %ROH-1.0< 50,50,51
     50 CONTINUE
          TERM1#%1.0-RNUF<*%SIGX**2&SIGY**2<-2.0*RNUF*SIGX*SIGY
          SUMSF#SUMSF&TERM1
          TERM2#TAUXY*TAUXY
          SUMTF#SUMTF&TERM2
          GO TO 52
     51 CONTINUE
```

```
      TERM3#%1.0-RNUM<**%SIGX**2&SIGY**2<-2.0*RNUM*SIGX*SIGY
      SUMSM#SUMSM&TERM3
      TERM4#TAUXY*TAUXY
      SUMTM#SUMTM&TERM4
   52 CONTINUE
   31 CONTINUE
   30 CONTINUE
      USF#SUMSF/%4.0*GF<
      UTF#SUMTF/%2.0*GF<
      USM#SUMSM/%4.0*GM<
      UTM#SUMTM/%2.0*GM<
      UDF#2.0*RPI*%GEF*USF&GGF*UTF<
      UDM#2.0*RPI*%GEM*USM&GGM*UTM<
      U#USF&USM&UTF&UTM
      GD22#%UDF&UDM</%2.0*RPI*U<
      RETURN
      END
C
C
C     ***FUNCTION FUNC%Z<***
      FUNCTION FUNC%Z<
      COMMON RMU,DELTA,RPI,AMDA,AMDAP,AMDA1,AMDA2,ALPHA,BETA,GAMMA,
     1    EF,GEF,GF,GGF,RNUF,GNUF,EM,GEM,GM,GGM,RNUM,GNUM,A%38<,B%38<,
     2    XI%20,20<,ETA%20,20<,IKS,ANP%19<,BNP%19<,D22S,GD22,VF,VM,D22SM,
     3    DATA%128,8<,XXX%3,3<,YYY%3,3<
      SUM#0.0
      DO 30 I#1,19
      II#I&19
      N#2*I&1
      RN#N
      ROH#RMU*DELTA/SIN%Z<
      COSM2#COS%%RN-2.0<*Z<
      COSNT#COS%RN*Z<
      COSM1#COS%%RN-1.0<*Z<
      COSP1#COS%%RN&1.0<*Z<
      COSP2#COS%%RN&2.0<*Z<
```

```
      ROHN#ROH**N
      ROHM2#ROHN/%ROH*ROH<
      ROHP2#ROHN*ROH*ROH
      P1#RN*%RN-1.0<*ROHM2*COSM2
      P2#RN*ROHN*%RN*COSM2-COSNT&2.0*COS%Z<*COSM1<
     1    &2.0*%1.0-2.0*RNUM<*%RN&1.0<*ROHN*COSNT
      P3#%RN*%RN&1.0</ROHP2<*COSP2
      P4#%RN/ROHN<*%RN*COSP2&COSNT-2.0*COS%Z<*COSP1<
     1    -2.0*%1.0-2.0*RNUM<*%RN-1.0<*COSNT/ROHN
      TERM#B%I<*P1&B%II<*P2&ANP%I<*P3&BNP%I<*P4
      SUM#SUM&TERM
   30 CONTINUE
      FUNC#%COS%Z</%%SIN%Z<<**3<<*SUM
      FUNC#FUNC*%%RMU*DELTA<**2</%2.0*GM<
      RETURN
      END
C
C
C
C     ***SUBROUTINE SQG5%XL,XU,FCT,Y<***
      SUBROUTINE SQG5%XL,XU,FCT,Y<
      A#0.5*%XU&XL<
      B#XU-XL
      C#.4530899*B
      Y#.1184634*%FCT%A&C<&FCT%A-C<<
      C#.2692347*B
      Y#Y&.2393143*%FCT%A&C<&FCT%A-C<<
      Y#B*%Y&.2844444*FCT%A<<
      RETURN
      END
C
C
C
C     ***SUBROUTINE STRES%X,Y,SIGX,SIGY,TAUXY<***
      SUBROUTINE STRES%X,Y,SIGX,SIGY,TAUXY<
      COMMON RMU,DELTA,RPI,AMDA,AMDAP,AMDA1,AMDA2,ALPHA,BETA,GAMMA,
     1    EF,GEF,GF,GGF,RNUF,GNUF,EM,GEM,GM,GGM,RNUM,GNUM,A%38<,B%38<,
```

```
     2    XI%20,20<,ETA%20,20<,IKS,ANP%19<,BNP%19<,D22S,GD22,VF,VM,D22SM,
     3    DATA%128,8<,XXX%3,3<,YYY%3,3<
      ROH#SQRT%X**2&Y**2<
      IF %X< 49,50,51
   49 TETA#RPI&ATAN%Y/X<
      GO TO 52
   50 TETA#0.5*RPI
      GO TO 52
   51 TETA#ATAN%Y/X<
   52 CONTINUE
      IF %ROH< 53,53,54
   53 CONTINUE
      SIGX#0.0
      SIGY#0.0
      TAUXY#0.0
      RETURN
   54 CONTINUE
      IF %ROH-1.0< 55,55,56
   55 CONTINUE
      SUM1#0.0
      SUM2#0.0
      SUM3#0.0
      DO 30 I#1,19
      N#2*I&1
      RN#N
      II#I&19
      ROHN#ROH**N
      ROHM2#ROHN/%ROH*ROH<
      ROHP2#ROHN*ROH*ROH
      COSNT#COS%RN*TETA<
      COSM2#COS%%RN-2.0<*TETA<
      COSP2#COS%%RN&2.0<*TETA<
      P1#RN*%RN-1.0<*ROHM2*COSM2
      P2#%RN&1.0<*ROHN*%RN*COSM2-2.0*COSNT<
      TERM1#-%A%I<*P1&A%II<*P2<
      TERM2#A%I<*P1&A%II<*%RN&1.0<*ROHN*%RN*COSM2&2.0*COSNT<
```

```
      SUM1#SUM1&TERM1
      SUM2#SUM2&TERM2
      TERM3#%A%I<*RN*%RN-1.0<*ROHM2&A%II<*RN*%RN&1.0<*ROHN<*
     1    SIN%%RN-2.0<*TETA<
      SUM3#SUM3&TERM3
   30 CONTINUE
      SIGX#SUM1
      SIGY#SUM2
      TAUXY#SUM3
      RETURN
   56 CONTINUE
      SUM1#0.0
      SUM2#0.0
      SUM3#0.0
      DO 31 I#1,19
      N#2*I&1
      II#I&19
      J#I
      RN#N
      ROHN#ROH**N
      ROHM2#ROHN/%ROH*ROH<
      ROHP2#ROHN*ROH*ROH
      COSNT#COS%RN*TETA<
      COSP2#COS%%RN&2.0<*TETA<
      COSM2#COS%%RN-2.0<*TETA<
      P1#RN*%RN-1.0<*ROHM2*COSM2
      P2#%RN&1.0<*ROHN*%RN*COSM2-2.0*COSNT<
      P3#RN*%RN&1.0<*COSP2/ROHP2
      P4#%RN-1.0<*%RN*COSP2&2.0*COSNT</ROHN
      TERM1#-%B%I<*P1&B%II<*P2&ANP%J<*P3&BNP%J<*P4<
      SUM1#SUM1&TERM1
      Q1#P1
      Q2#%RN&1.0<*ROHN*%RN*COSM2&2.0*COSNT<
      Q3#P3
      Q4#%RN-1.0<*%RN*COSP2-2.0*COSNT</ROHN
      TERM2#B%I<*Q1&B%II<*Q2&ANP%J<*Q3&BNP%J<*Q4
```

```
      SUM2#SUM2&TERM2
      R1#RN*%RN-1.0<*ROHM2
      R2#RN*%RN&1.0<*ROHN
      R3#RN*%RN&1.0</ROHP2
      R4#RN*%RN-1.0</ROHN
      TERM3#%B%I<*R1&B%II<*R2<*SIN%%RN-2.0<*TETA<
     1    -%ANP%J<*R3&BNP%J<*R4<*SIN%%RN&2.0<*TETA<
      SUM3#SUM3&TERM3
   31 CONTINUE
      SIGX#SUM1
      SIGY#SUM2
      TAUXY#SUM3
      RETURN
      END
C
C
C     ***SUBROUTINE ATA%A,B<***
      SUBROUTINE ATA%A,B<
      DIMENSION A%78,38<,B%38,38<
      DO 30 I#1,38
      DO 31 J#1,38
      B%I,J<#0.0
      DO 32 M#1,78
      B%I,J<#B%I,J<&A%M,I<*A%M,J<
   32 CONTINUE
   31 CONTINUE
   30 CONTINUE
      RETURN
      END
C     ***SUBROUTINE ATB%A,B,C<***
      SUBROUTINE ATB%A,B,C<
      DIMENSION A%78,38<,B%78<,C%38<
      DO 30 I#1,38
      C%I<#0.0
      DO 31 J#1,78
      C%I<#C%I<&A%J,I<*B%J<
```

```
   31 CONTINUE
   30 CONTINUE
      RETURN
      END
C
C
C     ***SUBROUTINE PT9***
      SUBROUTINE PT9
      COMMON RMU,DELTA,RPI,AMDA,AMDAP,AMDA1,AMDA2,ALPHA,BETA,GAMMA,
     1   EF,GEF,GF,GGF,RNUF,GNUF,EM,GEM,GM,GGM,RNUM,GNUM,A%38<,B%38<,
     2   XI%20,20<,ETA%20,20<,IKS,ANP%19<,BNP%19<,D22S,GD22,VF,VM,D22SM,
     3   DATA%128,8<,XXX%3,3<,YYY%3,3<
      DO 30 I#1,3
      RI#I
      DO 31 J#1,3
      RJ#J
      XXX%I,J<#%RJ-1.0<*RMU/2.0
      YYY%I,J<#RMU*DELTA-%RI-1.0<*RMU*DELTA/2.0
   31 CONTINUE
   30 CONTINUE
      RETURN
      END
C
C
C     *****DATA DECK FOR HEADING - COMPD22*****
C
C
%46X,@*****BORON-EPOXY A*****@,///<
%46X,@*****BORON-EPOXY B*****@,///<
%41X,@*****BORON-ALUMINUM 2024-T3*****@,///<
%45X,@*****E GLASS-EPOXY A*****@,///<
%45X,@*****E GLASS-EPOXY B*****@,///<
%33X,@*****TRANSVERSE FLEXURAL STIFFNESS D22/D22M*****@,///<
%1H1,////////////,31X,@DATA 1  ELASTIC AND DAMPING PROPERTIES OF BORON@,///<
%1H1,////////////,30X,@DATA 2  ELASTIC AND DAMPING PROPERTIES OF EPOXY A@,///<
%1H1,////////////,30X,@DATA 3  ELASTIC AND DAMPING PROPERTIES OF EPOXY B@,///<
```

```
%1H1,/////////////,30X,@DATA 4  ELASTIC AND DAMPING PROPERTIES OF ALU 2224@,///<
%1H1,/////////////,29X,@DATA 5  ELASTIC AND DAMPING PROPERTIES OF E-G_ASS@,///<
%1H1,/////////////,33X,@NOMINAL ELASTIC PROPERTIES OF SELECTE) MATERIALS@,///<
```

```
C       *****LEAD-IN FOR COMPD66*****
        DIMENSION FMT2%20,6<,FNT2%20<
        COMMON RMU,DELTA,AMDA,AMDA1,RPI,EF,GEF,GF,GGF,RNUF,GNUF,
       1    EM,GEM,GM,GGM,RNUM,GNUM,A%23<,B%23<,XI%20,60<,ETA%20,60<,
       2    IKS,D66S,GD66,GAMA,D66SM,DATA%128,8<
C       ***DATA INPUT
        READ %5,2000< FMT2
 2000 FORMAT %20A4<
        CALL GIVEN
C       *READ GEOMETRICAL PARAMETERS RMU AND DELTA
        IDATA#1
        RPI#3.1415927
  700 READ %5,106< RMU,DELTA
  106 FORMAT %2F10.3<
        IF %RMU< 999,999,800
  800 CONTINUE
        CALL P1200
        RTK#TK%3.0/DELTA<
        VF#RPI/%4.0*RMU**2*DELTA<
        VM#1.0-VF
        IBEG#1
        IBEG#6
        IEND#6
        IINC#1
        DO 31 IJK#IBEG,IEND,IINC
        IF %IJK-5< 50,50,51
   50 NBEG#12*%IJK-1<&1
        NEND#NBEG&11
        NINC#1
        GO TO 52
   51 NBEG#61
        NEND#NBEG&3
        NINC#1
   52 CONTINUE
        WRITE %6,107< IDATA,RMU,DELTA,VF
  107 FORMAT %1H1,////////////,28X,@IDATA#@,I3,@      RMU#@,F7.3,
```

```
    1@      DELTA#@,F7.3,@      VF#@,F7.3,////<
     DO 2222 LMN#1,20
2222 FNT2%LMN<#FMT2%LMN,IJK<
     WRITE %6,FNT2<
     IF %IJK-5< 53,53,54
  53 CONTINUE
     WRITE %6,330<
 330 FORMAT %15X,13H   FREQUENCY ,13H       D66S    ,13H       GD55    ,
    113H      GF/GM    ,13H     D66/D66M ,13H       RTK     ,7H    IKS ,/<
     WRITE %6,331<
 331 FORMAT %15X,13H      HERTZ    ,13H     1.E6 PSI ,13H     PER CENT ,///<
     GO TO 55
  54 WRITE %6,332<
 332 FORMAT %27X,20H        FIBER          <
     WRITE %6,333<
 333 FORMAT %27X,20H  VOLUME FRACTION    ,13H      GF/GM    ,
    1    13H     D66/D66M ,13H       RTK     ,///<
  55 CONTINUE
     DO 30 I#NBEG,NEND,NINC
     II#I&64
     FREQ#DATA%I,1<
     EF#DATA%I,3<
     GEF#DATA%I,4<
     GF#DATA%I,5<
     GGF#DATA%I,6<
     RNUF#DATA%I,7<
     GNUF#DATA%I,8<
     EM#DATA%II,3<
     GEM#DATA%II,4<
     GM#DATA%II,5<
     GGM#DATA%II,6<
     RNUM#DATA%II,7<
     GNUM#DATA%II,8<
     AMDA#GF/GM
     AMDAP#EF/EM
     AMDA1#%AMDA-1.0</%AMDA&1.0<
```

```
      AMDA2#%AMDA*%1.0-2.0*RNUM<-%1.0-2.0*RNUF<</%AMDA&1.0-2.0*RNUF<
      ALPHA#AMDA*%3.0-4.0*RNUM&1.0</%3.0-4.0*RNUF&AMDA<
      BETA#4.0*AMDA*%1.0-RNUM</%AMDA-1.0<
      GAMMA#BETA-1.0
      CALL COMPD66
      GO TO %81,81,81,81,81,82<,IJK
   81 WRITE %6,109< FREQ,D66S,GD66,AMDA,D66SM,RTK,IKS
  109 FORMAT %15X,6E13.4,I5<
      GO TO 83
   82 WRITE %6,110< VF,AMDA,D66SM,RTK
  110 FORMAT %32X,F7.3,8X,3E13.4<
   83 CONTINUE
   30 CONTINUE
   31 CONTINUE
      IDATA#IDATA&1
      GO TO 700
  999 STOP
      END
C
C
C     *****SUBROUTINE GIVEN*****
C
C
C     ***SUBROUTINE P1200***
      SUBROUTINE P1200
      COMMON RMU,DELTA,AMDA,AMDA1,RPI,EF,GEF,GF,GGF,RNUF,GNUF,
     1   EM,GEM,GM,GGM,RNUM,GNUM,A%23<,B%23<,XI%20,60<,ETA%20,60<,
     2   IKS,D66S,GD66,GAMA,D66SM,DATA%128,8<
      XX#RMU/20.0
      YY#RMU*DELTA/20.0
      DO 30 I#1,20
      RI#I
      DO 31 J#1,60
      RJ#J
      XI%I,J<#%RJ-0.5<*XX
      ETA%I,J<#%RMU*DELTA<-%RI-0.5<*YY
```

```
   31 CONTINUE
   30 CONTINUE
      RETURN
      END
C
C
C     *****SUBROUTINE COMPD66*****
      SUBROUTINE COMPD66
      DIMENSION DDD%49,23<,DD%23,23<,D%23,23<,BB%49<
      COMMON RMU,DELTA,AMDA,AMDA1,RPI,EF,GEF,GF,GGF,RNUF,GNUF,
     1    EM,GEM,GM,GGM,RNUM,GNUM,A%23<,B%23<,XI%20,60<,ETA%20,60<,
     2    IKS,D66S,GD66,GAMA,D66SM,DATA%128,8<
      GAMA#2.0*RMU
      V#RMU*DELTA/8.0
      H#RMU/8.0
      AREA#RMU**2*DELTA/400.0
C     ***FIRST EDGE-9 POINTS
      Y#RMU*DELTA
      DO 30 I#1,9
      RI#I
      X#%RI-1.0<*H
      ROH#SQRT%X**2&Y**2<
      IF%X< 50,50,51
   50 TETA#0.5*RPI
      GO TO 52
   51 TETA#ATAN%Y/X<
   52 CONTINUE
      BB%I<#0.5*ROH**2
      DDD%I,1<#1.0
      DDD%I,9<#0.0
      DO 31 J#2,8
      K#2*%J-1<
      RK#K
      DDD%I,J<#%ROH**K&AMDA1*ROH**%-K<<<*COS%RK*TETA<
   31 CONTINUE
      DO 32 JJ#10,23
```

```
      DDD%I,JJ<#0.0
   32 CONTINUE
   30 CONTINUE
C     ***SECOND EDGE-8POINTS X 16 EQUATIONS
      X#RMU
      DO 132 I#10,17
      RI#I
      Y#%RI-10.0<*V
      ROH#SQRT%X**2&Y**2<
      TETA#ATAN%Y/X<
      II#I&8
      BB%I<#2.0*RMU*AMDA1*ROH**%-1<*COS%TETA<
      DDD%I,1<#1.0
      DDD%I,9<#-1.0
      BB%II<# 2.0*RMU*AMDA1*ROH**%-2<*COS%2.0*TETA<
      DDD%II,1<#0.0
      DDD%II,9<#0.0
      DO 33 J#2,8
      K#2*%J-1<
      RK#K
      DDD%I,J<#%ROH**K&AMDA1*ROH**%-K<<*COS%RK*TETA<
      DDD%II,J<#RK*%ROH**%K-1<*COS%%RK-1.0<*TETA<
     1    -AMDA1*ROH**%-K-1<*COS %%RK&1.0<*TETA<<
   33 CONTINUE
      DO 34 JJ#10,23
      K#JJ-9
      RK#K
      DDD%I,JJ<#-%%-1.0<**K<**ROH**K&AMDA1*ROH**%-K<<*COS%RK*TETA<
      DDD%II,JJ<#%%-1.0<**K<*RK*%ROH**%K-1<*COS%%RK-1.0<*TETA<
     1    -AMDA1*ROH**%-K-1<*COS%%RK&1.0<*TETA<<
   34 CONTINUE
  132 CONTINUE
C     ***THIRD EDGE-16 POINTS
      Y#RMU*DELTA
      DO 35 I#26,41
      RI#I
```

```
      X#RMU&%RI-25.0<*H
      ROH#SQRT%%X-GAMA<**2&Y**2<
      IF %X-GAMA< 53,54,55
   53 TETA#RPI&ATAN%Y/%X-GAMA<<
      GO TO 56
   54 TETA#0.5*RPI
      GO TO 56
   55 TETA#ATAN%Y/%X-GAMA<<
   56 CONTINUE
      BB%I<#0.5*%X**2&Y**2<&GAMA*AMDA1*ROH**%-1<*COS%TETA<
      DDD%I,1<#0.0
      DDD%I,9<#1.0
      DO 36 J#2,8
      DDD%I,J<#0.0
   36 CONTINUE
      DO 37 JJ#10,23
      K#JJ-9
      RK#K
      DDD%I,JJ<#%ROH**K&AMDA1*ROH**%-K<<*COS%RK*TETA<
   37 CONTINUE
   35 CONTINUE
C     ***FOURTH EDGE-8POINTS
      X#3.0*RMU
      DO 38 I#42,49
      RI#I
      Y#%RI-42.0<*V
      ROH#SQRT%RMU**2&Y**2<
      TETA#ATAN%Y/RMU<
      BB%I<#0.5*%X**2&Y**2<&2.0*RMU*AMDA1*ROH**%-1<*COS%TETA<
      DDD%I,1<#0.0
      DDD%I,9<#1.0
      DO 39 J#2,8
      DDD%I,J<#0.0
   39 CONTINUE
      DO 40 JJ#10,23
      K#JJ-9
```

```
      RK#K
      DDD%I,JJ<#%ROH**K&AMDA1 *ROH* **-K<<*COS%RK*TETA<
   40 CONTINUE
   38 CONTINUE
C     ***SOLVE FOR COEFFICIENTS USING BPLS METHOD
      CALL MATAS%DDD,D<
      CALL ATB%DDD,BB,B<
      CALL SIMQ%D,B,23,KS<
      IKS#KS
C     ***COMPUTE FIBER REGION COEFFICIENTS A%23<***
      A%1<#%B%1<&0.5*%AMDA-1.0<</AMDA
      DO 42 I#2,8
      A%I<#2.0*B%I</%AMDA&1.0<
   42 CONTINUE
      A%9<#%B%9<&0.5*%AMDA-1.0<**1.0&GAMA**2<</AMDA
      A%10<#2.0*B%10</%AMDA&1.0<&AMDA1*GAMA
      DO 43 I#11,23
      A%I<#2.0*B%I</%AMDA&1.0<
   43 CONTINUE
C     ***COMPUTE D66S AND GD66
      SUM1#0.0
      SUM2#0.0
      SUM3#0.0
      DO 44 I#1,20
      DO 44 J#1,20
      CALL PSIC%XI%I,J<,ETA%I,J<,PSIP<
      CALL TXYC%XI%I,J<,ETA%I,J<,TXZ,TYZ<
      ROH#SQRT%XI%I,J<**2&ETA%I,J<**2<
      IF %ROH-1.0< 59,59,60
   59 TERM1#PSIP
      TERM2#TXZ**2&TYZ**2
      SUM2#SUM2&TERM2
      GO TO 61
   60 TERM1#PSIP
      TERM3#TXZ**2&TYZ**2
      SUM3#SUM3&TERM3
```

```
61 CONTINUE
   SUM1#SUM1&TERM1
44 CONTINUE
   SUMP1#SUM1
   UF1#SUM2/GF
   UM1#SUM3/GM
   SUM4#0.0
   SUM5#0.0
   SUM6#0.0
   DO 45 I#1,20
   DO 45 J#21,60
   CALL PSIC%XI%I,J<,ETA%I,J<,PSIP<
   CALL TXYC%XI%I,J<,ETA%I,J<,TXZ,TYZ<
   ROH#SQRT%%XI%I,J<-GAMA<**2&ETA%I,J<**2<
   IF %ROH-1.0< 62,62,63
62 TERM4#PSIP
   TERM5#TXZ**2&TYZ**2
   SUM5#SUM5&TERM5
   GO TO 64
63 TERM4#PSIP
   TERM6#TXZ**2&TYZ**2
   SUM6#SUM6&TERM6
64 CONTINUE
   SUM4#SUM4&TERM4
45 CONTINUE
   SUMP2#SUM4
   UF2#SUM5/GF
   UM2#SUM6/GM
   SUMP#%SUMP1&SUMP2<*AREA
   D66S#GM*SUMP/%6.0*TK%3.0/DELTA<*RMU**4*DELTA**3<
   D66SM#D66S/GM
   UF#UF1&UF2
   UM#UM1&UM2
   GD66#%UF*GGF&UM*GGM</%UF&UM<
   RETURN
   END
```

```
C
C C
C       ***SUBROUTINE MATAS%A,B< FOR TRITORC 49X23***
        SUBROUTINE MATAS%A,B<
        DIMENSION A%49,23<,B%23,23<
        DO 30 I#1,23
        DO 31 J#I,23
        B%I,J<#0.0
        DO 32 M#1,49
        B%I,J<#A%M,I<*A%M,J<&B%I,J<
   32 CONTINUE
   31 CONTINUE
   30 CONTINUE
        DO 33 I#2,23
        II#I-1
        DO 34 J#1,II
        B%I,J<#B%J,I<
   34 CONTINUE
   33 CONTINUE
        RETURN
        END
C       ***SUBROUTINE ATB%A,B,C<***
        SUBROUTINE ATB%A,B,C<
        DIMENSION A%49,23<,B%49<,C%23<
        DO 30 I#1,23
        C%I<#0.0
        DO 31 J#1,49
        C%I<#C%I<&A%J,I<*B%J<
   31 CONTINUE
   30 CONTINUE
        RETURN
        END
C       ***SUBROUTINE PSIC%X,Y,PSIP<
        SUBROUTINE PSIC%X,Y,PSIP<
        COMMON RMU,DELTA,AMDA,AMDA1,RPI,EF,GEF,GF,GGF,RNUF,GNU=,
      1    EM,GEM,GM,GGM,RNUM,GNUM,A%23<,B%23<,XI%20,60<,ETA%20,60<,
```

```
     2    IKS,D66S,GD66,GAMA,D66SM,DATA%128,8<
      IF %X-RMU< 50,50,51
   50 ROH#SQRT%X**2&Y**2<
      IF %X< 52,53,54
   52 TETA#RPI&ATAN%Y/X<
      GO TO 55
   53 TETA#0.5*RPI
      GO TO 55
   54 TETA#ATAN%Y/X<
   55 IF %ROH-1.0< 56,56,57
   56 IF %ROH< 64,64,65
   64 PSIP#A%1<*AMDA
      ERR#0.0
      ROUTE#1.0
      RAD#ROH
      DEG#9.99
      RETURN
   65 SUMF#0.0
      DO 30 J#2,8
      K#2*%J-1<
      RK#K
      TERMF#A%J<*ROH**K*COS%RK*TETA<
      SUMF#SUMF&TERMF
   30 CONTINUE
      PSIP#%A%1<&SUMF-0.5*ROH**2<*AMDA
      ERR#TERMF*AMDA
      ROUTE#2.0
      RAD#ROH
      DEG#TETA*180.0/RPI
      RETURN
   57 SUMM#0.0
      DO 31 J#2,8
      K#2*%J-1<
      RK#K
      TERMM#B%J<*%ROH**K&AMDA1*ROH**%-K<<*COS%RK*TETA<
      SUMM#SUMM&TERMM
```

```
31 CONTINUE
   PSIP#B%I<&SUMM-0.5*ROH**2
   ERR#TERMM
   ROUTE#3.0
   RAD#ROH
   DEG#TETA*180.0/RPI
   RETURN
51 GAMA#2.0*RMU
   ROH#SQRT%%X-GAMA<**2&Y**2<
   IF %X-GAMA< 58,59,60
58 TETA#RPI&ATAN%Y/%X-GAMA<<
   GO TO 61
59 TETA#0.5*RPI
   GO TO 61
60 TETA#ATAN%Y/%X-GAMA<<
61 IF %ROH-1.0< 62,62,63
62 IF %ROH< 66,66,67
66 PSIP#%A%9<-0.5*%X**2&Y**2<<*AMDA
   ERR#0.0
   ROUTE#4.0
   RAD#ROH
   DEG#8.88
   RETURN
67 SUMF#0.0
   DO 32 J#10,23
   K#J-9
   RK#K
   TERMF#A%J<*ROH**K*COS%RK*TETA<
   SUMF#SUMF&TERMF
32 CONTINUE
   PSIP#%A% 9<&SUMF-0.5*%X**2&Y**2<<*AMDA
   ERR#TERMF*AMDA
   ROUTE#5.0
   RAD#ROH
   DEG#TETA*180.0/RPI
   RETURN
```

```
   63 SUMM#0.0
      DO 33 J#10,23
      K#J-9
      RK#K
      TERMM#B%J<*%ROH**K&AMDA1*ROH**%-K<<*COS%RK*TETA<
      SUMM#SUMM&TERMM
   33 CONTINUE
      PSIP#B%9<&SUMM-GAMA*AMDA1*ROH**%-1<*COS%TETA<
     1    -0.5*%X**2&Y**2<
      ERR#TERMM
      ROUTE#6.0
      RAD#ROH
      DEG#TETA*180.0/RPI
      RETURN
      END
C
C
C     ***SUBROUTINE TXYC%X,Y,TAUX,TAUY<
      SUBROUTINE TXYC%X,Y,TAUX,TAUY<
      COMMON RMU,DELTA,AMDA,AMDA1,RPI,EF,GEF,GF,GGF,RNUF,GNUF,
     1    EM,GEM,GM,GGM,RNUM,GNUM,A%23<,B%23<,XI%20,60<,ETA%20,60<,
     2    IKS,D66S,GD66,GAMA,D66SM,DATA%128,8<
      GAMA#2.0*RMU
      IF%X-RMU< 50,50,51
   50 ROH#SQRT%X**2&Y**2<
      IF %X< 52,53,54
   52 TETA#RPI&ATAN%Y/X<
      GO TO 55
   53 TETA#0.5*RPI
      GO TO 55
   54 TETA#ATAN%Y/X<
   55 IF %ROH-1.0< 56,56,57
   56 IF %ROH< 64,64,65
   64 TAUX#-AMDA*Y
      TAUY#AMDA*X
      CHANL#1.0
```

```
      RETURN
   65 SUMFX#0.0
      SUMFY#0.0
      DO 30 J#2,8
      K#2*%J-1<
      RK#K
      TERMFX#RK*A%J<*ROH***%K-1<*SIN%%RK-1.0<*TETA<
      SUMFX#SUMFX&TERMFX
      TERMFY#RK*A%J<*ROH***%K-1<*COS%%RK-1.0<*TETA<
      SUMFY#SUMFY&TERMFY
   30 CONTINUE
      TAUX#-AMDA*%SUMFX&Y<
      TAUY#-AMDA*%SUMFY-X<
      CHANL#2.0
      RETURN
   57 SUMMX#0.0
      SUMMY#0.0
      DO 31 J#2,8
      K#2*%J-1<
      RK#K
      TERMMX#RK*B%J<**%ROH***%K-1<*SIN%%RK-1.0<*TETA<&
     1    AMDA1*ROH**%-K-1<*SIN%%RK&1.0<*TETA<<
      TERMMY#RK*B%J<**%ROH***%K-1<*COS%%RK-1.0<*TETA<-
     1    AMDA1*ROH**%-K-1<*COS%%RK&1.0<*TETA<<
      SUMMX#SUMMX&TERMMX
      SUMMY#SUMMY&TERMMY
   31 CONTINUE
      TAUX#-SUMMX-Y
      TAUY#-SUMMY&X
      CHANL#3.0
      RETURN
   51 ROH#SQRT%%X-GAMA<**2&Y**2<
      IF %X-GAMA< 58,59,60
   58 TETA#RPI&ATAN%Y/%X-GAMA<<
      GO TO 61
   59 TETA#0.5*RPI
```

```
      GO TO 61
   60 TETA#ATAN%Y/%X-GAMA<<
   61 IF %ROH-1.0< 62,62,63
   62 IF %ROH< 66,66,67
   66 TAUX#-AMDA*Y
      TAUY#AMDA*%-A%10<&X<
      CHANL#4.0
      RETURN
   67 SUMFX#0.0
      SUMFY#0.0
      DO 32 J#11,23
      K#J-9
      RK#K
      TERMFX#RK*A%J<*ROH**%K-1<*SIN%%RK-1.0<*TETA<
      TERMFY#RK*A%J<*ROH**%K-1<*COS%%RK-1.0<*TETA<
      SUMFX#SUMFX&TERMFX
      SUMFY#SUMFY&TERMFY
   32 CONTINUE
      TAUX#-AMDA*%SUMFX&Y<
      TAUY#AMDA*%-A%10<-SUMFY&X<
      CHANL#5.0
      RETURN
   63 SUMMX#0.0
      SUMMY#0.0
      DO 33 J#11,23
      K#J-9
      RK#K
      TERMMX#RK*B%J<*%ROH**%K-1<*SIN%%RK-1.0<*TETA<
     1    &AMDA1*ROH**%-K-1<*SIN%%RK&1.0<*TETA<<
      TERMMY#RK*B%J<*%ROH**%K-1<*COS%%RK-1.0<*TETA<
     1    -AMDA1*ROH**%-K-1<*COS%%RK&1.0<*TETA<<
      SUMMX#SUMMX&TERMMX
      SUMMY#SUMMY&TERMMY
   33 CONTINUE
      TAUX#-SUMMX-AMDA1*%B%10<-GAMA<*SIN%2.0*TETA</%ROH**2<-Y
      TAUY#-SUMMY-B%10<&AMDA1*%B%10<-GAMA<*COS%2.0*TETA</%ROH**2<&X
```

```
      CHANL#6.0
      RETURN
      END
C
C
C     ***FUNCTION TK%X<***
      FUNCTION TK%X<
      RPI#3.1415927
      SUM#0.0
      DO 30 I#1,9,2
      RI#I
      TERM#TANH%RI*RPI*X/2.0</%RI**5<
      SUM#SUM&TERM
      IF %ABS%TERM<-1.0E-4< 50,50,51
   51 CONTINUE
   30 CONTINUE
   50 TK#%1.0-192.0*SUM/%RPI**5*X<</3.0
      RETURN
      END
C
C
C     *****DATA DECK FOR HEADING - COMPD66*****
C
C
%46X,@*****BORON-EPOXY A*****@,///<
%46X,@*****BORON-EPOXY B*****@,///<
%41X,@*****BORON-ALUMINUM 2024-T3*****@,///<
%45X,@*****E GLASS-EPOXY A*****@,///<
%45X,@*****E GLASS-EPOXY B*****@,///<
%39X,@*****TWISTING STIFFNESS D66/D66M*****@,///<
%1H1,//////////////,31X,@DATA 1  ELASTIC AND DAMPING PROPERTIES OF BORON@,///<
%1H1,//////////////,30X,@DATA 2  ELASTIC AND DAMPING PROPERTIES OF EPOXY A@,///<
%1H1,//////////////,30X,@DATA 3  ELASTIC AND DAMPING PROPERTIES OF EPOXY B@,///<
%1H1,//////////////,30X,@DATA 4  ELASTIC AND DAMPING PROPERTIES OF ALJ 2224@,///<
%1H1,//////////////,29X,@DATA 5  ELASTIC AND DAMPING PROPERTIES OF E-G_ASS@,///<
%1H1,//////////////,33X,@NOMINAL ELASTIC PROPERTIES OF SELECTED MATERIALS@,///<
```

```
C       *****LEAD-IN FOR COMPG55*****
        DIMENSION FMT2%20,6<,FNT2%20<
        COMMON RMU,DELTA,AMDA,AMDAP,AMDA1,RPI,IKS,SHAPE,EF,GEF,GF,GGF,
       1   RNUF,GNUF,FM,GEM,GM,GGM,RNUM,GNUM,RNUBA,B%20<,A%20<,XI%20,20<,
       2   ETA%20,20<,G55,GG55,K,G55S
C       ***DATA INPUT
        READ %5,2000< FMT2
 2000   FORMAT %20A4<
        CALL GIVEN
C       *READ GEOMETRICAL PARAMETERS RMU AND DELTA
        IDATA#1
        RPI#3.1415927
  700   READ %5,106< RMU,DELTA
  106   FORMAT %2F10.3<
        IF %RMU< 999,999,800
  800   CONTINUE
        CALL PT4CC
        VF#RPI/%4.0*RMU**2*DELTA<
        VM#1.0-VF
        IBEG#1
        IEND#6
        IINC#1
        DO 31 IJK#IBEG,IEND,IINC
        IF %IJK-5< 50,50,51
   50   NBEG#12*%IJK-1<&1
        NEND#NBEG&11
        NINC#1
        GO TO 52
   51   NBEG#61
        NEND#NBEG&3
        NINC#1
   52   CONTINUE
        WRITE %6,107< IDATA,RMU,DELTA,VF
  107   FORMAT %1H1,////////////,28X,@IDATA#@,I3,@      RMU#@,F7.3,
       1@      DELTA#@,F7.3,@      VF#@,F7.3,////<
        DO 2222 LMN#1,20
```

```
2222 FNT2%LMN<#FMT2%LMN,IJK<
     WRITE %6,FNT2<
     IF %IJK-5< 53,53,54
  53 CONTINUE
     WRITE %6,330<
 330 FORMAT %15X,13H   FREQUENCY ,13H       G55     ,13H      GG55     ,
    113H     GF/GM     ,13H     G55/GM    ,13H      SHAPE    ,7H    IKS ,/<
     WRITE %6,331<
 331 FORMAT %15X,13H      HERTZ    ,13H     1.E6 PSI ,13H     PER CENT ,//<
     GO TO 55
  54 WRITE %6,332<
 332 FORMAT %27X,20H        FIBER          <
     WRITE %6,333<
 333 FORMAT %27X,20H  VOLUME FRACTION    ,20H        GF/GM         ,
    1    20H        G55/GM         ,//<
  55 CONTINUE
     DO 30 I#NBEG,NEND,NINC
     II#I&64
     FREQ#DATA%I,1<
     EF#DATA%I,3<
     GEF#DATA%I,4<
     GF#DATA%I,5<
     GGF#DATA%I,6<
     RNUF#DATA%I,7<
     GNUF#DATA%I,8<
     EM#DATA%II,3<
     GEM#DATA%II,4<
     GM#DATA%II,5<
     GGM#DATA%II,6<
     RNUM#DATA%II,7<
     GNUM#DATA%II,8<
     AMDA#GF/GM
     AMDAP#EF/EM
     AMDA1#%AMDA-1.0</%AMDA&1.0<
     AMDA2#%AMDA*%1.0-2.0*RNUM<-%1.0-2.0*RNUF<</%AMDA&1.0-2.0*RNUF<
     ALPHA#AMDA*%3.0-4.0*RNUM&1.0</%3.0-4.0*RNUF&AMDA<
```

```
      BETA#4.C*AMDA*%1.0-RNUM</%AMDA-1.0<
      GAMMA#BETA-1.0
      RNUBA#VF*RNUF&VM*RNUM
      CALL CCMPG55
      GO TO %81,81,81,81,81,82<,IJK
   81 WRITE %6,109< FREQ,G55,GG55,AMDA,G55S,SHAPE,IKS
  109 FORMAT %15X,6F13.4,I5<
      GO TO 83
   82 WRITE %6,110< VF,AMDA,G55S
  110 FORMAT %32X,F7.3,11X,F13.4,8X,E13.4<
   83 CONTINUE
   30 CONTINUE
   31 CONTINUE
      IDATA#ICATA&1
      GO TO 7CC
  999 STOP
      END
C
C
C     ***SUBRCLTINE GIVEN***
C
C
C
C     ***PT400 ***
      SUBROUTINE PT400
      COMMON RMU,DELTA,AMDA,AMDAP,AMDA1,RPI,IKS,SHAPE,EF,GEF,GF,GGF,
     1   RNUF,GNUF,EM,GEM,GM,GGM,RNUM,GNUM,RNUBA,B%20<,A%20<,XI%20,20<,
     2   ETA%20,20<,G55,GG55,G55S,DATA%128,8<
      H#RMU/20.0
      V#RMU*DELTA/20.0
      DO 30 I#1,20
      RI#I
      DO 30 J#1,20
      RJ#J
      Y#RMU*DELTA-%RI-0.5<*V
      X#%RJ-C.5<*H
      XI%I,J<#X
```

```
      ETA%I,J<#Y
   30 CONTINUE
      RETURN
      END
C     *****SUBROUTINE COMPG55*****
      SUBROUTINE COMPG55
      DIMENSION CCC%40,20<,CC%20,20<,C%20,20<,BB%40<
      COMMON RMU,DELTA,AMDA,AMDAP,AMDA1,RPI,IKS,SHAPE,EF,GEF,GF,GGF,
     1   RNUF,GNUF,EM,GEM,GM,GGM,RNUM,GNUM,RNUBA,B%20<,A%20<,XI%20,20<,
     2   ETA%20,20<,G55,GG55,G55S,DATA%128,8<
      H#RMU/20.0
      V#RMU*DELTA/20.0
      XX#RMU
      Y#RMU*DELTA
      DO 30 I#1,20
      RI#I
      X#RI*H
      ROH#SQRT%X**2&Y**2<
      YY#RMU*DELTA-RI*V
      ROHV#SQRT%XX**2&YY**2<
      TETA#ATAN%Y/X<
      TETAV#ATAN%YY/XX<
      II#I&20
      BB%I<#%AMDA1/4.0<**%-%3.0&2.0*RNUBA<*SIN%2.0*TETA</%ROH*ROH<
     1   &3.0*SIN%4.0*TETA</%ROH**4<<-%2.0&RNUBA<*X*Y
      BB%II<#%AMDA1/4.0<**%-%3.0&2.0*RNUBA<*COS%2.0*TETAV</%ROHV*ROHV<
     1   &3.0*COS%4.0*TETAV</%ROHV**4<<-0.5*RNUBA*XX*XX-%1.0-0.5*RNUBA<
     2   *YY*YY
      CCC%I,1<#AMDA1*SIN%2.0*TETA</%ROH*ROH<
      CCC%II,1<#1.0&AMDA1*COS%2.0*TETAV</%ROHV*ROHV<
      DO 31 J#2,20
      K#2*J-1
      RK#K
      CCC%I,J<#-RK*%ROH**%K-1<*SIN%%RK-1.0<*TETA<&AMDA1*ROH**%-K-1<*
     1   SIN%%RK&1.0<*TETA<<
      CCC%II,J<#RK*%ROHV**%K-1<*COS%%RK-1.0<*TETAV<&AMDA1*ROHV**%-K-1<*
```

```
     1    COS%%RK&1.0<*TETAV<<
   31 CONTINUE
   30 CONTINUE
      CALL MATA%CCC,CC,40,20,0<
      CALL GTPRD%CCC,BB,B,40,20,1<
      CALL MSTR%CC,C,20,1,0<
      CALL SIMQ%C,B,20,KS<
      IKS#KS
      A%1<#2.0*B%1</%AMDA&1.0<-AMDA1*%3.0&2.0*RNUBA</4.0
      A%2<#2.0*B%2</%AMDA&1.0<&AMDA1/4.0
      CONST#2.0/%AMDA&1.0<
      DO 32 I#3,20
      A%I<#CONST*B%I<
   32 CONTINUE
      CALL CHICO
      RETURN
      END
C
C
C     ***SUBROUTINE CHICO***
      SUBROUTINE CHICO
      COMMON RMU,DELTA,AMDA,AMDAP,AMDA1,RPI,IKS,SHAPE,EF,GEF,GF,GGF,
     1    RNUF,GNUF,EM,GEM,GM,GGM,RNUM,GNUM,RNUBA,B%20<,A%20<,XI%20,20<,
     2    ETA%20,20<,G55,GG55,G55S,DATA%128,8<
      SHAPE#10.0*%1.0&RNUBA</%12.0&11.0*RNUBA<
      UPPER#2.0*%1.0&RNUM<*%%AMDA-1.0<*RPI/4.0&4.0*RMU**4*DELTA/3.0<
      BOT1#2.0*RNUBA*RMU**4*DELTA*%DELTA*DELTA-1.0</3.0
      BOT2#-%%RMU**4<*%DELTA**3<</3.0
      SUM#0.0
      AREA#%RMU**2<*DELTA/400.0
      DO 30 I#1,20
      DO 30 J#1,20
      CALL XCHI%XI%I,J<,ETA%I,J<,CHIX<
      SUM#SUM&CHIX
   30 CONTINUE
      BOT3#-3.0*SUM/%4.0*RMU*RMU<
```

```
      BOTOM#SHAPE**%BOT1&BOT2&BOT3<
      G55S#UPPER/BOTOM
      G55#GM*G55S
      SUMF#0.0
      SUMM#0.0
      DO 32 I#1,20
      DO 33 J#1,20
      CALL SGXYZ%XI%I,J<,ETA%I,J<,TAUXZ,TAUYZ<
      ROH#SQRT%XI%I,J< **2&ETA%I,J<**2<
      IF %ROH-1.0< 50,50,51
   50 TERMF#TAUXZ**2&TAUYZ**2
      SUMF#SUMF&TERMF
      GO TO 52
   51 TERMM#TAUXZ**2&TAUYZ**2
      SUMM#SUMM&TERMM
   52 CONTINUE
   33 CONTINUE
   32 CONTINUE
      UF#AMDA*SUMF
      UM#SUMM
      UDF#2.0*RPI*GGF*UF
      UDM#2.0*RPI*GGM*UM
      U#UF&UM
      UD#UDF&UDM
      GG55#UD/%2.0*RPI*U<
      RETURN
      END
C
C
C     ***SUBROUTINE XCHI%X,Y,CHIX<***
      SUBROUTINE XCHI%X,Y,CHIX<
      COMMON RNU,DELTA,AMCA,AMCAP,AMDA1,RPI,IKS,SHAPE,EF,GEF,GF,GGF,
     1   RNUF,GNUF,EM,GEM,GM,GGM,RNUM,GNUM,RNUBA,B%20<,A%20<,XI%20,20<,
     2   ETA%20,20<,G55,GG55,G55S,DATA%128,8<
      ROH#SQRT%X**2&Y**2<
      TETA#ATAN%Y/X<
```

```
      IF %ROH-1.0< 50,50,51
   50 CONTINUE
      SUMF#0.0
      DO 30 I#1,20
      K#2*I-1
      RK#K
      TERMF#A%I<*%ROH**K<*COS%RK*TETA<
      SUMF#SUMF&TERMF
   30 CONTINUE
      CHIX#X*SUMF
      RETURN
   51 CONTINUE
      SUMM#0.0
      DO 31 I#1,20
      K#2*I-1
      RK#K
      TERMM#B%I<*%ROH**K-AMDA1*ROH***-K<<<*COS%RK*TETA<
      SUMM#SUMM&TERMM
   31 CONTINUE
      EXTRA#%0.25*AMDA1<**-%3.0&2.0*RNUBA<*COS%TETA</ROH&COS%3.0*TETA<
     1    /%ROH**3<<
      CHIX#X*%SUMM&EXTRA<
      RETURN
      END
C
C
C     ***SUBROUTINE SGXYZ%X,Y,TAUXZ,TAUYZ<***
      SUBROUTINE SGXYZ%X,Y,TAUXZ,TAUYZ<
      COMMON PMU,DELTA,AMDA,AMDAP,AMDA1,RPI,IKS,SHAPE,EF,GEF,GF,GGF,
     1    RNUF,GNUF,EM,GEM,GM,GGM,RNUM,GNUM,RNUBA,B%20<,A%20<,XI%20,20<,
     2    ETA%20,20<,G55,GG55,G55S,DATA%128,8<
      ROH#SQRT%X**2&Y**2<
      IF %X< 50,51,52
   50 TETA#RPI&ATAN%Y/X<
      GO TO 53
   51 TETA#0.5*RPI
```

```
      GO TO 53
   52 TETA#ATAN%Y/X<
   53 CONTINUE
      IF %ROH< 54,54,55
   54 TAUXZ#A%1<*AMDA
      TAUYZ#0.0
      RETURN
   55 CONTINUE
      SUMX#0.0
      SUMY#0.0
      IF %ROH-1.0< 56,56,57
   56 CONTINUE
      DO 30 I#2,20
      K#2*I-1
      RK#K
      TERMX#RK*A%I<*ROH**%K-1<*COS%%RK-1.0<*TETA<
      TERMY#-RK*A%I<*ROH**%K-1<*SIN%%RK-1.0<*TETA<
      SUMX#SUMX&TERMX
      SUMY#SUMY&TERMY
   30 CONTINUE
      TAUXZ#AMDA*%SUMX&0.5*RNUBA*X**2&%1.0-0.5*RNUBA<*Y**2<&A%1<
      TAUYZ#AMDA*%SUMY&%2.0&RNUBA<*X*Y<
      RETURN
   57 DO 31 I#2,20
      K#2*I-1
      RK#K
      TERMX#RK*B%I<*%ROH**%K-1<*COS%%RK-1.0<*TETA<&
     1    AMDA1*ROH**%-K-1<*COS%%RK&1.0<*TETA<<
      TERMY#-RK*B%I<*%ROH**%K-1<*SIN%%RK-1.0<*TETA<-
     1    AMDA1*ROH**%-K-1<*SIN%%RK&1.0<*TETA<<
      SUMX#SUMX&TERMX
      SUMY#SUMY&TERMY
   31 CONTINUE
      TAUXZ#0.25*AMDA1*%%3.0&2.0*RNUBA<*COS%2.0*TETA</%ROH*ROH<
     1    -3.0*COS%4.0*TETA</%ROH**4<<&0.5*RNUBA*X*X&%1.0-0.5*RNUBA<*
     2    Y*Y&SUMX&B%1<*AMDA1*COS%2.0*TETA</%ROH*ROH<
```

```
      TAUYZ#0.25*AMDA1**3.0E2.0*RNUBA<*SIN**2.0*TETA</*ROH*ROH<
     1    -3.0*SIN**4.0*TETA</*ROH**4<<E**2.0ERNUBA<*X*YESUMY
     2    EB*I<*AMDAI*SIN**2.0*TETA</*ROH*ROH<
      RETURN
      END
C
C
C     *****DATA DECK FOR HEADING - COMPG55*****
C
C
**46X,@*****BORON-EPOXY A*****@,///<
**46X,@*****BORON-EPOXY B*****@,///<
**41X,@*****BORON-ALUMINUM 2024-T3*****@,///<
**45X,@*****E GLASS-EPOXY A*****@,///<
**45X,@*****E GLASS-EPOXY B*****@,///<
**31X,@*****TRANSVERSE THICKNESS-SHEAR STIFFNESS G55/GM*****@,///<
**1H1,////////////,31X,@DATA 1  ELASTIC AND DAMPING PROPERTIES OF BORON@,///<
**1H1,////////////,30X,@DATA 2  ELASTIC AND DAMPING PROPERTIES OF EPOXY A@,///<
**1H1,////////////,30X,@DATA 3  ELASTIC AND DAMPING PROPERTIES OF EPOXY B@,///<
**1H1,////////////,30X,@DATA 4  ELASTIC AND DAMPING PROPERTIES OF ALU 2224@,///<
**1H1,////////////,29X,@DATA 5  ELASTIC AND DAMPING PROPERTIES OF E-GLASS@,///<
**1H1,////////////,33X,@NOMINAL ELASTIC PROPERTIES OF SELECTED MATERIALS@,///<
```

```
C       *****LEAD-IN FOR COMPG44*****
        DIMENSION FMT2%20,6<,FNT2%20<
        COMMON RMU,DELTA,AMDA,AMDAP,AMDA1,AMDA2,EF,GEF,GF,GGF,RNUF,GNUF,
       1    EM,GEM,GM,GGM,RNUM,GNUM,RPI,VF,VM,E11S,DATA%128,8<,G44,G44S,
       2    GG44,RK
C       ***DATA INPUT
        READ %5,2000< FMT2
 2000 FORMAT %20A4<
        CALL GIVEN
C       *READ GEOMETRICAL PARAMETERS RMU AND DELTA
        IDATA#1
        RPI#3.1415927
  700 READ %5,106< RMU,DELTA
  106 FORMAT %2F10.3<
        IF %RMU< 999,999,800
  800 CONTINUE
        VF#RPI/%4.0*RMU**2*DELTA<
        VM#1.0-VF
        IBEG#1
        IEND#6
        IINC#1
        DO 31 IJK#IBEG,IEND,IINC
        IF %IJK-5< 50,50,51
   50 NBEG#12*%IJK-1<&1
        NEND#NBEG&11
        NINC#1
        GO TO 52
   51 NBEG#61
        NEND#NBEG&3
        NINC#1
   52 CONTINUE
        WRITE %6,107< IDATA,RMU,DELTA,VF
  107 FORMAT %1H1,////////////,28X,@IDATA#@,I3,@      RMU#@,F7.3,
      1@      DELTA#@,F7.3,@      VF#@,F7.3,////<
        DO 2222 LMN#1,20
 2222 FNT2%LMN<#FMT2%LMN,IJK<
```

```
      WRITE %6,FNT2<
      IF %IJK-5< 53,53,54
   53 CONTINUE
      WRITE %6,330<
  330 FORMAT %15X,14H     FREQUENCY ,14H         G44      ,
     1    14H         GG44     ,14H        GF/GM     ,14H        G44/GM   ,
     2    14H        SHAPE     ,/<
      WRITE %6,331<
  331 FORMAT %15X,14H       HERTZ     ,14H      1.E6 PSI  ,
     1    14H      PER CENT  ,//<
      GO TO 55
   54 WRITE %6,332<
  332 FORMAT %15X,12H        FIBER<
      WRITE %6,333<
  333 FORMAT %15X,20H   VOLUME FRACTION    ,21H                GF/GM     ,
     1    21H                G44/GM   ,21H                SHAPE     ,//<
   55 CONTINUE
      DO 30 I#NBEG,NEND,NINC
      II#I&64
      FREQ#DATA%I,1<
      EF#DATA%I,3<
      GEF#DATA%I,4<
      GF#DATA%I,5<
      GGF#DATA%I,6<
      RNUF#DATA%I,7<
      GNUF#DATA%I,8<
      EM#DATA%II,3<
      GEM#DATA%II,4<
      GM#DATA%II,5<
      GGM#DATA%II,6<
      RNUM#DATA%II,7<
      GNUM#DATA%II,8<
      AMDA#GF/GM
      AMDAP#EF/EM
      AMDA1#%AMDA-1.0</%AMDA&1.0<
      AMDA2#%AMDA*%1.0-2.0*RNUM<-%1.0-2.0*RNUF<</%AMDA&1.0-2.0*RNUF<
```

```
      ALPHA#AMDA*%3.0-4.0*RNUM&1.0</%3.0-4.0*RNUF&AMDA<
      BETA#4.0*AMDA*%1.0-RNUM</%AMDA-1.0<
      GAMMA#BETA-1.0
      CALL COMPG44
      GO TO %81,81,81,81,81,82<,IJK
   81 WRITE %6,109< FREQ,G44,GG44,AMDA,G44S,RK
  109 FORMAT %15X,6E14.4<
      GO TO 83
   82 WRITE %6,110< VF,AMDA,G44S,RK
  110 FORMAT %15X,E15.4,5X,3E21.4<
   83 CONTINUE
   30 CONTINUE
   31 CONTINUE
      IDATA#IDATA&1
      GO TO 700
  999 STOP
      END
C
C
C     *****SUBROUTINE GIVEN*****
C
C
C     ***SUBROUTINE G4GG4
      SUBROUTINE G4GG4
      EXTERNAL FF1,FF2,FF3,FF4
      COMMON RMU,DELTA,AMDA,AMDAP,AMDA1,AMDA2,EF,GEF,GF,GGF,RNUF,GNU=,
     1    EM,GEM,GM,GGM,RNUM,GNUM,RPI,VF,VM,E11S,DATA%128,8<,G44,G44S,
     2    GG44,RK
      CALL QG5%0.0,1.0,FF1,F1<
      CALL QG5%0.0,1.0,FF2,F2<
      CALL QG5%-1.0,1.0,FF3,F3<
      CALL QG5%-1.0,1.0,FF4,F4<
      RNUAV#0.5*%RNUF&RNUM<
      RK#10.0*%1.0&RNUAV</%12.0&11.0*RNUAV<
      G44#%GM/%3.0*DELTA*RK<</%0.4*%RMU-1.0</%RMU*DELTA<&0.75
     1    *%F1/AMDA&F2<<
```

```
      UF1#9.0*F1/%8.0*GF<
      UF2#3.0*AMDAP*F3/%4.0*EM**%RMU*DELTA<**6<
      UM1#3.0/GM**%%RMU-1.0</%5.0*RMU*DELTA<&3.0*F2/8.0<
      UM2#3.0/%4.0*EM**%RMU*DELTA<**3<**%2.0/3.0*%RMU-1.0<**%1.0&RMU&
     1    4.0*RMU**2<&F4<
      UBAR#UF1&UF2&UM1&UM2
      UDBAR#GEF*UF1&GGF*UF2&GEM*UM1&GGM*UM2
      GG44#UDBAR/%2.0*RPI*UBAR<
      G44S#G44/GM
      RETURN
      END
C
C
C     ***FUNCTION FF1%X<***
      FUNCTION FF1%X<
      COMMON RMU,DELTA,AMDA,AMDAP,AMDA1,AMDA2,EF,GEF,GF,GGF,RNUF,GNUF,
     1    EM,GEM,GM,GGM,RNUM,GNUM,RPI,VF,VM,E11S,DATA%128,8<,G44,G44S,
     2    GG44,RK
      Y#1.0-X**2
      SQRY#SQRT%Y<
      Z#RMU*DELTA
      ZZ#Z*Z
      ZZZ#Z*ZZ
      A#%%AMDAP-1.0<*Y&ZZ<**2*SQRY
      B#-%2.0/3.0<*%%AMDAP-1.0<*Y&ZZ<*AMDAP*SQRY**3
      C#0.2*AMDAP**2*SQRY**5
      D#%ZZZ&%AMDAP-1.0<*SQRY**3<**2
      FF1#%A&B&C</D
      RETURN
      END
C
C
C     ***FUNCTION FF2%X<***
      FUNCTION FF2%X<
      COMMON RMU,DELTA,AMDA,AMDAP,AMDA1,AMDA2,EF,GEF,GF,GGF,RNUF,GNUF,
     1    EM,GEM,GM,GGM,RNUM,GNUM,RPI,VF,VM,E11S,DATA%128,8<,G44,G44S,
```

```
     2    GG44,RK
          Y#1.0-X**2
          SQRY#SQRT%Y<
          Z#RMU*DELTA
          ZZ#Z*Z
          ZZZ#Z*ZZ
          A#8.0*ZZ*ZZZ/15.0
          B#-SQRY*%Z*ZZZ-2.0/3.0*ZZ*Y&0.2*Y*Y<
          C#%ZZZ&%AMDAP-1.0<*SQRY**3<**2
          FF2#%A&B</C
          RETURN
          END
C
C
C         ***FUNCTION FF3%X<***
          FUNCTION FF3%X<
          COMMON RMU,DELTA,AMDA,AMDAP,AMDA1,AMDA2,EF,GEF,GF,GGF,RNUF,GNJF,
     1    EM,GEM,GM,GGM,RNUM,GNUM,RPI,VF,VM,E11S,DATA%128,8<,G44,G44S,
     2    GG44,RK
          Y#1.0-X**2
          Z#RMU*DELTA
          SQRY#SQRT%Y<
          ZZ#Z*Z
          ZZZ#Z*ZZ
          FF3#%%RMU-X</%1.0-%AMDAP-1.0</ZZZ*SQRY**3<<**2*SQRY**3
          RETURN
          END
C
C
C         ***FUNCTION FF4%X<***
          FUNCTION FF4%X<
          COMMON RMU,DELTA,AMDA,AMDAP,AMDA1,AMDA2,EF,GEF,GF,GGF,RNUF,GNJF,
     1    EM,GEM,GM,GGM,RNUM,GNUM,RPI,VF,VM,E11S,DATA%128,8<,G44,G44S,
     2    GG44,RK
          Y#1.0-X**2
          Z#RMU*DELTA
```

```
      SQRY#SQRT%Y<
      ZZ#Z*Z
      ZZZ#Z*ZZ
      FF4#%%RMU-X</%1.0E%AMDAP-1.0</ZZZ*SQRY**3<<**2*%ZZZ-SQRY**3<
      RETURN
      END
C
C
C     ***SUBROUTINE QGS%XL,XU,FCT,Y<***
      SUBROUTINE QGS%XL,XU,FCT,Y<
      A#0.5*%XU&XL<
      B#XU-XL
      C#.4530899*B
      Y#.1184634*%FCT%A&C<&FCT%A-C<<
      C#.2692347*B
      Y#Y&.2393143*%FCT%A&C<&FCT%A-C<<
      Y#B*%Y&.2844444*FCT%A<<
      RETURN
      END
C
C
C     *****DATA DECK FOR HEADING - COMPG44******
C
C
%46X,23H*****BORON-EPOXY A*****,///<
%46X,23H*****BORON-EPOXY B*****,///<
%41X,32H*****BORON-ALUMINUM 2024-T3*****,///<
%45X,25H*****E GLASS-EPOXY A*****,///<
%45X,25H*****E GLASS-EPOXY B*****,///<
%31X,53H*****TRANSVERSE THICKNESS-SHEAR STIFFNESS G44/GM*****,///<
%1H1,/////////////,31X,47HDATA 1  ELASTIC AND DAMPING PROPERTIES OF BORON,///<
%1H1,/////////////,30X,49HDATA 2  ELASTIC AND DAMPING PROPERTIES OF EPOXY A,///<
%1H1,/////////////,30X,49HDATA 3  ELASTIC AND DAMPING PROPERTIES OF EPOXY B,///<
%1H1,/////////////,30X,50HDATA 4  ELASTIC AND DAMPING PROPERTIES OF ALU 2224,///<
%1H1,/////////////,29X,49HDATA 5  ELASTIC AND DAMPING PROPERTIES OF E-GLASS,///<
%1H1,/////////////,33X,48HNOMINAL ELASTIC PROPERTIES OF SELECTED MATERIALS,///<
```